Platelets promote insulin secretion of pancreatic β-cells

♦♦♦♦♦

Thrombozyten fördern die Insulinsekretion von pankreatischen β-Zellen

Doctoral thesis for a doctoral degree
at the Graduate School of Life Sciences,
Julius-Maximilians-Universität Würzburg,
Section Biomedicine

Submitted by

Till Karwen

from Großburgwedel

Würzburg, Novermber 2022

Submitted on: _____

Office stamp

Members of the *Promotionskomitee*:

Chairperson:	Prof. Dr. med. Manfred Gessler
Primary Supervisor:	Dr. Grzegorz Sumara
Supervisor (Second):	Prof. Dr. Bernhard Nieswandt
Supervisor (Third):	Prof. Dr. Patrik Rorsman
Supervisor (Fourth):	Prof. Dr. Antje Gohla

Date of Public Defense: _____

Date of Receipt of Certificates: _____

TABLE OF CONTENTS

SUMMARY

The pancreas is the key organ for the maintenance of euglycemia. This is regulated in particular by α-cell-derived glucagon and β-cell-derived insulin, which are released in response to nutrient deficiency and elevated glucose levels, respectively. Although glucose is the main regulator of insulin secretion, it is significantly enhanced by various potentiators.

Platelets are anucleate cell fragments in the bloodstream that are essential for hemostasis to prevent and stop bleeding events. Besides their classical role, platelets were implemented to be crucial for other physiological and pathophysiological processes, such as cancer progression, immune defense, and angiogenesis. Platelets from diabetic patients often present increased reactivity and basal activation. Interestingly, platelets store and release several substances that have been reported to potentiate insulin secretion by β-cells. For these reasons, the impact of platelets on β-cell functioning was investigated in this thesis.

Here it was shown that both glucose and a β-cell-derived substance/s promote platelet activation and binding to collagen. Additionally, platelet adhesion specifically to the microvasculature of pancreatic islets was revealed, supporting the hypothesis of their influence on glucose homeostasis. Genetic or pharmacological ablation of platelet functioning and platelet depletion consistently resulted in reduced insulin secretion and associated glucose intolerance. Further, the platelet-derived lipid fraction was found to enhance glucose-stimulated insulin secretion, with *20-hydroxyeicosatetraenoic acid* (20-HETE) and possibly also *lyso-precursor of platelet-activating factor* (lysoPAF) being identified as crucial factors. However, the acute platelet-stimulated insulin secretion was found to decline with age, as did the levels of platelet-derived 20-HETE. In addition to their direct stimulatory effect on insulin secretion, specific defects in platelet activation have also been shown to affect glucose homeostasis by potentially influencing islet vascular development. Taking together, the results of this thesis suggest a direct and indirect mechanism of platelets in the regulation of insulin secretion that ensures glucose homeostasis, especially in young individuals.

ZUSAMMENFASSUNG

Der Pankreas ist das Schlüsselorgan für die Aufrechterhaltung der Glukosehomöostase. Diese wird insbesondere durch das von α-Zellen stammende Glukagon und von β-Zellen stammende Insulin reguliert, die als Reaktion auf Nährstoffmangel beziehungsweise erhöhte Glukosespiegel freigesetzt werden. Obwohl Glukose der Hauptregulator der Insulinsekretion ist, wird sie durch verschiedene Potentiatoren erheblich gesteigert.

Thrombozyten sind kernlose Zellfragmente im Blutkreislauf, die für die Hämostase unerlässlich sind. Neben ihrer klassischen Funktion sind sie auch an anderen physiologischen und pathophysiologischen Prozessen beteiligt, etwa an der Tumorentwicklung, der Immunabwehr und der Angiogenese. Thrombozyten von Diabetikern weisen häufig eine erhöhte Reaktivität und basale Aktivierung auf. Außerdem speichern und sekretieren sie Substanzen, von denen bekannt ist, dass sie die Insulinsekretion durch β-Zellen verstärken. Aus diesen Gründen wurde in dieser Arbeit der Einfluss von Thrombozyten auf die Funktion von β-Zellen untersucht.

Es konnte gezeigt werden, dass sowohl Glukose als auch eine aus β-Zellen stammende Substanz/en die Thrombozytenaktivierung und die Bindung an Kollagen fördern. Darüber hinaus wurde eine spezifische Thrombozytenadhäsion an der Mikrovaskulatur der pankreatischen Inseln festgestellt, was die Hypothese ihres Einflusses auf die Glukosehomöostase unterstützt. Eine genetische oder pharmakologische Ablation der Thrombozytenfunktion sowie eine Depletion von Thrombozyten führten zu einer verminderten Insulinsekretion und einer damit verbundenen Glukoseintoleranz. Hierbei erwies sich die Lipidfraktion von Thrombozyten als essentieller Potentiator für die glukosestimulierte Insulinsekretion, wobei *20-Hydroxyeicosatetraensäure* (20-HETE) und die *Lyso-Vorstufe des Plättchen-Aktivierenden Faktors* (LysoPAF) als entscheidende Faktoren identifiziert werden konnten. Weiterhin wurde festgestellt, dass sowohl der direkte stimulierende Effekt von Thrombozyten auf die Insulinsekretion, als auch deren 20-HETE Sekretion mit zunehmendem Alter abnimmt. Thrombozyten beeinflussten außerdem die Inselvaskularisierung, welche mutmaßlich zusätzlich zu Glukoseintoleranz führt. Insgesamt deuten die Ergebnisse dieser Arbeit auf einen direkten und indirekten Mechanismus der Thrombozyten bei der Regulierung der Insulinsekretion hin, der die Glukosehomöostase insbesondere bei jungen Menschen gewährleistet.

1 INTRODUCTION

1.1 The pancreas

1.1.1 Pancreas morphology and functions

The pancreas is a composite, glandular organ that affects the functioning of the entire body due to its exocrine and endocrine functions. In humans, the pancreas weighs about 90 g, whereas in mice its mass ranges from 0.2-0.4 g[1,2]. From a macro perspective, it can be divided into the head, which is connected with the intestine, the body, and the tail extending across the midline close to the spleen. It is crossed by a pancreatic duct, which enters the duodenum through the greater papilla[3].

The pancreas can be further divided into the exocrine and endocrine pancreas. The exocrine part consists of acinar cells, that form so-called acinus units, which are connected to the ductal system. They produce and secrete pancreatic juice through the pancreatic duct into the intestine. This iso-osmotic, alkaline pancreatic juice contains enzymes that digest carbohydrates, proteins, fats, and nucleic acids essential for food digestion. The secretion is regulated by food consumption and resulting hormonal and neurohormonal mechanisms[4]. The endocrine pancreas is organized in pancreatic islets, also called islets of Langerhans, which are located between the clusters of acinar cells and are evenly distributed within the pancreas[5]. The mouse pancreas contains a couple of thousand islets, whereas humans possess a few million islets, making only 1-2 % of the total mass of the pancreas[2,6]. They are mainly composed of insulin-secreting β-cells and glucagon-secreting α-cells, but additionally contain δ-cells and *pancreatic polypeptide* (PP)-cells, which release somatostatin and pancreatic polypeptide, respectively[7-10]. The released polypeptide hormones execute the principal function of the endocrine pancreas, which is the control of cellular mobilization and storage of glucose, amino acids, and triglycerides. Thus, the secretion of respective hormones is regulated by circulating metabolites, autonomic nerves, and local or circulating hormones[6].

Islets range widely in size, with a typical islet being between 50-400 µm in diameter in humans and between 100-200 µm in rodents. Factors like age, metabolic requirements, and body size influence islet size[11]. Regarding cellularity, islets of rodents tend to have more β-cells (60-80 %) than islets from humans (~50 %), but fewer α-cells (15-20 % in rodents, ~40 % in humans), as well as roughly 10 % δ-cells

and 1 % PP-cells[12-16]. They further differ in their architecture, as cells are rather randomly distributed throughout the human pancreatic islets, whereas in rodent islets β-cells form a core surrounded by the other endocrine cells[12,13,15].

Despite their small percentage of the pancreas mass, pancreatic islets can get up to 20 % of its blood supply[7]. Their vascularization is 5- to 10-fold higher than that of the exocrine pancreas, ensuring a ready exposure to blood glucose concentrations and a rapid release of corresponding hormones into the blood stream[17,18]. Additionally, the blood flow through islets microvasculature can be adjusted in a glucose-dependent manner. Contractile pericytes relax during high blood glucose, enabling higher blood flow through the islets, thereby favoring processes that restore euglycemia[19]. Almaca et al. stated that ATP mediates the relaxation of pericytes, which likely derives from β-cells co-released with insulin. This model implies a blood flow through pancreatic islets regulated by amounts of released insulin[20,21].

1.1.2 Pancreatic glucoregulatory control

The human organism depends on strict management of its blood glucose levels to ensure appropriate physiological function. Hypoglycemic levels below 50 mg/dL can be life-threatening, due to insufficient fuel supply to the brain. On the other hand, a hyperglycemic state with levels above 200 mg/dL causes adverse effects through glucotoxicity, upon others[22]. Therefore, blood glucose levels are typically regulated within a narrow physiological range of 80-140 mg/dL, with levels in mice being slightly above[23]. As blood glucose levels are affected by varying nutritional supply and different states of organs being involved in nutritional absorption, storage, and consumption, it requires a complex regulatory mechanism to maintain normoglycemia. The endocrine pancreas plays a key role in this and ensures an accurate interplay of several organs. This is mainly accomplished by the opposing actions of glucagon and insulin, which are released from α-cells and β-cells, respectively (Figure 1). During low blood glucose levels, as they occur during sleep, prolonged fasting, exercise, or between periods of food ingestion, α-cells release glucagon[24]. This catabolic hormone promotes hepatic gluconeogenesis and glycogenolysis leading to elevated blood glucose levels[25-27]. It further induces lipolysis in adipocytes, producing lipolytic byproducts that act as additional energy substrates[28,29]. In contrast, β-cells release insulin during hyperglycemic conditions, as it occurs after food ingestion[30]. Insulin

executes an anabolic action, that induces translocation and integration of *glucose transporter* (GLUT)4 into the plasma membrane of cells in insulin-sensitive tissue like muscle, liver, and adipose tissue. This enables glucose uptake, which results in decreasing blood glucose levels[31]. In addition, it inhibits catabolic mechanisms like lipolysis, gluconeogenesis, and glycogenolysis[32-34].

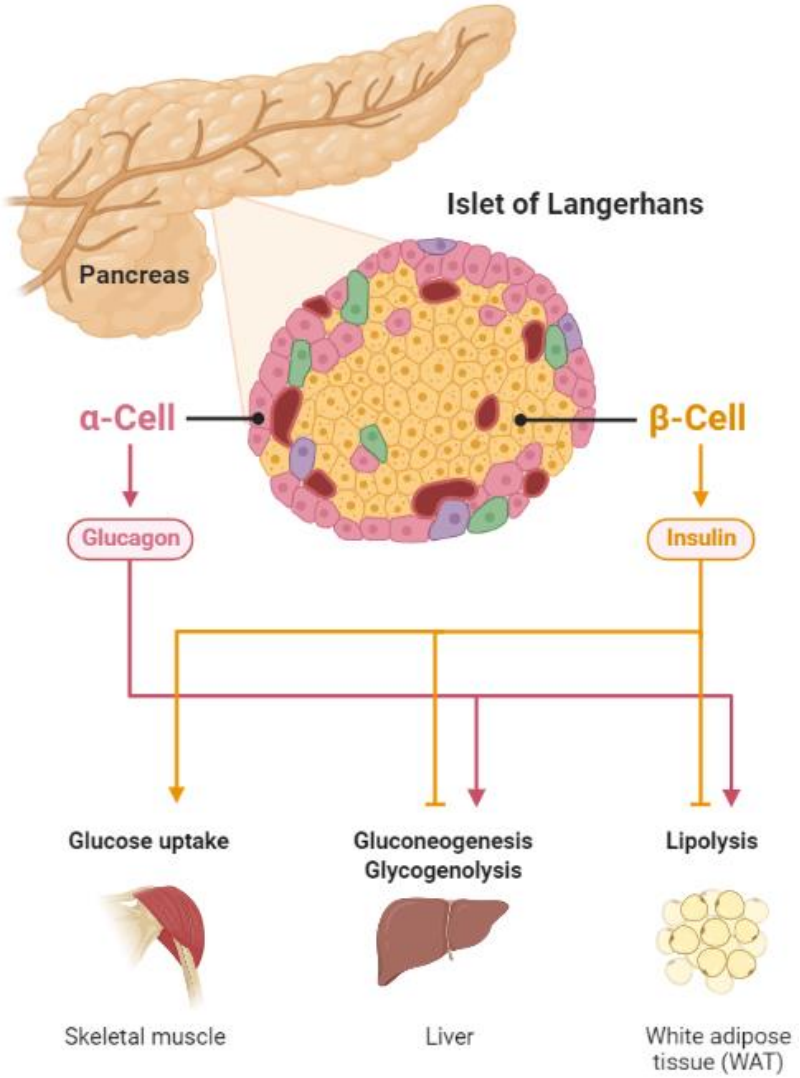

Figure 1: Glucoregulatory control of the pancreas. Islets of Langerhans contain α-cells that release glucagon during hypoglycemia, which elevates blood glucose levels through stimulation of gluconeogenesis and glycogenolysis. During hyperglycemic conditions, β-cells release insulin, thus mediating glucose uptake into insulin-sensitive tissue and consequently decreasing blood glucose levels. (Created with BioRender.com)

Counteracting insulin and glucagon are getting released in response to signals initiated by circulating metabolites, endocrine and paracrine hormones, and autonomic nerves. The sensitivity to certain metabolites enables α-cells and β-cells to respond to

metabolic conditions. Insulin secretion is induced by glucose and further stimulated by f*atty acids* (FA) and amino acids, whereas glucagon secretion is inhibited by increasing glucose concentration but stimulated by FA and amino acids, whose levels are elevated with fasting[35]. In addition, both cells influence each other's secretion behavior in a paracrine manner. β-cells co-release amylin and zinc together with insulin, which were all shown to inhibit glucagon secretion[36-40]. On the other hand, glucagon executes stimulative actions on β-cells insulin secretion[41,42]. Other cell types of pancreatic islets regulate the coordinated secretion of insulin and glucagon as well, as δ-cell-derived somatostatin acts as a paracrine suppressor of both insulin and glucagon secretion[43]. Similarly, PP-cells release PP through vagal and enteric nervous inputs, which has inhibitory actions on glucagon and somatostatin secretion[44]. Additional cells that are present in small numbers (<1 %) in pancreatic islets are ε-cells. They release ghrelin during fasting conditions, which inhibits insulin secretion, but stimulates glucagon release and further regulates appetite[45-48]. Besides paracrine stimuli, the function of pancreatic islets is also regulated by several endocrine mechanisms. Incretins are hormones released by the gastrointestinal system. The secretion of integrins like *glucose-dependent insulinotropic polypeptide* (GIP) or *glucagon-like peptide* (GLP)-1 is stimulated by nutrient ingestion and boosts glucose-induced insulin secretion[49,50]. Also, ghrelin gets released by the stomach during periods of fasting to promote nutritional supply and inhibit insulin secretion[51,52]. Finally, autonomic nerves innervate pancreatic islets and regulate hormone secretion of endocrine cells. Hence, hypoglycemia and hyperglycemia can be sensed in the brain causing sympathetic or parasympathetic activity, that leads to glucagon or insulin secretion, respectively[53-56]. In mouse islets nerve branches are therefore in direct contact with endocrine cells, whereas in humans the sparsely innervated nerves are rather connected with smooth muscles, indicating regulation of endocrine action by the blood flow[7,57,58].

1.2 β-Cells

1.2.1 Core regulation of insulin secretion

Pancreatic β-cells are able to convert metabolic changes into an electrical potential, which in turn is translated into corresponding secretory actions. The master regulator

for insulin secretion is glucose. It is considered an initiator of insulin secretion, because of its capability to stimulate insulin secretion without the need for any other co-stimulus (Figure 2). Hence, healthy β-cells convert small changes in blood glucose levels into substantial changes in insulin secretion to maintain euglycemia. Therefore, as an initial step, β-cells need to uptake circulating glucose by facilitated diffusion, which in mice is mediated by GLUT2 and in humans primarily by GLUT1[59,60]. Once in the cytosol, g*lucokinase* (GCK) catalyzes glucose phosphorylation to form *glucose-6-phosphate* (G6P)[61]. The low affinity of GLUT and GCK of β-cells allows rapid equilibration between intracellular and extracellular glucose concentrations, which reduces their rate-limiting potential for insulin secretion within a brought range of physiological glucose concentrations[59,62,63]. Generated G6P enters glycolysis leading to the formation of pyruvate, which gets oxidized through the *tricarboxylic acid* (TCA) cycle in the mitochondria of β-cells. The resulting NADH and *flavin adenine dinucleotide* ($FADH_2$) undergo further metabolic oxidation to produce ATP. Thus, the large majority of glucose entering glycolysis is further metabolized in the TCA cycle, yielding high ATP conversion[64]. Rising ATP/ADP ratio as a result of increased glycolytic flux in β-cells leads to the closure of ATP-sensitive K^+ (K_{ATP}) channels in the plasma membrane, which maintain the negative membrane potential (-70 mV) at non-stimulatory glucose levels[65]. The decrease in K^+ efflux results in a depolarization of the membrane, which upon reaching a threshold of about -50 mV increases the likability of *voltage-dependent Ca^{2+} channel* (VDCC) to open. Some differences exist in the composition and nature of VDCCs between mice and humans. In humans, the closure of K_{ATP} channels is associated with an increased membrane resistance, causing the spontaneous opening of low-voltage activated T-type Ca^{2+} channels, which's opening amplifies with increasing depolarization. Once the depolarization reaches a threshold of above -40 mV, L-type VDCCs and Na^{2+} channels open to further amplify depolarization[66]. When a peak of the action potential is reached (≥-20 mV) P/Q-type Ca^{2+}-channels open, resulting in the maximal influx of Ca^{2+}. In mice, L-type VDCC channels account for the majority of Ca^{2+} currents[67]. They do not possess T-type Ca^{2+} channels but instead R-type VDCC that are essential for second-phase insulin secretion[68]. When the action potentials are reached, mechanisms like the lowering effect of *sarcoendoplasmic reticulum Ca^{2+}-ATPase* (SERCA) on the intracellular ATP/ADP ratio, which causes the reopening of K_{ATP} and further mediates Ca^{2+} extrusion through its pump activity, or voltage-gated and calcium-activated

potassium channels mediate repolarization of the cell[69]. These glucose-induced $[Ca^{2+}]_i$ oscillations are coupled between adjacent β-cells through gap junctions, causing a synchronized state across the whole islet in mice. This effect is less pronounced in human islets, probably due to the nonhomogeneous β-cells distribution in human islets[12,70]. Of note, glucose does not only induce this process by increasing the ATP/ADP ratio. Intermediate metabolites can exit the TCA cycle to amplify K_{ATP}-dependent insulin release[71,72]. Additionally, instead of metabolization through glycolysis, G6P can get processed to result in the formation of Gly3P. This, in turn, enables the formation of lipid mediators such as *diacylglycerol* (DAG) and long-chain acyl-*coenzyme A* (CoA) which are mitochondria-independent promoters of insulin secretion[73-75]. It was shown, that the threshold glucose concentration for insulin secretion is about 50 mg/dL in humans and 90 mg/dL in mice, which goes in line with lower fasting blood glucose levels in humans[7,76,77]. In both humans and mice, insulin reaches the half-maximum secretion upon 180-220 mg/dL and saturates at levels above 360 mg/dL of glucose[7].

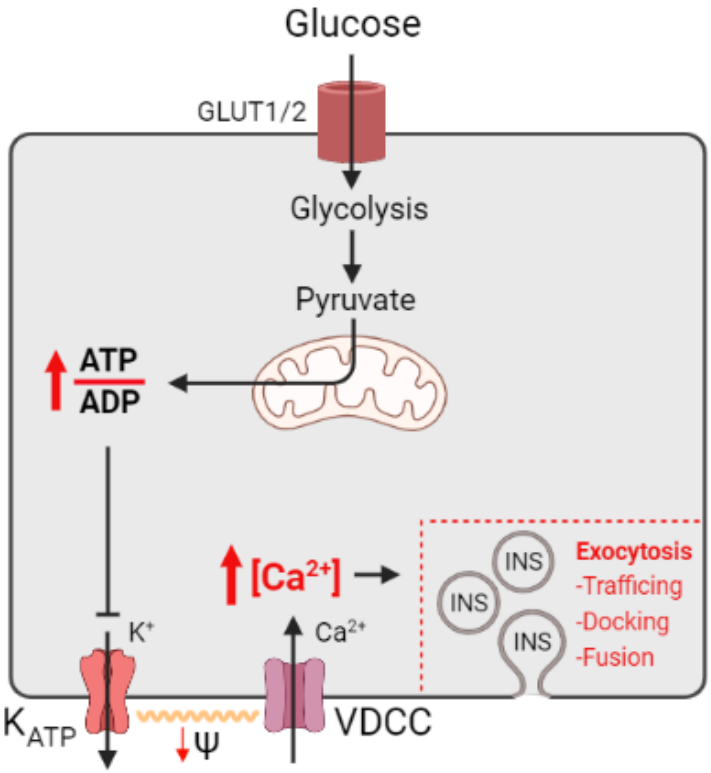

Figure 2: Regulation of glucose-stimulated insulin secretion in β-cells. The glycolytic and oxidative metabolization of glucose leads to an increasing intracellular ATP/ADP ratio. This is sensed by ATP-sensitive K_{ATP}-channels and mediates their closure. The inhibited K^+ efflux results in decreasing membrane potential (Ψ), causing the opening of VDCC and a respective influx of Ca^{2+} that finally triggers exocytosis of insulin granules. (Created with BioRender.com)

The rise of $[Ca^{2+}]_i$ that is reached during action potentials is the major driver of insulin secretion, as it primes essential exocytotic events like trafficking, priming, docking, and the release of secretory insulin granules[78]. The resulting initial degranulation process is called first-phase secretion and lasts for 5-10 min. Especially a readily releasable pool of insulin granules, which is already pre-docked or near the plasma membrane gets released and executes a first response to the elevated glucose levels[79,80]. The second phase of insulin secretion is mediated by granules from intracellular storage pools, which is depending on the reorganization of filamentous actin[81,82]. Thus, the secretion rate drops but remains constant until a euglycemic state is reached[80]. This phase contributes to about 85 % of the insulin secretion within the first hour of glucose stimulation[83]. Mechanistically, elevated $[Ca^{2+}]_i$ activates calcium-dependent *phospholipase C* (PLC), which hydrolyzes *phosphatidylinositol-4,5-bisphosphate* (PIP_2) in the membrane into DAG and *inositol (3,4,5)-trisphosphate* (IP_3)[84]. DAG induces activation of *protein kinases C* (PKC)s, which bind to PIP_2 and PS in the presence of calcium, thus translocating to the plasma membrane[85]. In their active state, PKCs affect insulin secretion by targeting several processes. It mediates a reorganization of the dense cortical network of actin close to the plasma membrane that acts as a barrier to vesicles[86]. This is partially mediated through MARCKS, which gets released from the plasma membrane by activated PKC and cross-links actin[87]. It is thought that the disassembly enables rapid initial vesicle release and sustained recruitment of vesicles from the reserve pool[88-90]. Similarly, MLCK gets activated by PKC, which is thought to contribute to vesicle movement through vesicle-localized myosin[91]. PKC further promotes localization and fusion of the secretory machinery with the plasma membrane. It phosphorylates N-type Ca^{2+} channels, thereby enabling the binding of syntaxin from granules[92,93]. With given high local Ca^{2+} concentrations due to the channel proximity, the release of this proportion of granules is thought to contribute to the first phase exocytotic response[94]. PKCs have many more targets involved in forming a granule plasma membrane complex. These include *synaptosomal-associated protein* (SNAP)23, VAMP2, m*ammalian uncoordinated* (munc)18, and synaptotagmin through which they are thought to enable docking and fusion of vesicles, thereby increasing the rate and number of exocytotic events[95,96].

Insulin derives from the insulin gene expression leading to the synthesis of preproinsulin. This precursor protein contains a C-terminal signal recognition peptide mediating entry into the secretory pathway and getting cleaved upon entry into the *endoplasmic reticulum* (ER)[97]. The resulting proinsulin consists of an A and B chain, together with a connecting C-peptide. Due to the oxidative environment of the ER, disulfide bonds are formed to gain the tertiary structure. In this state, it gets transported to the Golgi apparatus, where it is packed into immature secretory granules[98]. Peptidase machinery mediates the cleavage of the C-peptide leading to mature insulin, which is stored in a Zn_2-$insulin_6$ complex and accounts for 5-10 % of the β-cell protein content[99,100]. A β-cell contains about 10,000 insulin secretory granules, with each of them storing 8-9 fg insulin[101]. Despite the high abundance of insulin, less than 1 %/h gets released by exocytosis even at high glucose levels[80]. However, the regulation of insulin biosynthesis differs from that of exocytosis. The low threshold glucose concentration for proinsulin biosynthesis (40-70 mg/dL) enables the maintenance of an insulin reservoir also in the absence of glucose-stimulated insulin secretion[102]. Still, elevated blood glucose levels after food intake further stimulate the rapid translation of preproinsulin mRNA[103]. Also, insulin gene transcription was demonstrated to multiply upon high glucose conditions and additionally increased the stability of generated proinsulin mRNA[104,105]. Of note, glucose does not induce proinsulin biosynthesis through elevated cytosolic Ca^{2+} levels, but instead by secondary metabolites generated in the mitochondria of β-cells[106].

1.2.2 Potentiators of insulin secretion

Besides the glucose-mediated core mechanism of insulin secretion, several potentiators and inhibitors contribute to the adjustment of its release. Potentiators of insulin secretion are not able to induce insulin secretion on their own, but only in the presence of glucose even at sub-stimulatory concentrations[7]. This is due to their mechanism of action. They generate an inward current, that is supposed to amplify the depolarization process. However, in the absence of glucose, the hyperpolarization mediated by the K_{ATP} channels is too strong to counteract. Other potentiators execute their effect by enhancing the degranulation process. As exocytosis depends on Ca^{2+} entry, these potentiators can also act only in the presence of depolarizing glucose concentrations. However, if glucose-induced depolarization is assured, those

potentiators can substantially increase insulin secretion by enhancing depolarization or exocytotic events (Figure 3)[7].

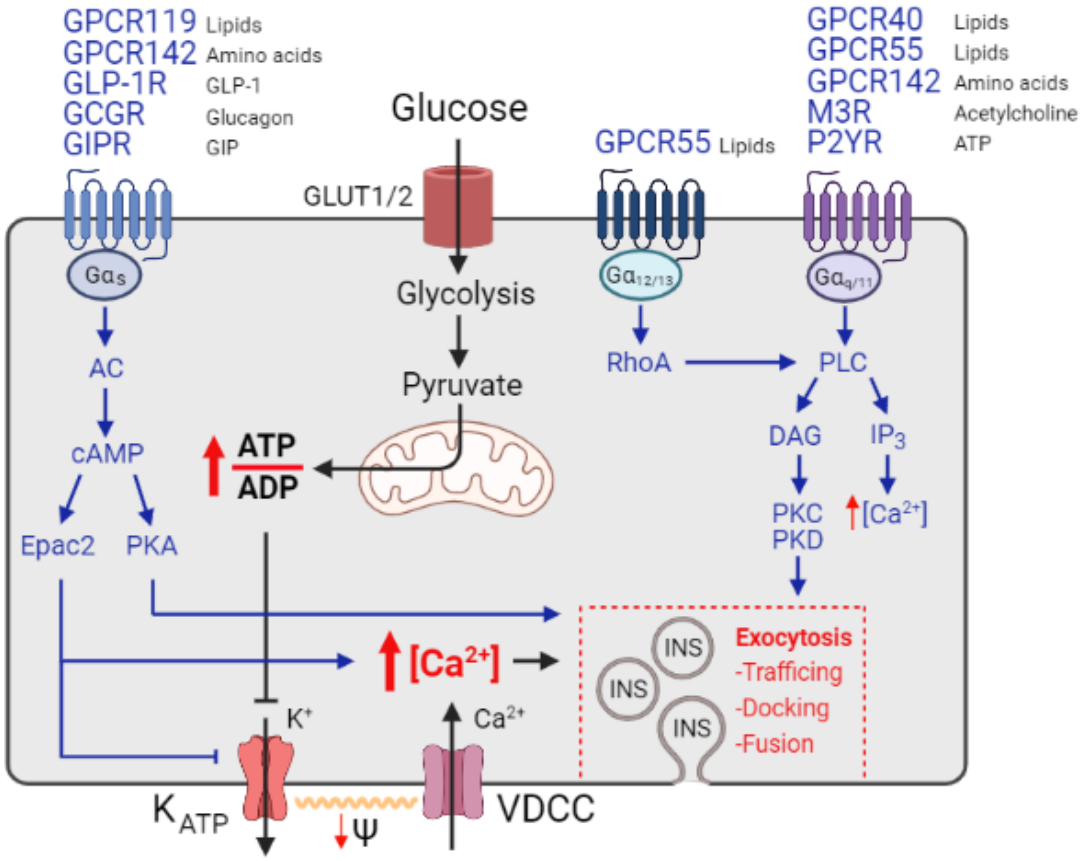

Figure 3: Potentiators of glucose-stimulated insulin secretion in β-cells. Different ligands bind to their respective receptors and stimulate insulin secretion through several signaling axes. $G\alpha_S$-dependent signaling results in elevated cAMP levels that activate *exchange protein directly activated by cAMP* (Epac)2 and PKA, thus strengthening the closure of K_{ATP}, elevating intracellular Ca^{2+} levels, and directly stimulating insulin granule exocytosis. Signaling through $G\alpha_{12/13}$ and $G\alpha_{q/11}$ mediates PLC-dependent DAG and IP_3 generation, finalizing in increasing intracellular Ca^{2+} levels and PKC and PKD-promoted exocytosis. (Created with BioRender.com)

Upon others, incretins are a prominent class of potentiators acting through the cAMP signaling pathway. GIP and GLP-1 are getting released upon glucose ingestion by enteroendocrine K cells and L cells, respectively[107,108]. By binding to their respective GIP or GLP-1 receptors, the receptors bind to a G-protein complex, mediating the release of the activated $G\alpha_s$ subunit, which activates plasma membrane-bound AC[109,110]. The resulting elevated cAMP levels activate PKA that augments *glucose-stimulated insulin secretion* (GSIS) by phosphorylating proteins involved in the exocytotic machinery[111]. Additionally, cAMP was shown to activate e*xchange protein directly activated by cAMP* (Epac)2, which promotes GSIS in a PKA-independent way.

This is mediated through several pathways including a change of action of K_{ATP} channels and activation of PLC-ε with the resulting release of intracellular Ca^{2+} sources[75]. Other hormones stimulate insulin secretion through the same signaling axis, as glucagon does by binding to GLP-1R or *glucagon receptor* (GCGR)[112]. On the other hand, the satiety hormone leptin primarily released by adipose tissue and enterocytes was shown to antagonize the cAMP-dependent stimulation of GSIS by activating PDE, which hydrolyzes cAMP[113].

Another molecule class executing potentiating effects on insulin secretion are lipids. They can either act intracellularly as metabolic coupling factors or extracellular by signaling through certain *G-protein coupled receptors* (GPCR)[114]. For the latter, GPCR40 (also called FFR1), which couples to the G protein subunit $G\alpha_{q/11}$, executes an important function in the acute stimulatory effect of FFAs on GSIS. It is predominately expressed in pancreatic β-cells and can be activated by mono- or poly-unsaturated, medium to long-chain fatty acids like α- and γ-linoleic acids, *arachidonic acid* (AA), *docosahexaenoic acid* (DHA), oleic acid, *lysophosphatidylcholine* (LPC), or *20-hydroxyeicosatetraenoic acid* (20-HETE)[115-117]. The binding of FFA induces PLC-mediated hydrolysis of PIP_2 into DAG and IP_3. The latter results in the release of intracellular Ca^{2+} stores, whereas DAG activates PKC, thus boosting GSIS[35,118]. In this context, agonism of GPCR40 also revealed a PKC-dependent opening of the *nonselective cation channel* (NSCC) of the *transient receptor potential* (TRP) channel class, which increases Ca^{2+} influx[119]. Similarly, also L-type VDCCs were demonstrated to be involved in FFA-amplified GSIS, however, the exact mechanisms remain unsolved[120]. DAG further activates PKD1, which mediates cortical F-actin reorganization resulting in granule recruitment[115,121]. GPCR40 signaling was also demonstrated to act through the impairment of voltage-gated K^+ channels, which usually open during glucose stimulation to induce repolarization with subsequent closure of VDCC. Thus, GPCR40 stimulation sustains $[Ca^{2+}]_i$ by delaying repolarization[122]. GPCR119 is another receptor mediating the potentiation of GSIS. It gets activated by *phospholipids* (PL)s and fatty acid amides like LPC, *platelet-activating factor* (PAF), *lyso-precursor of platelet-activating factor* (lysoPAF), N-oleoyldopamine, N-vanillyloleoylamide, or *oleoylethanolamide* (OEA)[123,124]. It is associated with the $G\alpha_s$, and thus executes its action through the elevation of cAMP

as described for incretins and others above[124,125]. GSIS can further be promoted through GPCR55, which is coupled to $G\alpha_q$ or $G\alpha_{12/13}$. Initially identified as a cannabinoid receptor, it can get activated by *tetrahidrocannabinol* (THC), but also by *L-α-lysophosphatidylinositol* (LPI), LPC, *2-arachidonoyglycerol* (2-AG), *N-arachidonoylethanolamine* (AEA), and *phosphatidylethanolamine* (PEA). Its signaling was shown to cause activation of PLC, Rho-associated protein, and ERK, thus leading to increased $[Ca^{2+}]_i$[117,126-130]. However, the cannabinoid receptors CB_1R and CB_2R get agonized by THC, AEA, and 2-AG as well, which is associated with inhibited insulin secretion. Both receptors signal through $G_{i/o}$ proteins leading to inhibited AC activation and respectively reduced cAMP levels[131-134]. Besides their function as signaling molecules, lipids were also demonstrated to contribute to exocytosis in a rather direct manner. *Monoacylglycerol* (MAG), which is generated during triacylglycerol catabolism upon glucose stimulation enhances insulin secretion by binding and thereby activating the vesicle priming protein munc13[135].

Of note, different lipid species involved in the enhancement of GSIS can derive from different origins. They were shown to be part of the nutritional supply, as treatment of rats with an antilipolytic agent abolished GSIS, whereas increasing endogenous FFA levels by inhibition of hepatic fatty acid oxidation stimulated GSIS[136]. On the other hand, β-cells release several lipid classes that stimulate insulin secretion in an autocrine fashion. Hence, it was shown that 20-HETE, acyl-CoAs, and glycerolipids like MAG are released by mouse and human islets during glucose stimulation and regulate insulin secretion[116,135,137].

In addition to autocrine factors belonging to the lipid class, β-cells release additional autocrine regulators of insulin secretion through the process of exocytosis. Released ATP was shown to bind to ATP-sensing GPCRs (P2Y receptors) or ATP-gated cation channels (P2X receptor channels), which directly, or indirectly through activation of PLC leads to inward currents of cations [7,138,139]. It is further known, that pancreatic β-cells release *γ-aminobutyric acid* (GABA), which can act in an autocrine manner[140,141]. Binding to ionotropic $GABA_A$ receptors enables efflux of Cl^- which contributes to depolarization and consequently insulin secretion in humans, but not in mice[140,142]. A similar insulinotropic and autocrine mechanism has been demonstrated to be mediated by serotonin and its different receptors present on β-cells[143,144].

Certain amino acids can stimulate insulin secretion as well. They do not only act through the induced release of incretins but also their metabolites. Leucine activates glutamate dehydrogenase, which converts glutamate, previously formed from glutamine in the cytosol, into α-ketoglutarate[145]. This in turn can enter the TCA cycle where it serves as a substrate for ATP production, thereby rising insulin secretion[146]. Both leucine and glutamine need to be present for this effect. However, as this pathway acts independently of present glucose concentrations, it can be considered an inducing mechanism for insulin secretion, rather than a potentiating one. Arginine, due to its cationic nature, can be taken up by CAT causing a depolarizing current that promotes GSIS[147]. Further, aromatic amino acids can act through GPCR142 of β-cells that is coupled to $G\alpha_q$ or $G\alpha_s$, hence stimulating GSIS through the PLC and AC axis[148,149].

Finally, neurotransmitters and neuropeptides from parasympathetic nerves, that innervate pancreatic islets, are capable to boost GSIS. When parasympathetic nerves get activated during the preabsorptive and absorptive phases of feeding, they release acetylcholine that binds to $G\alpha_q$-coupled muscarinic acetylcholine receptor M3 of β-cell receptors, thereby mediating PLC depending enhancement of insulin secretion[53,150]. This process is additionally stimulated through increasing levels of cAMP mediated by *pituitary adenylate cyclase-activating polypeptide* (PACAP), which is located in nerve endings within pancreatic islets and binds to the PAC1 receptor of β-cell[151,152].

1.2.3 β-Cell failure

Failure of pancreatic β-cells is the key mechanism that leads to the development of diabetes. The expansion of this disease has the dimensions of a pandemic, as approximately 451 million people worldwide had diabetes in 2017, and by 2045, that number is anticipated to rise to 693 million[153]. There are two main forms of diabetes existing, T1D and T2D, which differ in their development, but both result in hyperglycemia. The dysglycemic condition can be used to diagnose diabetes through various parameters. Commonly, it is defined as fasted blood glucose levels of ≥126 mg/dL, 2 h post-oral *glucose tolerance test* (GTT) levels of ≥200 mg/dL or

glycated *hemoglobin* (Hb)A1c levels of ≥ 6.5 %, however, values are considered higher in rodents (fasting glucose levels >250 mg/dL, depending on the strain)[22,154,155].

T1D is a chronic autoimmune disorder, that leads to the destruction of the β-cell mass of pancreatic islets. Of note, only 5-10 % of diabetic patients suffer from T1D. The development is complex and yet, not completely understood. However, there is a certain polygenetic susceptibility of developing T1D with additional environmental factors and activators that contribute to its pathogenesis[156]. Thus, first-degree relatives exhibit an 8-15-fold lifetime risk to develop T1D[157]. One major group of genetic determinators is related to class I/II *human leukocyte antigen* (HLA) alleles. HLA are surface receptors that present antigens to T-cells. Hence, mutations affect the repertoire and binding affinity of peptides that are presented to T-cells[158,159]. The resulting generation of β-cell targeted autoantibodies induces the autoimmune response, with the titer and specificity of the antibodies determining the progression of the disease[22]. This can be further triggered by certain environmental factors such as infections, dietary factors, and the composition of the intestinal microbiome[160]. In more than 90 % of T1D cases, patients exhibit autoantibodies directed against islet-enriched proteins such as proinsulin, g*lutamic acid decarboxylase* (GAD), *insulinoma-associated antigen* (IA)-2, *zinc transporter* (ZnT)8, or *tetraspanin* (Tspan)7, upon others[161]. However, more than 50 non-HLA loci have been identified in genome-wide association studies that were associated with increased risk of T1D, including insulin gene and variable number tandem repeat and other β-cell associated genes[162-164]. Thus, genetic mutations can lead to differential expression or post-translational modifications in the target cell compared to thymus, where negative T-cell selection takes place. Consequently, the immune system is not tolerant to respective variants, which promotes autoimmunity[165-167]. Additionally, several loci commonly mutated in T1D patients were shown to be involved in the regulation or suppression of T-cell activation or cytotoxicity, as it was shown in the case of lymphoid-specific phosphatase, *cytotoxic T-lymphocyte associated protein 4* (CTLA-4), or *interleukin-2 receptor subunit alpha* (IL2RA)[168-170]. Of note, the number and combination of these mutations, together with resulting autoantibody titers, age, and BMI defines the pathogenesis of T1D in patients[171-173]. A consequence of the above-mentioned pathological mechanisms is autoreactive T-cells that lead to insulitis, which is the

hallmark of T1D and describes an inflammatory lesion of pancreatic islets[174]. Due to the inflammatory environment, β-cells and other islet cells release cytokines like *interferon* (IFN)α, which further promote the recruitment of immune cells. Upon them are macrophages, which additionally induce pro-apoptotic signaling cascades, thereby accelerating β-cell destruction[175]. The inflammatory microenvironment also interferes with metabolic and electrical activity, gap junction coupling, and insulin granule production of β-cells[176,177]. All together culminates in a reduction of 70-80 % in β-cell mass and additional loss of glucose sensitivity of the remaining β-cells, both leading to insulin deficiency and associated hyperglycemia[178,179].

More than 90 % of all diabetic patients suffer from T2D. It is a chronic metabolic disease that derives from insufficient relative insulin amounts that are needed for maintaining normoglycemia. The cause for this is a combination of tissue insulin resistance, insufficient compensatory mechanisms, and resulting defective insulin secretion. The main driver for the development of T2D is insulin resistance, which is present in more than 80 % of the patients[180]. However, only genetically susceptible individuals, whose β-cells are not able to compensate for increasing insulin demands develop T2D[181]. Insulin resistance can arise from lipotoxicity. On one hand, saturated FFAs are cytotoxic for β-cells, as they inhibit proliferation, function, and induce apoptosis[182,183]. On the other hand, elevated plasma FFA and intracellular lipid levels inhibit insulin signaling in muscle cells, thus reducing their capability to uptake glucose from the blood leading to prolonged elevations in blood glucose levels[184-187]. As these conditions are commonly found in obese subjects, more than 85 % of T2D patients are overweight or obese, making obesity a critical risk factor for its development[188,189]. Resulting increased blood glucose levels can cause glucotoxicity with related inhibited insulin expression and irreversible β-cell damage and apoptosis due to *reactive oxygen species* (ROS) and related oxidative stress, as well as ER stress[190-193]. Also, hyperglycemia and hyperlipidemia together execute a glucolipotoxic effect on β-cells' functioning. Here, high glucose concentrations lead to increasing levels of malonyl CoA. This in turn inhibits *carnitine-palmitoyl-transferase* (CPT)-1, which transports FFA into mitochondria for energy generation. Respective accumulating levels of long-chain fatty acyl-CoAs are thought to directly act as lipid mediators or as their precursors, thereby interfering with β-cell functioning[194-196]. Another relevant aspect in

the development of T2D are inflammatory processes. Adipocytes can secrete hormones and cytokines, such as leptin, *tumor necrosis factor* (TNF)-α, *interleukin* (IL)-6, and IL-1, being elevated in obese subjects[197,198]. The endothelium and macrophages were found to contribute to increased levels as well[199]. These are linked with insulin resistance and further can induce an immune response[197,200,201]. The triggered innate immune system, together with the above-described apoptotic events, leads to inflammatory responses within pancreatic islets that can finalize in the development of autoimmunity against β-cell as observed in T1D[202-205]. Thus, chronic hyperglycemia and hyperlipidemia lead to inflammation and β-cell stress finally leading to dysfunction, atrophy, and in the later stage a reduction of β-cell mass of up to 50 %[206]. Due to the presence of insulin resistance, β-cells are not able to compensate for the increased insulin demand, which due to insulin deficiency puts the organism into a chronic hyperglycemic state[207].

Diabetes is one of the most often fatal diseases due to related dysglycemia, which raises the risk for several cardiovascular problems. Thus, microvascular and macrovascular complications lead to nephropathy, retinopathy, and neuropathy, or ischemic heart disease, cerebrovascular disease, and peripheral vascular disease, respectively. These complications result in functional and structural changes, finally culminating in tissue damage and multi-organ dysfunction in up to half of diabetic patients[208]. Nephropathy, retinopathy, and neuropathy arise from the disability of cells in the renal, retina, and nerve glomeruli to downregulate glucose uptake. Hence, in the presence of hyperglycemia increased metabolization of glucose leads to elevated levels of ROS in the mitochondria mediating oxidative stress[209]. Macrovascular issues are not unique to diabetes, but diabetic patients have an increased risk to develop atherosclerosis and to suffer from a macrovascular disease, therefore contributing to earlier mortality[210]. In this case, hyperglycemia is associated with oxidative stress damaging the endothelium[211]. It also leads to the non-enzymatic formation of *advanced glycation end products* (AGE) in plasma, vessel walls, and tissues and further promotes the synthesis of the extracellular matrix of endothelial cells[212,213]. Additionally, it promotes the death of endothelial cells and slows down their replication[214]. These structural and functional changes increase arterial stiffness and therefore systolic hypertension. Furthermore, monocytes and leucocytes are more

prone to transendothelial migration upon chronic hyperglycemia, and platelets were found to be hyperreactive in diabetic patients[215,216]. Together with increased levels of proinflammatory cytokines observed in diabetic individuals, this promotes the formation of atherosclerotic plaque[214,217]. All these events make diabetic patients two to four times more prone to develop cardiovascular diseases, making it the major cause of morbidity and mortality in these individuals[218-220].

1.3 Platelets

1.3.1 Platelet morphology and functions

Platelets are small anucleate cell fragments that are produced by *megakaryocytes* (MK)s in the bone marrow and primarily function as regulators of hemostasis. The average platelet count in humans ranges from 150-400 $x10^3$/µL, whereas mice typically exhibit a platelet count of about 1,100 $x10^3$/µL. With an average size of 4.7 fl in humans and 7.5-10 fl in mice, platelets represent the smallest component of the blood[221,222]. The lifespan of human and mouse platelets ranges from 7-10 days and 4-5 days, respectively[223,224]. The clearance of aged or activated platelets from the bloodstream occurs by the spleen and Kupffer cells in the liver, which detect markers of platelet activation or glycan modifications of surface proteins[225].

Due to the absence of genomic *deoxyribonucleic acid* (DNA) in platelets, *de novo* protein biosynthesis is restricted to MK-derived mRNA. As platelets exhibit translational machinery, they are capable to synthesize protein in a signal-dependent manner[226]. Different from red blood cells platelets contain mitochondria. They serve as a rapid and highly efficient source of energy during energy-demanding hemostatic events and further directly promote platelet activation by the generation of ROS[227,228]. Furthermore, platelets contain three major kinds of granules: α-granules, dense granules, and lysosomes. The most abundant are the α-granules (40-80 per platelet) which contain a large variety of proteins affecting adhesive properties (*von Willebrand Factor* (vWF), fibrinogen, fibronectin), coagulation factors (V, XI, and XIII), pro-inflammatory and immune-modulating factors, glycoproteins and mitogenic factors, such as *vascular endothelial growth factor* (VEGF), *platelet-derived growth factor* (PDGF), e*pidermal growth factor* (EGF)[229-233]. In contrast, dense granules (3-8 per platelet) contain smaller molecules such as ATP, ADP, serotonin, calcium,

pyrophosphate, and polyphosphate. They act as a positive feedback mechanism on hemostatic events, thereby amplifying primary hemostasis[234,235]. Lysosomes store mainly hydrolytic enzymes to execute several extracellular processes like receptor cleavage, degradation of extracellular matrix components, remodeling of thrombus and vasculature as well as apoptosis and necrosis[231,236-238]. Additionally, platelets contain two membrane systems: the *open canalicular system* (OCS) and the *dense tubular system* (DTS). The latter serves primarily as a Ca^{2+} reservoir, whereas the OCS is involved in the uptake of molecules and granule release as well as serving as a membrane reservoir during activation-mediated shape change of the platelet[231,239].

The primary function of platelets is the mediation of hemostasis to stop and prevent bleeding events. Because they are involved in the entire hemostatic process, including vasoconstriction, platelet plug formation, and clot formation, they are irreplaceable in maintaining vascular integrity[240]. In recent years, however, there has been increasing recognition that platelets perform much broader physiological functions. Thus, it was shown that platelets promote metastasis and protect tumor cells from the innate immune system thereby accelerating cancer progression[241,242]. In addition, interactions between platelets and leukocytes have led to a closer examination of the function of platelets in the context of immune defense. Thus, activated platelets express P-selectin on their cell surface, facilitating leucocytes to bind via the *P-selectin glycoprotein ligand-1* (PSGL-1) to enable retainment at extravasation sites and tissue infiltration[243]. A similar effect has been observed between the high-affinity conformation of the integrin αIIbβ3 receptor, crosslinking with fibrinogen, and the integrin *macrophage-1 antigen* (Mac-1) of neutrophils[244]. Further, platelets contribute to innate immunity by their ability to bind and bundle bacteria in order to trap them or present them to phagocytes[245,246]. Finally, several proangiogenic factors like VEGF and anti-angiogenic factors like *platelet factor* (PF)4 are stored and released by platelets, which makes them relevant modulators of angiogenesis and neovascularization[247-249]. Of note, platelet function can change due to the progression of various diseases. For example, diabetic patients often possess hyperreactive platelets, whereas others such as virus-mediated diseases can lead to hypo-responsiveness[250-252].

1.3.2 Mechanism of hemostasis

Under regular physiological conditions, platelets do not come in direct contact with the ECM and therefore remain inactivated for their whole life span. However, during vascular injury, the cascade of thrombus formation gets induced to stop bleeding events and generate an environment favorable for wound healing. This whole process requires three major steps, that need to be well coordinated in terms of time and place. First, platelets bind to the exposed ECM creating a monolayer of activated platelets. In the second step, these platelets recruit additional platelets through a local release of major platelet agonists. Finally, cross-linking of the platelets forms a stable blood clot enabling further wound-healing processes (Figure 4)[253].

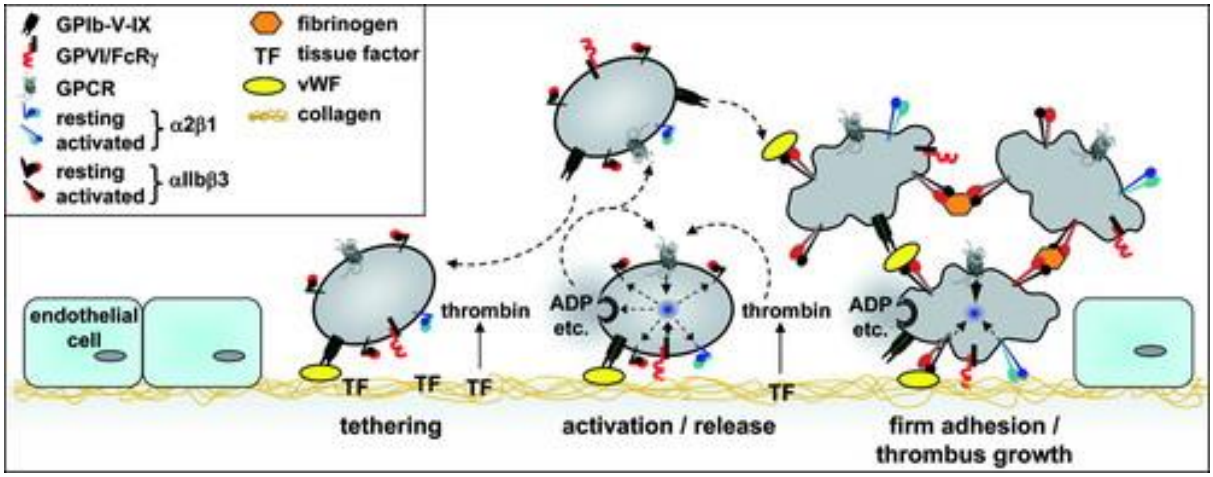

Figure 4: Schematic mechanism of thrombus formation on ECM. Platelets bind to exposed ECM by the interaction of GPIb-V-IX with collagen-bound vWF. Initial tethering allows GPVI to directly bind to collagen triggering platelet activation, which is characterized by the release of second-wave mediators such as ADP and *thromboxane* $(Tx)A_2$ as well as functional upregulation of the integrin αIIbβ3. Thrombin, which is locally generated by exposed TF, together with released mediators triggers the activation of additional platelets and recruitment to the growing thrombus. Finally, integrins bind to ECM components, fibrinogen, and vWF, thereby crosslinking platelets and causing firm adhesion. (taken from Varga-Szabo et al., 2008)[254]

The initial tethering of platelets to the site of injury is depending on the GPIb-V-IX complex, which consists of a GPIbα subunit linked to two molecules of GPIbβ, and non-covalently linked GPIX and GPV in a 2:4:2:1 ratio[255]. The GPIbα subunit binds to immobilized vWF on the surface of the endothelium or in the subendothelial matrix, which is a multimeric adhesive protein secreted from activated platelets and endothelial cells[256]. This initial tethering is transient, but it retains the platelet close to the vessel wall allowing further activation processes. These are initiated by the binding of the platelet GPVI receptor to the collagens of the ECM. GPVI induces platelet

activation by intracellular signaling processes via an *immunoreceptor tyrosine-based activation motif* (ITAM) in the associated *Fc receptor* (FcR) γ-chain, which triggers intracellular signaling events mediating platelet degranulation, integrin activation, and shape change of platelets[257]. Consequently, dense granule-derived ADP as well as synthesized t*hromboxane* (Tx)A_2 activate surrounding platelets, thereby amplifying the hemostatic event by positive feedback signaling[258]. Thrombin, which gets generated at the site of injury due to the action of the *tissue factor* (TF) contributes to this effect[259]. Further, adhesive molecules such as vWF or fibrinogen are released by α-granules and promote thrombus formation. In addition, this degranulation process leads to the translocation of receptors such as GPVI, P-selectin, or integrins into the platelet plasma membrane, thereby amplifying platelet aggregation[260]. All signaling pathways resulting in platelet activation converge in the last common event, namely integrin activation. Integrins are heterodimeric transmembrane receptors that consist of α- and β-subunits and mediate cell-cell and cell-matrix interactions[261]. Thereby, they play a critical role in converting the transient binding of platelets into stable adhesion. To do so, they need to undergo a conformational change from their resting state to a state of high affinity to their natural ligands. This event is referred to as inside-out signaling and is induced to a small extent by binding of GPIb to vWF but is mainly promoted by GPVI activation with an enhancing action of released soluble mediators such as ADP and Tx, and at the site of injury generated thrombin[257,262]. Platelet membranes include five different integrins exhibiting high binding affinities to different ECM components like collagen, fibronectin, laminin, and vitronectin[263-266]. However, the most abundant and relevant integrin for firm adhesion and crosslinking of platelets is αIIbβ3 integrin with the ability to bind to fibrinogen, vWF, fibronectin, thrombospondin, vitronectin, and further yet unidentified ligands[267-270]. In the last step, thrombin converts fibrinogen into fibrin monomers, which upon crosslinking turn into an insoluble fibrin clot that ultimately closes the injury[271].

1.3.3 Platelet signaling

The mechanism of hemostasis needs to be tightly regulated, to ensure a rapid stop of bleeding events, but avoid undesired thrombus formation. To meet these requirements, hemostasis is regulated by finely tuned signaling pathways. In principle, platelets get activated through two different kinds of signaling pathways. On the one

hand, surface receptors bind directly or indirectly to components of the ECM, thereby inducing intracellular signaling leading to platelet activation. On the other hand, released soluble second mediators bind to different GPCRs triggering activation through additional pathways. Both of these events get integrated through the two central mediator families PLC and *phosphoinositide 3 kinase* (PI3K), which finally leads to an increased concentration of cytosolic Ca^{2+}. Ca^{2+} acts as a second messenger essential for the three key events of platelet activation: induction of degranulation, integrin activation, and change to a more reactive cell shape (Figure 5)[272,273].

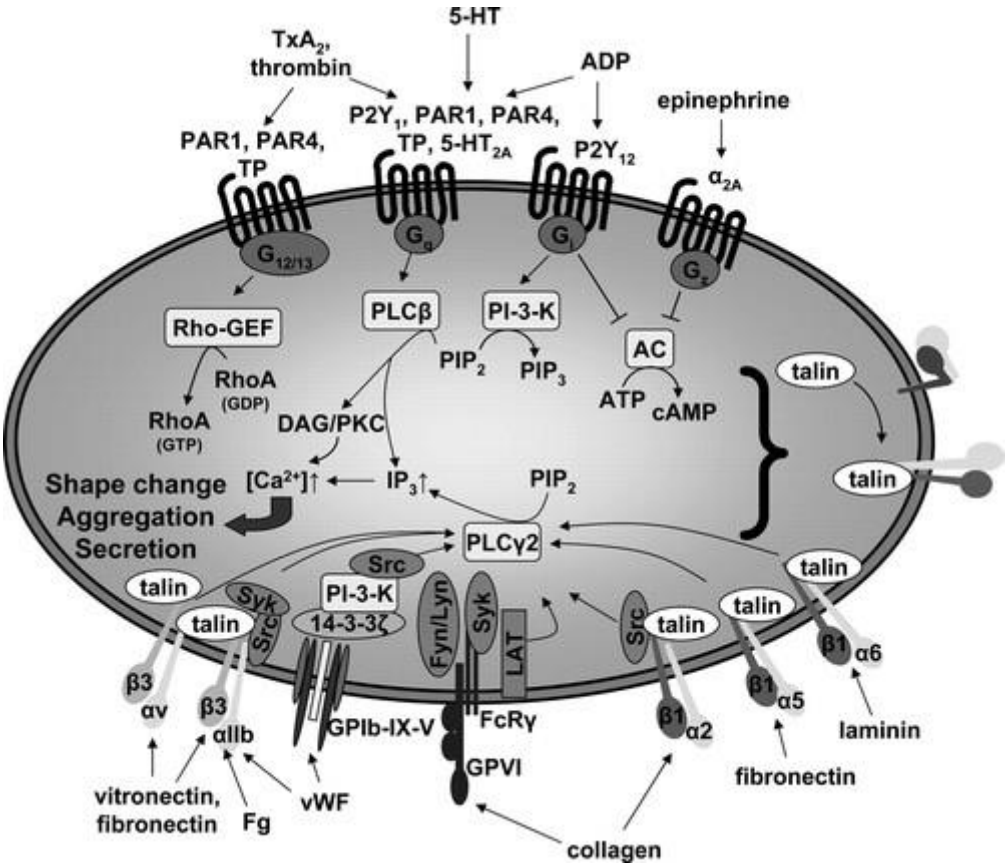

Figure 5: Signaling events regulating platelet activation. Soluble factors like *thromboxane* $(Tx)A_2$, thrombin, ADP, and serotonin signal through GPCR that are associated with $G_{12/13}$, G_q, G_i, or G_z leading to activation of Rho GTPase, PLCβ, PI3K, or inhibition of AC. Ligand binding of adhesion receptors such as GPVI and activated integrins activate PLCγ2. RhoA induces rearrangement of the cytoskeleton, whereas PLC catalyzes the formation of DAG and IP_3, which results in increasing intracellular Ca^{2+} levels that is essential for aggregation, granule secretion, and shape change. (taken from Varga-Szabo et al., 2008)[254]

Adhesion receptors bearing ITAM signal through the PLCγ2 axis. Crosslinking of GPVI by agonists causes Src kinase (Fyn, Lyn) mediated tyrosine phosphorylation of ITAM,

resulting in recruitment and activation of Syk kinase[274]. This in turn triggers a signaling cascade including LAT and several other adaptors and effector proteins leading to an upregulation of PLCγ2 activity[275,276]. Similarly, upon clustering integrin αIIbβ3 activates PLCγ2 by the sequential activation of Scr and Syk tyrosine kinases[277]. The signaling machinery of integrin αIIbβ3 is shared with other platelet integrins. However, their function in outside-in signaling remains unclear due to their relatively low expression levels[278]. On the other hand, activation of PLCβ is induced by soluble secondary mediators acting through Gq-coupled GPCRs such as the ADP receptor P2Y1, thrombin *protease-activated receptor* (PAR)1 and 4 in humans (3 and 4 in mice), TxA_2 receptor TP or *5-hydroxytryptamine* (5HT or serotonin) receptor 5HT-A_2. Both PLC isoforms mediate the cleavage of PIP_2 into DAG, which activates PKC, and IP_3. IP_3 induces Ca^{2+} influx into the cytosol by activating IP_3 receptors on the DTS, whereas substrates of different PKC isoforms are involved in integrin activation, degranulation mechanisms, and cytoskeleton rearrangement[279,280]. Additionally, ADP acts also through the G_i-coupled $P2Y_{12}$ receptor, causing activation of PI3K, which catalyzes the conversion of PIP_2 into the secondary messenger *phosphatidylinositol (3,4,5)-trisphosphate* (PIP_3). This interacts with the *pleckstrin homology* (PH) domain of PLCγ2 facilitating its recruitment to the plasma membrane and activation, which induces *protein kinase B* (Akt)-dependent signaling that prompts granule secretion through phosphorylation of *soluble N-ethylmaleimide-sensitive-factor attachment receptor* (SNARE) proteins[281-284]. One essential signaling axis particularly involved in the mediation of platelet shape change depends on the small GTPase Rho, which is downstream of $G_{12/13}$ and activates MLC kinase. Hereby, phosphorylation of MLC induces cytoskeletal reorganization and increases actomyosin contractility[285,286]. The epinephrine receptor (α2) in platelets is coupled to G_z, which is another G_i subtype[287]. Besides regulators of platelet activation, there are a few inhibitory mechanisms that ensure platelet circulation in a resting state. *Nitric oxide* (NO) and *prostaglandin* (PG)I_2 are released by intact vascular endothelial cells and increase intracellular levels of *cyclic guanosine monophosphate* (cGMP) and cAMP by activation of soluble g*uanylate cyclase* (GC) and a*denylyl cyclase* (AC), respectively. The resulting activation of PKG and PKA suppresses several key nodes in pro-thrombotic platelet signaling such as calcium release as well as calcium-independent mechanisms[288-291].

1.4 Platelet lipidomics

Lipids play essential structural, signaling, and metabolic roles in platelets. Upon platelet activation, different lipid species regulate intracellular signaling and further affect surrounding cells to control hemostasis and thrombosis-related processes. Thus, lipidome analysis revealed the presence of about 8000 different lipids in healthy human platelets[292]. Of note, only 15 lipids comprise 70 % of the lipidome in resting platelets, whereas less than 20 % of the lipidome changes upon activation with thrombin or c*ollagen-related peptide* (CRP), involving mainly lipids containing arachidonic acid. Further, from the 15 most abundant lipids only PIs change significantly after activation, as most of the lipids that change during activation are of low abundance[293].

As described in the previous chapter, DAG, IP_3, and PIs are PLC and PI3K-derived lipids produced during platelet activation that play important roles as signaling molecules governing PKC activation, calcium mobilization, and integrin activation, which are all fundamental processes regulating platelet function[279,281]. In addition, activated platelets reveal *phospholipids* (PL)s like *phosphatidylserine* (PS), which are part of the platelet plasma membrane, providing the necessary negatively charged platform for the formation of the coagulation complex[294]. Besides PLC and PI3K, $cPLA_2$ is one key player in thrombin-stimulated platelets, that generates numerous lipid species by hydrolysis of the sn-2 bond of PLs, generating lyso-PL and FA like AA, palmitic acid, linoleic acid, and stearic acid[295]. These provide mitochondria with substrates for energy generation and hence play an important role in platelet activation and procoagulant function[292]. As some of the $cPLA_2$ isoforms require Ca^{2+} for translocation to the membrane, they exhibit an increased catalytic activity upon platelet activation[296,297]. Further, the $cPLA_2$-mediated release of AA, which makes up to 25 % of glycerophospholipids of the platelet plasma membrane, serves as an important precursor for oxidative transformation to several eicosanoids essential for numerous signaling events[298]. *Cyclooxygenase* (COX)-1 converts AA into PGG_2, and further to PGH_2, which undergoes additional modification by Tx synthase, PGD isomerase, or PGE synthase to finally generate TxA_2, PGD_2, or PGE_2, respectively[298,299]. In expansion to the high variety of prostaglandins, COX1 can also mediate the synthesis of 11-HETE and 15-HETE[300]. Another important branch of AA modification besides COX is mediated by *lipoxygenase* (LOX). Depending on the isoform, LOX oxidizes AA

by the addition of a hydroperoxyl group at a certain carbon thus generating oxylipins. A very abundant one in platelets is 12-LOX, which adds oxygen preferentially at position C-12 of AA, thereby generating 12(S)HpETE, which is reduced due to the reducing conditions in platelets to its hydroxyl derivative 12-HETE[301]. Hereby, not only AA was shown to be a substrate of 12-LOX, but other FA like e*icosapentaenoic acid* (EPA), d*ocosahexaenoic acid* (DHA), and *α-Linolenic acid* (ALA) were demonstrated to be oxidized by this enzyme to oxylipins as well[302,303]. In addition to 12-LOX, products of 15-LOX were detected in human platelets[304,305]. The third important AA modifying mechanism is mediated by c*ytochrome* (CY)P450. Different isozymes exhibit a hydroxylase or epoxygenase activity, leading to the formation of 19-HETE and 20-HETE or *epoxyeicosatrienoic acids* (EET), respectively[306-309]. It has been shown, that CYP450 products are integral components of the human platelet membrane, which can be released upon receptor-mediated de-esterification of phospholipids[310]. Due to their presence in the plasma membrane, it is understood that CYP450 products might also be actively taken up by platelets and integrated into the membrane to be released during activation[303,306,311]. However, platelets exhibit the CYP450 enzymatic machinery to synthesize these products independently[309]. Of note, products of COX-1-, LOX-, and CYP450-dependent biosynthesis can later be re-esterified into phospholipids like *phosphatidylethanolamine* (PE) by *fatty acyl Co-A ligases* (FACL)[312,313].

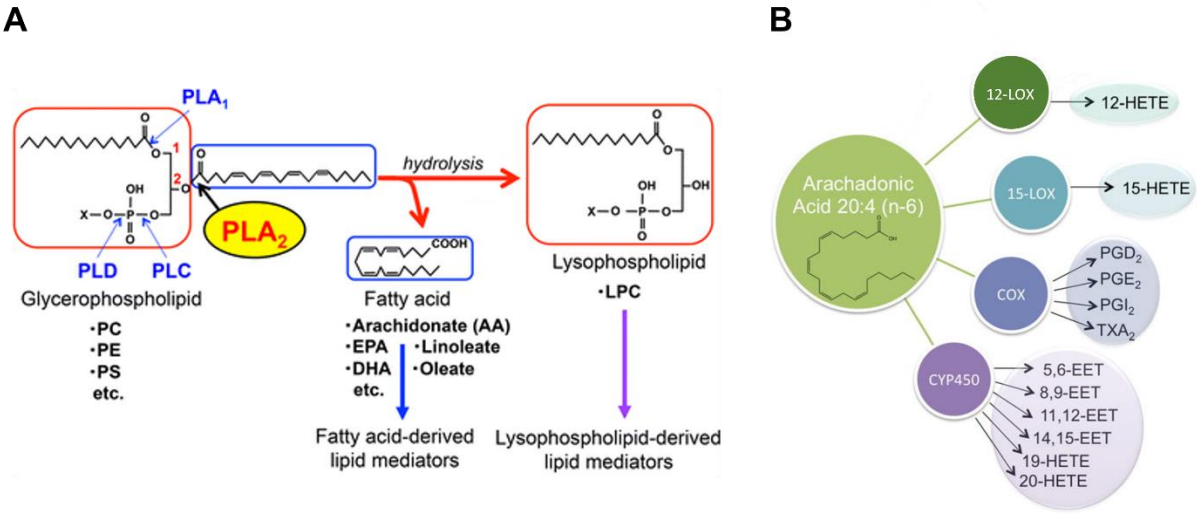

Figure 6: Lipidomics in platelets. (**A**) Hydrolyzation sites of PLA_1, PLA_2, PLC, and PLD of phospholipids. PLA_2 hydrolyzation at position sn-2 yields FA and lyso-PL, which can be further metabolized to other lipid mediators (taken from Sato et al., 2016)[314]. (**B**) AA-derived oxylipins generated by LOX, COX, and CYP450 mediated oxidation (modified from Yeung et al., 2017)[303].

In addition to numerous AA-depending products, platelets contain a high variety of additional lipids and PL. Lyso-PL, including *lysophosphatidylcholine* (LPC), *lysophosphatidylethanolamine* (LPE), *L-α-lysophosphatidylinositol* (LPI), and *lysophosphatidylserine* (LPS), arise through the action of PLA_1, PLA_2, and PLD, or phosphorylation of 1,2-diacylglycerol[315,316]. LPC can be converted into PAF, which is an important signaling molecule, by the addition of an acetyl group mediated by LPC-acetyltransferase[317]. Sphingolipids form another lipid class and are built of a sphingoid base backbone, which in the case of ceramide contains sphingosine and a FA. Their function is associated with membrane dynamics, but they also execute intracellular signaling, even though their exact function in platelets remains uncertain[318]. Further, sphingosine can get phosphorylated by sphingosine kinase 1 and 2 resulting in *sphingosine-1-phosphate* (S1P), which can induce several signaling events through GPCRs[319-323].

Bioactive lipids can act in an autocrine and paracrine manner and regulate a high variety of processes. Prostanoids and oxylipins can diffuse through plasma membranes to act on respective receptors[324,325]. By binding to GPCR they can modulate intracellular signaling in an auto- and paracrine manner[312,326]. Products of COX have been identified a long time ago as platelet effectors and many of their signaling axes are well understood. TxA_2 activates platelets through the TP receptor, whereas several prostaglandins, like PGD_2 and PGI_2, inhibit platelet activation through prostaglandin and prostacyclin receptors, as well as through the *peroxisome proliferator-activated receptor* (PPAR)[327,328]. Others, such as PGE_2, execute opposite actions. It can be pro- (low dose) or anti-aggregatory by acting through PGE_2 receptor EP3 or prostacyclin receptor IP, respectively[329]. The same counts for different oxylipins, for example, different products of 12-LOX can execute pro- and anti-thrombotic effects[302,330]. The high variety of LOX products is less understood in their function. Some are known to agonize or antagonize platelet receptors, as 19-HETE activates the prostacyclin receptor, whereas 12-HETE prevents binding of PGH_2 and TxA_2 to their respective receptors, thus inhibiting platelet activation[331-334]. They can also activate PPAR, thereby regulating gene expression of other cell types[335,336]. Furthermore, generated oxylipins are able to directly inhibit further oxylipin production

or metabolic transformation of lipids, hence affecting platelet functioning[303]. Products of CYP450 consistently execute anti-thrombotic effects, however, different products were demonstrated to either cause vasoconstriction or vasodilation[331,337,338]. Some lipid species are thought to execute their function from the plasma membrane. For instance, oxidized phospholipids, like PG-PE, are anchored by the sn1 FA into the membrane, allowing to signal through receptors of other cells[339]. Other lipids species like S1P can get stored and released by degranulation. In the case of S1P, it has been evidenced that it gets released from α-granules during platelet activation and regulates several physiological processes through GPCRs like vascular integrity, angiogenesis, cell migration, maturation, and differentiation[340,341].

1.5 Changes in platelets during aging

Platelets from individuals of advancing age undergo several changes at molecular and cellular levels. Resulting differences in platelet function and structure are associated with altered platelet behavior that can lead to different pathophysiological conditions. A well-investigated characteristic of platelets from aged individuals is hyperreactivity, associated with decreasing bleeding times and faster clot formation[342,343]. Higher reactivity is known to arise from increased susceptibility to agonist-induced platelet aggregation since elderly individuals show lower threshold concentrations for platelet activation after ADP, epinephrine, collagen, or arachidonic acid stimulation[344-347]. The resulting hypersensitivity was demonstrated to increase by about 8 % per decade of age, as derived from a dose of ADP at which primary aggregation occurred at half its maximum rate from a cohort of 958 patients[348]. Of note, the aggregability was demonstrated to be generally more elevated in aged women than in aged men[345,348]. Until now, the exact underlying mechanism that is responsible for age-related platelet hyperactivity is not understood. Studies by Bastyr et al. measured an increased basal and stimulated phosphoinositide turnover in platelets of aged subjects, which positively correlated with platelet aggregation and levels of plasma β-thromboglobulin. As phosphoinositide turnover is linked to stimulus-coupled platelet activation, it is possible that the increased basal and stimulated phosphoinositide turnover contributes to the rise in platelet activity with age[349]. Other studies attribute the changes to functional or expressional changes in platelet α-adrenoreceptors, which

enhance platelet aggregation by binding with epinephrine. However, these findings are inconclusive, as some studies reported an increase in α-adrenoreceptor binding capacity in platelets of aged subjects without a change in binding affinity whereas other studies showed a decrease in α-adrenoreceptor binding capacity[344,350,351]. Results from another investigation indicated decreased affinity of the aggregation inhibiting β-adrenoreceptor but no change in binding capacity in elderlies[352]. Also, serotonin, which is an enhancer of epinephrine- and ADP-induced activation, was shown to be more potent on platelets in terms of sensitivity and responsiveness in 72-86 years old subjects compared to 18-27 years old ones[353,354]. On the other hand, age-related declines in platelet serotonin content were observed[354,355]. The same findings were made in patients suffering from diabetes or peripheral vascular diseases which were further associated with elevated plasma serotonin levels. Together, this allows the hypothesis, that platelet hyperactivity can lead to increased serotonin release further promoting platelet hyperactivity[354]. In general, RNA-sequencing of platelets derived from <45 years and >64 years old subjects revealed altered expression of 514 genes[356]. A similar observation has been made regarding age-related changes of the proteome, which allows the assumption that changes of the transcriptome might contribute to hyperactivation with age[357]. Also senescence, which is characterized by persistent hyporeplicative cells and an altered secretome consisting of inflammatory cytokines, growth factors, and proteases, is one prominent age-related alteration that is thought to affect platelet functioning[358,359].

Another relevant factor influencing platelet functionality is oxidative stress and resulting ROS, which are known to rise along with the aging process in both humans and animals[360,361]. ROS have been proven to increase the risk of cardiovascular events through different mechanisms. They can act as a second messenger or lead to oxidized proteins thereby promoting platelet aggregation[362]. With increasing age, free radicals promote the carbonylation of proteins in platelets with even more pronounced effects in diabetic patients of the same age, which might cause a thinkable contribution to platelet dysfunction[363,364]. ROS can also directly or indirectly by activation of platelet membrane protein disulfide isomerase promote the formation of disulfide bonds[365,366]. This can lead to the activation of several integrins like αIIbβ3 or α2β1 due to disulfide bond isomerization[365,367-369]. In accordance with this, H_2O_2

production in platelets of aged mice was increased upon stimulation, but catalytic degradation of it resulted in a complete loss of age-dependent platelet hyperactivation. The origin of increased H_2O_2 generation was claimed to be due to an upregulated NADPH oxidase dismutase pathway in 18-month-old mice[370]. Another result is an increased lipid peroxide membrane composition causing lipid-protein interactions that decrease membrane fluidity[371]. This is further promoted by additional age-related compositional changes of the membrane, like increased amounts of cholesterol[372]. Of note, altered structures of the platelet membrane were associated with increased sensitivity to agonist-induced aggregation[373,374].

Also, inhibitory pathways of platelets are altered in the process of aging. GC, which is activated by NO and consequently generates cGMP leading to reduced intracellular free calcium levels has been shown to have reduced activity in elderly men (mean age of 51 years) compared to younger ones (mean age of 29 years)[361,375,376]. Other studies confirmed an inverse correlation between age and platelet cGMP levels, strengthening the theory of a disturbed NO/GC/cGMP inhibitory mechanism with age[377,378]. Isolated endothelial cells from elderlies displayed reduced production of prostacyclin an NO, potentially contributing to platelet hyperaggregability[379,380]. Surprisingly, platelet *nitric oxide synthase* (NOS) was demonstrated to have increased activity in elderly humans and rats[377,381]. This contradictory finding was explained by the fact that NO can lead to the generation of oxidative species such as $ONOO^-$ that might inhibit GC activity[377]. In addition to the latter mentioned inhibitory axis, also receptors of PGI_2, a negative regulator of platelet function, are known to be less present on the platelets of aged individual[382].

With age, not only the platelets themselves change, but also their natural environment. The vasculature undergoes several changes upon aging due to increasing oxidative stress, impaired proteostasis, genomic instability, and cellular senescence upon others, which leads to inflammatory events finally resulting in atherosclerosis[383-388]. Kurabayashi et al. investigated platelet activity in the context of atherosclerosis. They investigated the platelet state determined by shape change and peroxidase content of young and old individuals with or without atherosclerosis. Interestingly, they found no significant differences between young and old subjects, however, the platelets from

elderly patients with atherosclerosis were identified to be more often in an activated state[389]. Despite the limited sample size, they highlight a crucial aspect by speculating as to whether platelet hyperactivity in the elderly is brought on by aging or by the concurrent beginning of an atherosclerotic state. Furthermore, plasma composition changes in the process of aging, as elderly subjects were shown to exhibit significantly elevated plasma levels of β-thromboglobulin and PF4. As these proteins are specifically released from platelet granules, this goes in line with age-related hyperaggregability and gives evidence for enhanced platelet secretion events *in vivo*[349,390]. On the other hand, PF4 is known to have a procoagulant effect, hence possibly exerting its effect on platelets and further promoting hyperaggregation[391,392]. In this context, also plasma concentrations and activities of other coagulation factors like fibrinogen, vWF, and factors V, VII, VIII, and IX have been shown to be elevated during the physiological process of aging[393-395].

Despite changes in platelets themselves, it has been shown that platelet count is inversely associated with age. Studies with a cohort of more than 12,000 subjects revealed a significant decrease in platelet counts of 7 x 10^3/µL in 60-69 years old subjects, and 18 x 10^3/µL in 70-90 years old subjects compared to young 20-59 years old individuals. This effect was still present after adjustment of various covariates like medication, illnesses, nutritional deficiencies, or consumption of alcohol and tobacco, indicating that age-related changes in platelet count are at least partially due to a systemic biological aging process[396]. The same inverse correlation has been demonstrated by other studies, which additionally pointed out significantly elevated platelet counts in older women compared to men of the same age[397,398]. However, the mechanistic origin causing this observation remains unknown. It is thought, that lower stem cell reserve in elderly subjects might lead to this phenotype. Further, reduced platelet counts might lead to a biological advantage causing better chances to reach an older age for subjects fulfilling this feature[396].

Finally, platelet precursor cells, MKs, also contribute to age-related platelet changes. Here, senescence, which is characterized by persistent hyporeplicative cells and an altered secretome consisting of inflammatory cytokines, growth factors, and proteases, is one prominent age-related alteration that is thought to affect platelet

functioning[358,359]. Released inflammatory mediators such as IL6 were suggested to affect thrombopoiesis resulting in platelets with a more thrombotic phenotype and a higher platelet volume[399]. Similarly, the pro-inflammatory cytokine TNF-α was shown to promote metabolic reprogramming of MKs, mitochondrial dysfunction of platelets, and hyperreactivity with increasing age of humans and mice[400]. In the same study, they further found through transcriptome analysis, that *aldehyde dehydrogenase* (ALDH)-1A and the pentose phosphate pathway were highly upregulated in older mouse MKs. As these contribute to cellular detoxification, the authors suggest a compensatory mechanism by which aged megakaryocytes and platelets aim to reduce oxidative stress, which contributes to increased reactivity of platelets[400].

1.6 Aim of the study

Platelets of diabetic patients are commonly associated with increased reactivity and basal activation[250,251]. They further possess a highly diverse secretome containing several insulinotropic substances like purines, serotonin, histamine, and lipids, thus potentially affecting β-cell functioning[114,138,139,234,315,316,401-404]. For this reason, their contribution to glucose homeostasis was investigated in this work. First, the response of platelets to hyperglycemic stimuli was investigated by flow cytometry, flow adhesion assay, and *in vivo.* Additionally, the behavior of platelets within the microvasculature of pancreatic islets was investigated using *in vivo* imaging and classic histological approaches. To study their effect on glucose homeostasis, various genetic and pharmacological mouse models were used that exhibit defective platelet adhesion, activation, degranulation, or platelet deficiency. Furthermore, *in vitro* β-cell models together with biochemical and lipidomic approaches were performed to determine specific platelet-derived factors that stimulate insulin secretion. The action of these factors was evaluated *in vivo* and *in vitro* by modulating the proposed signaling pathways. Finally, not only a direct effect of platelets on β-cells was studied, but also their influence on the islet vasculature.

2 MATERIALS AND METHODS

2.1 Materials

2.1.1 Equipment

Table 1: List of used equipment.

Equipment	Specification	Manufacturer
Animal ear punch	2 mm	Fine Science Tools
Autoclave	VX-120	Systec
Autoclave sterilizer	DX-100	Systec
Bench-top homogenizer	PT 1600E	Polytron
Camera	CoolSNAP-EZ	Visitron
Centrifuge	5415C	Eppendorf
Centrifuge	5424 R	Eppendorf
Centrifuge	5810 R; rotor: A-4-62	Eppendorf
Confocal microscope	TCS SP8	Leica
Dionex Ultimate 3000 UHPLC system	Q exactive mass spectrometer equipped with a heated electrospray probe	Thermo Fisher Scientific
Flow cytometer	Celesta	(BD Biosciences
Freezer (-20°C)	Profi line GG4310	Liebherr
Freezer (-20°C)	Comfort	Liebherr
Freezer (-80°C)	HERAfreeze HFU666 basic	Thermo Fisher Scientific
Freezing chamber		Thermo Fisher Scientific
Fridge	profi line FKS5000	Liebherr
Fridge-freezer	CP3523-21	Liebherr
Glass bottles	2000 mL; 1000 mL; 500 mL; 250 mL; 100 mL	Duran
Hematology Analyzer	KX-21N	Sysmex
Hematology Analyzer	ScilVet	Scil animal care company GmbH
HPLC column	Acclaim 120 C8 (3 µm particles, 100 × 2.1 mm)	Thermo Fisher Scientific
Hydrophobic pen; Roti®-Liquid barrier marker	AN91.1	Roth
Ice machine		Ziegra
Imager for Gels	Typhoon TRIO	GE Healthcare

Equipment	Specification	Manufacturer
Imager for Proteins	Amersham Imager 600	GE Healthcare
Incubator	C150	Binder
Incubator	Heracell 240	Heraeus
Inverted microscope	CKX31	Olympus
Inverted microscope	IX71	Olympus
Inverted microscope	Axiovert 200	Zeiss
Laminar flow cabinet	SB-1200	BDK Luft- und Reinraumtechnik
Magnetic stirrer	MR Hei-Standard	Heidolph
Mechanical piece counter	T120	IVO
Mice cage	GM500PFS; lid: for water bottles; water bottle: 300 mL; lid: full length	Tecniplast
Mice cage rack system	Green Line IVC	Tecniplast
Microm Cool Cut microtome		Thermo Scientific
Microcentrifuge	Galaxy Ministar	VWR
Microscope	DMI6000B	Leica
Microwave		Dynamic
MilliQ water purification system	X-CAD	Millipore
Multi-channel pipette	Transferpette S12 (20 – 200 µL)	Brand
Multimode microplate reader	Spark™ 10M	TECAN
Multiplex ELISA reader	Bio-Plex® MAGPIX™ Multiplex reader	Bio-Rad
Neubauer chamber	0.1 mm Depth	Hecht-Assistant
Nitrogen cell storage tank	Cryosytem 4000	MVE
Nitrogen storage tank	Cryotherm	Apollo
Nuclear magnetic resonance (NMR) analyzer	The minispec LF50	Bruker
Orbitrap analyzer	Orbitrap LC-MS	Thermo Fisher Scientific
Orbitrap fusion	Orbitrap Fusion™ Tribrid™ Mass spectrometer	Thermo Fisher Scientific
pH-meter	FiveEasy	Mettler Toledo
Pipette	Transferpette S (0.5 – 10 µL)	Brand
Pipette Boy		Gilson
Pipette controller	Accu-Jet Pro	Brand
Power supply	PowerPac HC	Bio-Rad

Equipment	Specification	Manufacturer
Real-time PCR system	QuantStudio 5 real-time PCR system	Thermo Fisher Scientific
Repetitive pipet	Repetman	Gilson
Scissors (micro)	Spiky; 8.5 cm	Fine Science Tools
Scissors (standard)	Blunt; 13 cm	Fine Science Tools
Scissors (tissue)	Spiky; 10.5 cm	Fine Science Tools
Thermal cycler	T100	Bio-Rad
Thermal cycler	7900HT Fast Real Time PCR	Thermo Fisher Scientific
Thermo block	Thermomixer Comfort	Eppendorf
Fluorescence microscope	TriM Scope II multiphoton system	LaVision BioTec
Tweezer (fine)	Tip: 0.8 mm x 0.7 mm	Fine Science Tools
Tweezer (standard)	15.5 cm	Fine Science Tools
UV-/Vis-spectral photometer	Nanodrop 2000c	Thermo Fisher Scientific
UV-transilluminator	UVT-28 ME; camera: EASY 440K	Herolab
Vacuum concentrator	Concentrator 5301	Eppendorf
Vacuum pump	BVC 21	Vacuubrand
Volumetric flask	2000 mL; 1000 mL; 250 mL; 100 mL	Vitlab
Vortexer	RS-VA 10	Phoenix Instrument
Water bath	TW8	Julabo
Water bath	WB20	P-D Industriegesellschaft

2.1.2 Chemicals and reagents

Table 2: List of used chemicals.

Chemicals and reagents	Manufacturer
AAA (20-hydroxyicosa-6Z,15Z-dienoyl)aspartate	Cayman Chemical
2'-deoxynucleoside 5'-triphosphate (dNTP) mix	Thermo Fisher Scientific
Agarose	Roth
Ammonium peroxidisulphate (APS)	Roth
Bovine serum albumin (BSA)	Sigma-Aldrich
Bromphenolblue	Roth

Chemicals and reagents	**Manufacturer**
Calcium chloride ($CaCl_2$)	Roth
Citric acid	Sigma-Aldrich
Chloroform	Roth
Cold water fish skin gelatin	Sigma-Aldrich
CRT 0066101	Tocris
D7-cholesterol	Merck
D7-7-*dehydrocholesterol* (DHC)	Merck
D31-hexadecanoic acid	Merck
Dimethyl sulfoxide (DMSO)	Sigma-Aldrich
Dipotassium phosphate (K_2HPO_4)	Roth
Disodium hydrogen phosphate (Na_2HPO_4)	Roth
DNA loading dye solution	Sigma-Aldrich
Enhanced chemiluminescence (ECL) substrate	Bio-Rad
Eosin G solution	Roth
Ethanol, absolute	Roth
Ethanol, denatured	Roth
Ethylenediaminetetraacetic acid (EDTA)	Roth
Fc-block	Abcam
Fentanyl	Janssen-Cilag
Fura-2 a*cetoxymethyl ester* (AM)	Invitrogen
GeneRuler 1 kbp DNA ladder	Thermo Fisher Scientific
GeneRuler 100 bp DNA ladder	Thermo Fisher Scientific
Goat serum	Sigma-Aldrich
GW1100	Cayman Chemical
HET0016	Sigma-Aldrich
Heparin	Ratiopharm
Hydrogen chloride (HCl)	Sigma-Aldrich
(4-(2-hydroxyethyl)-1-piperazineethanesulfonic acid) HEPES	Sigma-Aldrich
Insulin (100 I.E./mL)	Sanofi Aventis
Isopropanol	Roth
Lyso-platelet activating factor (16:0)	Sigma-Aldrich
L*ysophosphatidic acid* (LPA)-(17:0)	Merck
Lysophosphatidylcholine (LPC)-(17:0)	Merck
Lysine	Sigma-Aldrich
Magnesium chloride (MgCl2)	Roth

Chemicals and reagents	**Manufacturer**
Magnesium sulfate ($MgSO_4$)	Sigma-Aldrich
Mayer's hematoxylin solution	Sigma-Aldrich
Medetomidin (Dormitor)	Pfizer
Methanol	Sigma-Aldrich
Midazolam (Dormicum)	Roche
Midori green advance DNA stain	Nippon Genetics
Mounting medium; Roti®-Mount	Roth
Platelet activating factor (16:0)	Sigma-Aldrich
PageRuler® prestained protein ladder	Thermo Fisher Scientific
Paraformaldehyde	Roth
Prostaglandin ($PG)I_2$	Sigma-Aldrich
Potassium chloride (KCl)	Sigma-Aldrich
PowerUp™ SYBR™ green master mix	Thermo Fisher Scientific
ProLong Gold Antifade Mountant with *4',6-diamidino-2-phenylindole* (DAPI) mounting reagent	Thermo Fisher Scientific
Proteinase K inhibitor	Calbiochem
Sodium chloride (NaCl)	Roth
Sodium dihydrogen phosphate (NaH_2PO_4)	Roth
Sodium dodecyl sulfate (SDS)	Roth
Sodium hydroxide (NaOH)	Roth
Sodium periodate ($NaIO_4$)	Roth
SR27417	Sigma-Aldrich
Tetramethylethylenediamine (TEMED)	Roth
Tris(hydroxymethyl)aminomethane (TRIS)	Roth
Trisodium citrate dehydrate	Sigma-Aldrich
Tween 20	Roth
UltraPure™ distilled water (Dnase/Rnase Free)	Thermo Fisher Scientific
YM-254890	Tocris
β-mercaptoethanol	Sigma-Aldrich
20-HETE	Cayman Chemical

2.1.3 Buffers and solutions

Acid-Citrate-Dextrose (ACD) Buffer, pH 4.5

Trisodium citrate dihydrate	85 mM
Citric acid	65 mM
Glucose	110 mM

Blocking Buffer (for IF)

PBS	
Goat serum	5 % (v/v)
Cold water fish skin gelatin	1 % (w/v)
Fc-block	10 µg/mL

Collagenase Buffer

HBSS	
$CaCl_2$	1 mM
Collagenase P	1 U/mL

Fixation Buffer (for IF)

Para-formaldehyde	1 % (w/v)
Lysine	0.9 M
NaH_2PO_4	28 mM
$NaIO_4$	12 mM
Na_2HPO_4	9.4 mM

HBSS

HBSS	
$CaCl_2$	1 mM

Krebs-Ringer-Buffer (KRB), pH 7.4

NaCl	135 mM
HEPES	20 mM
KCl	5 mM
$CaCl_2$	1 mM
$MgSO_4$	1 mM
K_2HPO_4	0.4 mM

Laemmli Buffer (5x)

TRIS (pH 6.8)	300 mM
Glycerol	50 %
β-mercaptoethanol	25 %
SDS	10 %
Bromphenolblue	Spatual tip

Modified KRB, pH 7.4

NaCl	138 mM
HEPES	5 mM
$NaHCO_3$	5 mM
KCl	3.6 mM
$CaCl_2$	1.5 mM
$MgSO_4$	0.5 mM
NaH_2PO_4	0.5 mM

Lysis Buffer (for DNA extraction)

NaCl	200 mM
TRIS (pH 8.5)	100 mM
EDTA	5 mM

SDS	0.2 % (w/v)
Proteinase K (added freshly)	0.1 mg/mL

TRIS-acetic acid-EDTA (TAE) Buffer (50x)

TRIS	2 M
Acetic acid	1 M
EDTA	50 mM

TRIS-buffered saline (TBS) Buffer, pH 7.3

NaCl	137 mM
TRIS	20 mM

Tyrode's Buffer, pH 7.3

NaCl	137 mM
KCl	2.7 mM
$NaHCO_3$	12 mM
NaH_2PO_4	0.43 mM
Hepes	5 mM
$CaCl_2$	2 mM
$MgCl_2$	1 mM
BSA	0.35 %
Glucose	0.1 %

Washing Buffer (for IF)

PBS	
Tween 20	0.05 % (v/v)

2.1.4 Cell culture reagents, media, and buffers

Table 3: List of cell culture reagents, media, and buffers.

Reagent, medium, or buffer	Manufacturer
DharmaFECT Duo	Horizon
Dulbecco's Modified Eagle's Medium (DMEM)	Thermo Fisher Scientific
Dulbecco's phosphate-buffered saline (DPBS)	Thermo Fisher Scientific
Fetal bovine serum (FBS)	Thermo Fisher Scientific
*Fetal calf serum (*FCS)	Thermo Fisher Scientific
Gentamicin	Thermo Fisher Scientific
Glucose solution (200 g/L)	Thermo Fisher Scientific
Glutamine (100x)	Thermo Fisher Scientific
HEPES	Thermo Fisher Scientific
MatriGel	Corning
Lipofectamine RNAiMAX	Thermo Fisher Scientific
Nonessential amino acids (NEAA) (100x)	Thermo Fisher Scientific
Opti-MEM I	Thermo Fisher Scientific
Penicillin/Streptomycin (P/S) (10000 U/mL/10000 µg/mL)	Thermo Fisher Scientific
Radioimmunoprecipitation assay (RIPA) buffer	Thermo Fisher Scientific
Roswell Park Memorial Institute RPMI 1640	Thermo Fisher Scientific
Sodium pyruvate (100 mM)	Thermo Fisher Scientific
Trypan blue stain	Thermo Fisher Scientific
Trypsin (0.05 %)-EDTA	Thermo Fisher Scientific
ULTI-ST	Human Cell Design
ULTIβ1	Human Cell Design
βCOAT	Human Cell Design
βKREBS	Human Cell Design

HEK293 medium

DMEM (4.5 g/L D-Glucose)	
FBS	10 % (v/v)
Penicillin/Streptomycin	1 % (v/v)

INS1 medium	
RPMI 1640	
FBS	10 % (v/v)
Penicillin/Streptomycin	1 % (v/v)
HEPES	10 mM
Glutamine	2 mM
Sodium pyruvate	1 mM
β-mercaptoethanol	50 µM

MIN6 medium	
DMEM (4.5 g/L D-Glucose)	
FBS	15 % (v/v)
Penicillin/Streptomycin	1 % (v/v)
HEPES	20 mM
β-mercaptoethanol	50 µM

3T3L1 medium	
DMEM (4.5 g/L D-Glucose)	
FCS	10 % (v/v)
Gentamicin	0.4 % (v/v)

2.1.5 Kits

Table 4: List of used kits.

Kit	Manufacturer
20-HETE e*nzyme-linked immunosorbent assay* (ELISA) Kit	Abcam
BCA Protein Assay Kit	Thermo Fisher Scientific
First Strand cDNA Synthesis Kit	Thermo Fisher Scientific

Kit	Manufacturer
Human insulin ELISA	Crystal Chem
KAPA HiFi PCR Kit	Roche
Mouse Glucagon ELISA Kit	Crystal Chem
Pro-Platelet-Basic-Protein ELISA Kit	RayBiotech
Taq DNA Polymerase	Thermo Fisher Scientific
Ultra Sensitive Mouse Insulin ELISA Kit	Crystal Chem
Ultra Sensitive Rat Insulin ELISA Kit	Crystal Chem

2.1.6 Oligonucleotides

Table 5: List of used oligonucleotides.

Gene name	Full gene name	Forward primer (5' - 3') (upper) Reverse primer (5' - 3') (lower)
Ffar1	Free fatty acid receptor 1 (GPCR40)	5'-CCCTTGGTTATCACTGCTTTCTG-3' 5'-GAGCCTTCTAAGTCCGGGTTTAT-3'
Hprt1	Hypoxanthine phosphoribosyltransferase 1	5'-GCAGACTTTGCTTTCCTTGG-3' 5'-CCGCTGTCTTTTAGGCTTTG-3'

2.1.7 Antibodies

2.1.7.1 Primary antibodies

Table 6: List of used primary antibodies.

Antibody	Manufacturer
Anti-GAPDH	Sigma Aldrich
Anti-PECAM-1	Abcam
Anti-PKD/PKCμ pSer$^{744/748}$	Cell Signaling
Anti-PKD/PKCμ p^{Ser916}	Cell Signaling
Anti-Phospho-(Ser/Thr) PKD substrate	Cell Signaling
Anti-VEGF-A	Abcam
JAQ1-F(ab')2	Emfret Analytics
JAQ1-IgG	Emfret Analytics
JON/A-F(ab')2	Emfret Analytics
non-immune rat IgG	Emfret Analytics

Antibody	Manufacturer
p0p/B-Fab	Emfret Analytics
R300	Emfret Analytics

2.1.7.2 Fluorophore-coupled antibodies

Table 7: List of used fluorophore-coupled antibodies.

Antibody	Manufacturer
anti-GPIbβ-Dylight488	Emfret Analytics
WUG1.9-FITC	Emfret Analytics
JON/A-PE	Emfret Analytics
Rat anti-rabbit IgG Alexa Fluor 488	Thermo Sciences

2.1.7.3 In-house generated antibodies

Table 8: List of used in-house generated antibodies.

Antibody	Reference
α-P-selectin-FITC	unpublished
anti-CD105-Alexa647	unpublished
Anti-GPIX-Alexa594	Stegner et al., 2017
Anti-GPIX-Dylight488	Stegner et al., 2017

2.1.8 Enzymes

Table 9: List of used enzymes.

Enzyme	Manufacturer
Apyrase	Sigma-Aldrich
Collagenase P	Roche
Diamine oxidase	Sigma-Aldrich
Monoamine oxidase A	Sigma-Aldrich
Proteinase K	Sigma-Aldrich

2.1.9 Cell lines

Table 10: List of used cell lines.

Cell line	Manufacturer
EndoC-βH1	Endocell
EndoC-βH5	Human Cell Design
HEK293	ATCC
INS1	Prof. R. Ricci (University of Strasbourg)
MIN6	Prof. R. Ricci (University of Strasbourg)
3T3L1	ATCC

2.2 Methods

2.2.1 Genetically modified mice

$Gp6^{-/-}$ mice were previously described[405]. To sum it up, a targeting vector targeting intron 2 and exon 2 was electroporated into Sv129-derived embryonic stem cells to obtain homologous recombination. Cells that were successfully transformed were injected into C57BL/6 blastocysts. For germline transmission resulting chimeric mice were backcrossed with C57BL/6 mice. For further mouse line maintenance, heterozygous animals were intercrossed to generate $Gp6^{-/-}$ mice.

$GpIb\alpha^{-/-;TG}$ mice, in which most of the extracytoplasmic sequence of GpIbα has been replaced by an isolated domain of the α-subunit of the human interleukin-4 receptor (IL-4R), were described previously[406]. Briefly, residues 1-198 of the mature α-subunit of the ectodomain of IL-4R were ligated with residues 473-610 of the human GPIbα mature subunit, integrated into an expression vector, and transfected into heterologous cells. A promoter cassette was cloned followed by microinjection of the transgenic product into pronuclei. The resulting transgenic mice were bred to mice lacking mouse GpIbα alleles.

$Unc13d^{-/-}$ mice were generated by injection of $Unc13^{dtm1(KOMP)Vlcg}$ embryonic stem cells into C57BL/6 blastocysts as described previously[407]. The resulting chimeric mice were backcrossed with C57BL/6 mice for germ-line transmission.

For the generation of $G\alpha_q/G\alpha_{13}$ PF4-Cre double deficient mice, previously described $G\alpha_q^{fl/fl}$ mice, in which exon 6 from the *Gnaq* gene was flanked by *loxP* sites, were intercrossed with $G\alpha_{13}^{fl/fl}$ mice, that exhibit exon 2 of *Gna13* flanked with *loxP* sites (kindly contributed by Prof. Dr. Stefan Offermanns and Shaun R Coughlin, respectively)[408,409]. $G\alpha_q^{fl/fl}/G\alpha_{13}^{fl/fl}$ mice were bred with mice that carry the Cre-recombinase under the platelet factor 4 (PF4) promotor to obtain $G\alpha_q/G\alpha_{13}$ PF4-Cre mice, which are referred to as $G\alpha_qG\alpha_{13}$ PF4 Δ/Δ[410].

All mouse experiments were approved by the district government of Lower Franconia (Bezirksregierung Unterfranken, reference 2-1296 ; 500-46/20) and the local ethic

committee of Warsaw (I Lokalna Komisja Etyczna ds. Doświadczeń na Zwierzętach, reference: 1074/2020). Mice were held in groups of maximum five animals in cages (green line IVC-rack system, Tecniplast) under specific pathogen-free conditions in the animal facility of the Rudolf Virchow Centre and the Nencki Institute of Experimental Biology. They were kept on a 12 *hours* (h) light/dark cycle at a temperature of 23°C and 55 % humidity with *ad libitum* access to water and a regular chow diet. For experiments, male mice of the same age were taken.

2.2.1.1 Generation of bone marrow chimeras

5-7 weeks-old recipient C57BL/6JRj) mice were irradiated (Faxitron) with a single dose of 10 Gy. The femur and tibia of respective donor mice were prepared and bone marrow was washed out with a 22 G needle into 37°C DMEM. Recipient mice were reconstituted by *intravenous* (i.v.) injection with $4x10^6$ bone marrow cells and treated with drinking water containing 2 g/l neomycin sulfate for the following 2 weeks.

2.2.2 Mouse genotyping

2.2.2.1 Isolation of murine DNA

Mouse-ear biopsies were lysed in 500 µL lysis buffer over night at 55°C and 400 rpm on a thermomixer. For DNA extraction, 100 µL of 5 M NaCl was added, mixed, and centrifuged for 10 min at 13000 g at 4°C. The supernatant containing the nucleic acids was transferred to a new tube. After the addition of 500 µL isopropanol followed by thorough mixing, samples were kept for 30 min at -20°C. The samples were centrifuged under the remaining conditions and the supernatant was discarded. For washing, 1 mL of 70 % ethanol (absolute) was added to the remaining precipitated nucleic acid pellet. After centrifugation under the same conditions, the supernatant was discarded. The pellet was air-dried and resolved in 100 µL ddH_2O at 55 °C and 400 rpm for 10 min on a thermomixer. The final product was stored at -20°C until further usage.

2.2.2.2 *Polymerase chain reaction* (PCR) for genotyping

Reagents for PCR were either derived from the KAPA High Fidelity Kit or Taq DNA Polymerase Kit.

Genotyping of Unc13d$^{-/-}$ mice

PCR mix:	
DNA	5 µL
Thermo Buffer -$MgCl_2$	2.5 µL
$MgCl_2$	2.5 µL
dNTP (5 mM)	0.5 µL
Primer TU.for	1 µL
Primer TU.rev	1 µL
Primer SU	1 µL
Primer LacZ.rev	1 µL
DMSO	1 µL
Taq polymerase (5 U/µL)	0.25 µL
H_2O	11.25 µL

PCR program:		
Step 1	96°C	3 min
Step 2	94°C	30 s
Step 3	62°C	30 s
Step 4	72°C	1 min
→	go to step 2, 40x	
Step 5	72°C	5 min
Step 6	4°C	∞

Primer for Unc13d$^{+/+}$-PCR:

Unc13d-TU.for: 5'- GGG ACG CCG TGT CTT TCT AC -3'

Unc13d- TU.rev: 5'- ACA CTC TCC CAA CAT CTC CTC TTA C -3'

Predicted band size: 73 bp

Primer for Unc13d$^{-/-}$ PCR:

Unc13d-SU: 5'- CTC TCC CCA GAG CCT CCG TG -3'

Unc13d-LacZ.rev: 5'- GTC TGT CCT AGC TTC CTC ACT G -3'

Predicted band size: 392 bp

Genotyping of PF4-cre mice

PCR mix (20 µL final volume):	
DNA	2 µL
KAPA Buffer	5 µL
KAPA dNTP (10 mM)	0.75 µL
Primer PF4-for	0.75 µL
Primer PF4-rev	0.75 µL
KAPA polymerase (1 U/µL)	0.3 µL
H_2O	15.45 µL

PCR program:		
Step 1	98°C	3 min
Step 2	98°C	20 s
Step 3	59°C	30 s
Step 4	72°C	45 s
→	go to step 2, 35x	
Step 5	72°C	3 min
Step 6	4°C	∞

Primer for PF4-cre PCR:

PF4-for: 5'- CTCTGACAGATGCCAGGACA-3'

PF4-rev: 5'- TCTCTGCCCAGAGTCATCCT-3'

Predicted band size: 450 bp

Genotyping of Gαq$^{fl/fl}$ mice

PCR mix (20 µL final volume):	
DNA	2 µL
Thermo Buffer -$MgCl_2$	2.4 µL
$MgCl_2$	2.0 µL
dNTP (5 mM)	1 µL
Primer Gαq-for	1 µL
Primer Gαq-rev	1 µL
Taq polymerase (5 U/µL)	0.2 µL
H_2O	15.4 µL

PCR program:		
Step 1	94°C	3 min
Step 2	94°C	30 s
Step 3	61°C	30 s
Step 4	72°C	45 s
→	go to step 2, 35x	
Step 5	72°C	3 min
Step 6	4°C	∞

Primer for Gαq$^{fl/fl}$ PCR:

Gαq-for: 5'- GCATGCGTGTCCTTTATGTGAG-3'

Gαq-rev: 5'- CTTCTGAGCCATCTTGCCAGC-3'

Predicted band size: 300 bp (WT), 450 bp (fl/fl)

Genotyping of Gα13$^{fl/fl}$ mice

PCR mix (20 µL final volume):	
DNA	2 µL
Thermo Buffer -$MgCl_2$	2.4 µL
$MgCl_2$	2.0 µL
DMSO	1 µL
dNTP (5 mM)	1 µL
Primer Gαq-for	1 µL
Primer Gαq-rev	1 µL
Taq polymerase (5 U/µL)	0.2 µL
H_2O	14.4 µL

PCR program:		
Step 1	94°C	3 min
Step 2	94°C	15 s
Step 3	56°C	30 s
Step 4	72°C	45 s
→	go to step 2, 35x	
Step 5	72°C	3 min
Step 6	4°C	∞

Primer for Gα13$^{fl/fl}$ PCR:

Gα13-for: 5'-GCACTCTTACAGACTCCCAC-3'

Gα13-rev: 5'- GCCACAGAGGGATTCAGCAC-3'

Predicted band size: 450 bp (WT), 550 bp (fl/fl)

2.2.2.3 Agarose gel electrophoresis

The PCR products were separated by size on a 2 % agarose gel. For the preparation of the gel, 6 g agarose was dissolved in 300 mL TAE buffer by boiling the solution in a microwave. After 3 min of cooling down, 15 µL of a DNA stain (Midori Green Advance) was added and the gel was allowed to solidify in a comb-containing tray which was then placed into a TAE buffer-filled chamber. Then, 24 µL of PCR product were mixed with 6 µL of 6x loading dye and loaded together with a 100 bp DNA ladder onto the gel. Separation of the samples and ladder occurred at 120 V for 1 h. For visualization, an ultra violet device was used and an image was taken with a camera.

2.2.3 Mouse phenotyping

To phenotype mice regarding their presence of GPVI on the platelet surface, flow cytometry was used as described in 2.2.6.2 using a specific antibody against GPVI.

2.2.4 Treatment of mice with active ingredients

2.2.4.1 Application of antibodies

To induce platelet depletion 2 µg/g *body weight* (BW) of anti-GPIbα IgG R300 (Emfret, Germany) were i.v. injected. For functional blocking of GPVI, GPIbα, and αIIbβ3 4 µg/g BW of JAQ1-F(ab')$_2$, p0p/B-Fab, or JON/A-F(ab')$_2$ were injected i.v., respectively. GPVI was depleted by i.v. injection of 4 µg/g BW of JAQ1-IgG. Control mice received a dosage matching i.v. injection of non-immune rat IgG.

2.2.4.2 Application of clopidogrel and ASA

Clopidogrel and ASA were given as a solution of 150 mg/L *ad libitum* by drinking water to ensure an assumed daily dosage of 40 mg/kg BW.

2.2.4.3 Application of HET0016

Mice were injected *intraperitoneally* (i.p.) with 10 mg/kg HET0016 dissolved in DMSO 72 h, 48 h, 24 h, and 30 min before the experiment. Control mice received DMSO only.

2.2.4.4 Application of SR27417

Mice were injected i.p. with 10 mg/kg SR27417 dissolved in PBS 16 h before the experiment. Control mice received PBS only.

2.2.5 *In vivo* analysis

2.2.5.1 Glucose and insulin tolerance test

The *glucose tolerance test* (GTT) and *insulin tolerance test* (ITT) were executed with mice that were fasted 16 h or 4 h before the experiment, respectively. Unless otherwise stated, mice received an intraperitoneal (i.p.) injection of glucose (2 g/kg bodyweight (BW) for GTT and of insulin (0.5 U/kg BW) for ITT. Blood glucose levels were monitored by tail vein puncture just before injection (0) and 15, 30, 60, 90, and 120 min after injection with an Accu-chek glucometer.

2.2.5.2 *Glucose-stimulated insulin secretion* (GSIS)

To measure GSIS mice were fasted for 16 h followed by i.p. glucose injection (3 g/kg BW). Blood samples were taken by tail vein puncture just before injection (0) and 2, 5, 15, and 30 min after injection. After spinning down the samples at 13000 g and 4°C for 10 min, insulin concentrations of the resulting supernatants were measured by ELISA.

2.2.5.3 Body composition

For assessment of the body composition mice were placed into a nuclear magnetic resonance analyzer which allows quantification of fat mass, lean mass, and free fluids. Further, mice were dissected and the weight of different organs was measured.

2.2.5.4 Platelet activation upon glucose injection

Mice were fasted for 16 h and received an i.v. injection of glucose (2 g/kg in saline) or saline through the retroorbital plexus. After indicated timepoints, mice were bled from the retroorbital plexus into 300 µL heparin (20 U/mL in TBS) and platelet count was measured for normalization according to 2.2.6.2. Finally, samples were centrifuged at 2800 rpm at RT for 6 min and levels of PPBP of the resulting supernatant were measured by ELISA (RayBiotech) as described in the manufacturer’s manual.

2.2.5.5 Pancreas intra-vital imaging

For visualization of vasculature and platelets, fluorescently labeled antibodies against CD105 (0.4 µg/g BW, Alexa Fluor 647) and GPIX (0.6 µg/g BW, Alexa Fluor 594) respectively, were injected subcutaneously. Mice were anesthetized with 0.5 mg/kg BW Medetomidin, 5 mg/kg BW Midazolam, and 0.05 mg/kg Fentanyl. Afterwards, access to the pancreas was generated by laparotomy of the upper abdominal below the costal arch. For further microscopy, the intestine and stomach were carefully pushed aside with a cotton stick to expose a small part of the pancreas. The surrounding tissue was covered with a cloth soaked with physiological saline solution to avoid drying the tissue. Subsequently, mice were placed on an inverted Leica SP8 confocal microscope, and imaging was performed using a 25x objective.

For further analysis, image stacks were processed, visualized, and analyzed using Fiji. First, *three-dimensional* (3D) multicolor image stack files were preprocessed using Huygens Deconvolution software (Huygens Professional 20.10.0p1 64bit, Scientific Volume Imaging B.V., Hilversum, The Netherlands) to obtain higher contrast and better signal-to-noise ratio. For deconvolution, the *Classic Maximum Likelihood Estimation* (CMLE) model was used, applying a maximum of 40 iterations, a signal-to-noise ratio of 10, and automatic background estimation. Then, the results were converted to Imaris Classic format and segmented using Imaris (Imaris x64, version 9.6, Bitplane AG, Zurich, Switzerland). Two segmentations were executed with each stack. The fluorescence intensity of CD105-stained cells served to determine blood vessel walls, and the fluorescence signal from GPIX-positive cells was used to identify platelets. Both parameters were integrated into the Surface Model tool in combination with shortest distance calculation, rolling ball background subtraction, and manual threshold adjustment. Vascular objects smaller than <100 µm³ were excluded. A size filter (>8 µm³) was applied to distinguish adherent platelets from motile ones. In addition, the manual removal of scan-related artifacts was executed. Distance transformation was used to only obtain platelets, that are adhered to the vessel wall (distance=0 µm). The volumes of vessel walls and adherent platelets were used for further statistical analysis and the "Snapshot" tool was applied to generate 3D images.

2.2.6 *In vitro* analysis of platelet function

2.2.6.1 Purification of platelets from whole blood

To generate washed platelets from murine blood, anesthetized mice were bled from the retroorbital plexus into 300 µL heparin (20 U/mL in TBS). The tube was filled up with heparin to 1.3 mL and centrifuged for 6 min at 800 rpm and RT. Then, the upper *platelet-rich plasma* (PRP) phase was transferred together with the transition phase of the red blood cells into a fresh tube containing 300 µL heparin. After repeating the previous centrifugation step, only PRP was transferred into a new tube without touching the red blood cell phase. For platelet inhibition 2 µL apyrase (0.02 U/mL, f.c.) and 5 µL PGI_2, (0.1 µg/mL, f.c.) were added. When platelets were spun down at 2800 rpm for 5 min at RT, the supernatant was discarded and the platelet pellet was resuspended in 1 mL of Tyrode's buffer without Ca^{2+} containing 2 µL apyrase and 5 µL PGI_2. Centrifugation and resuspension steps were repeated once and platelet count was assessed in a 1/1 dilution in PBS using an automated cell analyzer (Sysmex). Depending on further experiments, the platelet pellet was resuspended in the respective buffer volume to obtain desired platelet count. Finally, platelets were allowed to rest for 30 min at 37°C until continuation with the following experiment.

For the preparation of washed platelets from human blood, blood was taken from the basilic vein and transferred into a 15 mL tube containing 0.2 mL/mL blood of sterile acid citrate dextrose (ACD, pH 4.5). After centrifugation for 20 min at 300 g at RT (acceleration at 9, break at 1), PRP was transferred into a new tube and supplemented with 2 µL/mL apyrase (0.02 U/mL, f.c.), 5 µL/mL PGI_2, (0.1 µg/mL, f.c.) and 100 µL/mL ACD. The samples were rested for 10 min at 37°C and centrifuged for 10 min at 500 g and RT (acceleration at 3, break at 3). The supernatant was discarded and the platelet pellet resuspended it 2 mL of Tyrode's buffer containing 2 µL/mL apyrase (0.02 U/mL, f.c.), 5 µL/mL PGI_2, (0.1 µg/mL, f.c.) and 150 µL/mL ACD. Platelet count was assessed with a 1/1 dilution in PBS by Sysmex while the previous centrifugation step was repeated once. Depending on the further experiment, the platelet pellet was resuspended in the desired buffer to obtain a defined platelet count. After 30 min of resting at 37°C, platelets were used for the following experiment.

2.2.6.2 Flow cytometry

To quantify the presence of GPVI on the platelet surface, 50 µL blood was bled from the retroorbital plexus of anesthetized mice into 300 µL heparin (20 U/mL in TBS). 1 mL of Tyrode's buffer w.o. Ca^{2+} was added and 50 µl of diluted blood was stained with saturating amount of fluorophore-conjugated antibody against GPVI (JAQ1-FITC) for 7 min at 37°C followed by 7 min at RT. The samples were diluted with 500 µL PBS and analyzed at a Celesta (BD BioSciences). Platelets were identified by their forward and side scatter characteristics and mean fluorescence intensity (MFI) was determined.

For the assessment of platelet count by flow cytometry, samples were prepared as described above and stained with saturating amount of fluorophore-conjugated antibody against GPIbα (15E2-PE) for 7 min at 37°C followed by 7 min at RT. After dilution with 500 µL PBS counts per second were measured. Alternatively, platelet count was measured in heparinized blood diluted 1:1 in PBS with a Sysmex analyzer.

To analyze integrin αIIbβ3 activation and P-selectin exposure upon platelet activation, mice were bled as described before. For heparin removal, blood was washed twice with 1 mL Tyrode's buffer w.o. Ca^{2+} (2,800 rpm, 5 min, RT) and finally resuspended in 750 µL Tyrode's buffer containing 2 mM Ca^{2+}. Platelets were stimulated for 7 min at 37°C, followed by 7 min at RT with agonists in the presence of saturating amounts of fluorophore-conjugated antibodies against activated αIIbβ3 integrins (JON/A-PE) and P-selectin (WUG.1.9-FITC). For stimulation experiments with different cell supernatants, the supernatants were adjusted to 25 mM glucose and added in a ratio of 1:3 in the presence of 1 µg/mL CRP. Stimulation was stopped by the addition of 500 µL PBS and samples were analyzed as described above.

2.2.6.3 Platelet adhesion to collagen under flow

For assessing the impact of glucose on platelet adhesion, 800 µL heparinized blood derived from mice or human donors was mixed with 400 µL Tyrode's-HEPES buffer and supplemented with 2.8 mM or 25 mM glucose. For experiments with different cell supernatants, 200 µL heparinized mouse blood was mixed with 100 µL cell supernatant and 100 µL Tyrode's-HEPES buffer supplemented with glucose to obtain

a final glucose concentration of 25 mM. Platelets were fluorescently labeled with a Dylight488-labeled anti-GPIX antibody derivative (0.1 µg/mL, for mouse samples) or a Dylight488-labeled anti-GPIbβ (0.1 µg/mL, for human samples) for 5 min at 37°C.

Coverslips (24 x 60 mm) were coated with 200 µg/mL fibrillar type I collagen in SFK buffer overnight at 37°C, followed by blocking for 30 min with 1 % w/v BSA in PBS at room temperature. The coated coverslip was inserted into a transparent flow chamber system with a slit depth of 50 µm. Perfusion of the blood sample occurred at a shear rate of 150 /s using a pulse-free pump at room temperature for 8 min. Subsequently, the chamber got washed for an additional 8 min using Tyrode's-HEPES buffer with 2 mM $CaCl_2$ and sample-matching glucose concentration. Microscope phase-contrast images were recorded in real-time during the perfusion and washing process using a Zeiss Axiovert 200 inverted microscope (40x/0.60 objective) equipped with a CoolSNAP-EZ camera (Visitron). After washing, phase contrast and fluorescence images were recorded from at least 6 random microscope fields. Image quantification was executed with Fiji to obtain relative coverage of platelets as well as integrated density of their fluorescence signal.

2.2.7 Generation of supernatant of activated platelets

To prepare the *supernatant of activated mouse platelets* (mPS) and *supernatant of activated human platelets* (hPS), platelets were washed as described in 2.2.6.1. The platelet pellet resulting from the last washing step was resuspended in Tyrode's buffer containing 2 mM $CaCl^2$, to obtain a final platelet count of 500,000 platelets/µL for mPS and 1000,000 platelets/µL for hPS. The platelets were allowed to rest for 30 min at 37°C, followed by inducing platelet activation with the addition of 10 ug/mL of collagen-related peptide (CRP). After 15 min of incubation at RT, platelet debris was removed by centrifugation for 10 min at 4°C and 800 g, followed by sterile filtration of the supernatant. The control solution was generated identically except for the presence of platelets.

For the digestion of proteins and peptides, hPS and the control solution were treated with 0.2 U/ml proteinase K for 16 h at 37°C, followed by 1 h incubation with 0.2 mM proteinase K inhibitor. Fractioning was obtained by using Amicon Ultra-0.5 mL

centrifugal filters (3 kDa). The fraction bigger than 3 kDa was diluted in Tyrodes-HEPES buffer containing 2 mM $CaCl_2$ to obtain the starting volume of the solution. To digest purines, histamine, and serotonin, 2 x 10^{-3} U/ml apyrase, 3 x 10^{-4} U/ml diamine oxidase, or 19 µg/ml monoamine oxidase A, respectively, were added for 16 h at 37°C. The treatment of monoamine oxidase A was followed by separation with a centrifugal filter unit and only the fraction of substances smaller than 3 kDa was used for further experiments. During the generation of modified hPS and control solutions, additional vials of hPS and control solution were subjected to the same treatment except for the presence of appropriate enzymes and inhibitors. For the extraction of lipids, hPS and control solution were added to twice the volume of 2:1 v/v mixture of chloroform and methanol, vortexed for 1 min, and centrifuged at 3000 g, 4°C for 10 min. The upper, aqueous phase was transferred to a new vial and the procedure was repeated two additional times. The final upper phase was used for the following experiments.

2.2.8 *In vitro* analysis of β-cell lines and isolated islets

2.2.8.1 Mouse islet isolation and GSIS

The mouse was euthanized by CO_2, sterilized with 70 % ethanol (v/v), and an incision was made around the upper abdomen to expose the liver and intestine. The ampulla was clamped with surgical thread and a small incision into the common bile duct was generated with micro scissors under a microscope. A 30 G needle was inserted into the duct towards the pancreas, and 3 mL of cold collagenase buffer was slowly injected. The inflated pancreas was removed from the body and transferred into a tube containing 5 mL of collagenase buffer. After digestion for 15 min at 37,5°C and 400 rpm, digestion was stopped by placing the sample on ice and adding 20 mL cold HBSS. Subsequently, the sample was centrifuged for 30 s at 290 g and 4°C. The supernatant was discarded and the pellet was resuspended in 20 mL HBSS. The centrifugation step was repeated and the resulting pellet was resuspended in 15 mL HBSS. Then, the suspension was filtered through a 70 µm mash and rinsed with 50 mL of HBSS. The mash was turned upside down over a petri dish and the remaining islets were washed out by rinsing with 15 mL of RPMI medium (10 % FBS, v/v). For further purification, islets were manually picked and transferred into 5 mL of fresh RPMI medium using a pipette and a microscope. Islets were distributed in a 96-well plate (V-bottom) containing 300 µL RPMI (10 % FBS, v/v) to obtain 8 size matching

islets per well. After equilibration for 2.5 h at 37°C, 90 % of the medium was carefully discarded and each well was washed twice with 200 µL of low glucose KRB (2.8 mM glucose, 0.5 % BSA, v/v). For stimulation, 100 µL of low glucose KRB was added and after 90 min of incubation, a sample of 15 µL was taken. Wells were washed twice with high glucose KRB (16.7 mM glucose, 0.5 % BSA, v/v) and 100 µL of high glucose KRB was added. Following another 90 min of incubation, 15 µL of the sample was taken. Insulin levels of samples were assessed by mouse insulin ELISA (2.2.10.4).

For experiments including mPS, islets were isolated and equilibrated as described above. Then, islets were stimulated with a 1/1 mixture of KRB and mPS or control solution, supplemented either with 2.8 mM or 16.7 mM glucose and 0.5 % BSA (w/v). After 90 min of incubation 15 µL sample was taken and analyzed with mouse insulin ELISA.

2.2.8.2 Cell culture and GSIS

To measure insulin secretion with MIN6 cells, 30,000 cells/well were plated 48 h before on a MatriGel-coated 96-well plate. For coating, 50 µL/well of 0.05 % MatriGel in PBS (v/v) was incubated for 30 min at 37°C with subsequent washing with sterile ddH_2O and PBS, respectively. Cells were kept in low glucose KRB (2.8 mM glucose, 0.5 % BSA (w/v) for 2 h before the experiment for equilibration. For stimulation, cells were incubated for 1 h with low glucose KRB, followed by 1 h stimulation with a 1/1 mixture of KRB and mPS or control solution respectively, supplemented with 25 mM glucose and 0.5 % BSA (w/v). Supernatant samples of 15 µL were taken from low and high-glucose-stimulated cells and insulin concentrations were quantified by mouse insulin ELISA.

For GSIS with INS1-cells, 100,000 cells/well were plated 48 h before the assay on a 48-well plate. Before the experiment, cells were kept for 1 h in low glucose KRB (2.8 mM glucose, 0.5 % BSA, w/v) for acclimation. Afterwards, cells were stimulated for 30 min with a 1/1 mixture of KRB and hPS or control solution respectively, containing 2.8 mM or 15 mM glucose and 0.5 % BSA (w/v). Supernatant samples of 15 µL were taken and insulin levels were determined by rat insulin ELISA.

For the co-culture of INS1-cells with human platelets, INS1-cells were prepared and acclimated as described above. Then, cells were stimulated for 30 min with a suspension of 10^6/ul platelets in Tyrode's buffer or control solution (2.2.6.1) supplemented with 2.8 mM glucose and 0.5 % BSA (w/v). The supernatant was carefully collected, spun down for 5 min at 2000 g and 4°C, and the resulting supernatant was used for insulin quantification by rat insulin ELISA.

To inhibit GPCR40, Gαq/11, and PKD1, INS1-cells were treated with 5 µM GW1100, 5 nM YM-254890, and 1 µM CRT0066101, respectively for 2 h before the experiment, as well as during 30 min of stimulation with a 1:1 mixture of KRB and hPS or control solution, containing 15 mM glucose and 0.5 % BSA (w/v).

For silencing of GPCR40 expression, INS1-cells were transfected with siRNA in suspension. siRNA and DharmaFECT Duo transfection reagent were diluted in Opti-MEM I, before being added to MatriGel-coated 48-well plates. 100,000 cells/well were added in an antibiotic-free medium. The final concentrations of siRNA and transfection reagent were 0.1 µM and 7.7 µl/ml, respectively. 48 h after transfection, the GSIS experiment was executed as described above.

For the determination of GSIS of EndoC-βH1 cells, 300,000 cells/well were plated onto 24-well plates. Before the experiment, cells were incubated overnight in a culture medium supplemented with 2.8 mM glucose, followed by 15 min incubation in modified KRB supplemented with 0.2 % BSA (w/v) and 1 mM glucose. Afterwards, cells were stimulated with a 1/1 mixture of modified KRB and either hPS or control solution, supplemented with 0.2 % BSA (w/v) and 2.5 mM or 20 mM glucose. Supernatants were collected and cellular insulin was extracted by acid ethanol treatment. Insulin concentrations were quantified by ELISA.

In the case of EndoC-βH5 cells, 100,000 cells/well were seeded onto βCOAT coated 96-well plates and cultivated in ULTIβ1 medium. 6 days after plating, cells were kept in ULTI-ST medium for 24 h. 1 h before the experiment, cells were incubated in βKREBS containing 0.1 % BSA (w/v, fraction V fatty acid-free). For stimulation, cells were incubated for 40 min in a 1/1 mixture of βKREBS with hPS or control solution, containing 0.1 % BSA (w/v, fraction V fatty acid-free) and 3.9 mM or 20 mM glucose.

The supernatant was collected and cells were lysed with RIPA buffer to measure cellular insulin content. Insulin levels were quantified by ELISA.

2.2.8.3 Measurement of Ca^{2+} influx

INS1-cells were plated 48 h before assay on a 24-well plate. For monitoring of intracellular Ca^{2+} concentrations, cells were incubated for 1 h in KRP supplemented with 2 µM fura-2 (AM) and 2.8 mM glucose. After washing twice with PBS, cells were cultivated in KRB (2.8 mM glucose, 0.5 % BSA, w/v) for several minutes, to obtain the basal level of cytosolic Ca^{2+}. This was followed by stimulation with a 1/1 mixture of KRB and either hPS or control solution, containing 15 mM glucose and 0.5 % BSA (w/v). Cytosolic Ca^{2+} concentrations were monitored with a microplate reader at excitation/emission 340/510 nm and 380/510 nm.

2.2.8.4 Generation of cell supernatants

MIN6, 3T3L1, or HEK293 cells were seeded on a MatriGel-coated 12-well plate (300,000 cells/well). After 48 h of cultivation in respective medium, cells were acclimated for 2 h in 2.8 mM glucose KRB, followed by stimulation in 250 µL KRB containing 2.8 mM or 25 mM glucose for 3 min. The supernatant was collected and spun down for 5 min at 300 g and 4°C. The resulting supernatant was centrifuged again for 5 min at 14000 g and 4°C. Finally, the supernatant was collected and stored at -80°C until further use. Control supernatant was generated following the same procedure but in the absence of cells.

2.2.9 Histological analysis

2.2.9.1 *Hematoxylin and Eosin* (H&E) staining

H&E staining was executed according to standard protocols. In summary, paraffinized pancreas tissues were cut into sections of 5 µm. For deparaffinization, sections were incubated twice in xylol for 10 min, followed by rehydration in an ethanol gradient (99 %, 99 %, 90 %, 80 %, 70 %, 50 %, 0 %, v/v with ddH_2O, 5 min each). Then, sections were stained in hematoxylin for 10 min and rinsed in tap water for an additional 10 min. After incubation for 2 min in 70 % and 80 % ethanol respectively, sections were counterstained for 1 min in eosin. Dehydration in ethanol was continued (96 %, 96 %, 99 %, 99 %, 2 min each) followed by xylol (2x 10 min). Finally, sections

were covered with a cover slip using xylene based mounting medium (RotiMount). An inverted microscope was used for further analysis (Olympus CKX31).

2.2.9.2 *Immunofluorescence* (IF)

Cryosections with a thickness of 7 µL were incubated for 30 min at RT in the fixation buffer. Three times washing with PBS was followed by 1 h blocking in blocking buffer. Afterwards, the primary antibody was added in blocking buffer overnight at 4°C. Sections were washed twice with washing buffer and secondary antibodies were added in blocking buffer for 1 h at RT. After washing twice with washing buffer and PBS, sections were covered with a coverslip using ProLong Gold Antifade Mountant with DAPI. Analysis was executed with a confocal microscope (Leica TCS SP8).

To analyze the localization of platelets in pancreatic islets, cryosections of pancreas tissue were stained with primary rabbit anti-PECAM-1 antibody (1/150, v/v). Afterwards, sections were labeled with secondary rat anti-rabbit Alexa Flour 488 antibody (1/500) together with an anti-GPIX Alexa Flour 594 derivative (10 µg/mL). Pancreatic islets were identified by higher nucleus density and fluorescence images of the exocrine and endocrine pancreas were recorded. For quantification, background fluorescence was subtracted and endothelial area, islet area, and platelet count were determined by Fiji.

For analysis of vascularization of islets and VEGF-A expression, pancreas sections were incubated with primary guinea pig anti-insulin antibody (1/180, v/v) together with primary rabbit anti-VEGF-A (1/250, v/v) or rabbit anti-PECAM-1 (1/500, v/v) antibody. Following day sections were stained with secondary anti-guineapig Alexa Flour 594 (1/200, v/v) and anti-rabbit Alexa Flour 488 (1/500, v/v) antibodies. Islets were located by insulin staining and VEGF-A fluorescence intensity, as well as endothelial area, were determined by Fiji.

2.2.9.3 Quantification of pancreatic islet size and area

Paraffin and cryosections of the whole pancreas were used for the quantification of islet size and area. Three sections with a distance of 50 µm were prepared from each tissue. In the case of paraffin sections, islets were identified by H&E staining (2.2.9.1) and images were taken with a Leica light microscope DM4000B system. For

cryosections, islets were localized by IF staining against insulin (2.2.9.2) and imaged with a confocal microscope (Leica TCS SP8). To normalize the islet area to the whole pancreas area, images of whole paraffin and cryosections were recorded using the *Tile Scanning* function. Finally, the area of islets and whole pancreas sections were quantified by Fiji.

2.2.10 Molecular biology and biochemical methods

2.2.10.1 Immunoblotting

Cells were lysed in RIPA buffer supplemented with protease and phosphatase inhibitor mix. Cell fragments were spun down by centrifugation at 13000 g and 4°C for 10 min. After quantification of protein concentrations using a BCA assay kit according to the manufacturer's manual, protein concentrations were adjusted with RIPA buffer to an equal volume. A respective volume of 5x Laemmli buffer was added and samples were incubated at 95°C for 5 min. Subsequently, samples were loaded on a 10 % SDS polyacrylamide gel, separated by electrophoresis, and transferred to a *polyvinylidene fluoride* (PVDF) membrane. The membrane was washed in TBST, blocked for 1 h at 4°C in blocking buffer, and blotted with primary antibodies in TBST containing 5 % BSA (w/v) overnight at 4°C. After washing three times in TBST, anti-rabbit horseradish peroxidase (HRP)–conjugated secondary antibody in TBST supplemented with 5 % BSA (w/v) was added for 1 -based signal detection.

2.2.10.2 Real-time quantitative *PCR* (qPCR)

RNA was isolated from cells using a Total RNA Mini Kit following the manufacturer's instructions. For the synthesis of *complementary DNA* (cDNA) First Strand cDNA Synthesis Kit was used and RNA concentration and quality were assessed with a NanoDrop spectral photometer. qPCR was executed with 2 µL of cDNA (5 ng), 5 µL SYBR Green and 0.4 µL of the respective primer sequences (1/10 in H_2O, stock: 1 µg/mL), filled up to 10 µL with RNase-free water. Finally, samples were analyzed on a QuantStudio 5 Real-Time PCR System.

RT-qPCR program:

Step 1	95°C	10 min
Step 2	95°C	15 s
Step 3	60°C	1 min

→ go to step 2, 40x

Step 4-6 for melting curve:

Step 4	95°C	15 s
Step 5	60°C	1 min
Step 6	95°C	15 s

Relative mRNA levels were calculated using the $\Delta\Delta C_T$ method normalized to the reference gene *Hprt1*.

2.2.10.3 Insulin extraction from tissue and cells

To determine pancreatic insulin levels, Mice were euthanized by CO_2 and blood was removed by heart puncture. A piece of 50 mg was dissected from the tail of the pancreas, which is directly connected with the spleen, and homogenized in 5 mL of 70 % ethanol supplemented with 1.5 % HCl using a Polytron homogenizer. After incubation for 24 70 % ethanol supplemented with 1.5 % HCl was added to the wells and kept at -20°C for 24 h, followed by the above-described procedure.**Quantification of signaling molecules**

For the determination of insulin concentrations, a commercially available sandwich-based ELISA kit (CrystalChem) was used according to the manual instructions. In short, serum was generated by centrifugation of blood samples for 10 min at 13,000 g and 4°C. 5 µL of serum or pancreas extract was added to 95 µL dilution buffer and incubated for 2 h at 4°C in antibody-coated wells. After washing, 100 µL of antibody solution was added and kept for 30 min at RT. Following washing, 100 uL of substrate solution was added and incubated at RT for 40 min. The reaction was stopped by the addition of 100 µL stop solution and absorption at 450 nm, together with background absorption at 630 nm, was measured with a Spark 10M microplate reader.

To quantify glucagon levels, a sandwich ELISA kit (CrystalChem) was used as described in the manufacturer's manual. In brief, blood was centrifuged for 10 min at 13,000 g and 4°C for serum generation. 10 µL of serum and 100 µL of labeled antibody were added into antibody-coated wells. After incubation for 20 h at 4°C, the wells were washed and filled with 100 µL substrate solution. This was followed by

incubation for 30 min at RT with subsequential addition of 100 µL stop solution. Finally, absorption at 450/630 nm was measured.

20-HETE was quantified by a competitive ELISA (Abcam) according to the manual instructions. In summary, serum was generated by keeping blood samples for 30 min at RT to allow coagulation. Subsequently, samples were spun down at 2000 g and 4°C for 10 min to obtain serum. 50 µL of serum or supernatant of activated platelets (PS) were loaded together with 50 µL of sample diluent and 100 µL of HRP conjugate into antibody-coated wells. After 2 h of incubation at RT, the wells were washed and filled with 200 µL substrate solution. The reaction was terminated after 20 min by the addition of 100 µL 1 N sulfuric acid and absorption was measured at 450 nm.

2.2.11 LC-MS Lipidomic Analysis

Lipid extraction was performed by mixing 10 µL of the sample with 170 µl of 10 mM HCl, 190 µL methanol, and 20 µL external standards (100 µM D7-cholesterol, 50 µM D7-7DHC, 10 µM each of D31-hexadecanoic acid, *lysophosphatidic acid* (LPA)-(17:0), and LPC-(17:0)) in 1/1 chloroform/methanol (v/v). Successively, 90 µl and 100 µl of chloroform were added and mixed thoroughly in between. Then, the resulting upper phase was reextracted with 300 µL of synthetical lower phase, and the combined lower phases were evaporated under a stream of nitrogen gas at 30°C. The residues were dissolved in 50 µL of 2-propanol for further analysis.

Solvent A		Solvent B	
Methanol	5 % (v/v)	Acetonitrile	45 % (v/v)
Water	94.9 % (v/v)	2-Propanol	45 % (v/v)
Formic acid	0.1 % (v/v)	Water	0.9 % (v/v)
		Formic acid	0.1 % (v/v)

3 µL of the sample were loaded on an Acclaim 120 C8 HPLC column. LC-separation occurred at a flow rate of 200 µL/min at 45°C, starting with 20 % solvent B for 2 min, which was linearly increased to 100 % within 7 min, kept for another 28 min, and finally returned to 20 % solvent B within 1 min and maintained like this for 5 min for

equilibration. Eluent accessed the heated electrospray unit of the Q Exactive mass spectrometer from 4 min to 34 min after sample injection. Chromatograms were recorded with a scan range of 200-1650 m/z in alternating negative and positive modes at 70,000 nm resolution. Peaks corresponding to calculated monoisotopic metabolite masses (+/- 3 mMU) were integrated using TraceFinder V3.3 software.

2.2.12 Statistical analysis

Results are presented as ± *standard error of the mean* (SEM) or ± *standard deviation* (SD), depending on the sample size. To assess the significance a two-tailed Student's t-test for independent groups was used and a two-way *analysis of variance* (ANOVA), followed by a post hoc Tukey's test served for multiple comparisons. P-values < 0.05 were considered statistically significant (* $P< 0.05$; ** $P < 0.01$; *** $P < 0.001$) and P-values ≥ 0.05 were considered *not significant* (NS).

3 RESULTS

3.1 Platelets get activated during hyperglycemia and specifically localize in the microvasculature of pancreatic islets

For decades, it has been known that platelets from diabetic patients often show an increased reactivity and basal activation[250,251]. Therefore, several *in vitro* and *in vivo* approaches were applied to investigate different influencing factors that might cause the platelet phenotype during the pathophysiological state of diabetes.

3.1.1 High glucose levels increase platelet activation, degranulation, and binding to collagen

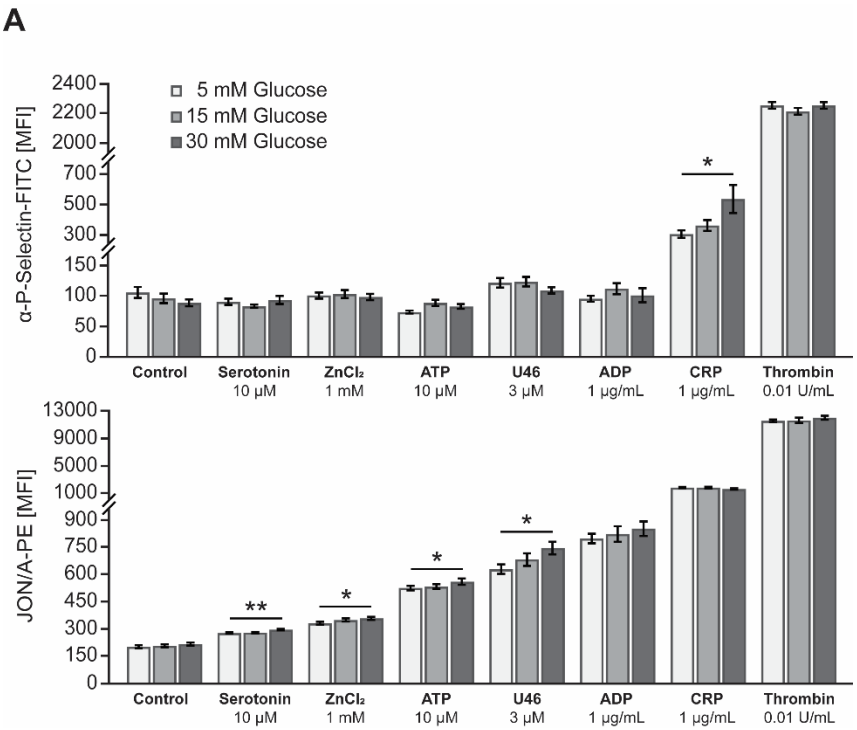

Figure 7: Glucose promotes platelet activation. (**A**) P-Selectin exposure and αIIbβ3 integrin activation of C57BL/6JRj mouse platelets after incubation of blood for 12 min with different platelet activators in the presence of 5 mM, 15 mM, and 30 mM glucose. n=12. Each n represents a measurement of a sample from distinct mice. *P < 0.05; **P < 0.01. Unpaired t-test. Data are mean ± SEM.

Diabetes is linked to the dysfunctional regulation of glucose homeostasis. Therefore, it is thinkable, that platelet hyperreactivity frequently observed in diabetics is caused by hyperglycemia, which is a result of improper glycemic control. To test the relevance

of glucose in the context of hyperreactive platelets, mouse blood was treated with different concentrations of glucose in the presence of common platelet activators. The subsequent flow cytometry analysis allowed the quantification of α-granule-specific P-selectin exposure (WUG1.9-FITC-antibody) and integrin αIIbβ3 activation (JON/A-PE-antibody) that determine the degree of platelet activation[411]. Although glucose itself did not affect P-selectin exposure, it further promoted the CRP-induced degranulation process (Figure 7A). Similarly, increasing glucose concentrations significantly stimulated serotonin-, $ZnCl_2$-, ATP-, and U46-induced integrin αIIbβ3 activation, the latter being a TxA_2 analog (Figure 7A)[412]. Even though the effect size is not large in the case of serotonin, $ZnCl_2$, and ATP, glucose seems to amplify platelet activation in the presence of additional activators.

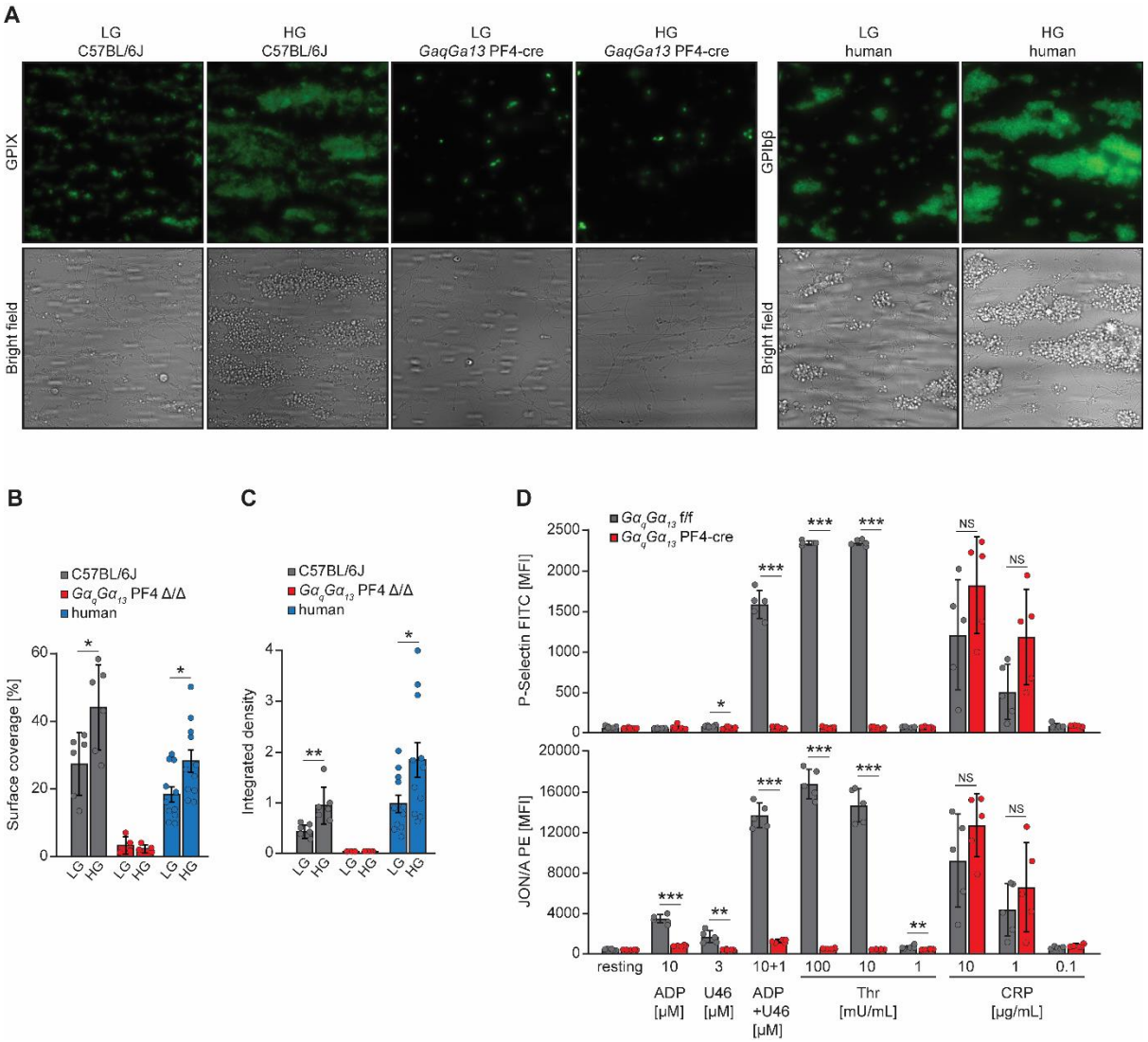

Figure 8: Glucose promotes the binding of platelets to collagen. (**A**) Representative fluorescence and brightfield microscopic images of platelets bound to collagen during flow conditions of anti-

coagulated whole blood from C57BL/6JRj mice, $G\alpha_qG\alpha_{13}$ PF4 Δ/Δ mice, or human donors. Before the assay, blood samples were incubated for 5 min with 2.4 mM (low glucose, LG) or 25 mM glucose (high glucose, HG). (**B and C**) Quantified surface coverage (B) and integrated density (C) of platelet aggregates formed under conditions described in (A). C57BL/6JRj, n=6; $G\alpha_qG\alpha_{13}$ PF4 Δ/Δ, n=4; human, n=11. (**D**) Flow cytometry was used to assess P-selectin exposure and integrin αIIbβ3 activation of platelets from $G\alpha_qG\alpha_{13}$ PF4 Δ/Δ and $G\alpha_qG\alpha_{13}$ f/f mice after stimulation with indicated agonists. n=5. Each n represents a measurement of a sample from distinct mice or humans. *P < 0.05; **P < 0.01; ***P < 0.001; NS, not significant. Unpaired t-test. Data are mean ± SEM for humans in (B, C) or ± SD for C57BL/6JRj and $G\alpha_qG\alpha_{13}$ PF4 Δ/Δ mice in (B-D).

To test whether the amplifying effect of glucose on platelet activation is strong enough to affect their binding to collagen, a whole blood perfusion system was applied. Therefore, whole blood of C57BL/6JRj mice and humans was incubated for 5 min with 2.4 mM or 25 mM glucose in the presence of Alexa488-coupled antibodies specific for mouse GPIX or human GPIbβ, respectively. Samples were run through a collagen-coated flow chamber, thus thrombus formation on collagen could be quantified afterwards (Figure 8A-C). To investigate the role of the activator machinery of platelets in glucose-stimulated platelet activation, mice with a platelet-specific deficiency for functional $G\alpha_q$ and $G\alpha_{13}$ using the Cre-Lox system were applied. In this model, the Cre-recombinase is expressed under the control of the MK-specific PF4 promoter[408-410]. Platelets of resulting $G\alpha_qG\alpha_{13}$ PF4 Δ/Δ mice exhibit a strongly reduced activation by major soluble agonists such as TxA_2, thrombin, and ADP, which we further confirmed by flow cytometry analysis (Figure 8D)[408,409,413]. Quantification of thrombus formation under flow conditions revealed, that high glucose conditions increased thrombus coverage and the integrated density of blood samples from wild-type mice and humans. However, blood samples from $G\alpha_qG\alpha_{13}$ PF4 Δ/Δ mice showed greatly reduced thrombus formation, whereas elevated glucose concentrations did not lead to an increase in thrombus formation (Figure 8B, C). It can be deduced that glucose promotes the binding of platelets to collagen and that this effect is dependent on their activation machinery.

3.1.2 A β-cell-derived factor/s promotes platelet activation, degranulation, and binding to collagen

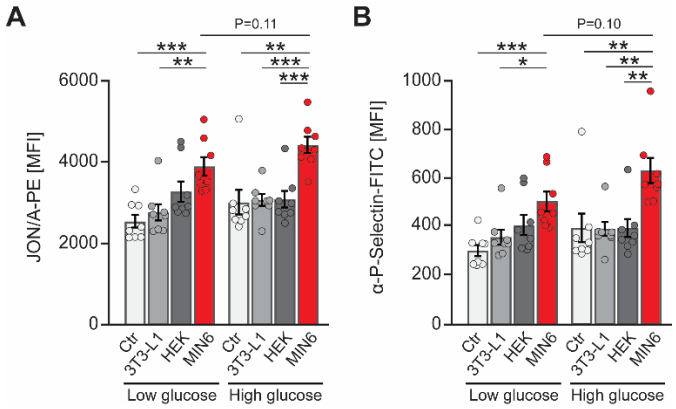

Figure 9: A β-cell-derived factor/s stimulates platelet activation. (**A and B**) Integrin αIIbβ3 activation (A) and P-selectin exposure (B) of platelets incubated for 12 min with low or high glucose medium supernatants of indicated cells or control supernatant (Ctr) in the presence of 1 µg/mL CRP. n=8. Each n represents a measurement of a sample from distinct mice. *P < 0.05; **P < 0.01; ***P < 0.001; Unpaired t-test. Data are mean ± SEM.

Elevated glucose levels in living organisms trigger the release of insulin by β-cells, to maintain euglycemia by enhancing peripheral glucose uptake[7]. In this process, β-cells co-release several other substances such as Zn^{2+} and ATP[139,414]. To assess the potential role of β-cell-derived factor/s on platelet activation, we generated medium supernatant of the mouse β-cell line MIN6, 3T3-L1 and HEK as control cells, and control supernatant that was generated in the absence of cells[415]. As MIN6-cells exhibit elevated degranulation rates upon high glucose conditions, those supernatants were generated in the presence of 2.8 mM or 25 mM glucose. Afterwards, glucose concentrations of resulting supernatants were adjusted to 25 mM and whole blood of C57BL/6JRj mice was incubated with resulting supernatants in a ratio of 1:3 in the presence of an additional 1 µg/mL CRP as a co-stimulus. Assessment of platelet activation by flow cytometry showed that the presence of high-glucose MIN6-supernatant significantly increased integrin αIIbβ3 activation and degranulation compared to different control supernatants (Figure 9A, B). Additionally, although the difference is not statistically significant, high-glucose MIN6-supernatant tends to enhance platelet activation to a greater extent than low-glucose MIN6-supernatant (Figure 9A, B). According to these results, β-cells seem to secrete a factor/s that increases platelet activation.

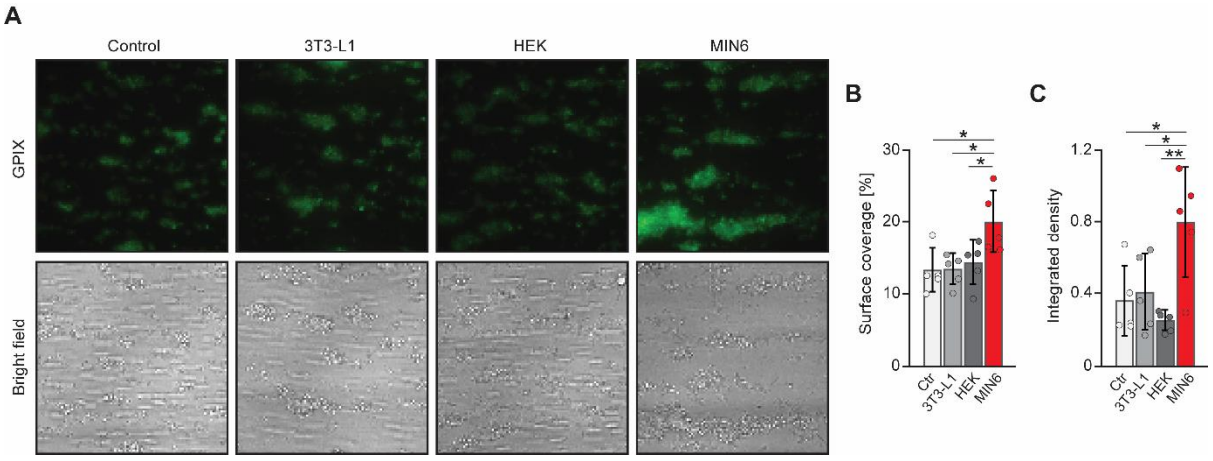

Figure 10: A β-cell-derived factor/s enhances platelet binding to collagen. (**A**) Representative fluorescence and bright field microscopic images of whole blood thrombus formed in a perfusion system on collagen. Before the assay, blood from C57BL/6JRj mice was incubated for 5 min with supernatants of indicated cells or control supernatant (Ctr). (**B, C**) Quantified surface coverage (A) and integrated density (B) of thrombi formed under conditions described in (A). n=5. Each n represents a measurement of a sample from distinct mice. *P < 0.05; **P < 0.01. Unpaired t-test. Data are mean ± SD.

Next, we were addressing whether the activatory action of β-cells' medium supernatant also promotes binding to collagen in the whole blood perfusion system. Preincubation of blood from C57BL/6JRj mice for 5 min with MIN6 high-glucose supernatant was sufficient to increase thrombus formation compared to respective control supernatants described in the previous section (Figure 10). In light of this functionality experiment, the results of flow cytometry on the activating impact of a substance/s released by β-cells may be confirmed.

3.1.3 Acute hyperglycemia induces platelet degranulation *in vivo*

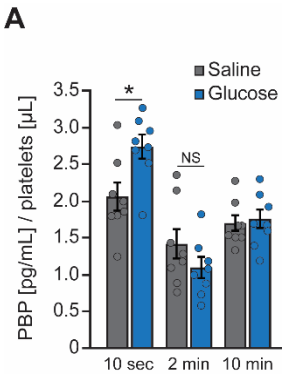

Figure 11: Acute hyperglycemia induces platelet degranulation *in vivo*. (**A**) Plasma levels of platelet basic protein (PBP) after i.v. injection of glucose or saline into C57BL/6JRj mice normalized to platelet count. n=8. Each n represents a measurement of a sample from distinct mice. *P < 0.05; NS, not significant. Unpaired t-test. Data are mean ± SEM.

Knowing that high glucose levels themselves, as well as a β-cell released factor/s, can promote platelet activation in the presence of an additional stimulus, hyperglycaemic conditions might be able to induce a certain degree of platelet activation. For this reason, 2 g/kg of glucose solution or saline was i.v. injected into fasted C57BL/6JRj mice and blood samples were subsequently collected after specific time points. Levels of PBP plasma levels served as a marker for platelet activation, as it gets released specifically from α-granules of platelets upon activation[416,417]. Of note, induced acute hyperglycemia caused immediately elevated PBP levels (Figure 11A). In conclusion, platelets are activated *in vivo* during hyperglycemia, which is likely caused by increased glucose levels and substance/s derived from β-cells, as demonstrated earlier.

3.1.4 Platelets localize specifically in the microvasculature of pancreatic islets

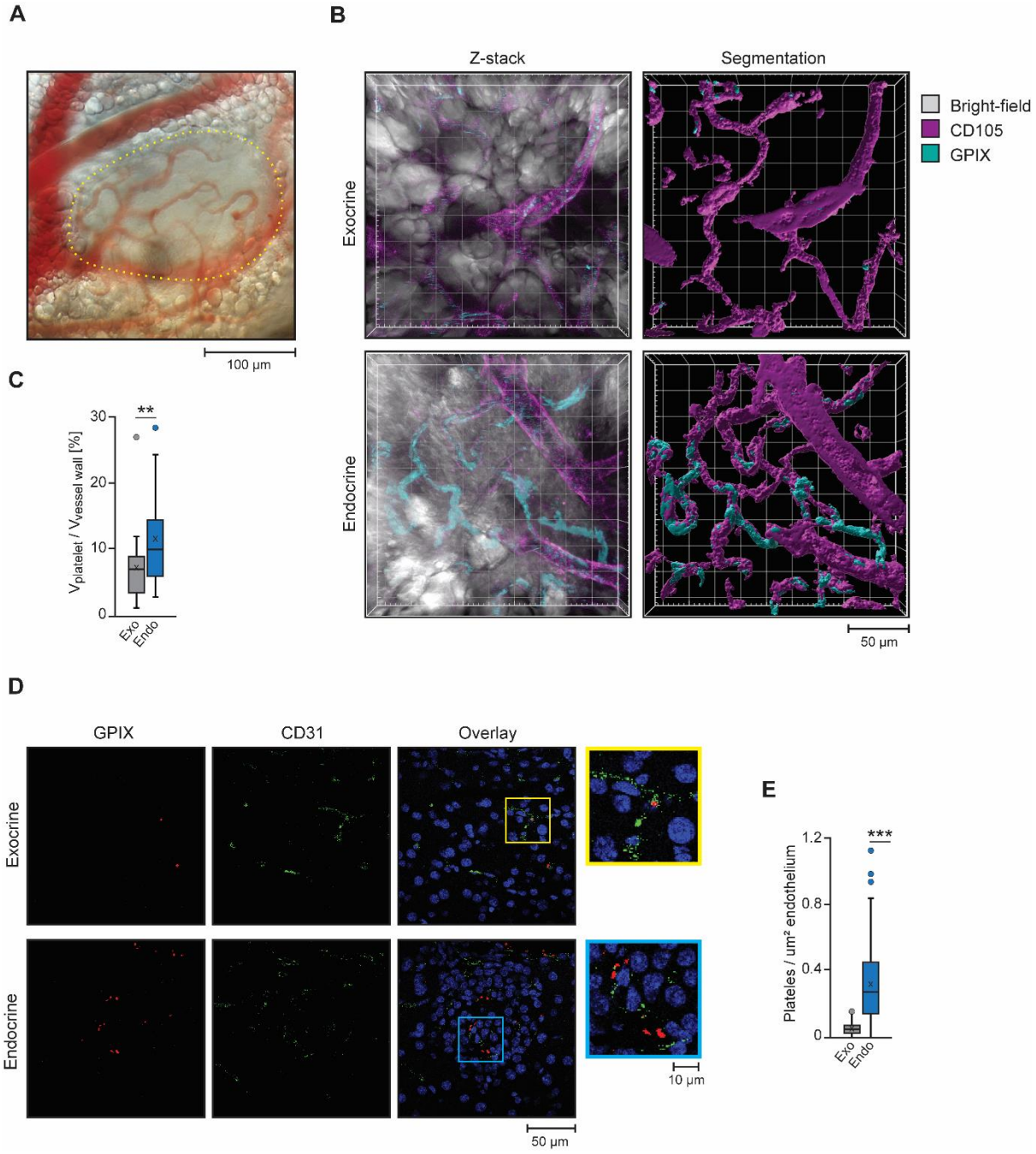

Figure 12: Platelets localize specifically in the microvasculature of the endocrine pancreas. (**A**) Representative image of C57BL/6JRj mouse pancreas obtained by bright-field microscopy during intra-vital imaging with highlighted localized pancreatic islet. (**B**) *In vivo* recorded representative z-stacks of exocrine and endocrine mouse pancreas both before and after segmentation. (**C**) The volume of vasculature-bound platelets normalized to the volume of endothelial cells from the exocrine (Exo) and endocrine (Endo) mouse pancreas. Exo, n=29; Endo, n=26 (five mice). Each n represents a z-stack of randomly selected exocrine tissue or an islet. (**D**) Representative fluorescence microscopy images of DAPI and immunostainings from mouse exocrine and endocrine pancreas. (**E**) Platelet count normalized to the endothelial area. Exo, n=131; Endo, n=112 (six mice). Each n represents an image of randomly selected exocrine tissue or an islet. **P < 0.01; ***P < 0.001. Unpaired t-test. Data are mean ± SEM.

It is hypothesized that platelets may regulate β-cell function. This is based on the fact that platelets store a variety of substances that can have a positive effect on these cells, and secondly on the fact that diabetics often exhibit platelet hyperreactivity. This assumption, together with our finding of platelets being activated by β-cell-derived substance/s raises the possibility, that platelets get transiently activated in the microvasculature of pancreatic islets. Therefore, we implemented intra-vital 3D confocal live imaging of mouse pancreas to investigate the platelet behavior within pancreatic islets *in vivo*. The distinct morphology of pancreatic endocrine tissue due to its increased cellular density and vascularization allowed the localization of islets through the brightfield channel of the microscope (Figure 12A). The application of fluorophore-labeled antibodies against CD105 and GPIX enabled the visualization of endothelium and platelets, respectively. Under these conditions, z-stacks of randomly selected exocrine tissue as well as identified endocrine tissue were recorded. Following image processing that took into account the platelet's distance from the endothelium and its size allowed discerning between adherent and free-floating platelets (Figure 12B). Interestingly, the normalization of the platelet volume to the volume of endothelial cells revealed a significantly increased amount of adherent platelets within the endocrine pancreas (Figure 12C). To verify this result, fixed cryosections of the pancreas from C57BL/6JRj mice were stained for GPIX and the endothelium marker CD31 (Figure 12D). Also here, quantification of the platelet count displayed an increased presence of platelets within the vasculature of endocrine tissue (Figure 12E).

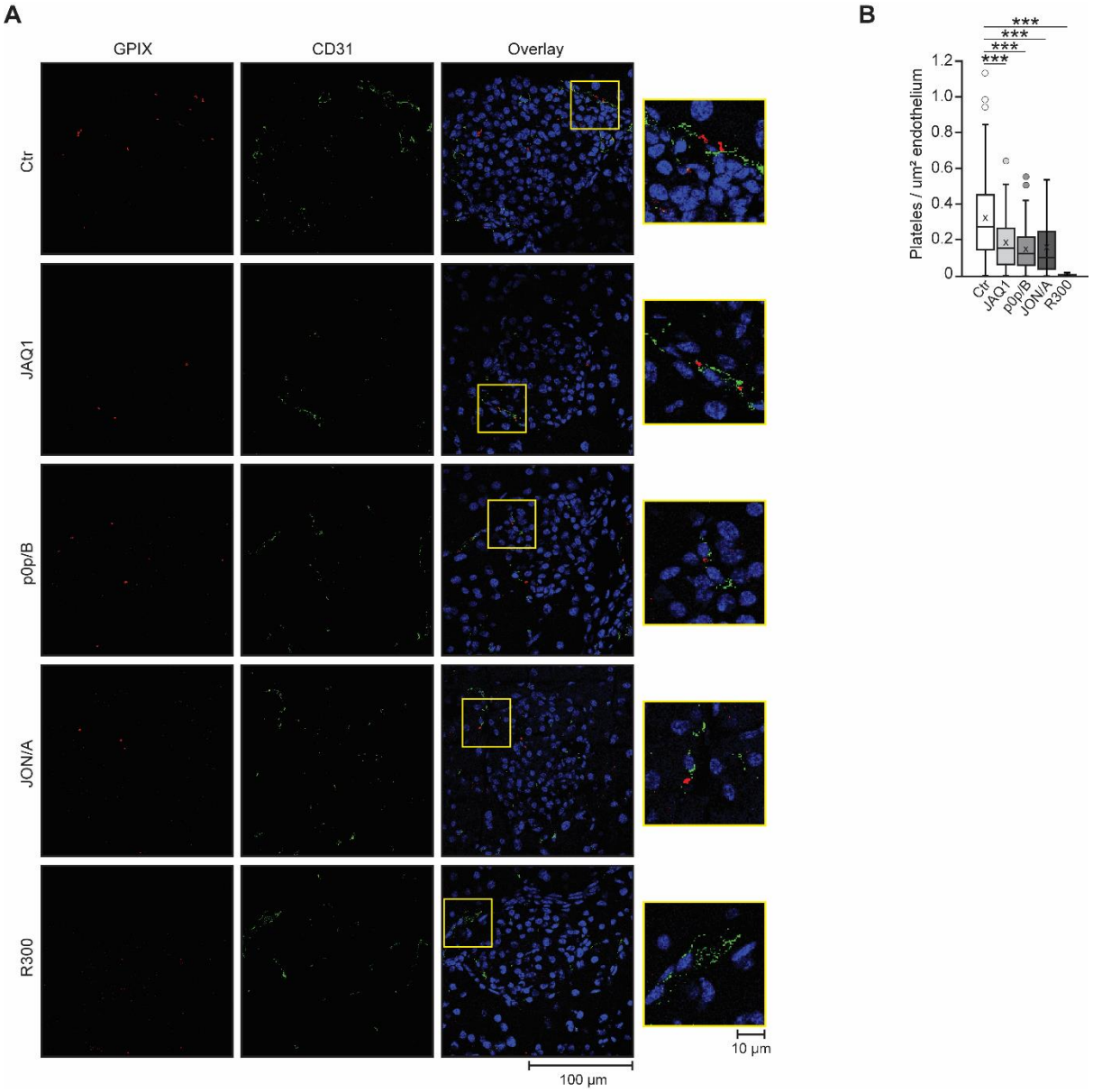

Figure 13: The binding of platelets to the microvasculature of pancreatic islets is mediated by platelet-specific surface receptors. (**A**) Representative fluorescence microscopy images of DAPI and immunostainings from the exocrine and endocrine pancreas of mice treated with indicated antibody constructs. (**B**) Platelet count normalized to the endothelial area. Control, n=131 (six mice); JAQ1 IgG, n=71 (six mice); p0p/B F(ab')$_2$, n=113 (six mice); JON/A F(ab')2, n=77 (six mice), R300 IgG, n=27 (three mice). Each n represents an image of an islet. ***P < 0.001. Unpaired t-test. Data are mean ± SEM.

To determine which platelet surface proteins are involved in the interaction with pancreatic islet microvasculature, several antibody constructs that block or deplete specific platelet receptors were used. C57BL/6JRj mice were injected with JAQ1 IgG to deplete the major platelet-activating receptor GPVI, p0p/B Fab-fragment or JON/A F(ab)$_2$-fragment to block the main ligand-binding site of GPIbα and integrin αIIbβ3, respectively, or the R300 mixture of different monoclonal antibodies against GPIbα

that mediates a rapid decrease of platelet count to less than 5 %[411,418-421]. After 24 hours, the pancreas was removed, whereby the removal took place after 5 days in the case of JAQ1 IgG injection since this antibody leads to transient thrombocytopenia that recovers after several days[418]. Fluorescence immunohistological analysis of cryosections of the pancreas from mice with depleted or blocked surface receptors showed reduced counts of platelets in pancreatic islets compared to mice that received a nonimmunological control IgG (Figure 13A, B). Moreover, the presence of platelets is completely diminished after platelet depletion, which is used as a negative control confirming the accuracy of the experiment (Figure 13B). Taking together, this result proves a specific adherence of platelets within pancreatic islets that is mediated by several platelet surface receptors (GPVI, GPIbα, and integrin αIIbβ3) potentially being triggered by β-cell-derived substance/s.

3.2 Inhibited platelet functionality decreases glucose-stimulated insulin secretion

Platelets store and release a high variety of substances from which some, such as purines, serotonin, histamine, and lipids are known to execute insulinotropic effects[114,138,139,234,315,316,401-404]. Further, diabetic subjects often exhibit an elevated basal platelet activation, suggesting a regulatory role of platelets in the maintenance of euglycemia[250,251]. The data described above reinforce this theory. Accordingly, glucose as well as β-cell-derived factor/s promote platelet activation. Additionally, platelets were demonstrated to adhere preferentially to the microvasculature of the endocrine pancreas. To finally assess whether platelets do affect β-cell function, different animal models with defined abnormalities in platelet function were used. This allowed determining whether these deficiencies were related to alterations in glucose homeostasis.

3.2.1 Genetic ablation of platelet functionality results in glucose intolerance due to decreased GSIS

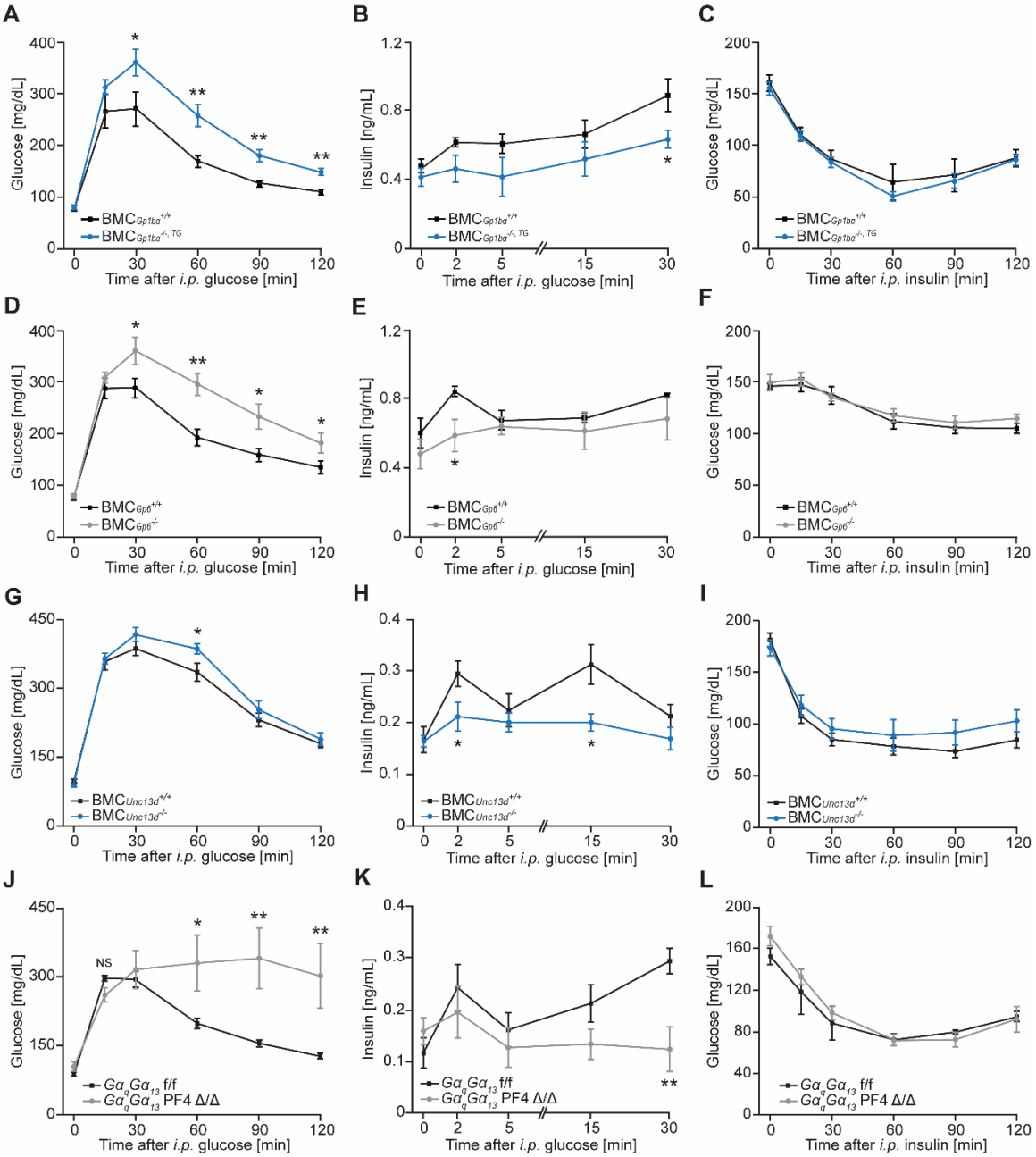

Figure 14: Genetic ablation of platelet functionality causes glucose intolerance through reduced insulin secretion. (**A-C**) Glucose tolerance test (GTT), glucose-stimulated insulin secretion (GSIS), and insulin tolerance test (ITT) of Gp1bα$^{-/-,TG}$ bone marrow chimeric mice (BMC) and respective control. BMC$_{Gp1bα}^{+/+}$, n=8; BMC$_{Gp1bα}^{-/-,TG}$, n=10 (A). BMC$_{Gp1bα}^{+/+}$, n=6; BMC$_{Gp1bα}^{-/-}$,TG, n=8 (B). BMC$_{Gp1bα}^{+/+}$, n=5; BMC$_{Gp1bα}^{-/-,TG}$, n=8 (C). (**D-F**) GTT, GSIS, and ITT of BMC$_{Gp6}^{+/+}$ mice and respective control. BMC$_{Gp6}^{+/+}$, n=15; BMC$_{Gp6}^{-/-}$, n=14 (D). BMC$_{Gp6}^{+/+}$, n=6; BMC$_{Gp6}^{-/-}$, n=6 (E). BMC$_{Gp6}^{+/+}$, n=12; BMC$_{Gp6}^{-/-}$, n=7 (F). (**G-I**) GTT, GSIS, and ITT of BMC$_{Unc13D}^{-/-}$ and respective control. BMC$_{Unc13D}^{+/+}$, n=9; BMC$_{Unc13D}^{-/-}$, n=9 (G). BMC$_{Unc13D}^{+/+}$, n=9; BMC$_{Unc13D}^{-/-}$, n=7 (H). BMC$_{Unc13D}^{+/+}$, n=9; BMC$_{Unc13D}^{-/-}$; n=9 (I). (**J-L**) GTT, GSIS, and ITT of Gα$_q$Gα$_{13}$ PF4 Δ/Δ mice and respective control. Gα$_q$Gα$_{13}$ f/f, n=9; Gα$_q$Gα$_{13}$ PF4 Δ/Δ, n=6 (J). Gα$_q$Gα$_{13}$ f/f, n=12; Gα$_q$Gα$_{13}$ PF4 Δ/Δ, n=9 (K). Gα$_q$Gα$_{13}$ f/f, n=8; Gα$_q$Gα$_{13}$ PF4 Δ/Δ, n=7 (L). For GTT 2 g/kg (A, G, J) or 1.5 g/kg (D) glucose, for GSIS 3 g/kg (B, H, K) or 2 g/kg (E) glucose, and for ITT 0.5 U (C, I, L) or 0.25 U (F) insulin was injected. Each n represents the measurement of a sample from distinct mice. *P < 0.05; **P < 0.01; NS, not significant. Unpaired t-test. Data are mean ± SEM.

Previous results have demonstrated reduced platelet localization within pancreatic islets when major platelet surface receptors were depleted or inhibited (Figure 13B). For this reason, a mouse model deficient for a functional GPIbα subunit that mediates binding of the GPIb-IX-V complex to vWF, thus being crucial for the initial tethering of platelets was established[255]. Deficiency of GPIbα is associated with severe impairment of platelet formation leading to macrothrombocytopenia[422]. This issue can be circumvented by the re-expression of an engineered GPIbα construct, in which the extracellular domain is replaced by the α-subunit of the human interleukin 4 receptor in GPIbα knockout mice. Resulting $Gp1b\alpha^{-/-,TG}$ mice exhibit normal platelet counts but retain a severe bleeding phenotype[406]. Although MKs and platelets are the primarily GPIbα expressing cells, BMC were generated to restrict the deficiency of functional GPIbα only to cells originating from bone marrow hematopoietic stem cells[423]. Therefore, C57BL/6JRj mice were lethally irradiated before being reconstituted with either C57BL/6JRj or $Gp1b\alpha^{-/-,TG}$ bone marrow. To investigate whether the present platelet defect leads to changes in glucose homeostasis, the mice were challenged with three different metabolic assays. For the *glucose tolerance test* (GTT), a defined dosage of glucose solution was injected i.p. and the insulin-mediated clearance from the blood over time was monitored. Strikingly, the rate of decline in glucose levels was slower in $BMC_{Gp1b\alpha}{}^{-/-,TG}$ mice, indicating glucose intolerance (Figure 14A). To evaluate whether this is due to reduced insulin secretion as a response to high blood glucose levels, the *glucose-stimulated insulin secretion* (GSIS) in these animals was measured. Indeed, i.p. administration of a glucose solution led to reduced serum insulin levels compared to respective control mice (Figure 14B). Finally, mice were subjected to an *insulin tolerance test* (ITT) to determine whether insulin tolerance has changed. However, i.p. injection of insulin caused comparable decreases in blood glucose levels, leading to the conclusion that the observed glucose intolerance is predominantly due to decreased insulin secretion rather than insulin intolerance (Figure 14C). Next, another mouse model was introduced to decipher the role of platelets in glucose homeostasis. This model was targeting GPVI, which is the major platelet signaling receptor for collagen-initiating platelet activation[257]. Also here, BMCs were generated to restrict the GPVI deletion to bone marrow-derived cells. Similar to $BMC_{Gp1b\alpha}{}^{-/-,TG}$ mice, $BMC_{Gp6}{}^{-/-}$ mice were demonstrated to be glucose intolerant through reduced insulin secretion upon glucose challenge, whereas insulin tolerance was unchanged (Figure 14D-F). Since it was demonstrated, that platelet attachment

and activation presumably affect insulin secretion, the question was raised to what extent amplification of hemostasis influences it. Once GPVI binds to collagen intracellular signaling cascades get induced that upon others lead to degranulation to induce a second wave platelet activation[257]. It was shown that Munc13-4 encoded by *Unc13d* plays a key function in the degranulation process, as its deletion led to an abrogation of dense granule secretion and a reduced α-granule secretion[407,424,425]. Consistent with the other mouse models, bone marrow-restricted deletion of Munc13-4 caused reduced glucose tolerance and insulin secretion without alterations in insulin sensitivity (Figure 14G-I). Finally, the relevance of the machinery responsible for second-wave activation was investigated in the context of glucose homeostasis. As mentioned earlier, $G\alpha_q G\alpha_{13}$ PF4 Δ/Δ mice displayed strongly diminished activation by soluble platelet activators, which was also associated with abolished glucose-promoted platelet binding to collagen (Figure 8A-D). The severe inability of platelet activation in these mice was transferrable to their glucose homeostasis, as the GTT revealed a strong glucose intolerance in these mice (Figure 14J). In line with this, insulin secretion was greatly reduced, while insulin sensitivity was unchanged (Figure 14K, L). To sum up, platelets seem to positively affect glucose tolerance by elevating GSIS. In addition, platelets appear to need to be fully functional for this effect.

3.2.2 Platelets do not affect islet morphology

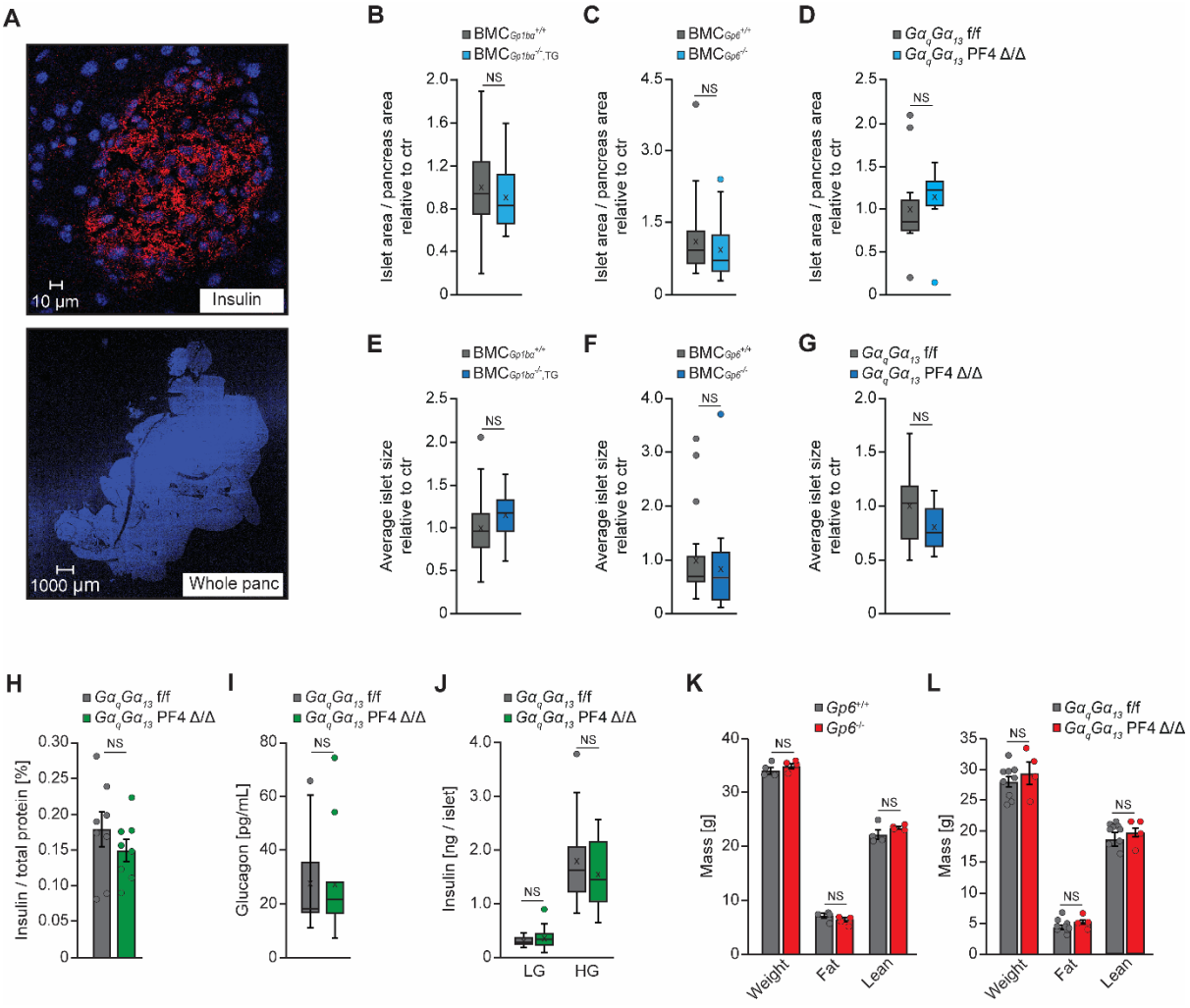

Figure 15: Mice with genetic platelet defects exhibit normal islet characteristics. (**A**) A representative fluorescence microscopy image of DAPI and anti-insulin immunostaining from a pancreatic islet (above) and the respective tile scan of the whole pancreas section (below) used to quantify the islet area and size. (**B-G**) Normalized islet area (B-D) and average islet size (E-G) relative to the respective control (ctr) of $BMC_{Gp1b\alpha}^{-/-,TG}$ (B, E), $BMC_{Gp6}^{-/-}$ (C, F), and $G\alpha_qG\alpha_{13}$ PF4 Δ/Δ (D, G) mice with respective control. $BMC_{Gp1b\alpha}^{+/+}$, n=32 (eight mice); $BMC_{Gp1b\alpha}^{-/-,TG}$, n=28 (seven mice, B, E). $BMC_{Gp6}^{+/+}$, n=24 (eight mice); $BMC_{Gp6}^{-/-}$, n=18 (six mice, C, F). $G\alpha_qG\alpha_{13}$ f/f, n=15 (five mice); $G\alpha_qG\alpha_{13}$ PF4 Δ/Δ, n=12 (four mice, D, G). Each n represents the average value of one tissue section. (**H**) Insulin content of pancreas from $G\alpha_qG\alpha_{13}$ PF4 Δ/Δ mice and respective control normalized to total protein. $G\alpha_qG\alpha_{13}$ f/f, n=8; $G\alpha_qG\alpha_{13}$ PF4 Δ/Δ, n=8. Each n represents the measurement of a sample from distinct mice. (**I**) Glucagon serum levels of $G\alpha_qG\alpha_{13}$ PF4 Δ/Δ mice fasted overnight with respective control. $G\alpha_qG\alpha_{13}$ f/f, n=12; $G\alpha_qG\alpha_{13}$ PF4 Δ/Δ, n=11. Each n represents the measurement of a sample from distinct mice. (**J**) Insulin release per islet isolated from $G\alpha_qG\alpha_{13}$ PF4 Δ/Δ or control mice upon 2.8 mM (LG) and 16.7 mM glucose (HG). $G\alpha_qG\alpha_{13}$ f/f, n=16; $G\alpha_qG\alpha_{13}$ PF4 Δ/Δ, n=38. Each n represents an independent biological replicate. (**K, L**) Body weight and composition of $Gp6^{-/-}$ (K) and $G\alpha_qG\alpha_{13}$ PF4 Δ/Δ (L) mice with respective control. $Gp6^{+/+}$, n=4; $Gp6^{-/-}$, n=4 (K). $G\alpha_qG\alpha_{13}$ f/f, n=9; $G\alpha_qG\alpha_{13}$ PF4 Δ/Δ, n=4 (L). Each n represents the measurement from distinct mice. NS, not significant. Unpaired t-test. Data are mean ± SEM. Data in boxplots: center line shows the median; the cross indicates the mean; the box defines the first and third quartiles; the whiskers indicate the 1.5 × interquartile range; outliers are individually plotted.

The decreased capacity of mice exhibiting platelet defects to release sufficient amounts of insulin in response to a glucose challenge may be caused by a reduction in the mass of pancreatic endocrine tissue or other developmental defects. This hypothesis is reinforced by the fact that platelets store and release various mitogenic substances and growth factors that could potentially affect pancreatic islet development[231-233]. Histological analysis of the pancreas was performed to address this possibility. IF staining for insulin enabled the identification of the endocrine pancreas and the DAPI signal was used to determine the entire pancreas size of each respective section using the tile-scan function of the confocal microscope (Figure 15A). No significant alterations were found when the endocrine pancreas area was quantified in relation to the total pancreatic area in $BMC_{Gp1b\alpha}^{-/-,TG}$, $BMC_{Gp6}^{-/-}$, and $G\alpha_qG\alpha_{13}$ PF4 Δ/Δ mice compared to their respective controls (Figure 15B-D). In addition, the average island size of these mouse models was unchanged (Figure 15E-G). Furthermore, performing an insulin extraction from pancreas tissue showed no difference in $G\alpha_qG\alpha_{13}$ PF4 Δ/Δ mice (Figure 15H), and also fasted glucagon serum levels in these mice were not altered, suggesting no change in function or mass of other endocrine cells (Figure 15I). For the assessment of the functionality of isolated islets, the whole pancreas was digested with collagenase and hand-picked islets were treated with low glucose (2.8 mM) and high glucose (16.7 mM) conditions. Of note, islets derived from $G\alpha_qG\alpha_{13}$ PF4 Δ/Δ mice showed normal induction of insulin secretion when stimulated with high glucose, indicating that these islets were fully functional when taken out of the *in vivo* environment (Figure 15J). Finally, neither body weight nor body composition was changed in mouse models presenting platelet defects (Figure 15K). These findings indicate no major developmental alterations of pancreatic islets in the presence of defective platelets, but rather an acute promoting effect of platelets on β-cell insulin secretion.

3.2.3 Pharmacological inhibition of platelet functioning results in glucose intolerance due to reduced GSIS

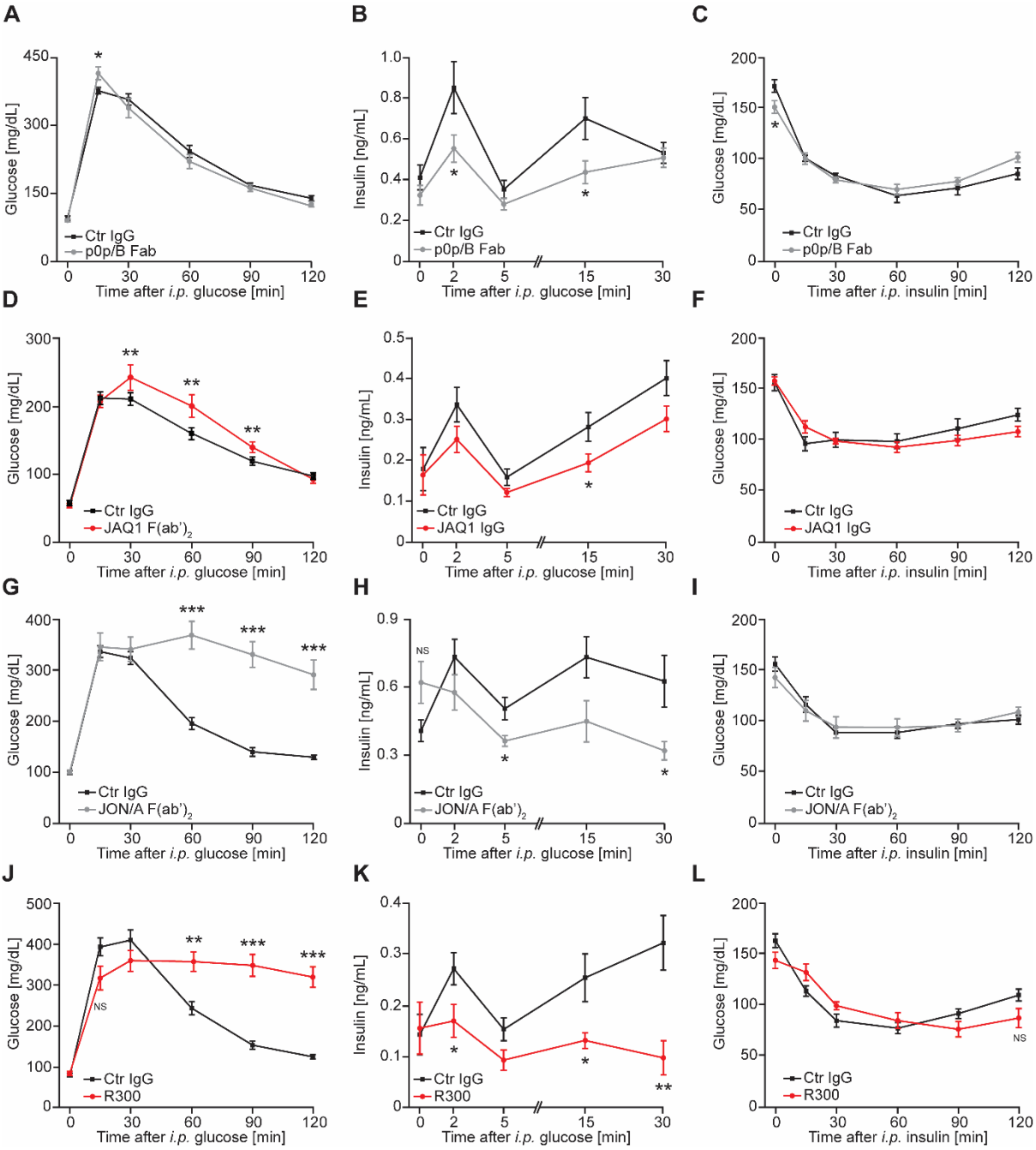

Figure 16: Pharmacologically induced platelet defects or depletion cause glucose intolerance due to reduced insulin secretion. (**A-C**) Glucose tolerance test (GTT), glucose-stimulated insulin secretion (GSIS), and insulin tolerance test (ITT) of p0p/B Fab and control IgG injected C57BL/6JRj mice. Ctr IgG, n=9; p0p/B Fab, n=10 (A). n=14 (B). n=10 (C). (**D-F**) GTT, GSIS, and ITT of JAQ1 F(ab')$_2$ (D) or JAQ IgG (E, F) and control IgG injected C57BL/6JRj mice. Ctr IgG, n=9; JAQ1 F(ab')$_2$, n=4 (D). n=11 (E). Ctr IgG, n=7; JAQ1 F(ab')$_2$, n=11 (F). (**G-I**) GTT, GSIS, and ITT of JON/A F(ab')$_2$ and control IgG injected C57BL/6JRj mice. Ctr IgG, n=8; JON/A F(ab')$_2$, n=10 (G). Ctr IgG, n=7; JON/A F(ab')$_2$, n=10 (H). Ctr IgG, n=8; JON/A-F(ab')$_2$, n=7 (I). (**J-L**) GTT, GSIS, and ITT of platelet-depleted C57BL/6JRj mice using R300 IgG (n=9) and mice receiving control IgG (n=9). Each n represents the measurement of a sample from distinct mice. *P < 0.05; **P < 0.01; ***P<0.001. Unpaired t-test. Data are mean ± SEM.

To prove that platelets exert a direct effect on β-cells, pharmacological tools were applied to induce a specific platelet defect in the short term, thereby eradicating any kind of long-term effect that platelets might execute. Thus, C57BL/6JRj mice received i.v. injections of p0p/B Fab to block Gp1bα, JAQ1 F(ab')$_2$ or JAQ1 IgG to block or deplete GPVI, respectively, or JON/A F(ab')$_2$, which blocks the main binding site of integrin αIIbβ3[411,418,419,421]. Additionally, the monoclonal antibody mix R300 was applied to mediate a rapid depletion of platelets from the circulation[420]. Mice were challenged with metabolic assays 24 h after the respective administration, or 5 days following in the case of JAQ1 IgG. Consistently, all models displayed a decreased glucose tolerance associated with reduced GSIS, whereas insulin sensitivity remained similar compared to their controls (Figure 16A-L). However, platelet defects seem to tendentially cause reduced blood glucose levels after 4 h of fasting as it is done for the ITT, which is significant for p0p/B Fab treated mice (Figure 16C). Further, observed glucose intolerance and abolished GSIS is very profound in integrin αIIbβ3 blocked and platelet-depleted mice (Figure 16G-L). In summary, this set of data supports the hypothesis that platelets directly stimulate β-cells to secrete insulin.

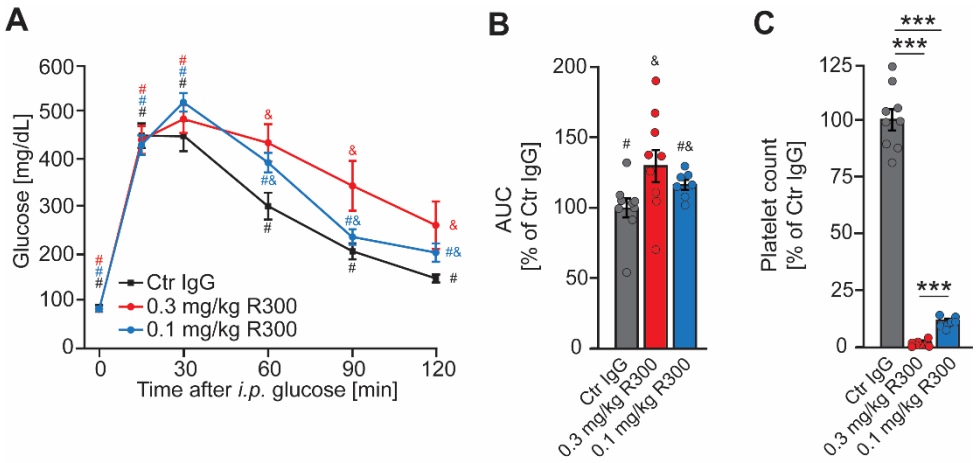

Figure 17: The stimulatory effect of platelets on β-cells insulin secretion is titratable. (**A, B**) Glucose tolerance test (A) and respective area under the curve (B) of platelet-depleted C57BL/6JRj mice using 0.3 mg/kg R300 IgG (n=9), 0.1 mg/kg R300 IgG (n=7), and mice receiving control IgG (n=9). (**C**) Platelet count of mice described in (A). Ctr IgG, n=9; 0.3 mg/kg R300 IgG, n=9; 0.1 mg/kg R300 IgG, n=7. Each n represents a measurement of a sample from distinct mice. ***P < 0.001. One-way ANOVA with post hoc Tukey test. The same symbols indicate no significant difference, whereas different symbols indicate significant differences (p<0.05) among groups (A, B). Unpaired t-test (C). Data are mean ± SEM.

To investigate the number of platelets that needs to be present to positively affect glucose tolerance, different concentrations of R300 were applied to C57BL/6JRj mice

to induce different degrees of platelet depletion. Thus, platelet count could be related to the respective glucose tolerance. From the results, it can be deduced that about 12 % of the regular platelet count is sufficient to maintain glucose tolerance (Figure 17A-C).

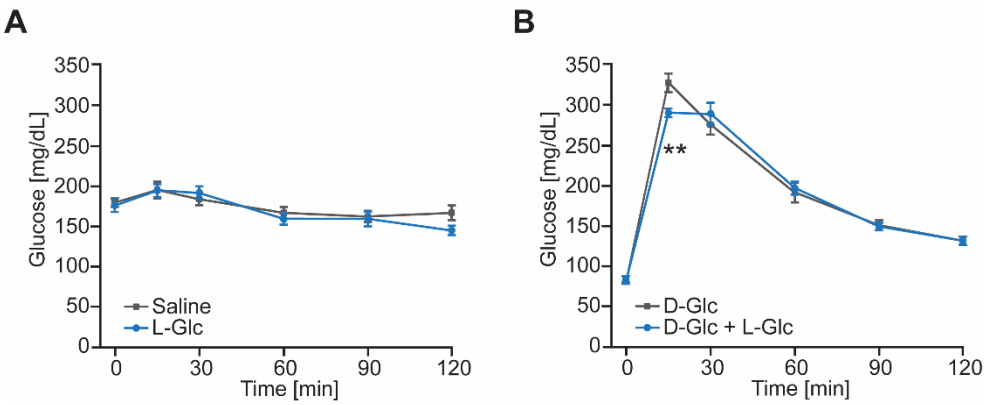

Figure 18: L-glucose promotes clearance of D-glucose from the blood. (**A**) Blood glucose levels of C57BL/6JRj mice injected with saline or 2 g/kg of L-glucose. n=10. (**B**) Glucose tolerance test of C57BL/6JRj mice injected with 1.5 g/kg D-glucose (n=10) or a mixture of 1.5 g/kg D-glucose and 1.5 g/kg L-glucose (n=12). **P < 0.01. Unpaired t-test. Data are mean ± SEM.

Previous results demonstrate abolished insulin secretion when platelet functioning was genetically or temporally inhibited (Figure 14, Figure 16). Thus, it is conceivable that raising platelet reactivity could ultimately result in increased insulin secretion. Glucose itself was shown to promote platelet activation and binding to collagen (Figure 7, Figure 8). Various sources indicated, that this effect is at least partially mediated by elevated osmolality and can be mimicked by mannitol or unmetabolizable L-glucose[216,426,427]. To see, whether L-glucose is able to mediate a lowering effect of blood D-glucose levels, C57BL/6JRj mice received a single i.v. injection of saline or 1.5 g/kg L-glucose solution. Mice were only fasted for 4 h to avoid too low blood glucose levels. The injection of L-glucose did not cause an increase in measured blood glucose levels, proving that the glucometer used for the quantification responded specifically to D-glucose (Figure 18A). However, no significant drop in blood glucose could be observed when L-glucose was injected into fasted mice (Figure 18A). Considering, that the promotive action of platelets on insulin secretion might only be present during high glucose conditions, 1.5 g/kg of L-glucose was co-injected with 1.5 g/kg of D-glucose to cause D-glucose mediated hyperglycemia. Here, the additional bolus of L-glucose led to a faster glucose clearance from the circulation

(Figure 18B). Based on these results, it can be speculated that the elevated osmolarity caused by L-glucose leads to increased platelet reactivity, which in turn improves glucose tolerance.

3.3 Platelets directly stimulate insulin secretion

The usage of pharmacological tools to induce platelet defects led to the conclusion that platelets acutely contribute to the promotion of β-cells' insulin secretion. However, the mechanism platelets mediate this effect could be of different natures. The mechanism might depend on the co-action of other cell types derived from the blood, vasculature, or endocrine pancreas. It is also conceivable that platelets positively influence β-cell sensing of glucose and corresponding insulin secretion through changes in blood circulation within the pancreatic islets. Finally, if platelets directly mediate their effect, it may be due to cell-cell interactions or an endocrine or autocrine process.

3.3.1 Platelet-derived factor/s potentiate insulin secretion

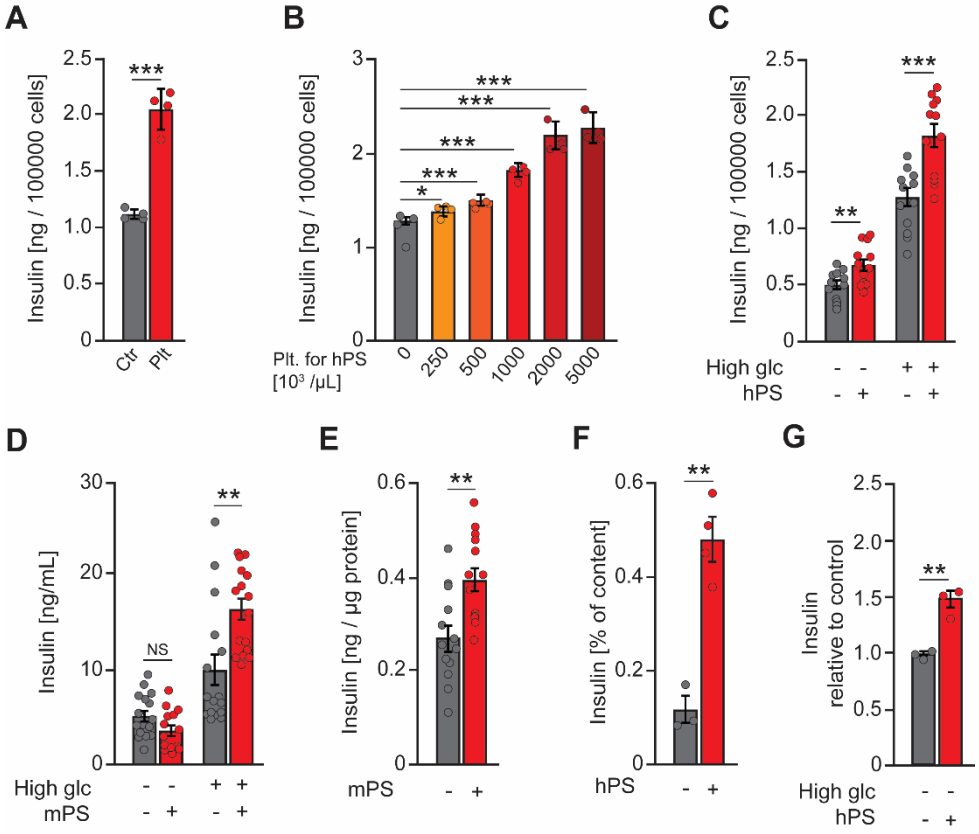

Figure 19: Factor/s released by platelets potentiate insulin secretion. (**A**) Normalized insulin secretion of INS1-cells co-cultured with human platelets (Plt) or control buffer (Ctr) at 2.8 mM glucose for 30 min. n=4. (**B**) Normalized insulin secretion of INS1-cells stimulated with human platelet

supernatant (hPS) generated with different platelet concentrations in the presence of 15 mM glucose. n=4. (**C**) Normalized insulin secretion of INS1-cells stimulated with hPS or control buffer upon low (2.8 mM) and high (15 mM) glucose. n=12. (**D**) Insulin secretion of isolated islets from C57BL/6JRj mice after 90 min of stimulation with mouse platelet supernatant (mPS) or control buffer during low (2.8 mM) or high (16.7 mM) glucose conditions. (-) High glc, (-) mPS, n=16; (+) High glc, (-) mPS, n=16; (-) High glc, (+) mPS, n=14; (+) High glc, (+) mPS, n=16. (**E**) Normalized insulin secretion of MIN6-cells stimulated with mPS or control buffer upon 25 mM glucose. n=13. (**F**) Normalized insulin secretion of human EndoC-βH5 cells stimulated with hPS upon 20 mM glucose. (-) hPS, n=3; (+) hPS, n=4. (**G**) Insulin secretion of human EndoC-βH1 cells after 15 min of stimulation with hPS or control buffer upon 2.5 mM glucose. n=3. Each n represents an independent biological replicate. *P < 0.05; **P < 0.01; ***P<0.001. Unpaired t-test. Data are mean ± SD (A, B, F, G) or ± SEM (C-E).

To address whether platelets alone mediate their insulinotropic action on β-cells or whether other cells are involved in this mechanism, a co-culture experiment of platelets and the rat pancreatic β-cell line INS1 was performed. Human platelets were isolated from whole blood through several centrifugation procedures. When added to INS1-cells, purified platelets were able to boost the insulin secretion of these cells (Figure 19A). Therefore, platelets seem to promote insulin secretion independently of additional cell types. The supernatant of activated human platelets was used to assess if the effect is mediated by cell contact or carried out by a released substance. Therefore, the *human platelet supernatant* (hPS) was prepared by the activation of isolated platelets with CRP, followed by centrifugation and sterile filtration to obtain cell fragment-free supernatant containing only platelet-released substances. Interestingly, the addition of hPS to INS1-cells resulted in increased insulin secretion, with the magnitude of this effect depending on the number of platelets used to generate the hPS (Figure 19B). Further investigations have demonstrated that hPS boosts insulin secretion of INS1-cells under low glucose (2.8 mM) and high glucose (15 mM) conditions (Figure 19C). Additionally, *mouse platelet supernatant* (mPS), which was generated analogously to hPS, showed the ability to increase insulin secretion from primary C57BL/6JRj islets under high glucose (16.7 mM) but not low glucose (2.8 mM) conditions (Figure 19D). This action was further confirmed with the mouse insulinoma β-cell line MIN6 (Figure 19E). Ultimately, also stimulation of human insulin releasing EndoC-βH1 cells (Figure 19F) or human β-cells derived from EndoC-βH5 pancreatic progenitors (Figure 19G) with hPS lead to elevated insulin secretion[428,429]. Collectively, these data indicated that a platelet-released factor/s boosts insulin secretion, thus mediating a *platelet-stimulated insulin secretion* (PSIS).

3.3.2 Platelet-derived lipid/s stimulate insulin secretion

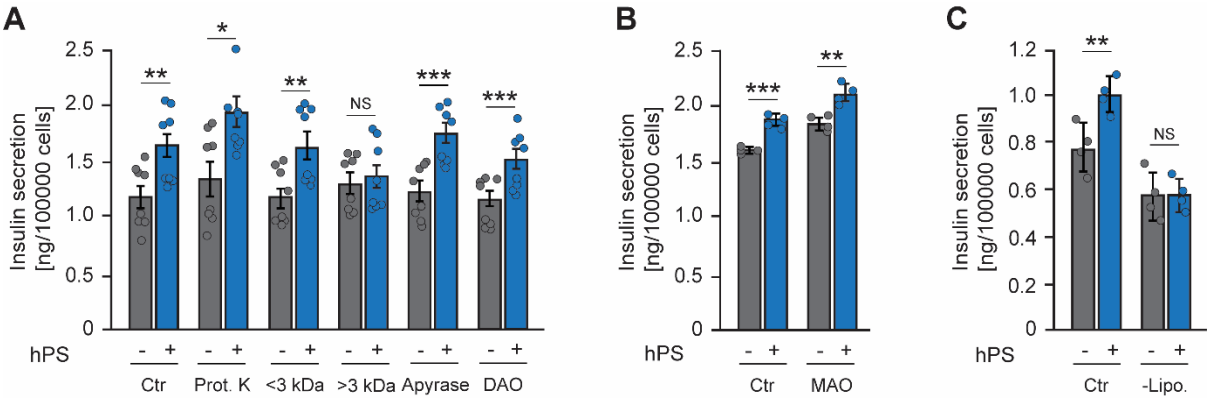

Figure 20: Platelet-derived lipid/s stimulate insulin secretion. (A**)** Normalized insulin secretion of INS1-cells stimulated with unmodified (Ctr), proteinase K treated, fractionated (<3 kDa, >3 kDa), apyrase or diamine oxidase (DAO) treated human platelet supernatant (hPS) in the presence of 15 mM glucose. n=8. (**B**) Normalized insulin secretion of INS1-cells stimulated with unmodified or monoamine oxidase A (MAO) treated hPS in the presence of 15 mM glucose. n=4. (**C**) Normalized insulin secretion of INS1-cells stimulated with unmodified or lipophilic fraction extracted (-Lipo.) hPS in the presence of 15 mM glucose. n=4. Each n represents an independent biological replicate. *P < 0.05; **P < 0.01; ***P < 0.001; NS, not significant. Unpaired t-test. Data are mean ± SEM (A) or ± SD (B, C).

To narrow down the actual substance/s that potentiates pancreatic β-cells' insulin release, hPS was subjected to different biochemical modifications. Respective modified hPS were added to INS1-cells upon high glucose (15 mM) conditions to evaluate whether they still carry out their promoting effect on insulin secretion. Therefore, hPS was incubated with proteinase K, to get rid of present peptides and proteins followed by the addition of proteinase K inhibitor. Modified hPS still demonstrated a similar stimulating effect on insulin secretion, suggesting that it is not a peptide or protein that promotes insulin secretion (Figure 20A). To gain information about the size of the substance/s, hPS was fractionated for substances smaller and larger than 3 kDa by using size exclusion filters. Here, only the fraction containing substances smaller than 3 kDa showed a stimulating effect on insulin secretion (Figure 20A). Several substances that fulfill the size criterium and potentially affect β-cell functioning are stored and released by platelets dense granules, such as ATP, ADP, serotonin, and histamine[138,139,234,401-404]. However, purine and histamine digestion using apyrase and diamine oxidase, respectively, followed by the inactivation of enzymatic activity by boiling, did not abolish the insulinotropic effect (Figure 20A). Similarly, hPS treated with monoamine oxidase A to degrade serotonin, followed by size separation to remove the added enzyme, still demonstrated a promoting action on insulin secretion (Figure 20B). Next, lipophilic substances were extracted from hPS

using organic solvents. Notably, depletion of those substances was associated with a loss of hPS potency to promote insulin secretion. These results suggest that the insulinotropic factor belongs to the family of lipid classes.

3.3.3 Liquid chromatography-mass spectrometry (LC-MS) analysis of platelet-released lipids

A

	Level in plt.depl. serum rel. to ctr serum	Level in mPS rel. to ctr
HETE	0,06	12,76
LPEA-(24:0)	0,39	57,80
FA-(20:5)	0,65	63,63
PA-(34:1)	0,74	2,56
AC-(16:0)	0,91	2,30
PEA-(38:6)	0,93	7,23
LPEA-(18:0)	0,94	10,22
LPEA-(16:0)	0,99	5,41
LPEA-(20:3)	1,07	2,27
BMP-(34:2)	1,07	13,34
BMP-(34:3)	1,09	4,69
PlasEA-(38:4)	1,09	3,72
LPI-(16:0)	1,16	36,46
Sphingosin-P	1,25	17,01
lysoPAF-(18:1)	1,31	7,23
LPC-(20:1)	1,33	2,08
PC-(36:0)	1,34	4,01
Cer-(24:1)	1,41	4,01
LPI-(18:0)	1,42	2,83
LPEA-(22:6)	1,70	5,03
Cer-(22:6)	1,81	14,24
PS-(40:3)	1,81	66,25

Figure 21: Platelets release a variety of lipid classes. (**A**) LC-MS analysis of mouse platelet supernatant (mPS) and serum of platelet-depleted mice using R300 IgG. The result is shown as relative values to the respective control supernatant (ctr) and serum of control IgG-treated mice (ctr serum). (n=4). *hydroxyeicosatetraenoic acid* (HETE), *lysophosphatidylethanolamine* (LPEA), *fatty acid* (FA), *phosphatidate* (PA), *acyl carnitines* (AC), *phosphatidylethanolamine* (PEA), *bis(monoacylglycerol)-phosphate* (BMP), *plasmalogenethanolamine* (PlasEA), *lysophosphatidylinositole* (LPI), *sphingosine phosphate* (Sphingosine-P), *lyso-platelet activating factor* (lysoPAF), *lysophosphatidylcholine* (LPC), *phosphatidylcholine* (PC), *cerebroside* (Cer), *phosphatidylserine* (PS).

In search for the exact lipophilic substance/s mediating the insulinotropic effect, semiquantitative lipidomic analysis was performed by an LC-MS approach. In the frame of this analysis, serum samples from platelet-depleted C57BL/6JRj mice using R300 antibody or from respective control IgG-treated mice, as well as mPS or control buffer samples were analyzed. In total, 22 different substances were detected to be significantly enriched ($p<0.05$) in mPS compared to the control buffer (Figure 21A). Furthermore, four of them were substantially decreased in serum from platelet-depleted mice compared to corresponding serum controls, indicating that platelets serve as the main source for these substances (Figure 21A).

3.3.4 Platelet secreted 20-HETE promotes insulin secretion

The lipidomic analysis revealed several lipid classes specifically released by platelets. Upon them, the family of HETEs has been demonstrated to be the most decreased in

serum from platelet-depleted mice (Figure 21A). Interestingly, HETEs and other AA-derived metabolites have been investigated already in the context of glucose homeostasis and were shown to promote insulin secretion, as shown in the case of 5-HETE[430,431]. Moreover, Tunaru et al. have identified 20-HETE to directly stimulate insulin secretion from β-cells by signaling through GPCR40[116]. As platelets possess the critical enzymatic machinery for the biosynthesis of 20-HETE, further work focused on its role in PSIS[308].

3.3.4.1 Inhibition of 20-HETE signaling reduces platelet-mediated insulin secretion *in vitro*

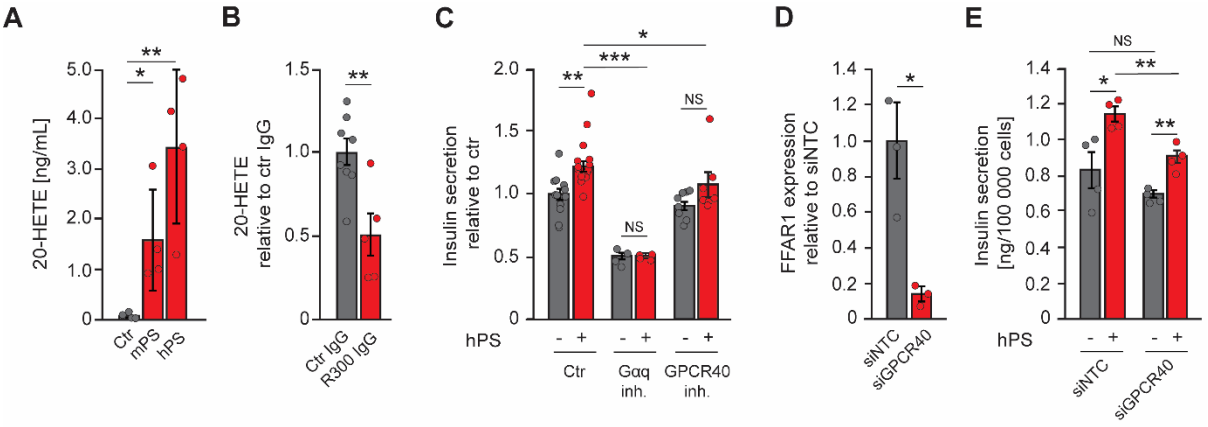

Figure 22: Platelets release 20-HETE and inhibition of its signaling axis diminishes the insulinotropic effect of human platelet supernatant (hPS). (**A**) Concentration of 20-HETE in mouse and human platelet supernatant (mPS, hPS) and control supernatant (Ctr) quantified by ELISA. n=4. (**B**) Serum levels of 20-HETE from platelet-depleted C57BL/6JRj mice using R300 antibodies and mice receiving control IgG. n=4. (**C**) Normalized insulin secretion of INS1-cells stimulated with hSN or control supernatant. INS1-cells were used untreated (Ctr), or treated with $G\alpha_{q/11}$ inhibitor YM-254890 or GPCR40 antagonist GW1100. Ctr, (-) hPS, n=12; Ctr, (+) hPS, n=16; $G\alpha_q$ inh., (-) hPS, n=4, $G\alpha_q$ inh., (+) hPS, n=4; GPCR40 inh., (-) hPS, n=8; GPCR40 inh., (+) hPS, n=7. Data are mean ± SEM for Ctr and GPCR40 inh. and mean ± SD for $G\alpha_q$ inh.. (**D**) Relative GPCR40 expression in INS1-cells transfected with siRNA against GPCR40 or non-targeting control (NTC). n=3. (**E**) Insulin secretion of INS1-cells transfected with siRNA against GPCR40 or NTC stimulated with hPS or control supernatant. n=4. Each n represents an independent biological replicate (A, C-E) or measurement of a sample from distinct mice (B). *P < 0.05; **P < 0.01; ***P < 0.001; NS, not significant. Unpaired t-test. Data are mean ± SEM (C) and ± SD (A, B, C-E).

Initially, it was planned to determine whether the results regarding the HETE family obtained by the lipidomic approach also apply specifically to the 20-HETE isoform. A 20-HETE-specific ELISA used to quantify mPS and hPS provided evidence of 20-HETE's existence in these samples (Figure 22A). Furthermore, 20-HETE levels in the serum of platelet-depleted C57BL/6JRj mice using R300 antibodies were reduced by 50 % (Figure 22B). These results confirm that the detected HETEs from the LC-MS

analysis originate at least partially from the 20-HETE isoform. In the previous paper of Tunaru et al., they postulated 20-HETE to act through $G\alpha_{q/11}$-coupled GPCR40 thereby stimulating insulin secretion[116]. Following this assumption, treatment of INS1-cells with $G\alpha_{q/11}$-inhibitor YM-254890 or antagonization of GPCR40 with GW1100 led to completely abolished or inhibited hPS-stimulated insulin secretion, respectively (Figure 22C). Similarly, the silencing of GPCR40 expression by siRNA (Figure 22D) resulted in a reduced potency of hPS to stimulate insulin secretion (Figure 22E).

3.3.4.2 20-HETE increases intracellular Ca^{2+} and acts PKD1 dependently

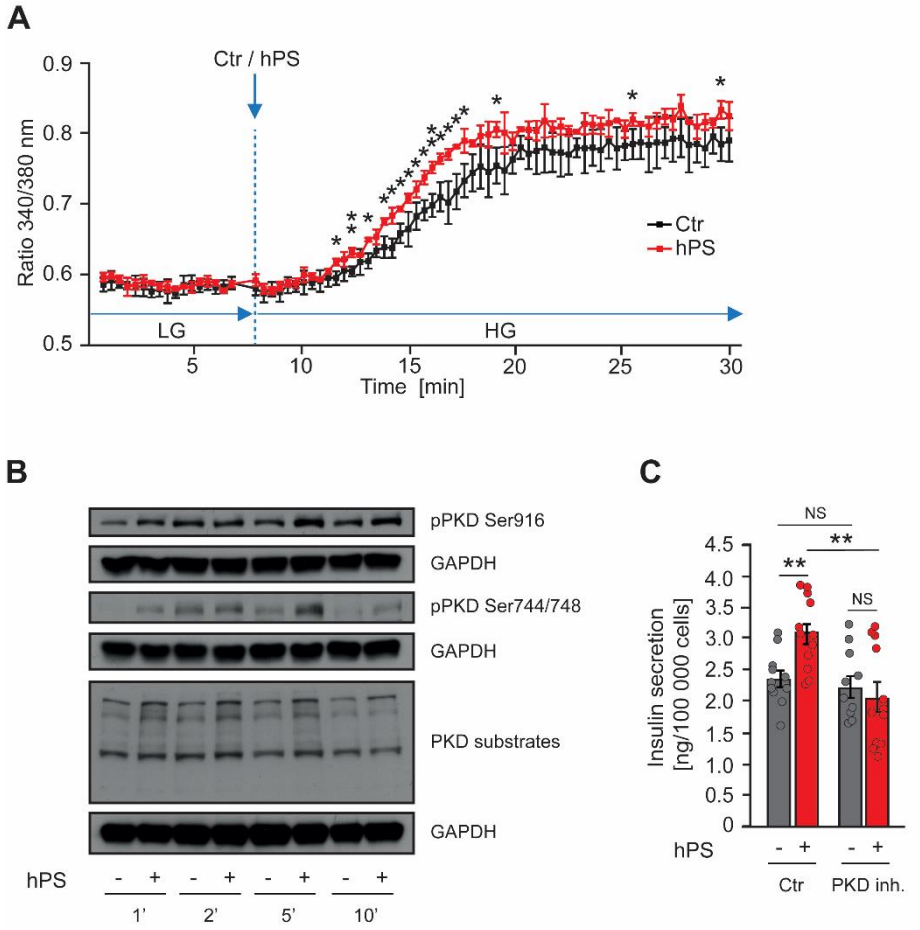

Figure 23: Platelet-induced insulin secretion acts through increased $[Ca^{2}]_i$ and depends on PKD. (**A**) $[Ca^{2+}]_i$ in INS1-cells upon stimulation human platelet supernatant (hPS) or control supernatant (Ctr) in the presence of 2.8 mM (LG) or 15 mM glucose (HG) using Fura-2 calcium tracer. n=3. (**B**) Western blot for indicated proteins with cell lysates of INS1-cells stimulated with hPS or control supernatant in the presence of 15 mM glucose for indicated time points. (**C**) Normalized insulin secretion of PKD inhibitor (PKD inh.) treated or control (Ctr) INS1-cells stimulated with hPS or control supernatant in the presence of 15 mM glucose. Ctr, (-) hPS, n=11; Ctr, (+) hPS, n=12; PKD inh., (-) hPS, n=10; PKD inh., (+) hPS, n=12. Each n represents an independent biological replicate. *P < 0.05; **P < 0.01; NS, not significant. Unpaired t-test. Data are mean ± SEM (C) and ± SD (A).

Additional experiments were applied to understand the signaling axis through which platelets execute their insulinotropic effect in more detail. It is well known that activation of GPCR40 leads to increasing levels of $[Ca^{2+}]_i$[432-434]. Application of the Ca^{2+} tracer Fura-2-AM, which displays a shift in fluorescence excitation spectrum upon forming a complex with Ca^{2+}, confirmed a potentiating effect of hPS on glucose-induced Ca^{2+} influx in INS1-cells (Figure 23A). According to earlier studies, stimulation of GPCR40 is associated with increased activity of PKD1, which is a common key regulator of glucose homeostasis and insulin secretion[115,121,435,436]. Indeed, short-term treatment of INS1-cells with hPS during high glucose conditions caused an elevated degree of PKD1 phosphorylation at serine 744/748 and 916, which is linked with the increased catalytic activity of the kinase and autophosphorylation, respectively (Figure 23B)[437]. In line with this, substrates of PKD1 were found to be increasingly phosphorylated when stimulated with hPS (Figure 23B). Finally, treatment of INS1-cells with the PKD1-specific inhibitor CRT 0066101 eliminated the potency of hPS to promote insulin secretion (Figure 23C).

3.3.4.3 Interference with 20-HETE signaling affects glucose tolerance *in vivo*

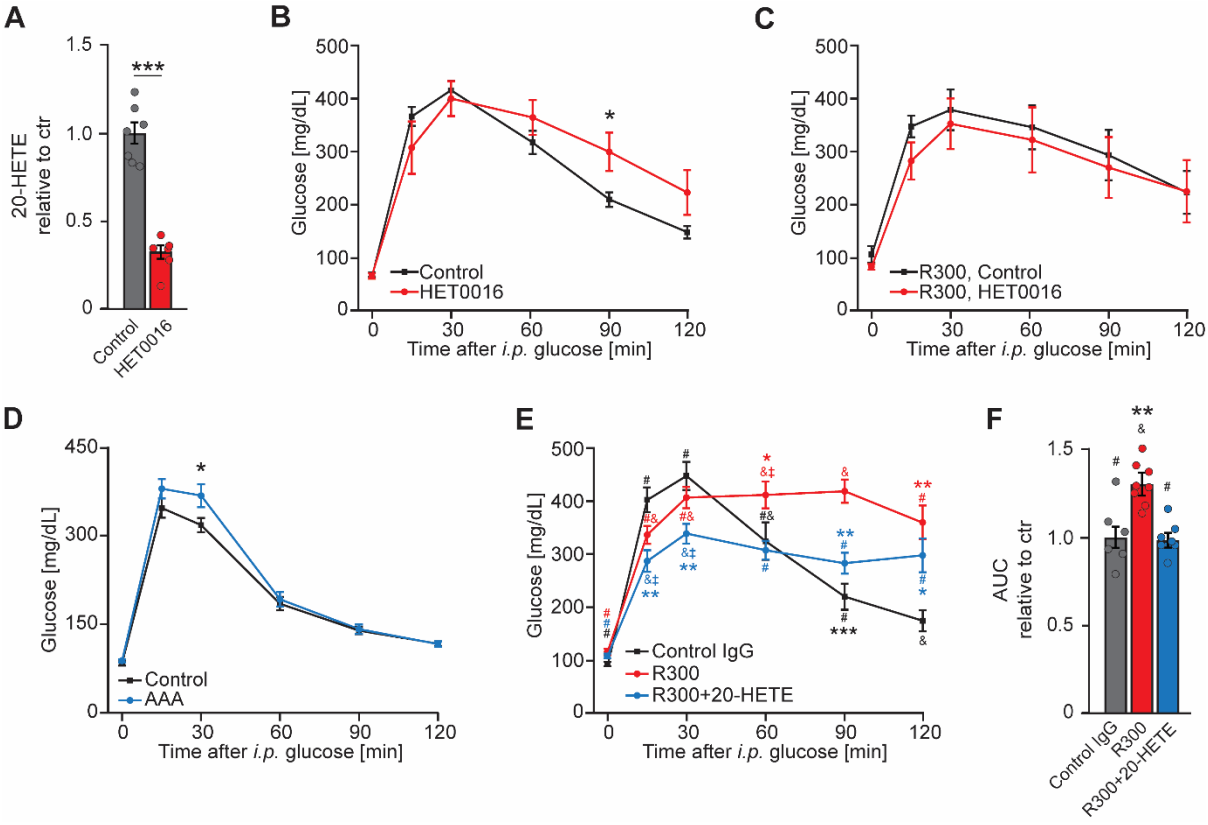

Figure 24: Interference with 20-HETE signaling affects glucose tolerance *in vivo*. (**A**) Relative 20-HETE serum levels of C57BL/6JRj mice injected i.p. with HET0016 or control diluent (Ctr) for four

consecutive days. Ctr, n=7, HET0016, n=6. (**B, C**) Glucose tolerance test (GTT) of C57BL/6JRj mice injected i.p. with HET0016 or control diluent 72 h, 48 h, 24 h, and 30 min before the assay (B). Control, n=8; HET0016, n=6. Other mice were additionally treated with R300 antibodies for platelet depletion or control IgG (C). R300, Control, n=6; R300, HET0016, n=6. (**D**) GTT of C57BL/6JRj mice i.p. injected with 2 mg/kg AAA 2 h before the assay and control mice. Control, n=11; AAA, n=7. (**E, F**) GTT (E) and calculated area under curve (AUC, F) of platelet depleted C57BL/6JRj mice using R300 antibodies or control IgG. For one group the glucose solution was supplemented with an additional 333.3 µg/kg of 20-HETE. Control IgG, n=7; R300, n=8; R300+20-HETE, n=7. Each n represents a measurement of a sample from distinct mice. *P < 0.05; **P < 0.01; ***P < 0.001. One-way ANOVA with post hoc Tukey test (E, F). The same symbols indicate no significant difference, whereas different symbols indicate significant differences among groups. Unpaired t-test. Data are mean ± SEM.

As disruption of the 20-HETE signaling pathway abrogated hPS-mediated insulin secretion in INS1-cells, it was investigated whether this mechanism is also present *in vivo*. CYP450, a vital enzyme in the biosynthesis of 20-HETE, was inhibited in C57BL/6JRj mice by i.p. injection of the specific inhibitor HET0016 for three consecutive days. This led to a corresponding reduction in the 20-HETE serum level by about 70 % (Figure 24A). Additionally, these animals displayed a reduced glucose tolerance (Figure 24C). No additive decrease in glucose tolerance was observed when platelet-depleted C57BL/6JRj mice were treated with HET0016 (Figure 24C). It has been previously shown in primary human and mouse islets that 20-HETE potentiates insulin secretion through GPCR40[116]. Further, deletion of this receptor was associated with inhibited glucose-stimulated insulin secretion[116,438]. However, GPCR75 has been identified to be an additional 20-HETE-specific receptor that also signals through $G\alpha_{q/11}$[439]. As an attempt to investigate the relevance of GPCR75 in PSIS, the GPCR75 specific inhibitor AAA was administered i.p. to C57BL/6JRj mice 2 h before they were challenged with a GTT. Application of the inhibitor caused a mild but significant reduction in glucose tolerance, suggesting that this receptor contributes to 20-HETE-induced signaling but does not mediate the main signaling event (Figure 24D). As inhibition of biosynthesis and signaling of 20-HETE had a negative impact on glucose homeostasis, the question arose whether agonizing the 20-HETE signaling axis would cause the opposite effect. Hence, platelet-depleted C57BL/6JRj mice received 333.3 µg/kg of 20-HETE co-injected together with glucose when challenged for a GTT. Notably, the single, immediate application of 20-HETE mediated a faster clearance of glucose from the blood, thus recovering the overall glucose intolerance induced by platelet depletion (Figure 24E, F).

3.3.5 PAF and lysoPAF stimulate insulin secretion

The lipidomic analysis of mPS provided various lipid classes specifically secreted by platelets upon activation (Figure 21). Besides the 20-HETE family, several other bioactive lipids were identified, including lysoPAF. Studies examining the lipid classes downstream of PLA2 discovered that PAF and its precursor lysoPAF stimulated the release of insulin from isolated rat islets under the conditions of 1.7 mM and 16.7 mM glucose in a concentration-dependent, reversible, and inhibitable manner[440]. The following section, therefore, addresses the possible role of PAF and lysoPAF in glucose homeostasis.

3.3.5.1 PAF and lysoPAF stimulate insulin secretion from β-cells

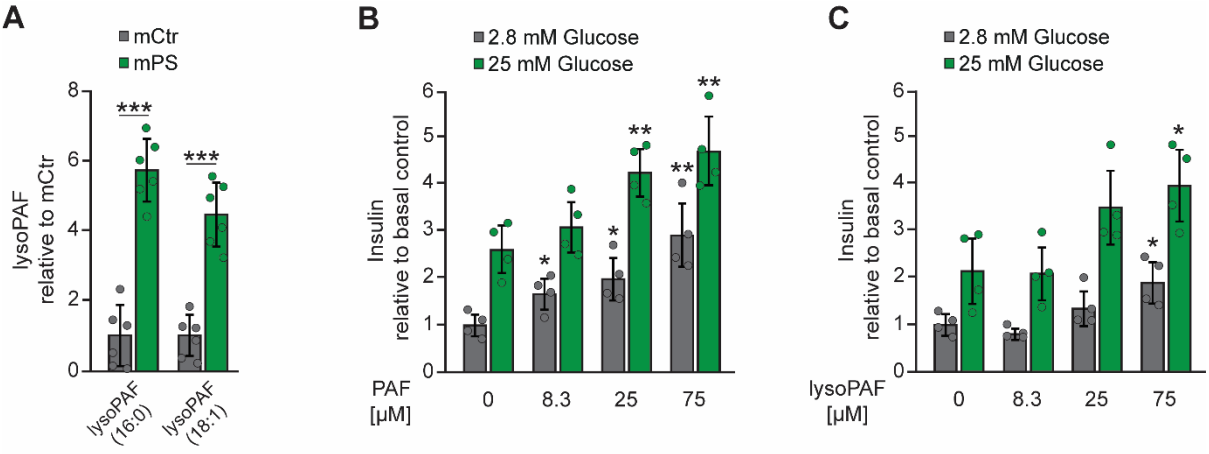

Figure 25: PAF and lysoPAF stimulate insulin secretion from β-cells. (**A**) Semi-quantitative analysis of lysoPAF in mouse platelet supernatant (mPS) obtained by LC-MS analysis. n=6. (**B, C**) Relative insulin secretion of MIN6-cells upon 2.8 mM and 25 mM glucose in the presence of different concentrations of PAF (B) or lysoPAF (C). n=4. Each n represents an independent biological replicate. *P < 0.05; **P < 0.01; ***P < 0.001. Significance refers to the respective basal value (B, C). Unpaired t-test. Data are mean ± SD.

The first LS-MS approach was designed to identify a wide range of different lipid classes. Therefore, the LC-MS protocol was optimized for the detection of lysoPAFs. The semi-quantitative analysis revealed elevated levels of lysoPAF-(16:0) and lysoPAF-(18:1) in mPS (Figure 25A). However, it appeared that the LC-MS method was insufficient for the detection of PAF, which is known to be continuously generated by platelets and released upon activation[441,442]. Since lysoPAF as well as PAF have been shown to promote insulin secretion in isolated rat islets, it was examined whether MIN6-cells display the same behavior. MIN6-cells were incubated with different concentrations of PAF-(16:0) or lysoPAF-(16:0) during 2.8 mM or 25 mM glucose

stimulation. The resulting insulin levels in the medium demonstrate a concentration-dependent promotion of insulin secretion by PAF and lysoPAF that is independent of the glucose concentration (Figure 25B, C). Therefore, data generated with isolated rat islets seem to be transferable to a single β-cell model.

3.3.5.2 Antagonization of PAFR abolishes the potency of mPS and reduces glucose tolerance in mice

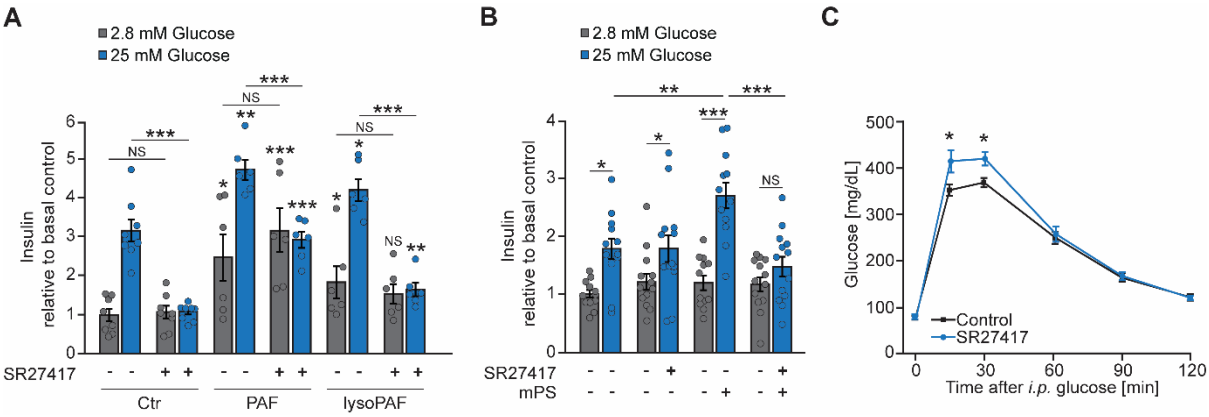

Figure 26: Antagonization of PAFR abolishes the potency of mPS and reduces glucose tolerance in mice. (**A**) Relative insulin secretion of MIN6-cells stimulated with 75 µL PAF, lysoPAF, or solvent control (Ctr) upon 2.8 mM and 25 mM glucose in the presence or absence of 2,5 µM PAFR antagonist SR27417. Ctr, n=8; PAF, n=6; lysoPAF, n=6. (**B**) Relative insulin secretion of MIN6-cells stimulated with mouse platelet supernatant (mPS) or control supernatant in the presence or absence of 2,5 µM SR27417 upon 2.8 mM and 25 mM glucose. n=12. (**C**) Glucose tolerance test of C57BL/6JRj mice injected with 10 mg/ kg SR27417 or solvent control 16 h before the assay. Control, n=8; SR27417, n=7. Each n represents an independent biological replicate (A, B) or measurement of a sample from distinct mice (C). *P < 0.05; **P < 0.01; ***P < 0.001; NS, not significant. If not indicated, significance refers to the Ctr value with identical glucose and SR27417 treatment (A). Unpaired t-test. Data are mean ± SEM.

The obtained results and data from the literature indicate that activated platelets release PAF and lysoPAF, which in turn are potent potentiators of insulin secretion (Figure 25)[440,442]. PAF is known to act through its PAFR, the gene of which is most highly transcribed in endocrine cells of the pancreas along with Kupffer cells[443]. To evaluate whether lysoPAF and PAF execute their insulinotropic potential through this receptor, MIN6-cells were additionally treated with 2.5 µM of the specific PAFR antagonist SR27417 during starvation, low glucose, and following high glucose stimulation of these cells[444]. Of note, the presence of SR27417 inhibited the glucose-mediated induction of insulin secretion in control, PAF, and lysoPAF-treated cells (Figure 26A). On the other hand, SR27417-treated cells that got treated with PAF and

lysoPAF still show elevated insulin secretion compared to their respective controls suggesting that PAFR is at least not solely responsible for the potentiating effect (Figure 26A). To further evaluate the role of PAFR in mPS-promoted insulin secretion, MIN6-cells were stimulated with mPS in the presence of SR27417. As the previous experiment demonstrated a completely abolished GSIS, the duration of SR27417 treatment was restricted only to the final high glucose stimulation period. The reduced exposure of MIN6-cells to SR27417 led to unchanged glucose-mediated insulin secretion (Figure 26B). However, the application of SR27417 diminished the potency of mPS (Figure 26B). Accordingly, mPS appears to exert its effect also in a PAFR-dependent manner. To study the impact of PAFR on glucose homeostasis *in vivo*, C57BL/6JRj mice were injected i.p. with 10 mg/kg SR27417 and challenged with a GTT 16 h later. Here, the antagonization of the PAFR resulted in glucose intolerance (Figure 26C). Altogether, these data indicate that PSIS is partially mediated through PAFR.

3.4 Platelet-stimulated insulin secretion decreases with age

The findings compiled up to this point consistently show that decreased platelet functionality or platelet count results in reduced insulin secretion. In addition, it was shown that this effect is mediated by lipids secreted by platelets. However, many drugs are existing, that reduce platelet functionality and are commonly prescribed to prevent thrombotic events. Therefore, in this section it will be examined to what extent the PSIS demonstrated in mice can be translated to humans.

3.4.1 Clopidogrel, but not acetylsalicylic acid reduces glucose tolerance through reduced insulin secretion

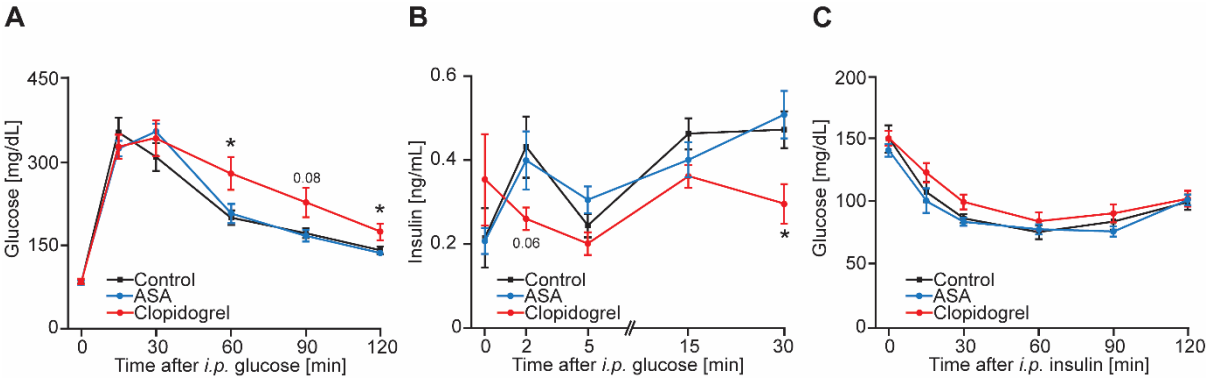

Figure 27: Clopidogrel causes glucose intolerance through reduced insulin secretion. (**A**) Glucose tolerance test of C57BL/6JRj mice treated with clopidogrel or *acetylsalicylic acid* (ASA) for 4 weeks with respective control. Control, n=9; ASA, n=10, Clopidogrel, n=10. (**B**) Glucose stimulated insulin secretion of C57BL/6JRj mice treated with clopidogrel or acetylsalicylic acid (ASA) for 6 weeks with respective control. Control, n=10; ASA, n=10, Clopidogrel, n=9. (**C**) Insulin tolerance test of C57BL/6JRj mice treated with clopidogrel or acetylsalicylic acid (ASA) for 7 weeks with respective control. Control, n=7; ASA, n=8, Clopidogrel, n=9. Each n represents a measurement of a sample from distinct mice. *P < 0.05. Unpaired t-test. Data are mean ± SEM.

Clopidogrel and a*cetylsalicylic acid* (ASA) are two commonly used drugs for the prevention of thrombotic events[445]. The active metabolite of clopidogrel inhibits P2Y12, which is the major receptor mediating ADP-stimulated platelet activation that is associated with integrin αIIbβ3 activation, enhanced degranulation, Tx production, and prolonged platelet activation[284,446,447]. ASA, on the other hand, irreversibly acetylates COX1, which hinders the conversion of AA into PGH_2, which is required for the synthesis of TxA_2[448]. Thus, it inhibits TxA_2-mediated platelet aggregation[449]. To investigate whether these antithrombotic drugs influence glucose homeostasis, C57BL/6JRj mice received a calculated dosage of 40 mg/kg of ASA or clopidogrel via the drinking water. After 4 weeks of treatment, clopidogrel-treated mice displayed glucose intolerance, whereas glucose tolerance was not changed in mice that received ASA (Figure 27A). Similarly, only clopidogrel-treated mice demonstrated a reduced GSIS (Figure 27B) without changed insulin tolerance in any of the treatment groups (Figure 27C). Based on these results, the frequently applied anti-platelet drug clopidogrel reduces GSIS and glucose tolerance in mice.

3.4.2 Anti-platelet treatment in aged mice does not reduce glucose homeostasis

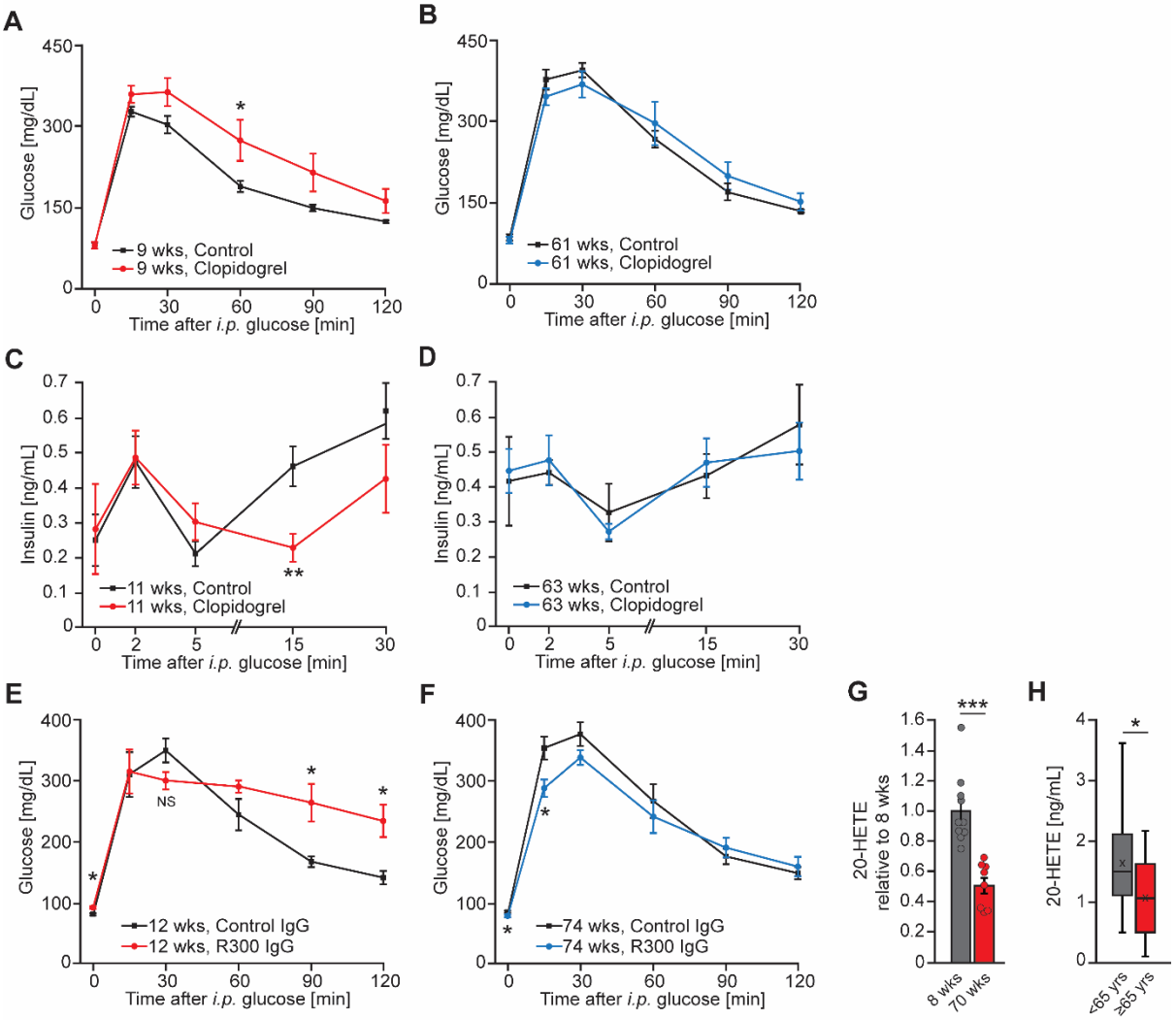

Figure 28: Anti-platelet treatment in aged mice does not affect glucose homeostasis. (**A, B**) Glucose tolerance test (GTT) of 9 weeks (A) and 61 weeks (B) old C57BL/6JRj mice treated with 40 mg/kg clopidogrel for 4 weeks and respective control animals. n=7. (**C, D**) Glucose stimulated insulin secretion of 11 weeks (C) and 63 weeks (D) old C57BL/6JRj mice treated with 40 mg/kg clopidogrel for 6 weeks and respective control animals. n=7. (**E, F**) GTT of 12 weeks (E) and 74 weeks (F) old C57BL/6JRj mice treated with R300 IgG for platelet depletion or control IgG. n=5. (**G**) Relative 20-HETE serum level from 8 and 70 weeks old C57BL/6JRj mice. 8 wks, n=10; 70 wks, n=8. (**H**) 20-HETE serum level from 30-64 years and 65-79 years old human. <65 yrs, n=24; ≥65 yrs, n=9. Each n represents a measurement of a sample from distinct mice (A-G) or humans (H). *P < 0.05; **P < 0.01; ***P < 0.001; NS, not significant. Unpaired t-test. Data are mean ± SEM. Data in boxplots: the center line shows the median; the cross indicates the mean; the box defines the first and third quartiles; the whiskers indicate the 1.5 × interquartile range; outliers are individually plotted.

Clopidogrel is commonly prescribed to prevent thrombotic events[445]. Therefore, it allows investigation of whether its inhibitory action on insulin secretion shown in mice is translatable to human individuals. However, the use of clopidogrel was not linked to any associated glucose intolerance, according to a thorough examination of the

literature. On the other hand, the mean age of patients receiving clopidogrel is 69 years[450]. To evaluate the relevance of age in PSIS, young and aged C57BL/6JRj mice were treated with 40 mg/kg clopidogrel for 4 weeks. Notably, in contrast to 9 weeks old mice, clopidogrel did not decrease glucose tolerance in 61 weeks old animals (Figure 28A, B). Further, GSIS was not reduced in aged mice treated with clopidogrel (Figure 28C, D). Platelet depletion in aged mice using R300 antibodies even lead to an improved glucose tolerance compared to control mice, whereas the opposite was demonstrated in young mice (Figure 28E, F). Since 20-HETE was demonstrated to be a platelet-released substance capable to potentiate insulin secretion, serum levels of 20-HETE in 8 weeks and 70 weeks old C57BL/6JRj mice were quantified (Figure 22)[116]. Strikingly, 20-HETE levels were reduced by 50 % in aged animals (Figure 28G). Additionally, the same tendency was demonstrated in human individuals (Figure 28H). Altogether, this set of data points to a mechanism whereby platelet-released 20-HETE potentiates insulin secretion in young subjects, whereas this mechanism appears to vanish with aging.

3.4.3 The loss of platelet-induced insulin secretion with age does not derive from MKs themself

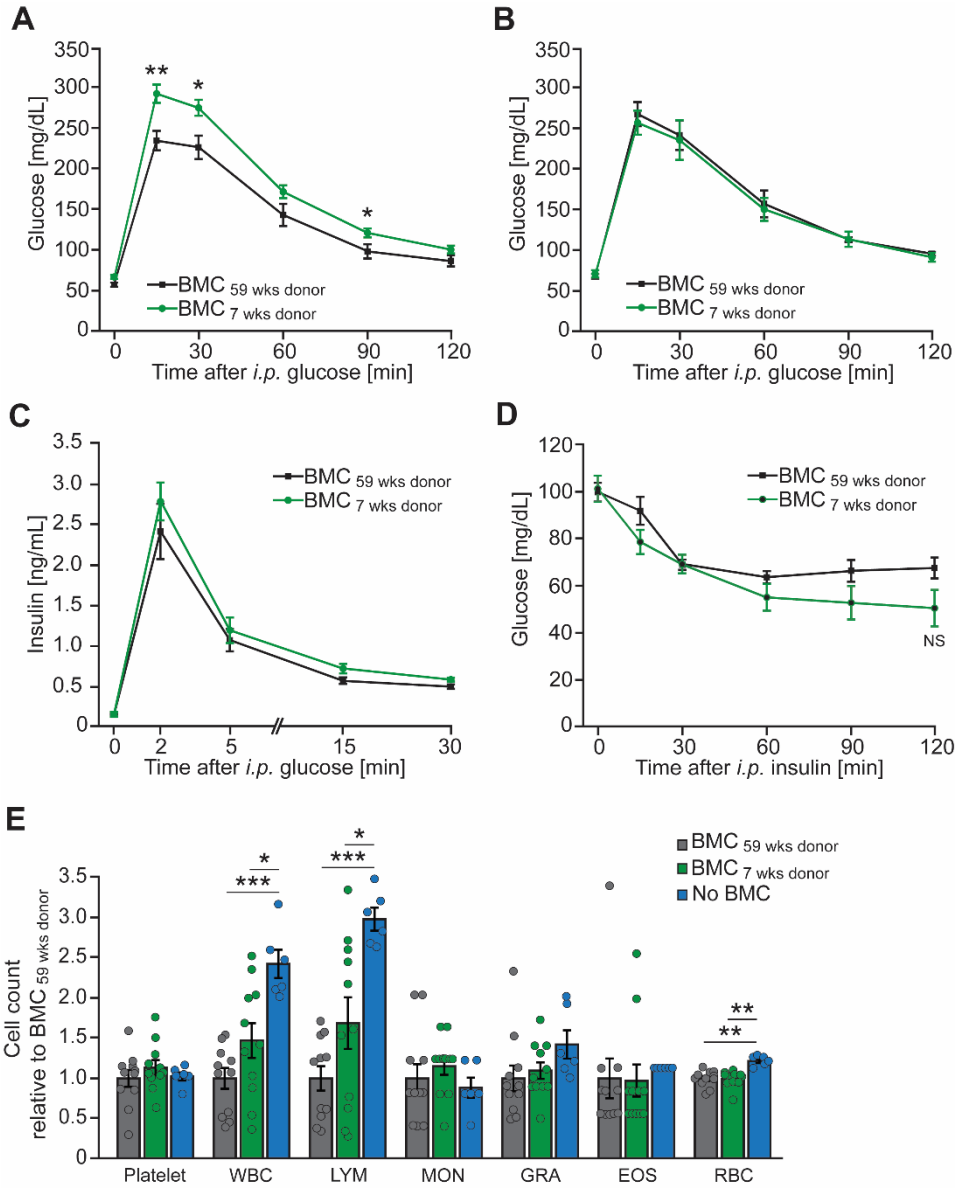

Figure 29: MKs from young mice do not improve metabolic characteristics in old mice. (**A, B**) Glucose tolerance test of irradiated 59 weeks old C57BL/6JRj mice that received bone marrow cells from 59 weeks or 7 weeks old C57BL/6JRj donor mice. Assays were performed 6 weeks (A) or 10 weeks (B) after bone marrow transplantation. $BMC_{59\ wks\ donor}$, n=11; $BMC_{7\ wks\ donor}$, n=12 (A). n=9 (B). (**C**) Glucose stimulated insulin secretion of the above-described mice measured 8 weeks after bone marrow transplantation. $BMC_{59\ wks\ donor}$, n=11; $BMC_{7\ wks\ donor}$, n=10. (**D**) Insulin tolerance test of the above-described mice measured performed 9 weeks after bone marrow transplantation. n=9. (**E**) Relative cell count of different blood cell populations of the above-described mice measured 8 weeks after bone marrow transplantation and 15 weeks old C57BL/6JRj mice that did not undergo a bone marrow transplantation. $BMC_{59\ wks\ donor}$, n=11; $BMC_{7\ wks\ donor}$, n=11; No BMC, n=6. *White blood cell* (WBC), *lymphocyte* (LYM), *monocyte* (MON), *granulocyte* (GRA), *eosinophil* (EOS), *red blood cell* (RBC). Each n represents a measurement of a sample from distinct mice. *P < 0.05; **P < 0.01; ***P < 0.001; NS, not significant. Unpaired t-test. Data are mean ± SEM.

The findings from the previous section imply that PSIS declines with age. This allows different speculations regarding the mechanistic basis of this association. It is conceivable that MKs undergo functional changes throughout aging, resulting in platelets with different morphological or functional characteristics. To examine the role of MKs in age-dependent loss of PSIS, a bone marrow transplantation approach was applied. Thus, 59 weeks old C57BL/6JRj mice were lethally irradiated before being reconstituted with bone marrow of 59 weeks or 7 weeks old C57BL/6JRj donor mice. Contrary to the proposed theory, 6 weeks after transplantation it was discovered that mice that received bone marrow from young donor animals were less glucose tolerant (Figure 29A). However, the effect was only transient, as it was not present anymore 10 weeks after transplantation (Figure 29B). Likewise, GSIS and ITT which were executed 8 weeks and 9 weeks after bone marrow transplantation, respectively, did not reveal significant changes (Figure 29C, D). To investigate whether the transplantation was associated with changes in the blood cell profile, cell counts of different blood cell populations were quantified. Including platelets, none of the analyzed cell populations were significantly changed between both BMC groups (Figure 29E). At the same time, the count of WBC, specifically LYM, as well as of RBC was reduced in both BMC groups compared to 15 weeks old C57BL/6JRj mice that did not undergo a bone marrow transplantation (Figure 29E). To sum up, these results suggest that the age-associated loss of platelet-induced insulin secretion does not derive from age-mediated changes in MKs.

3.4.4 $G\alpha_qG\alpha_{13}$ PF4 Δ/Δ mice exhibit decreased pancreatic islet vasculature

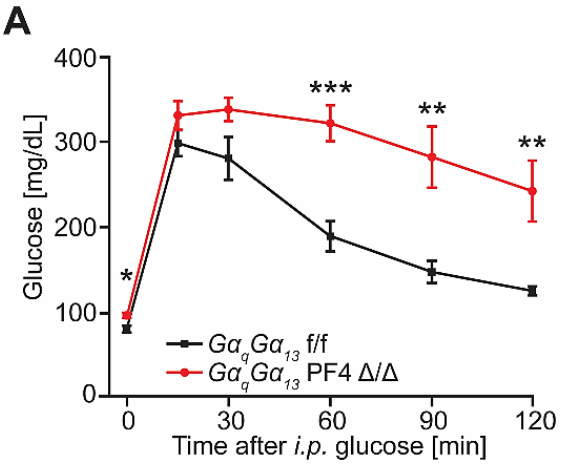

Figure 30: Aged $G\alpha_qG\alpha_{13}$ PF4 Δ/Δ mice display glucose intolerance. (**A**) Glucose tolerance test of 55 weeks old $G\alpha_qG\alpha_{13}$ PF4 Δ/Δ and control mice. $G\alpha_qG\alpha_{13}$ PF4 f/f, n=7; $G\alpha_qG\alpha_{13}$ PF4 Δ/Δ, n=6. Each n represents a measurement of a sample from distinct mice. *P < 0.05; **P < 0.01; ***P < 0.001. Unpaired t-test. Data are mean ± SEM.

In contrast to young mice, a pharmacologically induced platelet defect or platelet depletion did not alter insulin secretion in aged mice, which further correlated with reduced 20-HETE serum levels in aged animals (Figure 28). As an attempt to confirm this observation in a genetic model, aged $G\alpha_qG\alpha_{13}$ PF4 Δ/Δ mice were challenged with a GTT. Unexpectedly, 55 weeks old $G\alpha_qG\alpha_{13}$ PF4 Δ/Δ mice still showed severe glucose intolerance (Figure 30A) similar to what was seen in mice of this genotype at 14 weeks of age (Figure 14J).

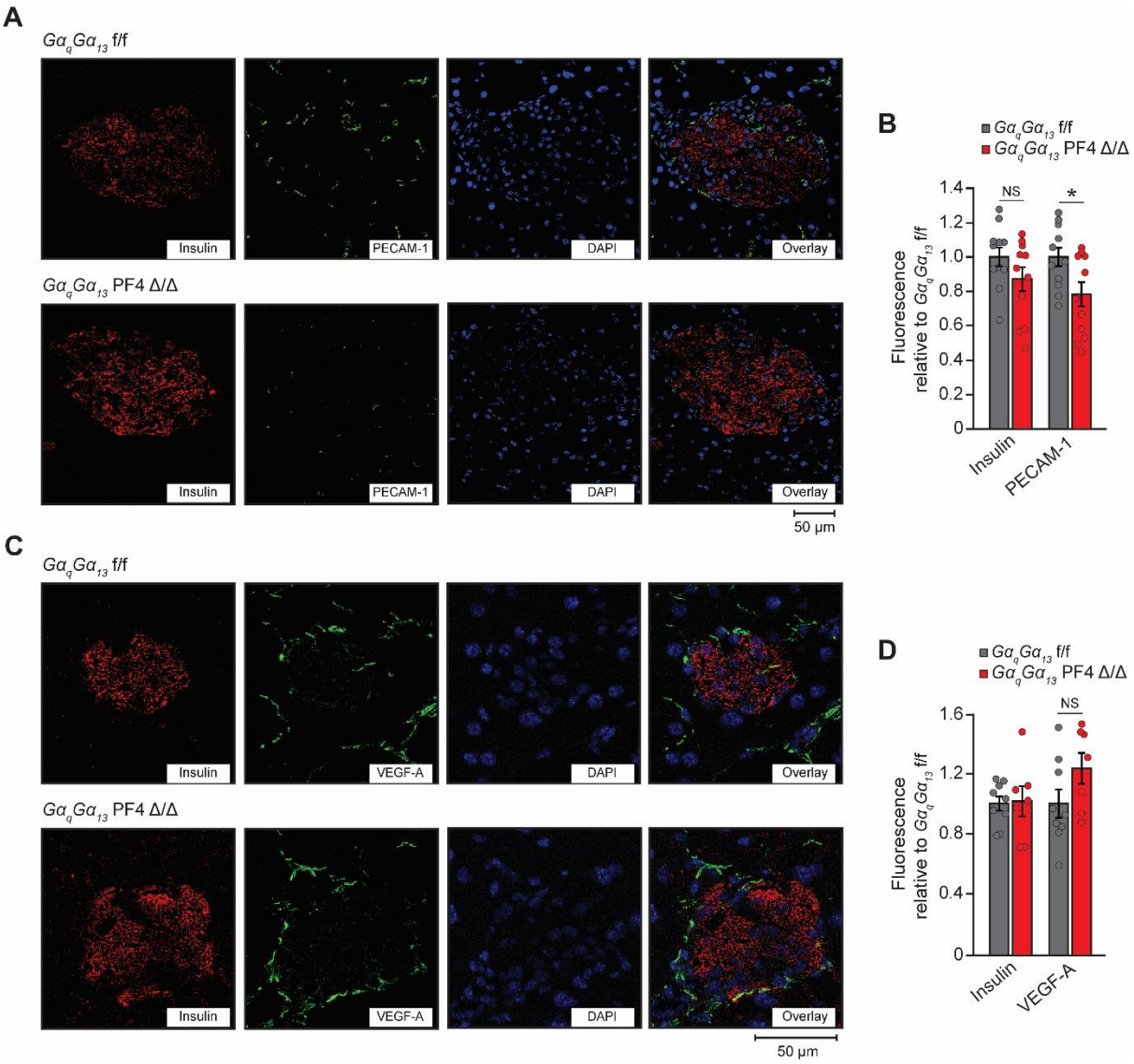

Figure 31: GαqGα13 PF4 Δ/Δ mice exhibit a decreased pancreatic islet vasculature. (**A**) Representative fluorescence microscopy images of DAPI and immunostainings against insulin and PECAM-1 from the endocrine pancreas of GαqGα13 PF4 Δ/Δ and control mice. (B) Relative mean fluorescence mediated by immunofluorescence staining against insulin and PECAM-1. n=11. (C) Representative fluorescence microscopy images of DAPI and immunostainings against insulin and VEGF-A from the endocrine pancreas of GαqGα13 PF4 Δ/Δ and control mice. (D) Relative mean

fluorescence mediated by immunofluorescence staining against insulin and VEGF-A. GαqGα13 PF4 Δ/Δ, n=9, GαqGα13 PF4 f/f, n=7. Each n represents a measurement of a sample from distinct mice. *P < 0.05; NS, not significant. Unpaired t-test. Data are mean ± SEM.

On the one hand, short-term pharmacological inhibition of platelet function or platelet depletion only decreases glucose tolerance in young but not aged mice (Figure 28). On the other hand, aged mice that exhibit a genetic platelet defect still display severe glucose intolerance (Figure 30A). This divergence might arise from an additional long-term effect that platelets might have on pancreatic islets. However, islets from $G\alpha_qG\alpha_{13}$ PF4 Δ/Δ mice did not differ in their average size and demonstrated a normal GSIS (Figure 15G, J). A critical islet compartment platelets might influence in a developmental or long-term manner, is the islet vasculature, as abnormalities were shown to be associated with insulin secretory defects and glucose intolerance[451,452]. Therefore, vascular morphology was investigated by IF-staining. Staining for the vascular marker PECAM-1 revealed a decrease in vasculature-mediated fluorescence in 16 week old GαqGα13 PF4 Δ/Δ mice (Figure 31A, B). Insulin-mediated fluorescence was not altered significantly (Figure 31B), confirming the result obtained by insulin extraction from the pancreas (Figure 15H). Reinert et al. have shown that a pancreas-restricted deficiency of angiogenetic VEGF-A leads to islet hypovascularization associated with strongly abolished glucose tolerance[452]. Platelets not only store and secrete VEGFs but also several growth factors that might potentially affect the expression of VEGF-A in other target cells[453,454]. Nevertheless, VEGF-A levels in islets from GαqGα13 PF4 Δ/Δ mice, as obtained by IF staining, tended to be elevated, suggesting a mechanism aiming to compensate for a lack of angiogenic stimulus in these animals (Figure 31C, D). Taking together, platelets do not only directly amplify insulin secretion by the secretion of insulinotropic lipids. They further seem to contribute to angiogenetic mechanisms ensuring an islet characteristic vasculature essential for proper insulin secretion. To this point, the exact mechanism of how platelets mediate this effect remains unknown.

4 DISCUSSION

The pancreas is a key organ for the maintenance of metabolic equilibrium and specifically glucose homeostasis. Its endocrine part is organized in pancreatic islets that are predominantly composed of α- and β-cells. Upon low blood glucose levels α-cells release the anabolic peptide hormone glucagon, which elevates blood glucose levels by stimulating hepatic glycogenolysis and gluconeogenesis[25,26]. In contrast, β-cells release insulin during hyperglycemia[30]. Insulin mediates the integration of GLUT4 into the cell membrane of insulin-sensitive cells, thus enabling the clearance of glucose from the circulation[31]. The respective release of glucagon and insulin is regulated by a complex interplay of circulating metabolites, endocrine, paracrine, and autocrine signaling molecules, and autonomic nerves[36,39,41,43,49,55]. Glucose is the most potent and indispensable inducer of insulin secretion. However, a plethora of substances have been identified to be promoters of glucose stimulated insulin secretion. These insulinotropic factors include a wide variety of substance classes, such as hormones, lipids, amino acids, purines, and neurotransmitters[53,110,117,139,147]. Insulin intolerance and the disability of pancreatic β-cells to release sufficient amounts of insulin lead to the development of diabetes[177,180]. Resulting poor glycemic control and chronic hyperglycemia is associated with microvascular and macrovascular complications that can finalize in tissue damage and multi-organ dysfunction making it one of the most fatal diseases[208,219,220].

Platelets are small anucleate cell fragments that primarily function as regulators of hemostasis[240]. More recently, however, platelets have emerged as multifunctional blood components involved in different physiological mechanisms including immune defense, inflammatory processes, angiogenesis, and cancer progression[241,243,245,249]. Platelets store and release a high variety of substances, of which some are known to execute insulinotropic effects[114,138,139,234,315,316,401-404]. Further, diabetes is linked to an increased risk of vascular disorders, which is driven in part by an increase in platelet reactivity[250,251]. All of this indicates a potential role of platelets in the systemic response to elevated glucose levels. For this reason, this thesis aimed to unravel the function of platelets on pancreatic β-cells and homeostatic function.

4.1 Platelets get activated during hyperglycemia and specifically localize in the microvasculature of pancreatic islets

Diabetes is commonly associated with a higher risk of vascular disorders, which is partially promoted by an increase in platelet reactivity[250,251]. Even though the exact mechanism is not fully understood, it is believed that among other factors, an enhanced capacity to be activated by agonists and a decreased efficiency of inhibitory mechanisms contribute to this effect[455]. Indeed, NO generation is inhibited by hyperglycemia by limiting *endothelial nitric oxide synthase* (eNOS) activation and increased production of NO-quenching reactive oxygen species, particularly superoxide anion (O2), in vascular smooth muscle cells and endothelial cells[456,457]. Similarly, vascular synthesis of PGI_2 has been reported to be reduced[458]. Furthermore, platelets of diabetic patients were demonstrated to display increased surface expression of GpIb and αIIbβ3 integrin as well as a stronger response to agonist-induced platelet activation[459,460].

Here, the sole role of glucose on platelet reactivity should first be examined. For this purpose, the whole blood of C57BL/6JRj mice was incubated with different concentrations of glucose in the presence of common platelet activators, followed by a flow cytometric analysis of αIIbβ3 integrin activation and P-selectin exposure as a marker for degranulation. High glucose (30 mM) was able to increase CRP-mediated platelet degranulation, as well as integrin activation in the presence of additional serotonin, $ZnCl_2$, ATP, or U46 (Figure 7). The high glucose-promoted amplification of αIIbβ3 integrin activation and platelet degranulation was demonstrated to be of functional significance since preincubation of blood in 30 mM glucose buffer promoted binding to collagen during flow conditions (Figure 8). However, the exact underlying mechanism of glucose to promote platelet activation remains a subject of speculation. Increased reactivity in the presence of ADP or t*hrombin receptor agonist peptide* (TRAP) was also shown when platelets were exposed to hyperosmolar solutions other than glucose, indicating that hyperglycemia may have a direct osmotic effect that is independent of the intra-platelet metabolism[216]. Sudic et al. attributed the effect to ROS formation induced by elevated osmolality generated by non-metabolizable sugars[426]. Platelets exhibit a basal production of ROS by NOX1/2 isoforms, which substantially increases upon platelet activation[461]. ROS was demonstrated to

contribute to platelet activation in different ways. It can act as a second messenger causing the phosphorylation and activation of PLCγ2, which is essential for converting adhesion receptor binding to platelet activation[462]. Additionally, ROS was shown to be released by activated but also resting platelets[463,464]. Thus, it can directly or indirectly by activation of the platelet membrane protein disulfide isomerase promote the formation of disulfide bonds[365,366]. Resulting structural alterations were demonstrated to be associated with stimulation of αIIβI and αIIbβ3 integrin activation and increased GPIbα-mediated platelet adhesion[365,367-369,465,466]. In contrast to Sudic et al., others claim that ROS production during hyperglycemia is not solely increased due to an osmotic effect, but as a result of glucose metabolization through the polyol pathway[467]. The polyol pathway accounts for only 3 % of glucose consumption during euglycemia, however, the proportion rises to 30 % during hyperglycemia. The increased rate is caused by the enhanced activity of the *aldose reductase* (AR), which is the first enzyme of this pathway[468]. The upregulation of the polyol route results in an exhaustion of reducing equivalents and increasing levels of polyols, which are associated with elevated oxidative and osmotic stress, respectively[469]. Tang et al. have found that the AR activity in human platelets is not only increased by high glucose concentrations but also by agonization of GPVI. Furthermore, pharmacological or genetic ablation of AR function abolished the augmented platelet aggregation and P-selectin exposure observed upon co-stimulation with high glucose and collagen. The same effect was created when ROS was scavenged[467]. Of note, high glucose does not only promote ROS generation through the polyol pathway but also leads to mitochondrial dysfunctions associated with the formation of ROS[470]. In this context, also AR was demonstrated to cause an amplifying effect, as high glucose-induced AR activity was shown to induce a signaling pathway finalizing in dysfunctional mitochondria and elevated oxidative stress[471]. In this thesis, increased P-selectin exposure during hyperglycemia was only observed upon co-stimulation of GPVI with CRP, but not with any of the other tested stimuli, thus confirming the findings of Tang et al. (Figure 7)[467]. Therefore, this putative mechanism provides a direct link to how glucose potentiates specifically GPVI-mediated platelet activation. However, αIIbβ3 integrin activation was shown to be unaffected under these conditions (Figure 7). Here, the strong effect of CRP on αIIbβ3 integrin activation might cover the additional effect of high glucose concentrations.

However, scavenging of generated ROS in human platelet only abolished the hyperglycemic enhancement of platelet P-selectin exposure, but not the elevated integrin activation[426]. Accordingly, hyperglycemia seems to promote platelet activation also in a ROS-independent way. Also here, increased integrin activation in the presence of high glucose levels and an additional stimulus were observed (Figure 7). Non-enzymatic glycation might be a mechanism that contributes to this effect. Studies suggest that *asparagine* (N)-glycosylation of β3 integrin at defined N-glycan sites causes conformational changes that affect ligand binding and positively regulate αIIbβ3 integrin activation[472]. Even small increases in blood glucose levels can cause a spontaneous, non-enzymatic reaction of glucose with amino groups of proteins[473]. Thus, high glucose levels might result in the glycation of platelet surface receptors, thereby affecting their affinity to certain ligands. Similarly, components of the blood might undergo glycation forming so-called AGE, thereby gaining or increasing the potency to activate platelets. Indeed, platelets express the *receptor for AGE* (RAGE) and stimulation with AGE-BSA in the presence of sub-threshold TRAP-6 increased platelet aggregation and P-selectin exposure, which was inhibitable by a specific RAGE inhibitor[474].

The generated data, together with existing literature indicates the potency of high glucose levels to promote platelet activation to a relevant degree. The effect seems to be at least partially dependent on ROS formation, however, whether its formation is promoted by an osmotic effect or dependent on glucose metabolism remains controversial. Therefore, measurement of platelet activation by flow cytometry and attachment to collagen under flow conditions may be repeated in the presence of glucose or unmetabolizable sugars, such as L-glucose. To address if glycation contributes to the effect, the existence of glycation of platelet adhesion receptors after high glucose treatment would need to be proven by structural analysis. Subsequently, the functional relevance of possibly identified glycations would need to be determined by genetic ablation of respective glycation sites. For testing the relevance of AGE, the attachment of platelets to collagen under flow could be repeated in the presence of a RAGE inhibitor.

To not only relate hyperglycemia to increased blood glucose levels but to consider it as an overall physiological state, the potential influence of β-cells on platelets was also

examined. Notably, stimulation of platelets with medium supernatant of the pancreatic β-cell line MIN6 promoted αIIbβ3 integrin activation and platelet degranulation in the presence of 1 µg/mL CRP as a co-stimulus (Figure 9). This effect tended to be more pronounced when MIN6-cells were maintained in a high glucose medium to ensure enhanced insulin-granule release (Figure 9). Also here, this effect reached functional relevance, as preincubation of mouse blood with MIN6-cell medium supernatant lead to enhanced platelet binding to collagen during flow conditions (Figure 10). The main substance secreted by β-cells during high glucose levels is insulin, which, however, was shown to attenuate agonist-induced platelet activation[475]. It is well known that β-cells co-release ATP and zinc in the process of degranulation[139]. ATP can act as a soluble secondary mediator of platelet activation through the P2X1 receptor that functions as a ligand-gated ion channel, thus mediating rapid influx of Ca^{2+} enhancing agonist-induced activation[476]. Also, extracellular zinc has been implemented to access platelets and induce tyrosine phosphorylation finalizing in potentiated GPVI activation and platelet aggregation that was reversible by chelator application[477]. The role of zinc and ATP in acute platelet activation is also conceivable, because their secretion by β-cells almost reaches its maximum after one minute of glucose stimulation, whereas insulin secretion continues to increase over a long period of time[139]. Last but not least, the peptide hormone amylin is known to be specifically released by β-cells synchronously with insulin[478,479]. In this context, RAGE was shown to not only bind AGE but also several amyloidogenic proteins, such as amylin, amyloid β, or serum amyloid A[480,481]. Additionally, amylin can aggregate to form complex amyloids, which have been shown to activate platelets through RAGE and GPIbα-mediated aggregation and agglutination[482,483]. As platelets express RAGE, this might provide another reasonable mechanism of how β-cells contribute to platelet activation[474]. To figure out which β-cell derived substance is responsible for the observed platelet activation, MIN6-cell supernatant could be subjected to biochemical modifications. The relevance of zinc could be tested by the application of a chelator, whereas apyrase or proteinase could be used to clear the supernatant from purines or proteins, respectively. Further, treatment of platelets with inhibitors of RAGE and P2X1 could verify their function in β-cell mediated activation.

Finally, the occurrence of platelet activation upon acute hyperglycemia was investigated *in vivo*. Thus, glucose was injected into C57BL/6JRj mice and plasma PBP levels were measured subsequently as a specific marker for platelet degranulation. Of note, PBP levels were shown to be significantly elevated immediately after glucose injection (Figure 11). This result proves the appearance of platelet activation during acute hyperglycemia *in vivo*. The above-discussed direct impact of glucose and β-cells on platelets may be the mechanism underlying this event. Furthermore, considering the entire organism, other factors such as the endothelium could also contribute to the observed effect. Hyperglycemia is known to reduce circulating NO levels due to an inhibited enzymatic machinery and increased ROS-mediated inactivation of it[456,457]. Along with also observed reduced PGI_2 secretion by the endothelium, these might reduce the inhibitory action on platelets[458]. Additionally, platelets possess a functional GLP-1R that upon activation reduces intracellular cAMP levels leading to inhibited platelet function and thrombus formation[484]. Thus, decreasing glucagon levels during high glucose levels might lower the inhibitory capacity. Acute glycation of the endothelium could also lead to increased platelet activation, which is also found to a greater extent in diabetic patients[485]. Finally, high glucose concentrations could alter the profile of proteins on the endothelial surface of certain tissues, thereby contributing to platelet activation. For instance, a high glucose-induced upregulation of *intercellular adhesion molecule* (ICAM)-1 was demonstrated in retinal endothelial cells[486].

Knowing that platelets store insulinotropic substances and get activated by β-cell-derived substance/s during hyperglycemia, interactions of platelets with the islet microvasculature were analyzed. Interestingly, intravital microscopy and histology of pancreatic cryosections revealed a substantially elevated attachment of platelets in the endocrine pancreas compared to the exocrine pancreas (Figure 12). This effect was greatly reduced when the functionality of platelet adhesion receptors GPVI, GPIbα, or αIIbβ3 integrin was inhibited, suggesting the binding is mediated by platelet-specific proteins (Figure 13). As described in the previous paragraph, this finding might be caused by β-cell-derived substances, such as ATP, zinc, or amylin, which might restrict platelet activation specifically within pancreatic islets. The localization analysis was executed with fasted mice, indicating that platelets constantly bind to the islet

endothelium including in euglycemic or hypoglycemic conditions. However, β-cells were demonstrated to degranulate and release ATP, zinc, and amylin also during low glucose concentrations, albeit to a lower degree[139,478,479]. This goes along with the finding that also medium supernatant obtained from low glucose treated MIN6-cells was potent to increase platelet activation (Figure 9Figure 10). Nevertheless, as it was shown here that a hyperglycemic environment increases platelet activation, it would be of interest to investigate platelet adhesion in islets after glucose application.

Besides soluble platelet activators, the pancreatic islet vasculature might possess a distinct expression of surface proteins allowing platelets to bind. Therefore, platelet adhesion receptors might exhibit interactions with yet unidentified counterparts. For example, GPIbα, αIIbβ3 integrin, and P-selectin showed binding to tumor cells, suggesting that these and other adhesion molecules may have additional interaction partners beyond those previously known[487-489]. The composition of the ECM and *basement membrane* (BM) within the endocrine pancreas is distinct from other tissues and provides β-cells with stimuli that regulate cell development as well as insulin expression and secretion[490-492]. Additionally, components of the ECM or BM display a high glucose-induced overexpression in endothelial cells[213]. Immobilized pancreatic endothelial cells (MS1), α-cells (α-TC1), and β-cells (β-TC6) were all shown to express α1(V) and α3(V) collagen[493]. Furthermore, MS1-cells were shown to secrete a truncated form of α1(V) and mice deficient for α3(V) exhibited a blunted GSIS[493]. Also, pericytes of the endocrine pancreas produce collagens, fibronectin, and laminins for the BM. This allows the speculative assumption of platelets getting activated by free, accessible components of the ECM or BM.

4.2 Inhibited platelet functionality decreases glucose-stimulated insulin secretion

As platelets release insulinotropic substances, get activated during hyperglycemia, and specifically adhere to the microvasculature of pancreatic islets, the assumption of platelets regulating glucose homeostasis grew stronger. Mice with a genetic platelet defect in adhesion ($BMC_{Gp1b\alpha^{-/-,TG}}$), activation ($BMC_{Gp6^{-/-}}$), degranulation ($BMC_{Unc13D^{-/-}}$), or second-wave activation consistently displayed glucose intolerance due to reduced GSIS (Figure 14). Nevertheless, the general islet characteristics such as size, insulin

expression, and GSIS *ex vivo* were not changed in these animals (Figure 15). Lastly, short-term induction of different platelet defects or platelet depletion for 24 h resulted in comparable phenotypes as observed in the genetic models, suggesting a direct effect of platelets on GSIS (Figure 16). Fasted glucose and insulin levels display larger differences between the different mouse models. These might arise from different experimental procedures that were performed with the animals, such as the performance of a bone marrow transplantation. Also, inbreeding of the mice strains might cause genetic shifts. Furthermore, the age of animals at the time of the metabolic assays was not always identical between the mouse models. However, littermates of the same age were used for each metabolic assay, implying that the observed metabolic changes can be referred specifically to the respective platelet defect.

All applied models exhibit a reduced GSIS, implying that platelets need to be fully functional to stimulate insulin secretion. Still, a comparison of the genetic and pharmacological mouse models reveals differences in their severity of glucose intolerance and GSIS inhibition. Effects are most pronounced when platelets are depleted, inhibited for second-wave activation through $G\alpha_q$ and $G\alpha_{13}$, or when the αIIbβ3 integrin binding site is blocked (Figure 14Figure 16). Previous results suggest an activation by β-cell-derived substance/s (Figure 9Figure 10), which potentially might be mediated through $G\alpha_q$ and $G\alpha_{13}$. The effect on GSIS further appears to depend on this activation route. The observed platelet adhesion to islet vasculature might especially rely on the adhesive properties of αIIbβ3 integrin, which was also shown to be decreased upon blockage of its binding site (Figure 13). Thus, the interference of platelets to specifically bind to islet vasculature appears to be crucial for the discovered reduction in GSIS. Nonetheless, ablation or blocking of GPVI and GPIbα reduced platelet localization within islets to a similar extent (Figure 13), whereas the effect on reduced insulin secretion is weaker in these models (Figure 14Figure 16). This raises the possibility that αIIbβ3 integrin does not only contribute to platelet binding within islets but also mediates crucial outside-in-signaling important for the impact on GSIS. This signaling might act through the known activatory αIIbβ3-PLCγ2 axis[277]. Hemostasis works as a feed-forward circle. This makes it difficult to distinguish whether certain platelet functions execute a direct effect on GSIS or whether they do it indirectly by affecting the general hemostatic event.

4.3 Platelets directly stimulate insulin secretion

The fact that mice in which platelets were pharmacologically inhibited or depleted demonstrate lower GSIS suggests a direct effect of platelets on β-cells. Indeed, co-culture with washed human platelets stimulated the GSIS of INS1-cells (Figure 19A). The application of supernatant of activated platelets to primary mouse islets or mouse, rat, and human β-cell lines shows that the effect is mediated by a released substance that acts in a concentration-dependent manner (Figure 19B-G). However, the potentiating effect of platelet-derived substances/s seems to be present only under high glucose conditions in primary islet cells, whereas INS1- and EndoC-βH1-cells show the effect even under low glucose conditions. This might be due to the heterogenic cellularity of pancreatic islets, whose paracrine interplay influences overall insulin secretion. Platelet-derived substance/s could stimulate δ- and ε-cells to release somatostatin and ghrelin, respectively, both of which downregulate insulin secretion[43,45]. Additionally, the substance/s might inhibit the release of PP from PP-cells, which is a known inhibitor of somatostatin secretion[44]. Consequently, increasing levels of somatostatin would lead to reduced insulin secretion.

Insulin secretion from β-cells is regulated by various metabolites as well as auto-, para-, and endocrine factors. To identify the exact substance/s that mediates the promoting effect on insulin secretion, hPS was biochemically modified to remove various bioactive substances. hPS with molecules greater than 3 kDa removed or free of proteins, purines, serotonin, and histamine still demonstrated a potent effect on β-cells (Figure 20A, B). Interestingly, this potency was depleted when lipophilic substances were extracted from the hPS (Figure 20C). This experiment suggests that the main insulinotropic effect is mediated by a lipid class. However, it needs to be considered that the biochemical elimination of proteins, purines, serotonin, histamine, and lipids occurred sequentially. In combination, these substances might further contribute to the potentiating effect on insulin secretion. Such synergistic potentiation has been demonstrated for ADP or ATP and Ach[401]. Furthermore, it is important to note that this experiment only considered the direct effect of hPS on INS1-cell's insulin secretion. Therefore, it excludes other pancreatic endocrine cells, the intra-islet nervous system, and the islet vasculature, which might be affected by platelets as well and are known to directly contribute to the regulation of insulin secretion[7,19,53,58]. ATP for instance is thought to be co-released with insulin to cause relaxation of islets

pericytes, which is associated with increased blood flow that favors insulin secretion[19-21]. Since platelets store ATP in their dense granules they could promote this mechanism[234]. To investigate the role of platelets on islet vasodynamics, parameters such as vessel diameter and flow rate could be studied in islets of mice exhibiting a platelet defect upon administration of a glucose bolus.

LC-MS analysis of mPS and serum from platelet-depleted mice was performed to gain insight into the lipid secretome of platelets. To take the full range of substances into account, no standards were used for this purpose, thus enabling a brought but semi-quantitative analysis. Several candidates were identified whose presence was significantly increased in mPS compared to the control buffer (Figure 21). The presence of these substances in the serum of platelet-depleted mice served as an additional parameter to assess how relevant the platelet-derived fraction of this substance is. The LC-MS method showed that the HETE family is present in mPS but is significantly reduced in the serum of mice with platelet depletion. HETEs like 5-HETE and 20-HETE as well as other AA-derived metabolites were shown already to stimulate insulin release[116,430,431]. Further work concentrated on 20-HETE, as platelets have been demonstrated to contain the necessary enzymatic machinery for its biosynthesis[308]. An isomer-specific ELISA confirmed the presence of 20-HETE in mPS and hPS as well as reduced levels in the serum of platelet-depleted mice. However, the reduction in HETE in serum from platelet-depleted mice determined by LC-MS was 96 %, whereas the reduction in 20-HETE quantified by ELISA was 50 %. This difference can only be explained if 20-HETE does not make up the largest proportion of all HETE isoforms. Indeed, others found 12-HETE to be the most abundant isoform in platelets[494]. Although 20-HETE presumably forms only a small fraction of platelet-derived HETEs, it seems to be specifically platelet-derived and appears in a nanomolar concentration in mPS. Thus, it makes it a plausible candidate to mediate platelet-induced insulin secretion. Additionally, hyperglycemia was shown to increase *de novo* synthesis of DAG, causing PKC and subsequent PLCA2 activation that finalizes in an increased production of AA metabolites[495]. It is therefore thinkable that platelets release 20-HETE in response to glucose stimulation. Thus, 20-HETE secretion by platelets following glucose stimulation could be measured *in vivo* and *in vitro*.

The injection of HET0016 to inhibit CYP450, which is essential for the biosynthesis of 20-HETE, resulted in a 70 % reduction in 20-HETE serum levels associated with glucose intolerance and reduced GSIS (Figure 24). Tunaru et al. have stated that a glucose-induced formation of 20-HETE by β-cells induces GSIS in an autocrine manner through GPCR40[116]. Therefore, reduced GSIS after HET0016 might be due to the inhibition of this autocrine mechanism. However, the application of HET0016 to platelet-depleted mice did not lead to a further reduction in glucose tolerance (Figure 24). This indicates that the platelet-derived 20-HETE fraction exerts the greatest effect on GSIS. Nevertheless, it cannot be excluded that the observed worsened glucose homeostasis is at least partially caused by the inhibition of the 20-HETE-mediated autocrine mechanism of β-cells. For this purpose, HET0016 would need to be applied to mice that obtain a genetic defect of 20-HETE synthesis specifically in β-cells, to see if the effect on GSIS is still as pronounced as observed in wild-type mice. In general, the HET0016-induced glucose intolerance and inhibition of GSIS are not as pronounced as demonstrated in platelet-depleted mice (Figure 16, Figure 24). HET0016 treatment did not completely deplete 20-HETE serum concentrations, which means that platelets may still partially exert a stimulatory influence on insulin secretion through this route. It further reinforces the assumption that other mechanisms are involved in PSIS.

Tunaru et al. demonstrated that 20-HETE promotes GSIS through $G\alpha_{q/11}$-coupled GPCR40[116]. Inhibition of $G\alpha_{q/11}$ in INS1-cells did not only abolish the potency of hPS but also general GSIS (Figure 22C). Thus, the platelet-derived substance/s appears to act in a $G\alpha_{q/11}$-dependent manner, as does an essential autocrine stimulus in INS1-cells. This autocrine stimulus might be ATP and/or 20-HETE, which get released by β-cells upon glucose stimulation and act through P2YR and GPCR40, respectively, both signaling through $G\alpha_{q/11}$[116,138,139]. Inhibition or silencing of the 20-HETE receptor GPCR40 led to a significantly reduced potency of hPS on GSIS but did not completely inhibit its effect (Figure 22C, E). Also, the characterization of mice with a global knockout of GPCR40 revealed essentially normal glucose tolerance and GSIS[496,497]. This indicates the existence of a compensatory mechanism ensuring accurate glucose homeostasis. Thus, a platelet-derived substance other than 20-HETE might exert an insulinotropic effect, or 20-HETE acts through additional receptors. Indeed, 20-HETE is also a high-affinity ligand of GPCR75, which like GPCR40 is also associated with

$G\alpha_{q/11}$[439,498]. Inhibition of GPCR75 in mice caused a mild but significant reduction in glucose tolerance (Figure 24D). Therefore, a combined blockage of these receptors could be evaluated in the future. In addition, platelets have an extensive secretome, which makes the involvement of other factors conceivable, as will be discussed later.

The injection of 20-HETE into mice lacking platelets rescued the overall glycemic dysregulation, yet resulted in a deviated curve of blood glucose levels compared with control mice (Figure 24E). On one hand, this might be caused by the lack of additional platelet-derived factors that potentially contribute to the accurate regulation of insulin secretion. On the other hand, the nonlocalized application of 20-HETE might cause this effect. In this thesis, an islet-specific platelet adhesion was demonstrated and a β-cell-derived substance/s was shown to promote platelet activation. This would allow an islet-restricted release of 20-HETE, possibly enabling much higher local concentrations to be achieved than with the i.p. injected 20-HETE bolus. Furthermore, injection of 20-HETE causes holistically elevated levels in the circulation, which, apart from β-cells, could trigger signaling events in the rest of the organism. 20-HETE is a known vasoconstrictor that upon others executes its action through GPCR75 of vascular smooth muscle cells[337,439]. The i.p. bolus of 20-HETE could therefore cause uncoordinated vasoconstriction that affects the blood supply of pancreatic islets. A generally accepted hypothesis suggests that the endocrine pancreas is divided into individual islets so that they can be regulated differently by blood flow depending on blood glucose levels[499]. Likewise, pancreatic islets exhibit different vascularization schemes, which allow blood to flow from periphery-to-center, center-to-periphery, or pole-to-pole[500]. In addition, induced pericyte depletion in pancreatic islets caused reduced functionality and insulin secretion from β-cells[501,502]. Due to this, a finely adjusted blood flow seems to be necessary to ensure proper insulin secretion. Islet-localized platelets might contribute to the control of the islet's blood supply, as described above. Holistically elevated 20-HETE levels by injection, however, could disrupt this regulatory mechanism. The literature as well as experiments from this work suggest a direct insulinotropic effect of 20-HETE through the GPCR40 signaling axis[116]. To investigate the potential acute effect of 20-HETE on the blood-circulation, knockout mice deficient for GPCR40 and/or GPCR75 specifically in β-cells could be used. A GTT and GSIS upon 20-HETE injection would thus reveal the indirect action on insulin secretion.

Here, hPS stimulation was demonstrated to cause increasing levels of $[Ca^{2+}]_i$ in INS1-cells. GPCR40 signaling in β-cells has also been associated with an elevation of $[Ca^{2+}]_i$[432,433]. This was shown to be caused by the PLC-mediated generation of IP_3 that enables the release of Ca^{2+} from the ER. Finally, exhaustion of ER Ca^{2+} levels induces the opening of the Ca^{2+} channel Orai1 through s*tromal interaction molecule* (STIM)1, further promoting Ca^{2+} entry[434]. Additionally, GPCR40 signaling leads to the opening of NSCC of the TRP channel class and inhibits voltage-gated K^+ channels, which delays the repolarization of the β-cell[119,122]. It should be noted that the hPS-induced increase in $[Ca^{2+}]_i$, although significant, is small in absolute terms and allows speculation of additional mechanisms. Interestingly, hPS stimulation was also associated with an elevated degree of PKD1 phosphorylation at serine 744/748 and 916 (Figure 23B), which is known to increase the catalytic activity of the kinase and autophosphorylation, respectively[437]. Its activation occurs by the PLC-mediated generation of DAG, which recruits PKD1 to the plasma membrane where it gets activated by DAG-activated PKC[503-505]. PKD1 has been shown to be critical for insulin secretion, presumably by promoting the fission of cell surface transport carriers from the TGN[121,506,507]. Furthermore, it was found to be activated through GPCR40 agonization, mediating cortical F-actin reorganization resulting in granule recruitment and respective promoted second phase insulin secretion[115]. Inhibition of PKD1 abolished hPS-mediated potentiation of insulin secretion, indicating a significant function in the underlying mechanism (Figure 23C). Of note, downstream signaling of DAG is known to increase insulin secretion partially independent of an additional increase of free $[Ca^{2+}]_i$[150]. This might serve as an explanation for relatively small changes of platelet-mediated $[Ca^{2+}]_i$ compared to the major change in insulin secretion. However, PKD1 was also proven to be activated through M3 and P2Y1 receptors[121,508,509]. To test the role of these receptors in hPS-stimulated insulin secretion, stimulation experiments using respective inhibitors could be executed. Furthermore, hPS could be generated in the presence of HET0016, to evaluate its potency when 20-HETE is ablated.

The LC-MS analysis indicated the presence of several lipid classes in platelets secretome, including lysoPAF (Figure 21). However, the detected lysoPAF species were solely annotated by their retention time and molecule masses. This raises the

possibility of substances with the same mass being confused for one another. Because of this, it would be crucial to confirm the annotation by substance-specific methods such as ELISA or by MS approaches in the future. PAF and its precursor lysoPAF displayed stimulatory actions on insulin secretion of isolated rat islets[440]. Even though PAF was not detected by the applied LC-MS approach, it is known to be continuously generated by platelets and released upon activation[441,442]. The fact that lysoPAF was presumably detected in mPS, but is increased in the serum of platelet-depleted mice might be explainable by platelet-derived enzymes that structurally modify or degrade it. In order to make a reliable conclusion, exact concentrations of PAF and lysoPAF in mPS/hPS and serum would need to be quantified. Here, a concentration-dependent stimulatory action of PAF and lysoPAF upon 2.8 mM and 25 mM glucose was confirmed in MIN6-cells (Figure 25B, C). PAF is known to act through the PAFR, with the respective gene being highly transcribed in the endocrine cells of the pancreas[443]. It has further been shown to be also associated with $G\alpha_q$[510]. The application of the PAFR antagonist SR27417 reduced the stimulatory action, proving that the observed effect is not due to cell destruction (Figure 26). It additionally inhibited overall GSIS, suggesting the existence of a stimulatory autocrine mechanism acting through PAFR or off-target effects of SR27417 (Figure 26). However, restricting the SR27417 application only to the high glucose stimulation period recovered GSIS but strikingly, abolished the promoting effect of mPS (Figure 26). Again, the total depletion of hPS-induced insulin secretion speaks for an off-target effect of SR27417, as also inhibition and silencing of GPCR40 caused a partial depletion of this effect. Although diminished GSIS upon PAFR antagonization, absolute values of insulin secretion were still significantly increased upon stimulation with PAF and lysoPAF (Figure 26). Therefore, at the applied concentrations, these substances could act through additional signaling pathways. GPCR119 is a thinkable candidate, as its signaling axis is known to promote GSIS and it additionally can be activated by PAF and lysoPAF[123,124]. As GPCR119 is associated with $G\alpha_s$, its activation by a platelet-derived substance/s could be investigated by the measurement of intracellular cAMP levels[124,125]. Furthermore, lysophospholipids were thought to act as membrane fusigens, thereby promoting degranulation processes[440].

In general, many lipids were identified to be released by platelets. Based on limited sensitivity, it can be assumed that other lipids are present at concentrations where

they may be bioactive. The lipid extraction from hPS has demonstrated that substances of the lipid class execute the major effect on insulin secretion. Although 20-HETE and PAF/lysoPAF have been validated to play a role in PSIS, other lipids might still contribute to this effect. The above-mentioned GPCR119 also gets activated by LPC, which was identified by LC-MS as well[125]. Similarly, GPCR55, which is associated with $G\alpha_q$ or $G\alpha_{12/13}$, can be activated by LPC, LPI, and PEA, upon others, leading to the activation of PLC, Rho-associated protein, and ERK, thus leading to increased $[Ca^{2+}]_i$[117,126-130]. These substances were also found by the LC-MS analysis, with LPI being drastically elevated in mPS. Here again, increased levels in the serum of platelet-depleted mice might be due to a reduced half-life in the presence of degranulating platelets. Independent of any signaling cascade, some lipids might diffuse into the cell directly prompting the fusion of granules with the cell membrane, as was shown for MAG[135]. To evaluate these hypotheses, the existence of these substances would first need to be verified by ELISA or MS approach. To study their potential influence on PSIS, the respective receptors and their associated G-proteins would further need to be silenced or inhibited in β-cells.

4.4 Platelet-stimulated insulin secretion decreases with age

To investigate whether antithrombotic drugs prescribed to humans affect glucose homeostasis, mice were administered clopidogrel and ASA. Notably, mice receiving clopidogrel showed reduced glucose tolerance and GSIS, whereas ASA did not affect glucose homeostasis (Figure 27). Above, it was described that platelets are presumably activated specifically in the vasculature of the pancreatic islets. Platelet-derived ADP is the major mediator of second-wave activation to amplify the hemostatic event[234,235]. Therefore, it can be hypothesized that inhibition of the ADP receptor P2Y12 results in reduced amplification of islet-restricted platelet activation, resulting in decreased platelet-induced insulin secretion. ASA inhibits the activity of COX1 and therefore the synthesis of TxA_2 and its mediated platelet activation[448,449]. Thus, its application should also reduce the second-wave activation of platelets. In general, lower daily dosages than 40 mg/kg of orally applied ASA have been demonstrated to significantly reduce TxA_2 generation and platelet aggregation[511,512]. Here, ASA was administered *ad libitum* via drinking water, which means that the calculated dose of

40 mg/kg may not be reached. The inhibition of TxA_2 production and corresponding inhibition of TxA_2-mediated platelet aggregation does not act linearly, as more than 95 % of TxA_2 needs to be depleted to affect platelet function[513]. Thus, the applied dosage might have been below this threshold. Furthermore, the GTT was performed after 4 weeks of ASA administration, possibly resulting in the development of ASA resistance, a phenomenon observed in 2 % to 57 % of patients[514-516]. In this context, also compensatory mechanisms such as the upregulation of other second-wave platelet receptors might play a role. Finally, ASA or depletion of systemic COX1 function was shown to reduce the generation of antiaggregatory PGD_2 and PGI_2 at non-platelet sites, potentially promoting thrombotic events[517]. To validate the inhibitory effect of the applied ASA administration, platelet activation and aggregation would need to be measured by flow cytometry and an *in vivo* vessel-occlusion model, respectively. Nevertheless, the absence of changes in glucose homeostasis with ASA administration may be taken as an indication that no insulinotropic platelet-derived substance originates downstream of the COX1 synthesis pathway.

The inhibitory effect of clopidogrel on GSIS has not been documented in humans, although the average age of clopidogrel patients is 69 years[450]. This raised the hypothesis that PSIS decreases with age. Indeed, clopidogrel administration to mice older than 61 weeks did not affect GTT or GSIS, and GTT was neither changed in aged platelet-depleted mice. Strikingly, this was accompanied by a decrease in 20-HETE serum levels in aged mice and humans (Figure 28). The question of what causes this reduction, as well as how glucose homeostasis occurs in aged individuals independently of platelets, remains a matter of speculation. Further lipidomic studies of the platelet secretome of young and aged individuals would need to be performed to determine whether the occurrence of other lipids is also changed by aging. On one hand, other lipids such as lysoPAF might be identified to be reduced as well, contributing to the loss of platelet-induced insulin secretion. On the other hand, the results might enable the identification of certain synthesis pathways that might be downregulated with advanced age. Subsequently, key enzymes of these pathways could be characterized regarding their expression and activity. Also, the source of 20-HETE needs to be determined. 20-HETE gets synthesized by CYP450 of the 4A and 4F gene families[518]. Furthermore, its synthesis can be also mediated by the CYP4502U1, which has been shown to be present in platelets[519]. However, CYP450

products were shown to be integral components of the platelet membrane in humans, which can be released by receptor-induced de-esterification of phospholipids[310]. Thus, CYP450 products including 20-HETE might be taken up by platelets and integrated into the membrane until they get released upon activation[303,306,311]. Therefore, the expression of the respective CYP450 enzymes needs to be analyzed in platelets. Studies focusing on the expression of different CYP450 enzymes in rat livers revealed that CYP450-4A1, which is one of the 20-HETE-producing isoforms, continuously decreases between the ages of 60 and 800 days[520]. Similar trends might be also present in other tissues and cell types, finally leading to a reduced amount of platelet-releasable 20-HETE. The finding that PSIS declines with age, while insulin secretion and glucose tolerance remain intact, raises questions. The occurrence of T2D strongly correlates with age, which is, upon others, due to a reduced baseline and compensatory β-cell replication[521,522]. Surprisingly, decoupling β-cells from the cell-division cycle was shown to increase the GSIS of β-cells in aged mice and humans. Hence, the senescence effector p16(Ink4a) is increasingly expressed in β-cells of aged humans and promotes GSIS through enhanced glucose uptake and mitochondrial activity[523]. Also, epigenetics were shown to be changed with age specifically in β-cells. The methylation status was demonstrated to be shifted favoring the activation of metabolic regulators resulting in improved β-cell functioning[524]. Furthermore, the expression of transcription factors like SIX2 and SIX3 were displayed to be elevated in β-cells from aged individuals, which was sufficient for elevated insulin content and secretion[525]. Thus, isolated islets from 27 months old WT mice presented a threefold GSIS compared to islets from 1 month old mice[523]. Therefore, the decreased impact of PSIS with advanced age might be covered up and compensated by these mechanisms. Of note, platelet-depletion in aged mice even improved glucose tolerance (Figure 28). This suggests an additional weak inhibitory effect of platelets on insulin secretion, which is overridden in young mice by the presence of the stronger positive stimulus.

In search for the origin of the reduced PSIS in aged mice, 59 weeks old C57BL/6JRj mice were lethally irradiated before being reconstituted with bone marrow of 59 weeks or 7 weeks old C57BL/6JRj donor mice. Even though there was a transient reduction in glucose tolerance of mice that received BM of young donor mice, no change in GTT,

GSIS, or ITT was observed after 8 weeks of BMC generation (Figure 29). In general bone marrow transplantation has been shown to cause transient glucose intolerance[526-528]. In comparison to patients who get autologous transplants, allogeneic hematopoietic stem cell transplantation recipients have a greater chance of developing posttransplant diabetes mellitus[529]. For this reason, the non-matching age of the donor animals might promote the allogenic phenotype causing a temporary reduction in glucose tolerance. The result of generated BMCs indicates that the reduced impact of platelets on insulin secretion in aged mice does not originate from age-dependent changes of MKs. However, the transplantation process might cause a selection process of MKs, by which only functional MKs are successfully reconstituting in recipient mice. Therefore, it can not be excluded that unfunctional or senescent MKs might cause reduced PSIS in aged mice. Furthermore, the platelet environment such as the vasculature and plasma components might affect platelets in a way that they execute reduced PSIS. Finally, an often observed age-dependent drop in platelet count might be explanational[396-398]. For further analysis, platelet transfusion experiments between young and aged mice could be performed to investigate whether this can restore PSIS in old animals. As described earlier, PSIS might also be mediated by alterations in blood circulation through pancreatic islets. Advanced age might therefore lead to changes in the vasculature that lead to a loss of this mechanism. Finally, reduced PSIS in aged individuals might be also partially due to alterations of β-cells. Therefore, the response of pancreatic islets isolated from aged mice and humans to the supernatant of activated platelets could be tested.

Whereas PSIS decreased with increasing age, glucose tolerance remained disturbed in 55 weeks old $G\alpha_q G\alpha_{13}$ PF4 Δ/Δ mice. Histological analysis revealed reduced islet vascularity in these animals (Figure 30). It has been shown that a pancreas-restricted knockdown of VEGF-A led to reduced islet vascularization, which was associated with strongly reduced glucose tolerance[452]. Platelets are important regulators of angiogenesis and release multiple angiogenic substances, such as VEGFs, PDGF, and *fibroblast growth factor* (FGF)-2), upon others[231-233]. Furthermore, it has been shown that platelet-derived angiogenic factors do not only promote angiogenesis after vascular injuries but also during developmental processes and for the maintenance of vasculature[530-534]. In this context, studies demonstrated that the binding of platelets

to the vasculature is a crucial step to execute their angiogenetic effect[532]. Here, increased adhesion of platelets to the vasculature of pancreatic islets was revealed, allowing the assumption that platelets might also affect angiogenesis in islets. It could be determined, whether platelets of $G\alpha_q G\alpha_{13}$ PF4 Δ/Δ mice display a reduced attachment within islets vasculature. In addition, the strongly inhibited response to soluble activators in $G\alpha_q G\alpha_{13}$ PF4 Δ/Δ mice might cause an insufficient supply of angiogenic stimuli. The upregulation of β-cells' VEGF-A expression might be due to a compensatory mechanism. In addition to the quantity of the islet vasculature, its integrity should be investigated as well. Furthermore, different mouse models could be applied to investigate the impact of platelets on islet vascularization. Mice deficient for the *neurobeachin-like* (*NBEAL*)*2* gene, that exhibit a defect in α-granule release in which most of the angiogenic factors are stored, could be used to screen for differences in the islet vasculature[249,535]. As an attempt to narrow down the actual angiogenic factor/s, mice with platelet-restricted depletion of VEGFs, PDGF, and other factors could be additionally used. However, the pharmacologically induced platelet defects prove a stimulating effect of platelets on insulin secretion independently of the degree of islet vascularization. Nevertheless, in all genetic models in which platelet defects were present for several weeks, it needs to be investigated whether these defects resulted in reduced islet vascularization and to what extent glucose homeostasis might be altered by this.

4.5 Closing remarks and future perspectives

In the here presented thesis, the impact of platelets on β-cells insulin secretion was studied. It was shown that both glucose and a β-cell-derived factor/s promote platelet activation. Further work needs to be done to identify this factor/s and the underlying mechanisms of these findings. In this context, also the contribution of the observed platelet adhesion within the islet vasculature needs to be determined. A stimulatory effect of platelets on insulin secretion was shown, which could be attributed to lipids, specifically to 20-HETE and presumably lysoPAF. Future studies need to investigate which other lipid receptors besides GPCR40, GPCR75, and PAFR might be involved in platelet-stimulated insulin secretion. The same counts for additional lipids that were identified in the secretome of platelets and potentially contribute to the insulinotropic

effect. Here it would also be important to understand how exactly the secretion of these lipids occurs and how it is initiated. Besides their direct action on β-cells, platelets were demonstrated to be crucial for the development or maintenance of the islet vasculature, hence indirectly affecting glucose homeostasis. Therefore, further studies need to be initiated to understand the exact angiogenic mechanism. Finally, it has been shown that the acute insulinotropic effect of platelets decreases with age, which was associated with declining serum levels of 20-HETE. On the one hand, it would be important to find out whether other properties of the platelets change with age and could thus contribute to this effect. On the other hand, it would be interesting to identify the origin that leads to these altered platelet characteristics in aged subjects. Finally, the mechanism of platelet-induced insulin secretion in humans would need to be examined, for example, in young humans undergoing clopidogrel administration.

In summary, an unexpected effect of platelets on β-cell function was discovered in this thesis. This work may serve as a basis for further research allowing a more detailed understanding of the unraveled mechanism. Thus, it may open new therapeutic avenues for the treatment of impaired glucose homeostasis.

6 REFERENCES

1 Innes, J. T. & Carey, L. C. Normal pancreatic dimensions in the adult human. *Am J Surg* **167**, 261-263 (1994). https://doi.org:10.1016/0002-9610(94)90088-4

2 Bock, T., Pakkenberg, B. & Buschard, K. Genetic background determines the size and structure of the endocrine pancreas. *Diabetes* **54**, 133-137 (2005). https://doi.org:10.2337/diabetes.54.1.133

3 Karpinska, M. & Czauderna, M. Pancreas-Its Functions, Disorders, and Physiological Impact on the Mammals' Organism. *Front Physiol* **13**, 807632 (2022). https://doi.org:10.3389/fphys.2022.807632

4 Murphy, J. A. *et al.* Direct activation of cytosolic Ca2+ signaling and enzyme secretion by cholecystokinin in human pancreatic acinar cells. *Gastroenterology* **135**, 632-641 (2008). https://doi.org:10.1053/j.gastro.2008.05.026

5 Ionescu-Tirgoviste, C. *et al.* A 3D map of the islet routes throughout the healthy human pancreas. *Sci Rep* **5**, 14634 (2015). https://doi.org:10.1038/srep14634

6 Da Silva Xavier, G. The Cells of the Islets of Langerhans. *J Clin Med* **7** (2018). https://doi.org:10.3390/jcm7030054

7 Rorsman, P. & Ashcroft, F. M. Pancreatic beta-Cell Electrical Activity and Insulin Secretion: Of Mice and Men. *Physiol Rev* **98**, 117-214 (2018). https://doi.org:10.1152/physrev.00008.2017

8 Briant, L., Salehi, A., Vergari, E., Zhang, Q. & Rorsman, P. Glucagon secretion from pancreatic alpha-cells. *Ups J Med Sci* **121**, 113-119 (2016). https://doi.org:10.3109/03009734.2016.1156789

9 Hauge-Evans, A. C. *et al.* Somatostatin secreted by islet delta-cells fulfills multiple roles as a paracrine regulator of islet function. *Diabetes* **58**, 403-411 (2009). https://doi.org:10.2337/db08-0792

10 Larsson, L. I., Sundler, F. & Hakanson, R. Immunohistochemical localization of human pancreatic polypeptide (HPP) to a population of islet cells. *Cell Tissue Res* **156**, 167-171 (1975). https://doi.org:10.1007/BF00221800

11 Nam, K. H. *et al.* Size-based separation and collection of mouse pancreatic islets for functional analysis. *Biomed Microdevices* **12**, 865-874 (2010). https://doi.org:10.1007/s10544-010-9441-2

12 Cabrera, O. *et al.* The unique cytoarchitecture of human pancreatic islets has implications for islet cell function. *Proc Natl Acad Sci U S A* **103**, 2334-2339 (2006). https://doi.org:10.1073/pnas.0510790103

13 Kim, A. *et al.* Islet architecture: A comparative study. *Islets* **1**, 129-136 (2009). https://doi.org:10.4161/isl.1.2.9480

14 Quesada, I., Tuduri, E., Ripoll, C. & Nadal, A. Physiology of the pancreatic alpha-cell and glucagon secretion: role in glucose homeostasis and diabetes. *J Endocrinol* **199**, 5-19 (2008). https://doi.org:10.1677/JOE-08-0290

15 Wieczorek, G., Pospischil, A. & Perentes, E. A comparative immunohistochemical study of pancreatic islets in laboratory animals (rats, dogs, minipigs, nonhuman primates). *Exp Toxicol Pathol* **50**, 151-172 (1998). https://doi.org:10.1016/S0940-2993(98)80078-X

16 Brissova, M. *et al.* Assessment of human pancreatic islet architecture and composition by laser scanning confocal microscopy. *J Histochem Cytochem* **53**, 1087-1097 (2005). https://doi.org:10.1369/jhc.5C6684.2005

17 Bonner-Weir, S. & Orci, L. New perspectives on the microvasculature of the islets of Langerhans in the rat. *Diabetes* **31**, 883-889 (1982). https://doi.org:10.2337/diab.31.10.883

18 Konstantinova, I. & Lammert, E. Microvascular development: learning from pancreatic islets. *Bioessays* **26**, 1069-1075 (2004). https://doi.org:10.1002/bies.20105

19 Ballian, N. & Brunicardi, F. C. Islet vasculature as a regulator of endocrine pancreas function. *World J Surg* **31**, 705-714 (2007). https://doi.org:10.1007/s00268-006-0719-8

20 Almaca, J., Weitz, J., Rodriguez-Diaz, R., Pereira, E. & Caicedo, A. The Pericyte of the Pancreatic Islet Regulates Capillary Diameter and Local Blood Flow. *Cell Metab* **27**, 630-644 e634 (2018). https://doi.org:10.1016/j.cmet.2018.02.016

21 Tamayo, A. *et al.* Pericyte Control of Blood Flow in Intraocular Islet Grafts Impacts Glucose Homeostasis in Mice. *Diabetes* **71**, 1679-1693 (2022). https://doi.org:10.2337/db21-1104

22 American Diabetes Association Professional Practice, C. 2. Classification and Diagnosis of Diabetes: Standards of Medical Care in Diabetes-2022. *Diabetes Care* **45**, S17-S38 (2022). https://doi.org:10.2337/dc22-S002

23 Nakrani, M. N., Wineland, R. H. & Anjum, F. in *StatPearls* (2022).

24 Walker, J. N. *et al.* Regulation of glucagon secretion by glucose: paracrine, intrinsic or both? *Diabetes Obes Metab* **13 Suppl 1**, 95-105 (2011). https://doi.org:10.1111/j.1463-1326.2011.01450.x

25 Freychet, L. *et al.* Effect of intranasal glucagon on blood glucose levels in healthy subjects and hypoglycaemic patients with insulin-dependent diabetes. *Lancet* **1**, 1364-1366 (1988). https://doi.org:10.1016/s0140-6736(88)92181-2

26 Finan, B., Capozzi, M. E. & Campbell, J. E. Repositioning Glucagon Action in the Physiology and Pharmacology of Diabetes. *Diabetes* **69**, 532-541 (2020). https://doi.org:10.2337/dbi19-0004

27 Sandoval, D. A. & D'Alessio, D. A. Physiology of proglucagon peptides: role of glucagon and GLP-1 in health and disease. *Physiol Rev* **95**, 513-548 (2015). https://doi.org:10.1152/physrev.00013.2014

28 Duncan, R. E., Ahmadian, M., Jaworski, K., Sarkadi-Nagy, E. & Sul, H. S. Regulation of lipolysis in adipocytes. *Annu Rev Nutr* **27**, 79-101 (2007). https://doi.org:10.1146/annurev.nutr.27.061406.093734

29 Billington, C. J., Briggs, J. E., Link, J. G. & Levine, A. S. Glucagon in physiological concentrations stimulates brown fat thermogenesis in vivo. *Am J Physiol* **261**, R501-507 (1991). https://doi.org:10.1152/ajpregu.1991.261.2.R501

30 Komatsu, M., Takei, M., Ishii, H. & Sato, Y. Glucose-stimulated insulin secretion: A newer perspective. *J Diabetes Investig* **4**, 511-516 (2013). https://doi.org:10.1111/jdi.12094

31 Leto, D. & Saltiel, A. R. Regulation of glucose transport by insulin: traffic control of GLUT4. *Nat Rev Mol Cell Biol* **13**, 383-396 (2012). https://doi.org:10.1038/nrm3351

32 Burns, T. W., Terry, B. E., Langley, P. E. & Robison, G. A. Insulin inhibition of lipolysis of human adipocytes: the role of cyclic adenosine monophosphate. *Diabetes* **28**, 957-961 (1979). https://doi.org:10.2337/diab.28.11.957

33 Mohan, C. & Bessman, S. P. Insulin "inhibition" of gluconeogenesis by stimulation of protein synthesis. *Biochem Med* **26**, 403-426 (1981). https://doi.org:10.1016/0006-2944(81)90016-8

34 Petersen, K. F., Laurent, D., Rothman, D. L., Cline, G. W. & Shulman, G. I. Mechanism by which glucose and insulin inhibit net hepatic glycogenolysis in humans. *J Clin Invest* **101**, 1203-1209 (1998). https://doi.org:10.1172/JCI579

35 Campbell, J. E. & Newgard, C. B. Mechanisms controlling pancreatic islet cell function in insulin secretion. *Nat Rev Mol Cell Biol* **22**, 142-158 (2021). https://doi.org:10.1038/s41580-020-00317-7

36 Akesson, B., Panagiotidis, G., Westermark, P. & Lundquist, I. Islet amyloid polypeptide inhibits glucagon release and exerts a dual action on insulin release from isolated islets. *Regul Pept* **111**, 55-60 (2003). https://doi.org:10.1016/s0167-0115(02)00252-5

37 Gedulin, B. R., Jodka, C. M., Herrmann, K. & Young, A. A. Role of endogenous amylin in glucagon secretion and gastric emptying in rats demonstrated with the selective antagonist, AC187. *Regul Pept* **137**, 121-127 (2006). https://doi.org:10.1016/j.regpep.2006.06.004

38 Franklin, I., Gromada, J., Gjinovci, A., Theander, S. & Wollheim, C. B. Beta-cell secretory products activate alpha-cell ATP-dependent potassium channels to inhibit glucagon release. *Diabetes* **54**, 1808-1815 (2005). https://doi.org:10.2337/diabetes.54.6.1808

39 Leung, Y. M. *et al.* Insulin regulates islet alpha-cell function by reducing KATP channel sensitivity to adenosine 5'-triphosphate inhibition. *Endocrinology* **147**, 2155-2162 (2006). https://doi.org:10.1210/en.2005-1249

40 Ishihara, H., Maechler, P., Gjinovci, A., Herrera, P. L. & Wollheim, C. B. Islet beta-cell secretion determines glucagon release from neighbouring alpha-cells. *Nat Cell Biol* **5**, 330-335 (2003). https://doi.org:10.1038/ncb951

41 Samols, E., Marri, G. & Marks, V. Promotion of Insulin Secretion by Glucagon. *Lancet* **2**, 415-416 (1965). https://doi.org:10.1016/s0140-6736(65)90761-0

42 Huypens, P., Ling, Z., Pipeleers, D. & Schuit, F. Glucagon receptors on human islet cells contribute to glucose competence of insulin release. *Diabetologia* **43**, 1012-1019 (2000). https://doi.org:10.1007/s001250051484

43 Rorsman, P. & Huising, M. O. The somatostatin-secreting pancreatic delta-cell in health and disease. *Nat Rev Endocrinol* **14**, 404-414 (2018). https://doi.org:10.1038/s41574-018-0020-6

44 Brereton, M. F., Vergari, E., Zhang, Q. & Clark, A. Alpha-, Delta- and PP-cells: Are They the Architectural Cornerstones of Islet Structure and Co-ordination? *J Histochem Cytochem* **63**, 575-591 (2015). https://doi.org:10.1369/0022155415583535

45 Sakata, N., Yoshimatsu, G. & Kodama, S. Development and Characteristics of Pancreatic Epsilon Cells. *Int J Mol Sci* **20** (2019). https://doi.org:10.3390/ijms20081867

46 Mani, B. K. *et al.* The role of ghrelin-responsive mediobasal hypothalamic neurons in mediating feeding responses to fasting. *Mol Metab* **6**, 882-896 (2017). https://doi.org:10.1016/j.molmet.2017.06.011

47 Mani, B. K. & Zigman, J. M. Ghrelin as a Survival Hormone. *Trends Endocrinol Metab* **28**, 843-854 (2017). https://doi.org:10.1016/j.tem.2017.10.001

48 Patterson, M., Bloom, S. R. & Gardiner, J. V. Ghrelin and appetite control in humans--potential application in the treatment of obesity. *Peptides* **32**, 2290-2294 (2011). https://doi.org:10.1016/j.peptides.2011.07.021

49 Dupre, J., Ross, S. A., Watson, D. & Brown, J. C. Stimulation of insulin secretion by gastric inhibitory polypeptide in man. *J Clin Endocrinol Metab* **37**, 826-828 (1973). https://doi.org:10.1210/jcem-37-5-826

50 Mojsov, S., Weir, G. C. & Habener, J. F. Insulinotropin: glucagon-like peptide I (7-37) co-encoded in the glucagon gene is a potent stimulator of insulin release in the perfused rat pancreas. *J Clin Invest* **79**, 616-619 (1987). https://doi.org:10.1172/JCI112855

51 Druce, M. R. *et al.* Ghrelin increases food intake in obese as well as lean subjects. *Int J Obes (Lond)* **29**, 1130-1136 (2005). https://doi.org:10.1038/sj.ijo.0803001

52 Dezaki, K. *et al.* Endogenous ghrelin in pancreatic islets restricts insulin release by attenuating Ca2+ signaling in beta-cells: implication in the glycemic control in rodents. *Diabetes* **53**, 3142-3151 (2004). https://doi.org:10.2337/diabetes.53.12.3142

53 Ahren, B. Autonomic regulation of islet hormone secretion--implications for health and disease. *Diabetologia* **43**, 393-410 (2000). https://doi.org:10.1007/s001250051322

54 Taborsky, G. J., Jr. & Mundinger, T. O. Minireview: The role of the autonomic nervous system in mediating the glucagon response to hypoglycemia. *Endocrinology* **153**, 1055-1062 (2012). https://doi.org:10.1210/en.2011-2040

55 Berthoud, H. R., Bereiter, D. A., Trimble, E. R., Siegel, E. G. & Jeanrenaud, B. Cephalic phase, reflex insulin secretion. Neuroanatomical and physiological characterization. *Diabetologia* **20 Suppl**, 393-401 (1981).

56 Thorens, B. Neural regulation of pancreatic islet cell mass and function. *Diabetes Obes Metab* **16 Suppl 1**, 87-95 (2014). https://doi.org:10.1111/dom.12346

57 Lundquist, I. & Ericson, L. E. beta-Adrenergic insulin release and adrenergic innervation of mouse pancreatic islets. *Cell Tissue Res* **193**, 73-85 (1978). https://doi.org:10.1007/BF00221602

58 Rodriguez-Diaz, R. & Caicedo, A. Neural control of the endocrine pancreas. *Best Pract Res Clin Endocrinol Metab* **28**, 745-756 (2014). https://doi.org:10.1016/j.beem.2014.05.002

59 Thorens, B. GLUT2, glucose sensing and glucose homeostasis. *Diabetologia* **58**, 221-232 (2015). https://doi.org:10.1007/s00125-014-3451-1

60 Heimberg, H., De Vos, A., Pipeleers, D., Thorens, B. & Schuit, F. Differences in glucose transporter gene expression between rat pancreatic alpha- and beta-cells are correlated to differences in glucose transport but not in glucose utilization. *J Biol Chem* **270**, 8971-8975 (1995). https://doi.org:10.1074/jbc.270.15.8971

61 Matschinsky, F. M. Regulation of pancreatic beta-cell glucokinase: from basics to therapeutics. *Diabetes* **51 Suppl 3**, S394-404 (2002). https://doi.org:10.2337/diabetes.51.2007.s394

62 Liang, Y. *et al.* Effects of glucose on insulin secretion, glucokinase activity, and transgene expression in transgenic mouse islets containing an upstream glucokinase promoter-human growth hormone fusion gene. *Diabetes* **43**, 1138-1145 (1994). https://doi.org:10.2337/diab.43.9.1138

63 Doliba, N. M. *et al.* Glucokinase activation repairs defective bioenergetics of islets of Langerhans isolated from type 2 diabetics. *Am J Physiol Endocrinol Metab* **302**, E87-E102 (2012). https://doi.org:10.1152/ajpendo.00218.2011

64 Prentki, M., Matschinsky, F. M. & Madiraju, S. R. Metabolic signaling in fuel-induced insulin secretion. *Cell Metab* **18**, 162-185 (2013). https://doi.org:10.1016/j.cmet.2013.05.018

65 Inagaki, N. *et al.* Reconstitution of IKATP: an inward rectifier subunit plus the sulfonylurea receptor. *Science* **270**, 1166-1170 (1995). https://doi.org:10.1126/science.270.5239.1166

66 Braun, M. *et al.* Voltage-gated ion channels in human pancreatic beta-cells: electrophysiological characterization and role in insulin secretion. *Diabetes* **57**, 1618-1628 (2008). https://doi.org:10.2337/db07-0991

67 Rorsman, P., Braun, M. & Zhang, Q. Regulation of calcium in pancreatic alpha- and beta-cells in health and disease. *Cell Calcium* **51**, 300-308 (2012). https://doi.org:10.1016/j.ceca.2011.11.006

68 Jing, X. *et al.* CaV2.3 calcium channels control second-phase insulin release. *J Clin Invest* **115**, 146-154 (2005). https://doi.org:10.1172/JCI22518

69 Jacobson, D. A. & Philipson, L. H. Action potentials and insulin secretion: new insights into the role of Kv channels. *Diabetes Obes Metab* **9 Suppl 2**, 89-98 (2007). https://doi.org:10.1111/j.1463-1326.2007.00784.x

70 Santos, R. M. *et al.* Widespread synchronous [Ca2+]i oscillations due to bursting electrical activity in single pancreatic islets. *Pflugers Arch* **418**, 417-422 (1991). https://doi.org:10.1007/BF00550880

71 Chang, T. W. & Goldberg, A. L. The metabolic fates of amino acids and the formation of glutamine in skeletal muscle. *J Biol Chem* **253**, 3685-3693 (1978).

72 Maechler, P. & Wollheim, C. B. Mitochondrial glutamate acts as a messenger in glucose-induced insulin exocytosis. *Nature* **402**, 685-689 (1999). https://doi.org:10.1038/45280

73 Eto, K. *et al.* Role of NADH shuttle system in glucose-induced activation of mitochondrial metabolism and insulin secretion. *Science* **283**, 981-985 (1999). https://doi.org:10.1126/science.283.5404.981

74 Bender, K., Newsholme, P., Brennan, L. & Maechler, P. The importance of redox shuttles to pancreatic beta-cell energy metabolism and function. *Biochem Soc Trans* **34**, 811-814 (2006). https://doi.org:10.1042/BST0340811

75 Fu, Z., Gilbert, E. R. & Liu, D. Regulation of insulin synthesis and secretion and pancreatic Beta-cell dysfunction in diabetes. *Curr Diabetes Rev* **9**, 25-53 (2013).

76 Henquin, J. C., Dufrane, D. & Nenquin, M. Nutrient control of insulin secretion in isolated normal human islets. *Diabetes* **55**, 3470-3477 (2006). https://doi.org:10.2337/db06-0868

77 Hedeskov, C. J. Mechanism of glucose-induced insulin secretion. *Physiol Rev* **60**, 442-509 (1980). https://doi.org:10.1152/physrev.1980.60.2.442

78 Curry, D. L., Bennett, L. L. & Grodsky, G. M. Requirement for calcium ion in insulin secretion by the perfused rat pancreas. *Am J Physiol* **214**, 174-178 (1968). https://doi.org:10.1152/ajplegacy.1968.214.1.174

79 Daniel, S., Noda, M., Straub, S. G. & Sharp, G. W. Identification of the docked granule pool responsible for the first phase of glucose-stimulated insulin secretion. *Diabetes* **48**, 1686-1690 (1999). https://doi.org:10.2337/diabetes.48.9.1686

80 Rorsman, P. & Renstrom, E. Insulin granule dynamics in pancreatic beta cells. *Diabetologia* **46**, 1029-1045 (2003). https://doi.org:10.1007/s00125-003-1153-1

81 Kalwat, M. A. & Thurmond, D. C. Signaling mechanisms of glucose-induced F-actin remodeling in pancreatic islet beta cells. *Exp Mol Med* **45**, e37 (2013). https://doi.org:10.1038/emm.2013.73

82 Ohara-Imaizumi, M. *et al.* Imaging analysis reveals mechanistic differences between first- and second-phase insulin exocytosis. *J Cell Biol* **177**, 695-705 (2007). https://doi.org:10.1083/jcb.200608132

83 Henquin, J. C., Dufrane, D., Kerr-Conte, J. & Nenquin, M. Dynamics of glucose-induced insulin secretion in normal human islets. *Am J Physiol Endocrinol Metab* **309**, E640-650 (2015). https://doi.org:10.1152/ajpendo.00251.2015

84 Thore, S., Dyachok, O., Gylfe, E. & Tengholm, A. Feedback activation of phospholipase C via intracellular mobilization and store-operated influx of Ca2+ in insulin-secreting beta-cells. *J Cell Sci* **118**, 4463-4471 (2005). https://doi.org:10.1242/jcs.02577

85 Steinberg, S. F. Structural basis of protein kinase C isoform function. *Physiol Rev* **88**, 1341-1378 (2008). https://doi.org:10.1152/physrev.00034.2007

86 Porat-Shliom, N., Milberg, O., Masedunskas, A. & Weigert, R. Multiple roles for the actin cytoskeleton during regulated exocytosis. *Cell Mol Life Sci* **70**, 2099-2121 (2013). https://doi.org:10.1007/s00018-012-1156-5

87 Hartwig, J. H. *et al.* MARCKS is an actin filament crosslinking protein regulated by protein kinase C and calcium-calmodulin. *Nature* **356**, 618-622 (1992). https://doi.org:10.1038/356618a0

88 Stevens, C. F. & Sullivan, J. M. Regulation of the readily releasable vesicle pool by protein kinase C. *Neuron* **21**, 885-893 (1998). https://doi.org:10.1016/s0896-6273(00)80603-0

89 Vitale, M. L., Seward, E. P. & Trifaro, J. M. Chromaffin cell cortical actin network dynamics control the size of the release-ready vesicle pool and the initial rate of exocytosis. *Neuron* **14**, 353-363 (1995). https://doi.org:10.1016/0896-6273(95)90291-0

90 Smith, C. A persistent activity-dependent facilitation in chromaffin cells is caused by Ca2+ activation of protein kinase C. *J Neurosci* **19**, 589-598 (1999).

91 Yu, W. *et al.* Synergism of protein kinase A, protein kinase C, and myosin light-chain kinase in the secretory cascade of the pancreatic beta-cell. *Diabetes* **49**, 945-952 (2000). https://doi.org:10.2337/diabetes.49.6.945

92 Yokoyama, C. T. *et al.* Mechanism of SNARE protein binding and regulation of Cav2 channels by phosphorylation of the synaptic protein interaction site. *Mol Cell Neurosci* **28**, 1-17 (2005). https://doi.org:10.1016/j.mcn.2004.08.019

93 Barg, S. *et al.* Fast exocytosis with few Ca(2+) channels in insulin-secreting mouse pancreatic B cells. *Biophys J* **81**, 3308-3323 (2001). https://doi.org:10.1016/S0006-3495(01)75964-4

94 Barg, S., Eliasson, L., Renstrom, E. & Rorsman, P. A subset of 50 secretory granules in close contact with L-type Ca2+ channels accounts for first-phase insulin secretion in mouse beta-cells. *Diabetes* **51 Suppl 1**, S74-82 (2002). https://doi.org:10.2337/diabetes.51.2007.s74

95 Snyder, D. A., Kelly, M. L. & Woodbury, D. J. SNARE complex regulation by phosphorylation. *Cell Biochem Biophys* **45**, 111-123 (2006). https://doi.org:10.1385/CBB:45:1:111

96 Foster, L. J. *et al.* Binary interactions of the SNARE proteins syntaxin-4, SNAP23, and VAMP-2 and their regulation by phosphorylation. *Biochemistry* **37**, 11089-11096 (1998). https://doi.org:10.1021/bi980253t

97 Goodge, K. A. & Hutton, J. C. Translational regulation of proinsulin biosynthesis and proinsulin conversion in the pancreatic beta-cell. *Semin Cell Dev Biol* **11**, 235-242 (2000). https://doi.org:10.1006/scdb.2000.0172

98 Molinete, M., Irminger, J. C., Tooze, S. A. & Halban, P. A. Trafficking/sorting and granule biogenesis in the beta-cell. *Semin Cell Dev Biol* **11**, 243-251 (2000). https://doi.org:10.1006/scdb.2000.0173

99 Davidson, H. W. (Pro)Insulin processing: a historical perspective. *Cell Biochem Biophys* **40**, 143-158 (2004). https://doi.org:10.1385/cbb:40:3:143

100 Orci, L. *et al.* Proteolytic maturation of insulin is a post-Golgi event which occurs in acidifying clathrin-coated secretory vesicles. *Cell* **49**, 865-868 (1987). https://doi.org:10.1016/0092-8674(87)90624-6

101 Olofsson, C. S. *et al.* Fast insulin secretion reflects exocytosis of docked granules in mouse pancreatic B-cells. *Pflugers Arch* **444**, 43-51 (2002). https://doi.org:10.1007/s00424-002-0781-5

102 Ashcroft, S. J. Glucoreceptor mechanisms and the control of insulin release and biosynthesis. *Diabetologia* **18**, 5-15 (1980). https://doi.org:10.1007/BF01228295

103 Boland, B. B., Rhodes, C. J. & Grimsby, J. S. The dynamic plasticity of insulin production in beta-cells. *Mol Metab* **6**, 958-973 (2017). https://doi.org:10.1016/j.molmet.2017.04.010

104 Giddings, S. J., Chirgwin, J. & Permutt, M. A. Effects of glucose on proinsulin messenger RNA in rats in vivo. *Diabetes* **31**, 624-629 (1982). https://doi.org:10.2337/diab.31.7.624

105 Welsh, M., Nielsen, D. A., MacKrell, A. J. & Steiner, D. F. Control of insulin gene expression in pancreatic beta-cells and in an insulin-producing cell line, RIN-5F cells. II. Regulation of insulin mRNA stability. *J Biol Chem* **260**, 13590-13594 (1985).

106 Leibowitz, G. *et al.* Mitochondrial regulation of insulin production in rat pancreatic islets. *Diabetologia* **48**, 1549-1559 (2005). https://doi.org:10.1007/s00125-005-1811-6

107 Drucker, D. J. Minireview: the glucagon-like peptides. *Endocrinology* **142**, 521-527 (2001). https://doi.org:10.1210/endo.142.2.7983

108 Meier, J. J., Nauck, M. A., Schmidt, W. E. & Gallwitz, B. Gastric inhibitory polypeptide: the neglected incretin revisited. *Regul Pept* **107**, 1-13 (2002). https://doi.org:10.1016/s0167-0115(02)00039-3

109 Doyle, M. E. & Egan, J. M. Mechanisms of action of glucagon-like peptide 1 in the pancreas. *Pharmacol Ther* **113**, 546-593 (2007). https://doi.org:10.1016/j.pharmthera.2006.11.007

110 El, K. *et al.* GIP mediates the incretin effect and glucose tolerance by dual actions on alpha cells and beta cells. *Sci Adv* **7** (2021). https://doi.org:10.1126/sciadv.abf1948

111 Jones, P. M. & Persaud, S. J. Protein kinases, protein phosphorylation, and the regulation of insulin secretion from pancreatic beta-cells. *Endocr Rev* **19**, 429-461 (1998). https://doi.org:10.1210/edrv.19.4.0339

112 Zhang, Y. *et al.* Glucagon Potentiates Insulin Secretion Via beta-Cell GCGR at Physiological Concentrations of Glucose. *Cells* **10** (2021). https://doi.org:10.3390/cells10092495

113 Zhao, A. Z., Bornfeldt, K. E. & Beavo, J. A. Leptin inhibits insulin secretion by activation of phosphodiesterase 3B. *J Clin Invest* **102**, 869-873 (1998). https://doi.org:10.1172/JCI3920

114 Prentki, M., Peyot, M. L., Masiello, P. & Madiraju, S. R. M. Nutrient-Induced Metabolic Stress, Adaptation, Detoxification, and Toxicity in the Pancreatic beta-Cell. *Diabetes* **69**, 279-290 (2020). https://doi.org:10.2337/dbi19-0014

115 Ferdaoussi, M. *et al.* G protein-coupled receptor (GPR)40-dependent potentiation of insulin secretion in mouse islets is mediated by protein kinase D1. *Diabetologia* **55**, 2682-2692 (2012). https://doi.org:10.1007/s00125-012-2650-x

116 Tunaru, S. *et al.* 20-HETE promotes glucose-stimulated insulin secretion in an autocrine manner through FFAR1. *Nat Commun* **9**, 177 (2018). https://doi.org:10.1038/s41467-017-02539-4

117 Drzazga, A. *et al.* Lysophosphatidylcholine and its phosphorothioate analogues potentiate insulin secretion via GPR40 (FFAR1), GPR55 and GPR119 receptors in a different manner. *Mol Cell Endocrinol* **472**, 117-125 (2018). https://doi.org:10.1016/j.mce.2017.12.002

118 Shapiro, H., Shachar, S., Sekler, I., Hershfinkel, M. & Walker, M. D. Role of GPR40 in fatty acid action on the beta cell line INS-1E. *Biochem Biophys Res Commun* **335**, 97-104 (2005). https://doi.org:10.1016/j.bbrc.2005.07.042

119 Yamada, H. *et al.* Potentiation of Glucose-stimulated Insulin Secretion by the GPR40-PLC-TRPC Pathway in Pancreatic beta-Cells. *Sci Rep* **6**, 25912 (2016). https://doi.org:10.1038/srep25912

120 Itoh, Y. *et al.* Free fatty acids regulate insulin secretion from pancreatic beta cells through GPR40. *Nature* **422**, 173-176 (2003). https://doi.org:10.1038/nature01478

121 Sumara, G. *et al.* Regulation of PKD by the MAPK p38delta in insulin secretion and glucose homeostasis. *Cell* **136**, 235-248 (2009). https://doi.org:10.1016/j.cell.2008.11.018

122 Feng, D. D. *et al.* Reduction in voltage-gated K+ currents in primary cultured rat pancreatic beta-cells by linoleic acids. *Endocrinology* **147**, 674-682 (2006). https://doi.org:10.1210/en.2005-0225

123 Soga, T. *et al.* Lysophosphatidylcholine enhances glucose-dependent insulin secretion via an orphan G-protein-coupled receptor. *Biochem Biophys Res Commun* **326**, 744-751 (2005). https://doi.org:10.1016/j.bbrc.2004.11.120

124 Overton, H. A., Fyfe, M. C. & Reynet, C. GPR119, a novel G protein-coupled receptor target for the treatment of type 2 diabetes and obesity. *Br J Pharmacol* **153 Suppl 1**, S76-81 (2008). https://doi.org:10.1038/sj.bjp.0707529

125 Overton, H. A. *et al.* Deorphanization of a G protein-coupled receptor for oleoylethanolamide and its use in the discovery of small-molecule hypophagic agents. *Cell Metab* **3**, 167-175 (2006). https://doi.org:10.1016/j.cmet.2006.02.004

126 Oka, S., Nakajima, K., Yamashita, A., Kishimoto, S. & Sugiura, T. Identification of GPR55 as a lysophosphatidylinositol receptor. *Biochem Biophys Res Commun* **362**, 928-934 (2007). https://doi.org:10.1016/j.bbrc.2007.08.078

127 McKillop, A. M., Moran, B. M., Abdel-Wahab, Y. H. & Flatt, P. R. Evaluation of the insulin releasing and antihyperglycaemic activities of GPR55 lipid agonists using clonal beta-cells, isolated pancreatic islets and mice. *Br J Pharmacol* **170**, 978-990 (2013). https://doi.org:10.1111/bph.12356

128 Henstridge, C. M. *et al.* The GPR55 ligand L-alpha-lysophosphatidylinositol promotes RhoA-dependent Ca2+ signaling and NFAT activation. *FASEB J* **23**, 183-193 (2009). https://doi.org:10.1096/fj.08-108670

129 Lauckner, J. E. *et al.* GPR55 is a cannabinoid receptor that increases intracellular calcium and inhibits M current. *Proc Natl Acad Sci U S A* **105**, 2699-2704 (2008). https://doi.org:10.1073/pnas.0711278105

130 Vong, C. T., Tseng, H. H. L., Kwan, Y. W., Lee, S. M. & Hoi, M. P. M. G-protein coupled receptor 55 agonists increase insulin secretion through inositol trisphosphate-mediated calcium release in pancreatic beta-cells. *Eur J Pharmacol* **854**, 372-379 (2019). https://doi.org:10.1016/j.ejphar.2019.04.050

131 Howlett, A. C. Cannabinoid receptor signaling. *Handb Exp Pharmacol*, 53-79 (2005). https://doi.org:10.1007/3-540-26573-2_2

132 Gonzalez-Mariscal, I., Krzysik-Walker, S. M., Kim, W., Rouse, M. & Egan, J. M. Blockade of cannabinoid 1 receptor improves GLP-1R mediated insulin secretion in mice. *Mol Cell Endocrinol* **423**, 1-10 (2016). https://doi.org:10.1016/j.mce.2015.12.015

133 Li, C. *et al.* Expression and function of monoacylglycerol lipase in mouse beta-cells and human islets of Langerhans. *Cell Physiol Biochem* **30**, 347-358 (2012). https://doi.org:10.1159/000339069

134 Juan-Pico, P. *et al.* Cannabinoid receptors regulate Ca(2+) signals and insulin secretion in pancreatic beta-cell. *Cell Calcium* **39**, 155-162 (2006). https://doi.org:10.1016/j.ceca.2005.10.005

135 Zhao, S. *et al.* alpha/beta-Hydrolase domain-6-accessible monoacylglycerol controls glucose-stimulated insulin secretion. *Cell Metab* **19**, 993-1007 (2014). https://doi.org:10.1016/j.cmet.2014.04.003

136 Stein, D. T. *et al.* Essentiality of circulating fatty acids for glucose-stimulated insulin secretion in the fasted rat. *J Clin Invest* **97**, 2728-2735 (1996). https://doi.org:10.1172/JCI118727

137 Prentki, M., Corkey, B. E. & Madiraju, S. R. M. Lipid-associated metabolic signalling networks in pancreatic beta cell function. *Diabetologia* **63**, 10-20 (2020). https://doi.org:10.1007/s00125-019-04976-w

138 Khan, S. *et al.* Autocrine activation of P2Y1 receptors couples Ca (2+) influx to Ca (2+) release in human pancreatic beta cells. *Diabetologia* **57**, 2535-2545 (2014). https://doi.org:10.1007/s00125-014-3368-8

139 Richards-Williams, C., Contreras, J. L., Berecek, K. H. & Schwiebert, E. M. Extracellular ATP and zinc are co-secreted with insulin and activate multiple P2X purinergic receptor channels expressed by islet beta-cells to potentiate insulin secretion. *Purinergic Signal* **4**, 393-405 (2008). https://doi.org:10.1007/s11302-008-9126-y

140 Braun, M. *et al.* Gamma-aminobutyric acid (GABA) is an autocrine excitatory transmitter in human pancreatic beta-cells. *Diabetes* **59**, 1694-1701 (2010). https://doi.org:10.2337/db09-0797

141 Braun, M. *et al.* Corelease and differential exit via the fusion pore of GABA, serotonin, and ATP from LDCV in rat pancreatic beta cells. *J Gen Physiol* **129**, 221-231 (2007). https://doi.org:10.1085/jgp.200609658

142 Gilon, P., Bertrand, G., Loubatieres-Mariani, M. M., Remacle, C. & Henquin, J. C. The influence of gamma-aminobutyric acid on hormone release by the mouse and rat endocrine pancreas. *Endocrinology* **129**, 2521-2529 (1991). https://doi.org:10.1210/endo-129-5-2521

143 Ohara-Imaizumi, M. *et al.* Serotonin regulates glucose-stimulated insulin secretion from pancreatic beta cells during pregnancy. *Proc Natl Acad Sci U S A* **110**, 19420-19425 (2013). https://doi.org:10.1073/pnas.1310953110

144 Cataldo Bascunan, L. R., Lyons, C., Bennet, H., Artner, I. & Fex, M. Serotonergic regulation of insulin secretion. *Acta Physiol (Oxf)* **225**, e13101 (2019). https://doi.org:10.1111/apha.13101

145 Dixon, G., Nolan, J., McClenaghan, N., Flatt, P. R. & Newsholme, P. A comparative study of amino acid consumption by rat islet cells and the clonal beta-cell line BRIN-BD11 - the functional significance of L-alanine. *J Endocrinol* **179**, 447-454 (2003). https://doi.org:10.1677/joe.0.1790447

146 Sener, A. & Malaisse, W. J. L-leucine and a nonmetabolized analogue activate pancreatic islet glutamate dehydrogenase. *Nature* **288**, 187-189 (1980). https://doi.org:10.1038/288187a0

147 Smith, P. A. *et al.* Electrogenic arginine transport mediates stimulus-secretion coupling in mouse pancreatic beta-cells. *J Physiol* **499 (Pt 3)**, 625-635 (1997). https://doi.org:10.1113/jphysiol.1997.sp021955

148 Wang, J., Carrillo, J. J. & Lin, H. V. GPR142 Agonists Stimulate Glucose-Dependent Insulin Secretion via Gq-Dependent Signaling. *PLoS One* **11**, e0154452 (2016). https://doi.org:10.1371/journal.pone.0154452

149 Al-Amily, I. M., Duner, P., Groop, L. & Salehi, A. The functional impact of G protein-coupled receptor 142 (Gpr142) on pancreatic beta-cell in rodent. *Pflugers Arch* **471**, 633-645 (2019). https://doi.org:10.1007/s00424-019-02262-7

150 Gilon, P. & Henquin, J. C. Mechanisms and physiological significance of the cholinergic control of pancreatic beta-cell function. *Endocr Rev* **22**, 565-604 (2001). https://doi.org:10.1210/edrv.22.5.0440

151 Yada, T. *et al.* Pituitary adenylate cyclase-activating polypeptide (PACAP) is an islet substance serving as an intra-islet amplifier of glucose-induced insulin secretion in rats. *J Physiol* **505 (Pt 2)**, 319-328 (1997). https://doi.org:10.1111/j.1469-7793.1997.319bb.x

152 Liu, M. *et al.* PACAP stimulates insulin secretion by PAC1 receptor and ion channels in beta-cells. *Cell Signal* **61**, 48-56 (2019). https://doi.org:10.1016/j.cellsig.2019.05.006

153 Cho, N. H. *et al.* IDF Diabetes Atlas: Global estimates of diabetes prevalence for 2017 and projections for 2045. *Diabetes Res Clin Pract* **138**, 271-281 (2018). https://doi.org:10.1016/j.diabres.2018.02.023

154 Qi, Z. *et al.* Characterization of susceptibility of inbred mouse strains to diabetic nephropathy. *Diabetes* **54**, 2628-2637 (2005). https://doi.org:10.2337/diabetes.54.9.2628

155 Fajardo, R. J., Karim, L., Calley, V. I. & Bouxsein, M. L. A review of rodent models of type 2 diabetic skeletal fragility. *J Bone Miner Res* **29**, 1025-1040 (2014). https://doi.org:10.1002/jbmr.2210

156 Skyler, J. S. *et al.* Differentiation of Diabetes by Pathophysiology, Natural History, and Prognosis. *Diabetes* **66**, 241-255 (2017). https://doi.org:10.2337/db16-0806

157 Parkkola, A. *et al.* Extended family history of type 1 diabetes and phenotype and genotype of newly diagnosed children. *Diabetes Care* **36**, 348-354 (2013). https://doi.org:10.2337/dc12-0445

158 Hu, X. *et al.* Additive and interaction effects at three amino acid positions in HLA-DQ and HLA-DR molecules drive type 1 diabetes risk. *Nat Genet* **47**, 898-905 (2015). https://doi.org:10.1038/ng.3353

159 Lee, K. H., Wucherpfennig, K. W. & Wiley, D. C. Structure of a human insulin peptide-HLA-DQ8 complex and susceptibility to type 1 diabetes. *Nat Immunol* **2**, 501-507 (2001). https://doi.org:10.1038/88694

160 Group, T. S. The Environmental Determinants of Diabetes in the Young (TEDDY) Study. *Ann N Y Acad Sci* **1150**, 1-13 (2008). https://doi.org:10.1196/annals.1447.062

161 Jacobsen, L. M. *et al.* The risk of progression to type 1 diabetes is highly variable in individuals with multiple autoantibodies following screening. *Diabetologia* **63**, 588-596 (2020). https://doi.org:10.1007/s00125-019-05047-w

162 Onengut-Gumuscu, S. *et al.* Fine mapping of type 1 diabetes susceptibility loci and evidence for colocalization of causal variants with lymphoid gene enhancers. *Nat Genet* **47**, 381-386 (2015). https://doi.org:10.1038/ng.3245

163 Farh, K. K. *et al.* Genetic and epigenetic fine mapping of causal autoimmune disease variants. *Nature* **518**, 337-343 (2015). https://doi.org:10.1038/nature13835

164 Bell, G. I., Horita, S. & Karam, J. H. A polymorphic locus near the human insulin gene is associated with insulin-dependent diabetes mellitus. *Diabetes* **33**, 176-183 (1984). https://doi.org:10.2337/diab.33.2.176

165 Diez, J. *et al.* Differential splicing of the IA-2 mRNA in pancreas and lymphoid organs as a permissive genetic mechanism for autoimmunity against the IA-2 type 1 diabetes autoantigen. *Diabetes* **50**, 895-900 (2001). https://doi.org:10.2337/diabetes.50.4.895

166 Dogra, R. S. *et al.* Alternative splicing of G6PC2, the gene coding for the islet-specific glucose-6-phosphatase catalytic subunit-related protein (IGRP), results in differential expression in human thymus and spleen compared with pancreas. *Diabetologia* **49**, 953-957 (2006). https://doi.org:10.1007/s00125-006-0185-8

167 Doyle, H. A. & Mamula, M. J. Autoantigenesis: the evolution of protein modifications in autoimmune disease. *Curr Opin Immunol* **24**, 112-118 (2012). https://doi.org:10.1016/j.coi.2011.12.003

168 Onengut-Gumuscu, S., Ewens, K. G., Spielman, R. S. & Concannon, P. A functional polymorphism (1858C/T) in the PTPN22 gene is linked and associated with type I diabetes in multiplex families. *Genes Immun* **5**, 678-680 (2004). https://doi.org:10.1038/sj.gene.6364138

169 Nistico, L. *et al.* The CTLA-4 gene region of chromosome 2q33 is linked to, and associated with, type 1 diabetes. Belgian Diabetes Registry. *Hum Mol Genet* **5**, 1075-1080 (1996). https://doi.org:10.1093/hmg/5.7.1075

170 Vella, A. *et al.* Localization of a type 1 diabetes locus in the IL2RA/CD25 region by use of tag single-nucleotide polymorphisms. *Am J Hum Genet* **76**, 773-779 (2005). https://doi.org:10.1086/429843

171 Insel, R. A. *et al.* Staging presymptomatic type 1 diabetes: a scientific statement of JDRF, the Endocrine Society, and the American Diabetes Association. *Diabetes Care* **38**, 1964-1974 (2015). https://doi.org:10.2337/dc15-1419

172 Florez, J. C. Found in Translation: A Type 1 Diabetes Genetic Risk Score Applied to Clinical Diagnosis. *Diabetes Care* **39**, 330-332 (2016). https://doi.org:10.2337/dci15-0029

173 Ferrara, C. T. *et al.* Excess BMI in Childhood: A Modifiable Risk Factor for Type 1 Diabetes Development? *Diabetes Care* **40**, 698-701 (2017). https://doi.org:10.2337/dc16-2331

174 Pugliese, A. Insulitis in the pathogenesis of type 1 diabetes. *Pediatr Diabetes* **17 Suppl 22**, 31-36 (2016). https://doi.org:10.1111/pedi.12388

175 Colli, M. L., Szymczak, F. & Eizirik, D. L. Molecular Footprints of the Immune Assault on Pancreatic Beta Cells in Type 1 Diabetes. *Front Endocrinol (Lausanne)* **11**, 568446 (2020). https://doi.org:10.3389/fendo.2020.568446

176 Vilas-Boas, E. A. *et al.* Early Cytokine-Induced Transient NOX2 Activity Is ER Stress-Dependent and Impacts beta-Cell Function and Survival. *Antioxidants (Basel)* **10** (2021). https://doi.org:10.3390/antiox10081305

177 Benninger, R. K. P., Dorrell, C., Hodson, D. J. & Rutter, G. A. The Impact of Pancreatic Beta Cell Heterogeneity on Type 1 Diabetes Pathogenesis. *Curr Diab Rep* **18**, 112 (2018). https://doi.org:10.1007/s11892-018-1085-2

178 Ferrannini, E. *et al.* Progression to diabetes in relatives of type 1 diabetic patients: mechanisms and mode of onset. *Diabetes* **59**, 679-685 (2010). https://doi.org:10.2337/db09-1378

179 Kloppel, G., Lohr, M., Habich, K., Oberholzer, M. & Heitz, P. U. Islet pathology and the pathogenesis of type 1 and type 2 diabetes mellitus revisited. *Surv Synth Pathol Res* **4**, 110-125 (1985). https://doi.org:10.1159/000156969

180 Bonora, E. *et al.* Prevalence of insulin resistance in metabolic disorders: the Bruneck Study. *Diabetes* **47**, 1643-1649 (1998). https://doi.org:10.2337/diabetes.47.10.1643

181 Horikawa, Y. *et al.* Genetic variation in the gene encoding calpain-10 is associated with type 2 diabetes mellitus. *Nat Genet* **26**, 163-175 (2000). https://doi.org:10.1038/79876

182 Shimabukuro, M., Zhou, Y. T., Levi, M. & Unger, R. H. Fatty acid-induced beta cell apoptosis: a link between obesity and diabetes. *Proc Natl Acad Sci U S A* **95**, 2498-2502 (1998). https://doi.org:10.1073/pnas.95.5.2498

183 Joseph, J. W. *et al.* Free fatty acid-induced beta-cell defects are dependent on uncoupling protein 2 expression. *J Biol Chem* **279**, 51049-51056 (2004). https://doi.org:10.1074/jbc.M409189200

184 Griffin, M. E. *et al.* Free fatty acid-induced insulin resistance is associated with activation of protein kinase C theta and alterations in the insulin signaling cascade. *Diabetes* **48**, 1270-1274 (1999). https://doi.org:10.2337/diabetes.48.6.1270

185 Schmitz-Peiffer, C. *et al.* Alterations in the expression and cellular localization of protein kinase C isozymes epsilon and theta are associated with insulin resistance in skeletal muscle of the high-fat-fed rat. *Diabetes* **46**, 169-178 (1997). https://doi.org:10.2337/diab.46.2.169

186 Yu, C. *et al.* Mechanism by which fatty acids inhibit insulin activation of insulin receptor substrate-1 (IRS-1)-associated phosphatidylinositol 3-kinase activity in muscle. *J Biol Chem* **277**, 50230-50236 (2002). https://doi.org:10.1074/jbc.M200958200

187 Lee, J. S. *et al.* Saturated, but not n-6 polyunsaturated, fatty acids induce insulin resistance: role of intramuscular accumulation of lipid metabolites. *J Appl Physiol (1985)* **100**, 1467-1474 (2006). https://doi.org:10.1152/japplphysiol.01438.2005

188 Mugharbel, K. M. & Al-Mansouri, M. A. Prevalence of obesity among type 2 diabetic patients in Al-khobar primary health care centers. *J Family Community Med* **10**, 49-53 (2003).

189 Daousi, C. *et al.* Prevalence of obesity in type 2 diabetes in secondary care: association with cardiovascular risk factors. *Postgrad Med J* **82**, 280-284 (2006). https://doi.org:10.1136/pmj.2005.039032

190 Donath, M. Y. & Halban, P. A. Decreased beta-cell mass in diabetes: significance, mechanisms and therapeutic implications. *Diabetologia* **47**, 581-589 (2004). https://doi.org:10.1007/s00125-004-1336-4

191 Donath, M. Y. *et al.* Mechanisms of beta-cell death in type 2 diabetes. *Diabetes* **54 Suppl 2**, S108-113 (2005). https://doi.org:10.2337/diabetes.54.suppl_2.s108

192 Robertson, R. P., Harmon, J., Tran, P. O., Tanaka, Y. & Takahashi, H. Glucose toxicity in beta-cells: type 2 diabetes, good radicals gone bad, and the glutathione connection. *Diabetes* **52**, 581-587 (2003). https://doi.org:10.2337/diabetes.52.3.581

193 Laybutt, D. R. *et al.* Endoplasmic reticulum stress contributes to beta cell apoptosis in type 2 diabetes. *Diabetologia* **50**, 752-763 (2007). https://doi.org:10.1007/s00125-006-0590-z

194 Prentki, M., Joly, E., El-Assaad, W. & Roduit, R. Malonyl-CoA signaling, lipid partitioning, and glucolipotoxicity: role in beta-cell adaptation and failure in the etiology of diabetes. *Diabetes* **51 Suppl 3**, S405-413 (2002). https://doi.org:10.2337/diabetes.51.2007.s405

195 Poitout, V. & Robertson, R. P. Glucolipotoxicity: fuel excess and beta-cell dysfunction. *Endocr Rev* **29**, 351-366 (2008). https://doi.org:10.1210/er.2007-0023

196 Poitout, V. & Robertson, R. P. Minireview: Secondary beta-cell failure in type 2 diabetes--a convergence of glucotoxicity and lipotoxicity. *Endocrinology* **143**, 339-342 (2002). https://doi.org:10.1210/endo.143.2.8623

197 Wajchenberg, B. L. Subcutaneous and visceral adipose tissue: their relation to the metabolic syndrome. *Endocr Rev* **21**, 697-738 (2000). https://doi.org:10.1210/edrv.21.6.0415

198 Ronti, T., Lupattelli, G. & Mannarino, E. The endocrine function of adipose tissue: an update. *Clin Endocrinol (Oxf)* **64**, 355-365 (2006). https://doi.org:10.1111/j.1365-2265.2006.02474.x

199 Pickup, J. C. Inflammation and activated innate immunity in the pathogenesis of type 2 diabetes. *Diabetes Care* **27**, 813-823 (2004). https://doi.org:10.2337/diacare.27.3.813

200 Xu, H. *et al.* Chronic inflammation in fat plays a crucial role in the development of obesity-related insulin resistance. *J Clin Invest* **112**, 1821-1830 (2003). https://doi.org:10.1172/JCI19451

201 Feinstein, R., Kanety, H., Papa, M. Z., Lunenfeld, B. & Karasik, A. Tumor necrosis factor-alpha suppresses insulin-induced tyrosine phosphorylation of insulin receptor and its substrates. *J Biol Chem* **268**, 26055-26058 (1993).

202 Pietropaolo, M., Barinas-Mitchell, E., Pietropaolo, S. L., Kuller, L. H. & Trucco, M. Evidence of islet cell autoimmunity in elderly patients with type 2 diabetes. *Diabetes* **49**, 32-38 (2000). https://doi.org:10.2337/diabetes.49.1.32

203 Tuomi, T. *et al.* Antibodies to glutamic acid decarboxylase reveal latent autoimmune diabetes mellitus in adults with a non-insulin-dependent onset of disease. *Diabetes* **42**, 359-362 (1993). https://doi.org:10.2337/diab.42.2.359

204 Bellone, M. *et al.* Processing of engulfed apoptotic bodies yields T cell epitopes. *J Immunol* **159**, 5391-5399 (1997).

205 Pickup, J. C., Mattock, M. B., Chusney, G. D. & Burt, D. NIDDM as a disease of the innate immune system: association of acute-phase reactants and interleukin-6 with metabolic syndrome X. *Diabetologia* **40**, 1286-1292 (1997). https://doi.org:10.1007/s001250050822

206 Butler, A. E. *et al.* Beta-cell deficit and increased beta-cell apoptosis in humans with type 2 diabetes. *Diabetes* **52**, 102-110 (2003). https://doi.org:10.2337/diabetes.52.1.102

207 Hudish, L. I., Reusch, J. E. & Sussel, L. beta Cell dysfunction during progression of metabolic syndrome to type 2 diabetes. *J Clin Invest* **129**, 4001-4008 (2019). https://doi.org:10.1172/JCI129188

208 UK Prospective Diabetes Study (UKPDS). VIII. Study design, progress and performance. *Diabetologia* **34**, 877-890 (1991).

209 Graves, L. E. & Donaghue, K. C. Vascular Complication in Adolescents With Diabetes Mellitus. *Front Endocrinol (Lausanne)* **11**, 370 (2020). https://doi.org:10.3389/fendo.2020.00370

210 Rawshani, A. *et al.* Excess mortality and cardiovascular disease in young adults with type 1 diabetes in relation to age at onset: a nationwide, register-based cohort study. *Lancet* **392**, 477-486 (2018). https://doi.org:10.1016/S0140-6736(18)31506-X

211 Baynes, J. W. Role of oxidative stress in development of complications in diabetes. *Diabetes* **40**, 405-412 (1991). https://doi.org:10.2337/diab.40.4.405

212 Vlassara, H. Recent progress in advanced glycation end products and diabetic complications. *Diabetes* **46 Suppl 2**, S19-25 (1997). https://doi.org:10.2337/diab.46.2.s19

213 Cagliero, E., Roth, T., Roy, S. & Lorenzi, M. Characteristics and mechanisms of high-glucose-induced overexpression of basement membrane components in cultured human endothelial cells. *Diabetes* **40**, 102-110 (1991). https://doi.org:10.2337/diab.40.1.102

214 Rahman, S., Rahman, T., Ismail, A. A. & Rashid, A. R. Diabetes-associated macrovasculopathy: pathophysiology and pathogenesis. *Diabetes Obes Metab* **9**, 767-780 (2007). https://doi.org:10.1111/j.1463-1326.2006.00655.x

215 Rattan, V., Sultana, C., Shen, Y. & Kalra, V. K. Oxidant stress-induced transendothelial migration of monocytes is linked to phosphorylation of PECAM-1. *Am J Physiol* **273**, E453-461 (1997). https://doi.org:10.1152/ajpendo.1997.273.3.E453

216 Keating, F. K., Sobel, B. E. & Schneider, D. J. Effects of increased concentrations of glucose on platelet reactivity in healthy subjects and in patients with and without diabetes mellitus. *Am J Cardiol* **92**, 1362-1365 (2003). https://doi.org:10.1016/j.amjcard.2003.08.033

217 Tedgui, A. & Mallat, Z. Anti-inflammatory mechanisms in the vascular wall. *Circ Res* **88**, 877-887 (2001). https://doi.org:10.1161/hh0901.090440

218 Ness, J., Nassimiha, D., Feria, M. I. & Aronow, W. S. Diabetes mellitus in older African-Americans, Hispanics, and whites in an academic hospital-based geriatrics practice. *Coron Artery Dis* **10**, 343-346 (1999). https://doi.org:10.1097/00019501-199907000-00012

219 Garcia, M. J., McNamara, P. M., Gordon, T. & Kannel, W. B. Morbidity and mortality in diabetics in the Framingham population. Sixteen year follow-up study. *Diabetes* **23**, 105-111 (1974). https://doi.org:10.2337/diab.23.2.105

220 Stamler, J., Vaccaro, O., Neaton, J. D. & Wentworth, D. Diabetes, other risk factors, and 12-yr cardiovascular mortality for men screened in the Multiple Risk Factor Intervention Trial. *Diabetes Care* **16**, 434-444 (1993). https://doi.org:10.2337/diacare.16.2.434

221 Peters, L. L. *et al.* Large-scale, high-throughput screening for coagulation and hematologic phenotypes in mice. *Physiol Genomics* **11**, 185-193 (2002). https://doi.org:10.1152/physiolgenomics.00077.2002

222 Daly, M. E. Determinants of platelet count in humans. *Haematologica* **96**, 10-13 (2011). https://doi.org:10.3324/haematol.2010.035287

223 Cohen, J. A. & Leeksma, C. H. Determination of the life span of human blood platelets using labelled diisopropylfluorophosphonate. *J Clin Invest* **35**, 964-969 (1956). https://doi.org:10.1172/JCI103356

224 Odell, T. T., Jr. & Mc, D. T. Life span of mouse blood platelets. *Proc Soc Exp Biol Med* **106**, 107-108 (1961). https://doi.org:10.3181/00379727-106-26252

225 Quach, M. E., Chen, W. & Li, R. Mechanisms of platelet clearance and translation to improve platelet storage. *Blood* **131**, 1512-1521 (2018). https://doi.org:10.1182/blood-2017-08-743229

226 Zimmerman, G. A. & Weyrich, A. S. Signal-dependent protein synthesis by activated platelets: new pathways to altered phenotype and function. *Arterioscler Thromb Vasc Biol* **28**, s17-24 (2008). https://doi.org:10.1161/ATVBAHA.107.160218

227 Hayashi, T. *et al.* Role of mitochondria in the maintenance of platelet function during in vitro storage. *Transfus Med* **21**, 166-174 (2011). https://doi.org:10.1111/j.1365-3148.2010.01065.x

228 Yamagishi, S. I., Edelstein, D., Du, X. L. & Brownlee, M. Hyperglycemia potentiates collagen-induced platelet activation through mitochondrial superoxide overproduction. *Diabetes* **50**, 1491-1494 (2001). https://doi.org:10.2337/diabetes.50.6.1491

229 Sander, H. J. *et al.* Immunocytochemical localization of fibrinogen, platelet factor 4, and beta thromboglobulin in thin frozen sections of human blood platelets. *J Clin Invest* **72**, 1277-1287 (1983). https://doi.org:10.1172/JCI111084

230 Wencel-Drake, J. D., Painter, R. G., Zimmerman, T. S. & Ginsberg, M. H. Ultrastructural localization of human platelet thrombospondin, fibrinogen, fibronectin, and von Willebrand factor in frozen thin section. *Blood* **65**, 929-938 (1985).

231 Rendu, F. & Brohard-Bohn, B. The platelet release reaction: granules' constituents, secretion and functions. *Platelets* **12**, 261-273 (2001). https://doi.org:10.1080/09537100120068170

232 Gleissner, C. A., von Hundelshausen, P. & Ley, K. Platelet chemokines in vascular disease. *Arterioscler Thromb Vasc Biol* **28**, 1920-1927 (2008). https://doi.org:10.1161/ATVBAHA.108.169417

233 Nurden, A. T., Nurden, P., Sanchez, M., Andia, I. & Anitua, E. Platelets and wound healing. *Front Biosci* **13**, 3532-3548 (2008). https://doi.org:10.2741/2947

234 McNicol, A. & Israels, S. J. Platelet dense granules: structure, function and implications for haemostasis. *Thromb Res* **95**, 1-18 (1999). https://doi.org:10.1016/s0049-3848(99)00015-8

235 Cloutier, N. *et al.* Platelets release pathogenic serotonin and return to circulation after immune complex-mediated sequestration. *Proc Natl Acad Sci U S A* **115**, E1550-E1559 (2018). https://doi.org:10.1073/pnas.1720553115

236 Kagedal, K., Johansson, U. & Ollinger, K. The lysosomal protease cathepsin D mediates apoptosis induced by oxidative stress. *FASEB J* **15**, 1592-1594 (2001). https://doi.org:10.1096/fj.00-0708fje

237 Jackson, S. P. & Schoenwaelder, S. M. Procoagulant platelets: are they necrotic? *Blood* **116**, 2011-2018 (2010). https://doi.org:10.1182/blood-2010-01-261669

238 Ciferri, S. *et al.* Platelets release their lysosomal content in vivo in humans upon activation. *Thromb Haemost* **83**, 157-164 (2000).

239 White, J. G. Interaction of membrane systems in blood platelets. *Am J Pathol* **66**, 295-312 (1972).

240 Periayah, M. H., Halim, A. S. & Mat Saad, A. Z. Mechanism Action of Platelets and Crucial Blood Coagulation Pathways in Hemostasis. *Int J Hematol Oncol Stem Cell Res* **11**, 319-327 (2017).

241 Mammadova-Bach, E. *et al.* Platelet glycoprotein VI promotes metastasis through interaction with cancer cell-derived galectin-3. *Blood* **135**, 1146-1160 (2020). https://doi.org:10.1182/blood.2019002649

242 Martins Castanheira, N., Spanhofer, A. K., Wiener, S., Bobe, S. & Schillers, H. Uptake of platelets by cancer cells and recycling of the platelet protein CD42a. *J Thromb Haemost* **20**, 170-181 (2022). https://doi.org:10.1111/jth.15543

243 Zuchtriegel, G. *et al.* Platelets Guide Leukocytes to Their Sites of Extravasation. *PLoS Biol* **14**, e1002459 (2016). https://doi.org:10.1371/journal.pbio.1002459

244 Weber, C. & Springer, T. A. Neutrophil accumulation on activated, surface-adherent platelets in flow is mediated by interaction of Mac-1 with fibrinogen bound to alphaIIbbeta3 and stimulated by platelet-activating factor. *J Clin Invest* **100**, 2085-2093 (1997). https://doi.org:10.1172/JCI119742

245 Gaertner, F. *et al.* Migrating Platelets Are Mechano-scavengers that Collect and Bundle Bacteria. *Cell* **171**, 1368-1382 e1323 (2017). https://doi.org:10.1016/j.cell.2017.11.001

246 White, J. G. Platelets are covercytes, not phagocytes: uptake of bacteria involves channels of the open canalicular system. *Platelets* **16**, 121-131 (2005). https://doi.org:10.1080/09537100400007390

247 Chatterjee, M. *et al.* Distinct platelet packaging, release, and surface expression of proangiogenic and antiangiogenic factors on different platelet stimuli. *Blood* **117**, 3907-3911 (2011). https://doi.org:10.1182/blood-2010-12-327007

248 Battinelli, E. M., Markens, B. A. & Italiano, J. E., Jr. Release of angiogenesis regulatory proteins from platelet alpha granules: modulation of physiologic and pathologic angiogenesis. *Blood* **118**, 1359-1369 (2011). https://doi.org:10.1182/blood-2011-02-334524

249 Italiano, J. E., Jr. *et al.* Angiogenesis is regulated by a novel mechanism: pro- and antiangiogenic proteins are organized into separate platelet alpha granules and differentially released. *Blood* **111**, 1227-1233 (2008). https://doi.org:10.1182/blood-2007-09-113837

250 Mahmoodian, R., Salimian, M., Hamidpour, M., Khadem-Maboudi, A. A. & Gharehbaghian, A. The effect of mild agonist stimulation on the platelet reactivity in patients with type 2 diabetes mellitus. *BMC Endocr Disord* **19**, 62 (2019). https://doi.org:10.1186/s12902-019-0391-2

251 Mylotte, D. *et al.* Platelet reactivity in type 2 diabetes mellitus: a comparative analysis with survivors of myocardial infarction and the role of glycaemic control. *Platelets* **23**, 439-446 (2012). https://doi.org:10.3109/09537104.2011.634932

252 Schrottmaier, W. C. *et al.* Adverse Outcome in COVID-19 Is Associated With an Aggravating Hypo-Responsive Platelet Phenotype. *Front Cardiovasc Med* **8**, 795624 (2021). https://doi.org:10.3389/fcvm.2021.795624

253 Cattaneo, M. *et al. Platelets*. Fourth edition. edn, (Academic Press, an imprint of Elsevier, 2019).

254 Varga-Szabo, D., Pleines, I. & Nieswandt, B. Cell adhesion mechanisms in platelets. *Arterioscler Thromb Vasc Biol* **28**, 403-412 (2008). https://doi.org:10.1161/ATVBAHA.107.150474

255 Luo, S. Z. *et al.* Glycoprotein Ibalpha forms disulfide bonds with 2 glycoprotein Ibbeta subunits in the resting platelet. *Blood* **109**, 603-609 (2007). https://doi.org:10.1182/blood-2006-05-024091

256 Huizinga, E. G. *et al.* Structures of glycoprotein Ibalpha and its complex with von Willebrand factor A1 domain. *Science* **297**, 1176-1179 (2002). https://doi.org:10.1126/science.107355

257 Nieswandt, B. & Watson, S. P. Platelet-collagen interaction: is GPVI the central receptor? *Blood* **102**, 449-461 (2003). https://doi.org:10.1182/blood-2002-12-3882

258 Andre, P. *et al.* P2Y12 regulates platelet adhesion/activation, thrombus growth, and thrombus stability in injured arteries. *J Clin Invest* **112**, 398-406 (2003). https://doi.org:10.1172/JCI17864

259 Walsh, P. N. Roles of factor XI, platelets and tissue factor-initiated blood coagulation. *J Thromb Haemost* **1**, 2081-2086 (2003). https://doi.org:10.1046/j.1538-7836.2003.00460.x

260 Blair, P. & Flaumenhaft, R. Platelet alpha-granules: basic biology and clinical correlates. *Blood Rev* **23**, 177-189 (2009). https://doi.org:10.1016/j.blre.2009.04.001

261 Hynes, R. O. Integrins: bidirectional, allosteric signaling machines. *Cell* **110**, 673-687 (2002). https://doi.org:10.1016/s0092-8674(02)00971-6

262 De Marco, L., Girolami, A., Zimmerman, T. S. & Ruggeri, Z. M. Interaction of purified type IIB von Willebrand factor with the platelet membrane glycoprotein Ib induces fibrinogen binding to the glycoprotein IIb/IIIa complex and initiates aggregation. *Proc Natl Acad Sci U S A* **82**, 7424-7428 (1985). https://doi.org:10.1073/pnas.82.21.7424

263 Marjoram, R. J. *et al.* alpha2beta1 integrin, GPVI receptor, and common FcRgamma chain on mouse platelets mediate distinct responses to collagen in models of thrombosis. *PLoS One* **9**, e114035 (2014). https://doi.org:10.1371/journal.pone.0114035

264 Nagae, M. *et al.* Crystal structure of alpha5beta1 integrin ectodomain: atomic details of the fibronectin receptor. *J Cell Biol* **197**, 131-140 (2012). https://doi.org:10.1083/jcb.201111077

265 Schaff, M. *et al.* Integrin alpha6beta1 is the main receptor for vascular laminins and plays a role in platelet adhesion, activation, and arterial thrombosis. *Circulation* **128**, 541-552 (2013). https://doi.org:10.1161/CIRCULATIONAHA.112.000799

266 Horton, M. A. The alpha v beta 3 integrin "vitronectin receptor". *Int J Biochem Cell Biol* **29**, 721-725 (1997). https://doi.org:10.1016/s1357-2725(96)00155-0

267 Takagi, J., Petre, B. M., Walz, T. & Springer, T. A. Global conformational rearrangements in integrin extracellular domains in outside-in and inside-out signaling. *Cell* **110**, 599-511 (2002). https://doi.org:10.1016/s0092-8674(02)00935-2

268 Li, R. *et al.* Activation of integrin alphaIIbbeta3 by modulation of transmembrane helix associations. *Science* **300**, 795-798 (2003). https://doi.org:10.1126/science.1079441

269 Vinogradova, O. *et al.* Membrane-mediated structural transitions at the cytoplasmic face during integrin activation. *Proc Natl Acad Sci U S A* **101**, 4094-4099 (2004). https://doi.org:10.1073/pnas.0400742101

270 Vinogradova, O. *et al.* A structural mechanism of integrin alpha(IIb)beta(3) "inside-out" activation as regulated by its cytoplasmic face. *Cell* **110**, 587-597 (2002). https://doi.org:10.1016/s0092-8674(02)00906-6

271 Fuss, C., Palmaz, J. C. & Sprague, E. A. Fibrinogen: structure, function, and surface interactions. *J Vasc Interv Radiol* **12**, 677-682 (2001). https://doi.org:10.1016/s1051-0443(07)61437-7

272 Shattil, S. J. & Brass, L. F. Induction of the fibrinogen receptor on human platelets by intracellular mediators. *J Biol Chem* **262**, 992-1000 (1987).

273 Hathaway, D. R. & Adelstein, R. S. Human platelet myosin light chain kinase requires the calcium-binding protein calmodulin for activity. *Proc Natl Acad Sci U S A* **76**, 1653-1657 (1979). https://doi.org:10.1073/pnas.76.4.1653

274 Ezumi, Y., Shindoh, K., Tsuji, M. & Takayama, H. Physical and functional association of the Src family kinases Fyn and Lyn with the collagen receptor glycoprotein VI-Fc receptor gamma chain complex on human platelets. *J Exp Med* **188**, 267-276 (1998). https://doi.org:10.1084/jem.188.2.267

275 Watson, S. P. *et al.* The role of ITAM- and ITIM-coupled receptors in platelet activation by collagen. *Thromb Haemost* **86**, 276-288 (2001).

276 Judd, B. A. *et al.* Differential requirement for LAT and SLP-76 in GPVI versus T cell receptor signaling. *J Exp Med* **195**, 705-717 (2002). https://doi.org:10.1084/jem.20011583

277 Goncalves, I. *et al.* Integrin alpha IIb beta 3-dependent calcium signals regulate platelet-fibrinogen interactions under flow. Involvement of phospholipase C gamma 2. *J Biol Chem* **278**, 34812-34822 (2003). https://doi.org:10.1074/jbc.M306504200

278 Watson, S. P., Auger, J. M., McCarty, O. J. & Pearce, A. C. GPVI and integrin alphaIIb beta3 signaling in platelets. *J Thromb Haemost* **3**, 1752-1762 (2005). https://doi.org:10.1111/j.1538-7836.2005.01429.x

279 Yang, X., Sun, L., Ghosh, S. & Rao, A. K. Human platelet signaling defect characterized by impaired production of inositol-1,4,5-triphosphate and phosphatidic acid and diminished Pleckstrin phosphorylation: evidence for defective phospholipase C activation. *Blood* **88**, 1676-1683 (1996).

280 Harper, M. T. & Poole, A. W. Diverse functions of protein kinase C isoforms in platelet activation and thrombus formation. *J Thromb Haemost* **8**, 454-462 (2010). https://doi.org:10.1111/j.1538-7836.2009.03722.x

281 Pasquet, J. M. *et al.* A collagen-related peptide regulates phospholipase Cgamma2 via phosphatidylinositol 3-kinase in human platelets. *Biochem J* **342 (Pt 1)**, 171-177 (1999).

282 Li, Z., Zhang, G., Marjanovic, J. A., Ruan, C. & Du, X. A platelet secretion pathway mediated by cGMP-dependent protein kinase. *J Biol Chem* **279**, 42469-42475 (2004). https://doi.org:10.1074/jbc.M401532200

283 Flevaris, P. *et al.* Two distinct roles of mitogen-activated protein kinases in platelets and a novel Rac1-MAPK-dependent integrin outside-in retractile signaling pathway. *Blood* **113**, 893-901 (2009). https://doi.org:10.1182/blood-2008-05-155978

284 Daniel, J. L., Dangelmaier, C., Jin, J., Kim, Y. B. & Kunapuli, S. P. Role of intracellular signaling events in ADP-induced platelet aggregation. *Thromb Haemost* **82**, 1322-1326 (1999).

285 Adelstein, R. S., Conti, M. A., Daniel, J. L. & Anderson, W., Jr. The interaction of platelet actin, myosin and myosin light chain kinase. *Ciba Found Symp* **35**, 101-109 (1975). https://doi.org:10.1002/9780470720172.ch6

286 Paul, B. Z. *et al.* Dynamic regulation of microtubule coils in ADP-induced platelet shape change by p160ROCK (Rho-kinase). *Platelets* **14**, 159-169 (2003). https://doi.org:10.1080/0953710031000092794

287 Yang, J. *et al.* Loss of signaling through the G protein, Gz, results in abnormal platelet activation and altered responses to psychoactive drugs. *Proc Natl Acad Sci U S A* **97**, 9984-9989 (2000). https://doi.org:10.1073/pnas.180194597

288 Dutta-Roy, A. K. & Sinha, A. K. Purification and properties of prostaglandin E1/prostacyclin receptor of human blood platelets. *J Biol Chem* **262**, 12685-12691 (1987).

289 Gorman, R. R., Bunting, S. & Miller, O. V. Modulation of human platelet adenylate cyclase by prostacyclin (PGX). *Prostaglandins* **13**, 377-388 (1977). https://doi.org:10.1016/0090-6980(77)90018-1

290 Smolenski, A. Novel roles of cAMP/cGMP-dependent signaling in platelets. *J Thromb Haemost* **10**, 167-176 (2012). https://doi.org:10.1111/j.1538-7836.2011.04576.x

291 Tertyshnikova, S., Yan, X. & Fein, A. cGMP inhibits IP3-induced Ca2+ release in intact rat megakaryocytes via cGMP- and cAMP-dependent protein kinases. *J Physiol* **512 (Pt 1)**, 89-96 (1998). https://doi.org:10.1111/j.1469-7793.1998.089bf.x

292 Slatter, D. A. *et al.* Mapping the Human Platelet Lipidome Reveals Cytosolic Phospholipase A2 as a Regulator of Mitochondrial Bioenergetics during Activation. *Cell Metab* **23**, 930-944 (2016). https://doi.org:10.1016/j.cmet.2016.04.001

293 Peng, B. *et al.* Identification of key lipids critical for platelet activation by comprehensive analysis of the platelet lipidome. *Blood* **132**, e1-e12 (2018). https://doi.org:10.1182/blood-2017-12-822890

294 Bevers, E. M., Comfurius, P., van Rijn, J. L., Hemker, H. C. & Zwaal, R. F. Generation of prothrombin-converting activity and the exposure of phosphatidylserine at the outer surface of platelets. *Eur J Biochem* **122**, 429-436 (1982). https://doi.org:10.1111/j.1432-1033.1982.tb05898.x

295 Derksen, A. & Cohen, P. Patterns of fatty acid release from endogenous substrates by human platelet homogenates and membranes. *J Biol Chem* **250**, 9342-9347 (1975).

296 Kramer, R. M. & Sharp, J. D. Structure, function and regulation of Ca2+-sensitive cytosolic phospholipase A2 (cPLA2). *FEBS Lett* **410**, 49-53 (1997). https://doi.org:10.1016/s0014-5793(97)00322-0

297 Adler, D. H. *et al.* Inherited human cPLA(2alpha) deficiency is associated with impaired eicosanoid biosynthesis, small intestinal ulceration, and platelet dysfunction. *J Clin Invest* **118**, 2121-2131 (2008). https://doi.org:10.1172/JCI30473

298 Paes, A. M. A. *et al.* Lipid Metabolism and Signaling in Platelet Function. *Adv Exp Med Biol* **1127**, 97-115 (2019). https://doi.org:10.1007/978-3-030-11488-6_7

299 Smith, W. L., DeWitt, D. L. & Garavito, R. M. Cyclooxygenases: structural, cellular, and molecular biology. *Annu Rev Biochem* **69**, 145-182 (2000). https://doi.org:10.1146/annurev.biochem.69.1.145

300 Rauzi, F. *et al.* Aspirin inhibits the production of proangiogenic 15(S)-HETE by platelet cyclooxygenase-1. *FASEB J* **30**, 4256-4266 (2016). https://doi.org:10.1096/fj.201600530R

301 Brash, A. R. Lipoxygenases: occurrence, functions, catalysis, and acquisition of substrate. *J Biol Chem* **274**, 23679-23682 (1999). https://doi.org:10.1074/jbc.274.34.23679

302 Ikei, K. N. *et al.* Investigations of human platelet-type 12-lipoxygenase: role of lipoxygenase products in platelet activation. *J Lipid Res* **53**, 2546-2559 (2012). https://doi.org:10.1194/jlr.M026385

303 Yeung, J., Hawley, M. & Holinstat, M. The expansive role of oxylipins on platelet biology. *J Mol Med (Berl)* **95**, 575-588 (2017). https://doi.org:10.1007/s00109-017-1542-4

304 Wong, P. Y. *et al.* 15-Lipoxygenase in human platelets. *J Biol Chem* **260**, 9162-9165 (1985).

305 Kim, H. Y., Karanian, J. W. & Salem, N., Jr. Formation of 15-lipoxygenase product from docosahexaenoic acid (22:6w3) by human platelets. *Prostaglandins* **40**, 539-549 (1990). https://doi.org:10.1016/0090-6980(90)90115-c

306 Fleming, I. Cytochrome p450 and vascular homeostasis. *Circ Res* **89**, 753-762 (2001). https://doi.org:10.1161/hh2101.099268

307 Panigrahy, D., Kaipainen, A., Greene, E. R. & Huang, S. Cytochrome P450-derived eicosanoids: the neglected pathway in cancer. *Cancer Metastasis Rev* **29**, 723-735 (2010). https://doi.org:10.1007/s10555-010-9264-x

308 Tsai, I. J., Croft, K. D., Puddey, I. B., Beilin, L. J. & Barden, A. 20-Hydroxyeicosatetraenoic acid synthesis is increased in human neutrophils and platelets by angiotensin II and endothelin-1. *Am J Physiol Heart Circ Physiol* **300**, H1194-1200 (2011). https://doi.org:10.1152/ajpheart.00733.2010

309 Dhers, L., Ducassou, L., Boucher, J. L. & Mansuy, D. Cytochrome P450 2U1, a very peculiar member of the human P450s family. *Cell Mol Life Sci* **74**, 1859-1869 (2017). https://doi.org:10.1007/s00018-016-2443-3

310 Zhu, Y., Schieber, E. B., McGiff, J. C. & Balazy, M. Identification of arachidonate P-450 metabolites in human platelet phospholipids. *Hypertension* **25**, 854-859 (1995). https://doi.org:10.1161/01.hyp.25.4.854

311 VanRollins, M., Kaduce, T. L., Fang, X., Knapp, H. R. & Spector, A. A. Arachidonic acid diols produced by cytochrome P-450 monooxygenases are incorporated into phospholipids of vascular endothelial cells. *J Biol Chem* **271**, 14001-14009 (1996). https://doi.org:10.1074/jbc.271.24.14001

312 Thomas, C. P. *et al.* Phospholipid-esterified eicosanoids are generated in agonist-activated human platelets and enhance tissue factor-dependent thrombin generation. *J Biol Chem* **285**, 6891-6903 (2010). https://doi.org:10.1074/jbc.M109.078428

313 Arnold, C. *et al.* Arachidonic acid-metabolizing cytochrome P450 enzymes are targets of {omega}-3 fatty acids. *J Biol Chem* **285**, 32720-32733 (2010). https://doi.org:10.1074/jbc.M110.118406

314 Sato, H., Taketomi, Y. & Murakami, M. Metabolic regulation by secreted phospholipase A2. *Inflamm Regen* **36**, 7 (2016). https://doi.org:10.1186/s41232-016-0012-7

315 Thomas, L. M. & Holub, B. J. Eicosanoid-dependent and -independent formation of individual [14C]stearoyl-labelled lysophospholipids in collagen-stimulated human platelets. *Biochim Biophys Acta* **1081**, 92-98 (1991). https://doi.org:10.1016/0005-2760(91)90255-g

316 O'Donnell, V. B., Murphy, R. C. & Watson, S. P. Platelet lipidomics: modern day perspective on lipid discovery and characterization in platelets. *Circ Res* **114**, 1185-1203 (2014). https://doi.org:10.1161/CIRCRESAHA.114.301597

317 Yost, C. C., Weyrich, A. S. & Zimmerman, G. A. The platelet activating factor (PAF) signaling cascade in systemic inflammatory responses. *Biochimie* **92**, 692-697 (2010). https://doi.org:10.1016/j.biochi.2010.02.011

318 Futerman, A. H. & Hannun, Y. A. The complex life of simple sphingolipids. *EMBO Rep* **5**, 777-782 (2004). https://doi.org:10.1038/sj.embor.7400208

319 Dahm, F. *et al.* Distribution and dynamic changes of sphingolipids in blood in response to platelet activation. *J Thromb Haemost* **4**, 2704-2709 (2006). https://doi.org:10.1111/j.1538-7836.2006.02241.x

320 Yatomi, Y., Ruan, F., Hakomori, S. & Igarashi, Y. Sphingosine-1-phosphate: a platelet-activating sphingolipid released from agonist-stimulated human platelets. *Blood* **86**, 193-202 (1995).

321 English, D. *et al.* Sphingosine 1-phosphate released from platelets during clotting accounts for the potent endothelial cell chemotactic activity of blood serum and provides a novel link between hemostasis and angiogenesis. *FASEB J* **14**, 2255-2265 (2000). https://doi.org:10.1096/fj.00-0134com

322 Yatomi, Y. *et al.* Sphingosine 1-phosphate, a bioactive sphingolipid abundantly stored in platelets, is a normal constituent of human plasma and serum. *J Biochem* **121**, 969-973 (1997). https://doi.org:10.1093/oxfordjournals.jbchem.a021681

323 Yatomi, Y. Plasma sphingosine 1-phosphate metabolism and analysis. *Biochim Biophys Acta* **1780**, 606-611 (2008). https://doi.org:10.1016/j.bbagen.2007.10.006

324 Chatterjee, M. Platelet lipidome: Dismantling the "Trojan horse" in the bloodstream. *J Thromb Haemost* **18**, 543-557 (2020). https://doi.org:10.1111/jth.14721

325 Tourdot, B. E., Ahmed, I. & Holinstat, M. The emerging role of oxylipins in thrombosis and diabetes. *Front Pharmacol* **4**, 176 (2014). https://doi.org:10.3389/fphar.2013.00176

326 Guo, Y. *et al.* Identification of the orphan G protein-coupled receptor GPR31 as a receptor for 12-(S)-hydroxyeicosatetraenoic acid. *J Biol Chem* **286**, 33832-33840 (2011). https://doi.org:10.1074/jbc.M110.216564

327 Whittle, B. J., Moncada, S. & Vane, J. R. Comparison of the effects of prostacyclin (PGI2), prostaglandin E1 and D2 on platelet aggregation in different species. *Prostaglandins* **16**, 373-388 (1978). https://doi.org:10.1016/0090-6980(78)90216-2

328 Nakahata, N. Thromboxane A2: physiology/pathophysiology, cellular signal transduction and pharmacology. *Pharmacol Ther* **118**, 18-35 (2008). https://doi.org:10.1016/j.pharmthera.2008.01.001

329 Fabre, J. E. *et al.* Activation of the murine EP3 receptor for PGE2 inhibits cAMP production and promotes platelet aggregation. *J Clin Invest* **107**, 603-610 (2001). https://doi.org:10.1172/JCI10881

330 Yeung, J. *et al.* 12(S)-HETrE, a 12-Lipoxygenase Oxylipin of Dihomo-gamma-Linolenic Acid, Inhibits Thrombosis via Galphas Signaling in Platelets.

Arterioscler Thromb Vasc Biol **36**, 2068-2077 (2016). https://doi.org:10.1161/ATVBAHA.116.308050

331 Tunaru, S., Chennupati, R., Nusing, R. M. & Offermanns, S. Arachidonic Acid Metabolite 19(S)-HETE Induces Vasorelaxation and Platelet Inhibition by Activating Prostacyclin (IP) Receptor. *PLoS One* **11**, e0163633 (2016). https://doi.org:10.1371/journal.pone.0163633

332 Sekiya, F. *et al.* Feedback regulation of platelet function by 12S-hydroxyeicosatetraenoic acid: inhibition of arachidonic acid liberation from phospholipids. *Biochim Biophys Acta* **1044**, 165-168 (1990). https://doi.org:10.1016/0005-2760(90)90232-m

333 Johnson, E. N., Brass, L. F. & Funk, C. D. Increased platelet sensitivity to ADP in mice lacking platelet-type 12-lipoxygenase. *Proc Natl Acad Sci U S A* **95**, 3100-3105 (1998). https://doi.org:10.1073/pnas.95.6.3100

334 Fonlupt, P., Croset, M. & Lagarde, M. 12-HETE inhibits the binding of PGH2/TXA2 receptor ligands in human platelets. *Thromb Res* **63**, 239-248 (1991). https://doi.org:10.1016/0049-3848(91)90287-7

335 Wahli, W. & Michalik, L. PPARs at the crossroads of lipid signaling and inflammation. *Trends Endocrinol Metab* **23**, 351-363 (2012). https://doi.org:10.1016/j.tem.2012.05.001

336 Madsen, L. *et al.* Adipocyte differentiation of 3T3-L1 preadipocytes is dependent on lipoxygenase activity during the initial stages of the differentiation process. *Biochem J* **375**, 539-549 (2003). https://doi.org:10.1042/bj20030503

337 Escalante, B., Sessa, W. C., Falck, J. R., Yadagiri, P. & Schwartzman, M. L. Vasoactivity of 20-hydroxyeicosatetraenoic acid is dependent on metabolism by cyclooxygenase. *J Pharmacol Exp Ther* **248**, 229-232 (1989).

338 Carroll, M. A., Balazy, M., Margiotta, P., Falck, J. R. & McGiff, J. C. Renal vasodilator activity of 5,6-epoxyeicosatrienoic acid depends upon conversion by cyclooxygenase and release of prostaglandins. *J Biol Chem* **268**, 12260-12266 (1993).

339 Greenberg, M. E. *et al.* The lipid whisker model of the structure of oxidized cell membranes. *J Biol Chem* **283**, 2385-2396 (2008). https://doi.org:10.1074/jbc.M707348200

340 Jonnalagadda, D., Sunkara, M., Morris, A. J. & Whiteheart, S. W. Granule-mediated release of sphingosine-1-phosphate by activated platelets. *Biochim Biophys Acta* **1841**, 1581-1589 (2014). https://doi.org:10.1016/j.bbalip.2014.08.013

341 Hla, T. Physiological and pathological actions of sphingosine 1-phosphate. *Semin Cell Dev Biol* **15**, 513-520 (2004). https://doi.org:10.1016/j.semcdb.2004.05.002

342 Jorgensen, K. A., Dyerberg, J., Olesen, A. S. & Stoffersen, E. Acetylsalicylic acid, bleeding time and age. *Thromb Res* **19**, 799-805 (1980). https://doi.org:10.1016/0049-3848(80)90007-9

343 Reilly, I. A. & FitzGerald, G. A. Eicosenoid biosynthesis and platelet function with advancing age. *Thromb Res* **41**, 545-554 (1986). https://doi.org:10.1016/0049-3848(86)91700-7

344 Yokoyama, M., Kusui, A., Sakamoto, S. & Fukuzaki, H. Age-associated increments in human platelet alpha-adrenoceptor capacity. Possible mechanism for platelet hyperactivity to epinephrine in aging man. *Thromb Res* **34**, 287-295 (1984). https://doi.org:10.1016/0049-3848(84)90385-2

345 Kasjanovova, D., Adameckova, D., Gratzlova, J. & Hegyi, L. Sex-related and age-related differences in platelet function in vitro: influence of hematocrit. *Mech Ageing Dev* **71**, 103-109 (1993). https://doi.org:10.1016/0047-6374(93)90039-t

346 O'Donnell, C. J. *et al.* Genetic and environmental contributions to platelet aggregation: the Framingham heart study. *Circulation* **103**, 3051-3056 (2001). https://doi.org:10.1161/01.cir.103.25.3051

347 Kasjanovova, D. & Balaz, V. Age-related changes in human platelet function in vitro. *Mech Ageing Dev* **37**, 175-182 (1986). https://doi.org:10.1016/0047-6374(86)90074-6

348 Meade, T. W. *et al.* Epidemiological characteristics of platelet aggregability. *Br Med J (Clin Res Ed)* **290**, 428-432 (1985). https://doi.org:10.1136/bmj.290.6466.428

349 Bastyr, E. J., 3rd, Kadrofske, M. M. & Vinik, A. I. Platelet activity and phosphoinositide turnover increase with advancing age. *Am J Med* **88**, 601-606 (1990). https://doi.org:10.1016/0002-9343(90)90525-i

350 Brodde, O. E., Anlauf, M., Graben, N. & Bock, K. D. Age-dependent decrease of alpha 2-adrenergic receptor number in human platelets. *Eur J Pharmacol* **81**, 345-347 (1982). https://doi.org:10.1016/0014-2999(82)90456-3

351 Winther, K. & Naesh, O. Platelet alpha-adrenoceptor function and aging. *Thromb Res* **46**, 677-684 (1987). https://doi.org:10.1016/0049-3848(87)90269-6

352 Winther, K. & Naesh, O. Aging and platelet beta-adrenoceptor function. *Eur J Pharmacol* **136**, 219-223 (1987). https://doi.org:10.1016/0014-2999(87)90713-8

353 Gleerup, G. & Winther, K. The effect of ageing on human platelet sensitivity to serotonin. *Eur J Clin Invest* **18**, 504-506 (1988). https://doi.org:10.1111/j.1365-2362.1988.tb01047.x

354 Barradas, M. A., Gill, D. S., Fonseca, V. A., Mikhailidis, D. P. & Dandona, P. Intraplatelet serotonin in patients with diabetes mellitus and peripheral vascular disease. *Eur J Clin Invest* **18**, 399-404 (1988). https://doi.org:10.1111/j.1365-2362.1988.tb01030.x

355 Flachaire, E. *et al.* Determination of reference values for serotonin concentration in platelets of healthy newborns, children, adults, and elderly subjects by HPLC with electrochemical detection. *Clin Chem* **36**, 2117-2120 (1990).

356 Campbell, R. A. *et al.* Granzyme A in Human Platelets Regulates the Synthesis of Proinflammatory Cytokines by Monocytes in Aging. *J Immunol* **200**, 295-304 (2018). https://doi.org:10.4049/jimmunol.1700885

357 Cini, C. *et al.* Differences in the resting platelet proteome and platelet releasate between healthy children and adults. *J Proteomics* **123**, 78-88 (2015). https://doi.org:10.1016/j.jprot.2015.04.003

358 Malaquin, N., Martinez, A. & Rodier, F. Keeping the senescence secretome under control: Molecular reins on the senescence-associated secretory phenotype. *Exp Gerontol* **82**, 39-49 (2016). https://doi.org:10.1016/j.exger.2016.05.010

359 He, S. & Sharpless, N. E. Senescence in Health and Disease. *Cell* **169**, 1000-1011 (2017). https://doi.org:10.1016/j.cell.2017.05.015

360 Violi, F., Loffredo, L., Carnevale, R., Pignatelli, P. & Pastori, D. Atherothrombosis and Oxidative Stress: Mechanisms and Management in

Elderly. *Antioxid Redox Signal* **27**, 1083-1124 (2017). https://doi.org:10.1089/ars.2016.6963

361 Fuentes, E. & Palomo, I. Role of oxidative stress on platelet hyperreactivity during aging. *Life Sci* **148**, 17-23 (2016). https://doi.org:10.1016/j.lfs.2016.02.026

362 Jang, J. Y. *et al.* Reactive oxygen species play a critical role in collagen-induced platelet activation via SHP-2 oxidation. *Antioxid Redox Signal* **20**, 2528-2540 (2014). https://doi.org:10.1089/ars.2013.5337

363 Goswami, K. & Koner, B. C. Level of sialic acid residues in platelet proteins in diabetes, aging, and Hodgkin's lymphoma: a potential role of free radicals in desialylation. *Biochem Biophys Res Commun* **297**, 502-505 (2002). https://doi.org:10.1016/s0006-291x(02)02241-6

364 Alexandru, N., Constantin, A. & Popov, D. Carbonylation of platelet proteins occurs as consequence of oxidative stress and thrombin activation, and is stimulated by ageing and type 2 diabetes. *Clin Chem Lab Med* **46**, 528-536 (2008). https://doi.org:10.1515/CCLM.2008.104

365 Gaspar, R. S., Trostchansky, A. & Paes, A. M. Potential Role of Protein Disulfide Isomerase in Metabolic Syndrome-Derived Platelet Hyperactivity. *Oxid Med Cell Longev* **2016**, 2423547 (2016). https://doi.org:10.1155/2016/2423547

366 Cremers, C. M. & Jakob, U. Oxidant sensing by reversible disulfide bond formation. *J Biol Chem* **288**, 26489-26496 (2013). https://doi.org:10.1074/jbc.R113.462929

367 Kim, K. *et al.* Platelet protein disulfide isomerase is required for thrombus formation but not for hemostasis in mice. *Blood* **122**, 1052-1061 (2013). https://doi.org:10.1182/blood-2013-03-492504

368 Levin, L. *et al.* A Single Disulfide Bond Disruption in the beta 3 Integrin Subunit Promotes Thiol/Disulfide Exchange, a Molecular Dynamics Study. *Plos One* **8** (2013). https://doi.org:ARTN e59175
10.1371/journal.pone.0059175

369 Essex, D. W. Redox control of platelet function. *Antioxid Redox Signal* **11**, 1191-1225 (2009). https://doi.org:10.1089/ARS.2008.2322

370 Pignatelli, P., Pulcinelli, F. M., Lenti, L., Gazzaniga, P. P. & Violi, F. Hydrogen peroxide is involved in collagen-induced platelet activation. *Blood* **91**, 484-490 (1998).

371 Hossain, M. S., Hashimoto, M., Gamoh, S. & Masumura, S. Association of age-related decrease in platelet membrane fluidity with platelet lipid peroxide. *Life Sci* **64**, 135-143 (1999). https://doi.org:10.1016/s0024-3205(98)00543-8

372 Cohen, B. M. & Zubenko, G. S. Aging and the biophysical properties of cell membranes. *Life Sci* **37**, 1403-1409 (1985). https://doi.org:10.1016/0024-3205(85)90079-7

373 Insel, P. A., Nirenberg, P., Turnbull, J. & Shattil, S. J. Relationships between membrane cholesterol, alpha-adrenergic receptors, and platelet function. *Biochemistry* **17**, 5269-5274 (1978). https://doi.org:10.1021/bi00617a029

374 Shattil, S. J., Anaya-Galindo, R., Bennett, J., Colman, R. W. & Cooper, R. A. Platelet hypersensitivity induced by cholesterol incorporation. *J Clin Invest* **55**, 636-643 (1975). https://doi.org:10.1172/JCI107971

375 Galley, H. F. & Webster, N. R. Physiology of the endothelium. *Br J Anaesth* **93**, 105-113 (2004). https://doi.org:10.1093/bja/aeh163

376 Michimata, T., Imamura, M., Mizuma, H., Murakami, M. & Iriuchijima, T. Sex and age differences in soluble guanylate cyclase activity in human platelets. *Life Sci* **58**, 415-419 (1996). https://doi.org:10.1016/0024-3205(95)02306-2

377 Kawamoto, E. M. *et al.* Oxidative state in platelets and erythrocytes in aging and Alzheimer's disease. *Neurobiol Aging* **26**, 857-864 (2005). https://doi.org:10.1016/j.neurobiolaging.2004.08.011

378 Origlia, C. *et al.* Platelet cGMP inversely correlates with age in healthy subjects. *J Endocrinol Invest* **27**, RC1-4 (2004). https://doi.org:10.1007/BF03346251

379 Celermajer, D. S., Sorensen, K. E., Bull, C., Robinson, J. & Deanfield, J. E. Endothelium-dependent dilation in the systemic arteries of asymptomatic subjects relates to coronary risk factors and their interaction. *J Am Coll Cardiol* **24**, 1468-1474 (1994). https://doi.org:10.1016/0735-1097(94)90141-4

380 Taddei, S. *et al.* Age-related reduction of NO availability and oxidative stress in humans. *Hypertension* **38**, 274-279 (2001). https://doi.org:10.1161/01.hyp.38.2.274

381 Kawamoto, E. M. *et al.* Age-related changes in nitric oxide activity, cyclic GMP, and TBARS levels in platelets and erythrocytes reflect the oxidative status in central nervous system. *Age (Dordr)* **35**, 331-342 (2013). https://doi.org:10.1007/s11357-011-9365-7

382 Modesti, P. A., Fortini, A., Abbate, R. & Gensini, G. F. Age related changes of platelet prostacyclin receptors in humans. *Eur J Clin Invest* **15**, 204-208 (1985). https://doi.org:10.1111/j.1365-2362.1985.tb00169.x

383 Kaushik, S. & Cuervo, A. M. Proteostasis and aging. *Nat Med* **21**, 1406-1415 (2015). https://doi.org:10.1038/nm.4001

384 Ungvari, Z. *et al.* Ionizing radiation promotes the acquisition of a senescence-associated secretory phenotype and impairs angiogenic capacity in cerebromicrovascular endothelial cells: role of increased DNA damage and decreased DNA repair capacity in microvascular radiosensitivity. *J Gerontol A Biol Sci Med Sci* **68**, 1443-1457 (2013). https://doi.org:10.1093/gerona/glt057

385 Csiszar, A. *et al.* Aging-induced phenotypic changes and oxidative stress impair coronary arteriolar function. *Circ Res* **90**, 1159-1166 (2002). https://doi.org:10.1161/01.res.0000020401.61826.ea

386 Morgan, R. G. *et al.* Age-related telomere uncapping is associated with cellular senescence and inflammation independent of telomere shortening in human arteries. *Am J Physiol Heart Circ Physiol* **305**, H251-258 (2013). https://doi.org:10.1152/ajpheart.00197.2013

387 Franceschi, C. *et al.* Inflamm-aging. An evolutionary perspective on immunosenescence. *Ann N Y Acad Sci* **908**, 244-254 (2000). https://doi.org:10.1111/j.1749-6632.2000.tb06651.x

388 Csiszar, A., Wang, M., Lakatta, E. G. & Ungvari, Z. Inflammation and endothelial dysfunction during aging: role of NF-kappaB. *J Appl Physiol (1985)* **105**, 1333-1341 (2008). https://doi.org:10.1152/japplphysiol.90470.2008

389 Kurabayashi, H., Kubota, K., Hishinuma, A. & Majima, M. Platelet activation is caused not by aging but by atherosclerosis. *Arch Gerontol Geriatr* **51**, 205-208 (2010). https://doi.org:10.1016/j.archger.2009.10.009

390 Zahavi, J. *et al.* Enhanced in-vivo platelet release reaction, increased thromboxane synthesis, and decreased prostacyclin release after tourniquet ischaemia. *Lancet* **2**, 663-667 (1980). https://doi.org:10.1016/s0140-6736(80)92706-3

391 Kowalska, M. A., Rauova, L. & Poncz, M. Role of the platelet chemokine platelet factor 4 (PF4) in hemostasis and thrombosis. *Thromb Res* **125**, 292-296 (2010). https://doi.org:10.1016/j.thromres.2009.11.023

392 Le Blanc, J. & Lordkipanidze, M. Platelet Function in Aging. *Front Cardiovasc Med* **6**, 109 (2019). https://doi.org:10.3389/fcvm.2019.00109

393 Franchini, M. Hemostasis and aging. *Crit Rev Oncol Hematol* **60**, 144-151 (2006). https://doi.org:10.1016/j.critrevonc.2006.06.004

394 Hager, K., Setzer, J., Vogl, T., Voit, J. & Platt, D. Blood coagulation factors in the elderly. *Arch Gerontol Geriatr* **9**, 277-282 (1989). https://doi.org:10.1016/0167-4943(89)90047-2

395 Sagripanti, A. & Carpi, A. Natural anticoagulants, aging, and thromboembolism. *Exp Gerontol* **33**, 891-896 (1998). https://doi.org:10.1016/s0531-5565(98)00047-3

396 Segal, J. B. & Moliterno, A. R. Platelet counts differ by sex, ethnicity, and age in the United States. *Ann Epidemiol* **16**, 123-130 (2006). https://doi.org:10.1016/j.annepidem.2005.06.052

397 Robbins, J. *et al.* Hematological and biochemical laboratory values in older Cardiovascular Health Study participants. *J Am Geriatr Soc* **43**, 855-859 (1995). https://doi.org:10.1111/j.1532-5415.1995.tb05526.x

398 Troussard, X. *et al.* Full blood count normal reference values for adults in France. *J Clin Pathol* **67**, 341-344 (2014). https://doi.org:10.1136/jclinpath-2013-201687

399 Burstein, S. A. *et al.* Cytokine-induced alteration of platelet and hemostatic function. *Stem Cells* **14 Suppl 1**, 154-162 (1996). https://doi.org:10.1002/stem.5530140720

400 Davizon-Castillo, P. *et al.* TNF-alpha-driven inflammation and mitochondrial dysfunction define the platelet hyperreactivity of aging. *Blood* **134**, 727-740 (2019). https://doi.org:10.1182/blood.2019000200

401 Bertrand, G., Chapal, J. & Loubatieres-Mariani, M. M. Potentiating synergism between adenosine diphosphate or triphosphate and acetylcholine on insulin secretion. *Am J Physiol* **251**, E416-421 (1986). https://doi.org:10.1152/ajpendo.1986.251.4.E416

402 Fotino, C., Dal Ben, D. & Adinolfi, E. Emerging Roles of Purinergic Signaling in Diabetes. *Med Chem* **14**, 428-438 (2018). https://doi.org:10.2174/1573406414666180226165204

403 El-Merahbi, R., Loffler, M., Mayer, A. & Sumara, G. The roles of peripheral serotonin in metabolic homeostasis. *FEBS Lett* **589**, 1728-1734 (2015). https://doi.org:10.1016/j.febslet.2015.05.054

404 Nagata, M. *et al.* Blockade of multiple monoamines receptors reduce insulin secretion from pancreatic beta-cells. *Sci Rep* **9**, 16438 (2019). https://doi.org:10.1038/s41598-019-52590-y

405 Bender, M. *et al.* Combined in vivo depletion of glycoprotein VI and C-type lectin-like receptor 2 severely compromises hemostasis and abrogates arterial thrombosis in mice. *Arterioscler Thromb Vasc Biol* **33**, 926-934 (2013). https://doi.org:10.1161/ATVBAHA.112.300672

406 Kanaji, T., Russell, S. & Ware, J. Amelioration of the macrothrombocytopenia associated with the murine Bernard-Soulier syndrome. *Blood* **100**, 2102-2107 (2002). https://doi.org:10.1182/blood-2002-03-0997

407 Stegner, D. *et al.* Munc13-4-mediated secretion is essential for infarct progression but not intracranial hemostasis in acute stroke. *J Thromb Haemost* **11**, 1430-1433 (2013). https://doi.org:10.1111/jth.12293

408 Wettschureck, N. *et al.* Absence of pressure overload induced myocardial hypertrophy after conditional inactivation of Galphaq/Galpha11 in cardiomyocytes. *Nat Med* **7**, 1236-1240 (2001). https://doi.org:10.1038/nm1101-1236

409 Moers, A. *et al.* G13 is an essential mediator of platelet activation in hemostasis and thrombosis. *Nat Med* **9**, 1418-1422 (2003). https://doi.org:10.1038/nm943

410 Tiedt, R., Schomber, T., Hao-Shen, H. & Skoda, R. C. Pf4-Cre transgenic mice allow the generation of lineage-restricted gene knockouts for studying megakaryocyte and platelet function in vivo. *Blood* **109**, 1503-1506 (2007). https://doi.org:10.1182/blood-2006-04-020362

411 Bergmeier, W. *et al.* Flow cytometric detection of activated mouse integrin alphaIIbbeta3 with a novel monoclonal antibody. *Cytometry* **48**, 80-86 (2002). https://doi.org:10.1002/cyto.10114

412 Karla, W., Shams, H., Orr, J. A. & Scheid, P. Effects of the thromboxane A2 mimetic, U46,619, on pulmonary vagal afferents in the cat. *Respir Physiol* **87**, 383-396 (1992). https://doi.org:10.1016/0034-5687(92)90019-s

413 Moers, A., Wettschureck, N., Gruner, S., Nieswandt, B. & Offermanns, S. Unresponsiveness of platelets lacking both Galpha(q) and Galpha(13). Implications for collagen-induced platelet activation. *J Biol Chem* **279**, 45354-45359 (2004). https://doi.org:10.1074/jbc.M408962200

414 Li, Y. V. Zinc and insulin in pancreatic beta-cells. *Endocrine* **45**, 178-189 (2014). https://doi.org:10.1007/s12020-013-0032-x

415 Ishihara, H. *et al.* Pancreatic beta cell line MIN6 exhibits characteristics of glucose metabolism and glucose-stimulated insulin secretion similar to those of normal islets. *Diabetologia* **36**, 1139-1145 (1993). https://doi.org:10.1007/BF00401058

416 Holt, J. C. *et al.* Occurrence of platelet basic protein, a precursor of low affinity platelet factor 4 and beta-thromboglobulin, in human platelets and megakaryocytes. *Exp Hematol* **16**, 302-306 (1988).

417 Brandt, E. *et al.* The beta-thromboglobulins and platelet factor 4: blood platelet-derived CXC chemokines with divergent roles in early neutrophil regulation. *J Leukoc Biol* **67**, 471-478 (2000). https://doi.org:10.1002/jlb.67.4.471

418 Nieswandt, B. *et al.* Long-term antithrombotic protection by in vivo depletion of platelet glycoprotein VI in mice. *J Exp Med* **193**, 459-469 (2001). https://doi.org:10.1084/jem.193.4.459

419 Nieswandt, B., Bergmeier, W., Rackebrandt, K., Gessner, J. E. & Zirngibl, H. Identification of critical antigen-specific mechanisms in the development of immune thrombocytopenic purpura in mice. *Blood* **96**, 2520-2527 (2000).

420 Bergmeier, W., Rackebrandt, K., Schroder, W., Zirngibl, H. & Nieswandt, B. Structural and functional characterization of the mouse von Willebrand factor receptor GPIb-IX with novel monoclonal antibodies. *Blood* **95**, 886-893 (2000).

421 Massberg, S. *et al.* A crucial role of glycoprotein VI for platelet recruitment to the injured arterial wall in vivo. *J Exp Med* **197**, 41-49 (2003). https://doi.org:10.1084/jem.20020945

422 Ware, J., Russell, S. & Ruggeri, Z. M. Generation and rescue of a murine model of platelet dysfunction: the Bernard-Soulier syndrome. *Proc Natl Acad Sci U S A* **97**, 2803-2808 (2000). https://doi.org:10.1073/pnas.050582097

423 Fujita, H., Hashimoto, Y., Russell, S., Zieger, B. & Ware, J. In vivo expression of murine platelet glycoprotein Ibalpha. *Blood* **92**, 488-495 (1998).

424 Ren, Q. *et al.* Munc13-4 is a limiting factor in the pathway required for platelet granule release and hemostasis. *Blood* **116**, 869-877 (2010). https://doi.org:10.1182/blood-2010-02-270934

425 Savage, J. S. *et al.* Munc13-4 is critical for thrombosis through regulating release of ADP from platelets. *J Thromb Haemost* **11**, 771-775 (2013). https://doi.org:10.1111/jth.12138

426 Sudic, D. *et al.* High glucose levels enhance platelet activation: involvement of multiple mechanisms. *Br J Haematol* **133**, 315-322 (2006). https://doi.org:10.1111/j.1365-2141.2006.06012.x

427 Ono, K., Takigawa, S. & Yamada, K. L-Glucose: Another Path to Cancer Cells. *Cancers (Basel)* **12** (2020). https://doi.org:10.3390/cancers12040850

428 Ravassard, P. *et al.* A genetically engineered human pancreatic beta cell line exhibiting glucose-inducible insulin secretion. *J Clin Invest* **121**, 3589-3597 (2011). https://doi.org:10.1172/JCI58447

429 Szczerbinska, I. *et al.* Large-Scale Functional Genomics Screen to Identify Modulators of Human beta-Cell Insulin Secretion. *Biomedicines* **10** (2022). https://doi.org:10.3390/biomedicines10010103

430 Laychock, S. G. Effects of hydroxyeicosatetraenoic acids on fatty acid esterification in phospholipids and insulin secretion in pancreatic islets. *Endocrinology* **117**, 1011-1019 (1985). https://doi.org:10.1210/endo-117-3-1011

431 Turk, J. *et al.* Arachidonic acid metabolism and insulin secretion by isolated human pancreatic islets. *Diabetes* **37**, 992-996 (1988). https://doi.org:10.2337/diab.37.7.992

432 Vettor, R. *et al.* Loss-of-function mutation of the GPR40 gene associates with abnormal stimulated insulin secretion by acting on intracellular calcium mobilization. *J Clin Endocrinol Metab* **93**, 3541-3550 (2008). https://doi.org:10.1210/jc.2007-2680

433 Schnell, S., Schaefer, M. & Schofl, C. Free fatty acids increase cytosolic free calcium and stimulate insulin secretion from beta-cells through activation of GPR40. *Mol Cell Endocrinol* **263**, 173-180 (2007). https://doi.org:10.1016/j.mce.2006.09.013

434 Usui, R. *et al.* GPR40 activation initiates store-operated Ca(2+) entry and potentiates insulin secretion via the IP3R1/STIM1/Orai1 pathway in pancreatic beta-cells. *Sci Rep* **9**, 15562 (2019). https://doi.org:10.1038/s41598-019-52048-1

435 Loffler, M. C. *et al.* Protein kinase D1 deletion in adipocytes enhances energy dissipation and protects against adiposity. *EMBO J* **37** (2018). https://doi.org:10.15252/embj.201899182

436 Kolczynska, K., Loza-Valdes, A., Hawro, I. & Sumara, G. Diacylglycerol-evoked activation of PKC and PKD isoforms in regulation of glucose and lipid metabolism: a review. *Lipids Health Dis* **19**, 113 (2020). https://doi.org:10.1186/s12944-020-01286-8

437 Rybin, V. O., Guo, J. & Steinberg, S. F. Protein kinase D1 autophosphorylation via distinct mechanisms at Ser744/Ser748 and Ser916. *J Biol Chem* **284**, 2332-2343 (2009). https://doi.org:10.1074/jbc.M806381200

438 Alquier, T. *et al.* Deletion of GPR40 impairs glucose-induced insulin secretion in vivo in mice without affecting intracellular fuel metabolism in islets. *Diabetes* **58**, 2607-2615 (2009). https://doi.org:10.2337/db09-0362

439 Garcia, V. *et al.* 20-HETE Signals Through G-Protein-Coupled Receptor GPR75 (Gq) to Affect Vascular Function and Trigger Hypertension. *Circ Res* **120**, 1776-1788 (2017). https://doi.org:10.1161/CIRCRESAHA.116.310525

440 Metz, S. A. Ether-linked lysophospholipids initiate insulin secretion. Lysophospholipids may mediate effects of phospholipase A2 activation on hormone release. *Diabetes* **35**, 808-817 (1986). https://doi.org:10.2337/diab.35.7.808

441 Ashraf, M. A. & Nookala, V. in *StatPearls* (2022).

442 Karhausen, J. *et al.* Platelets trigger perivascular mast cell degranulation to cause inflammatory responses and tissue injury. *Sci Adv* **6**, eaay6314 (2020). https://doi.org:10.1126/sciadv.aay6314

443 Karlsson, M. *et al.* A single-cell type transcriptomics map of human tissues. *Sci Adv* **7** (2021). https://doi.org:10.1126/sciadv.abh2169

444 Herbert, J. M. *et al.* Biochemical and pharmacological activities of SR 27417, a highly potent, long-acting platelet-activating factor receptor antagonist. *J Pharmacol Exp Ther* **259**, 44-51 (1991).

445 Investigators, C.-O. *et al.* Dose comparisons of clopidogrel and aspirin in acute coronary syndromes. *N Engl J Med* **363**, 930-942 (2010). https://doi.org:10.1056/NEJMoa0909475

446 Dorsam, R. T. & Kunapuli, S. P. Central role of the P2Y12 receptor in platelet activation. *J Clin Invest* **113**, 340-345 (2004). https://doi.org:10.1172/JCI20986

447 Caplain, H., Donat, F., Gaud, C. & Necciari, J. Pharmacokinetics of clopidogrel. *Semin Thromb Hemost* **25 Suppl 2**, 25-28 (1999).

448 Mitchell, J. A., Akarasereenont, P., Thiemermann, C., Flower, R. J. & Vane, J. R. Selectivity of nonsteroidal antiinflammatory drugs as inhibitors of constitutive and inducible cyclooxygenase. *Proc Natl Acad Sci U S A* **90**, 11693-11697 (1993). https://doi.org:10.1073/pnas.90.24.11693

449 Armstrong, P. C. *et al.* Aspirin and the in vitro linear relationship between thromboxane A2-mediated platelet aggregation and platelet production of thromboxane A2. *J Thromb Haemost* **6**, 1933-1943 (2008). https://doi.org:10.1111/j.1538-7836.2008.03133.x

450 Linder, M. & Andersen, M. Patient characteristics and safety outcomes in new users of ticagrelor and clopidogrel-An observational cohort study in Sweden. *Pharmacoepidemiol Drug Saf* **31**, 235-246 (2022). https://doi.org:10.1002/pds.5387

451 Anneren, C., Welsh, M. & Jansson, L. Glucose intolerance and reduced islet blood flow in transgenic mice expressing the FRK tyrosine kinase under the control of the rat insulin promoter. *Am J Physiol Endocrinol Metab* **292**, E1183-1190 (2007). https://doi.org:10.1152/ajpendo.00168.2006

452 Reinert, R. B. *et al.* Vascular endothelial growth factor-a and islet vascularization are necessary in developing, but not adult, pancreatic islets. *Diabetes* **62**, 4154-4164 (2013). https://doi.org:10.2337/db13-0071

453 Brouwers, J. *et al.* Platelet activation determines angiopoietin-1 and VEGF levels in malaria: implications for their use as biomarkers. *PLoS One* **8**, e64850 (2014). https://doi.org:10.1371/journal.pone.0064850

454 Salgado, R. *et al.* Platelets and vascular endothelial growth factor (VEGF): a morphological and functional study. *Angiogenesis* **4**, 37-43 (2001). https://doi.org:10.1023/a:1016611230747

455 Williams, S. B., Cusco, J. A., Roddy, M. A., Johnstone, M. T. & Creager, M. A. Impaired nitric oxide-mediated vasodilation in patients with non-insulin-dependent diabetes mellitus. *J Am Coll Cardiol* **27**, 567-574 (1996). https://doi.org:10.1016/0735-1097(95)00522-6

456 Du, X. L. *et al.* Hyperglycemia inhibits endothelial nitric oxide synthase activity by posttranslational modification at the Akt site. *J Clin Invest* **108**, 1341-1348 (2001). https://doi.org:10.1172/JCI11235

457 Rubanyi, G. M. & Vanhoutte, P. M. Superoxide anions and hyperoxia inactivate endothelium-derived relaxing factor. *Am J Physiol* **250**, H822-827 (1986). https://doi.org:10.1152/ajpheart.1986.250.5.H822

458 Gerrard, J. M. *et al.* Alteration in the balance of prostaglandin and thromboxane synthesis in diabetic rats. *J Lab Clin Med* **95**, 950-958 (1980).

459 Tschoepe, D. *et al.* Evidence for abnormal platelet glycoprotein expression in diabetes mellitus. *Eur J Clin Invest* **20**, 166-170 (1990). https://doi.org:10.1111/j.1365-2362.1990.tb02264.x

460 Tschope, D., Rosen, P. & Gries, F. A. Increase in the cytosolic concentration of calcium in platelets of diabetics type II. *Thromb Res* **62**, 421-428 (1991). https://doi.org:10.1016/0049-3848(91)90015-o

461 Bakdash, N. & Williams, M. S. Spatially distinct production of reactive oxygen species regulates platelet activation. *Free Radic Biol Med* **45**, 158-166 (2008). https://doi.org:10.1016/j.freeradbiomed.2008.03.021

462 Leoncini, G., Bruzzese, D. & Signorello, M. G. A role for PLCgamma2 in platelet activation by homocysteine. *J Cell Biochem* **100**, 1255-1265 (2007). https://doi.org:10.1002/jcb.21123

463 Caccese, D. *et al.* Superoxide anion and hydroxyl radical release by collagen-induced platelet aggregation--role of arachidonic acid metabolism. *Thromb Haemost* **83**, 485-490 (2000).

464 Wachowicz, B., Olas, B., Zbikowska, H. M. & Buczynski, A. Generation of reactive oxygen species in blood platelets. *Platelets* **13**, 175-182 (2002). https://doi.org:10.1080/09533710022149395

465 Kim, K., Li, J., Tseng, A., Andrews, R. K. & Cho, J. NOX2 is critical for heterotypic neutrophil-platelet interactions during vascular inflammation. *Blood* **126**, 1952-1964 (2015). https://doi.org:10.1182/blood-2014-10-605261

466 Begonja, A. J. *et al.* Platelet NAD(P)H-oxidase-generated ROS production regulates alphaIIbbeta3-integrin activation independent of the NO/cGMP pathway. *Blood* **106**, 2757-2760 (2005). https://doi.org:10.1182/blood-2005-03-1047

467 Tang, W. H. *et al.* Glucose and collagen regulate human platelet activity through aldose reductase induction of thromboxane. *J Clin Invest* **121**, 4462-4476 (2011). https://doi.org:10.1172/JCI59291

468 Bhatnagar, A. & Srivastava, S. K. Aldose reductase: congenial and injurious profiles of an enigmatic enzyme. *Biochem Med Metab Biol* **48**, 91-121 (1992). https://doi.org:10.1016/0885-4505(92)90055-4

469 Chung, S. S., Ho, E. C., Lam, K. S. & Chung, S. K. Contribution of polyol pathway to diabetes-induced oxidative stress. *J Am Soc Nephrol* **14**, S233-236 (2003). https://doi.org:10.1097/01.asn.0000077408.15865.06

470 Yu, T., Jhun, B. S. & Yoon, Y. High-glucose stimulation increases reactive oxygen species production through the calcium and mitogen-activated protein kinase-mediated activation of mitochondrial fission. *Antioxid Redox Signal* **14**, 425-437 (2011). https://doi.org:10.1089/ars.2010.3284

471 Tang, W. H. *et al.* Aldose reductase-mediated phosphorylation of p53 leads to mitochondrial dysfunction and damage in diabetic platelets. *Circulation* **129**, 1598-1609 (2014). https://doi.org:10.1161/CIRCULATIONAHA.113.005224

472 Cai, X., Thinn, A. M. M., Wang, Z., Shan, H. & Zhu, J. The importance of N-glycosylation on beta3 integrin ligand binding and conformational regulation. *Sci Rep* **7**, 4656 (2017). https://doi.org:10.1038/s41598-017-04844-w

473 Singh, V. P., Bali, A., Singh, N. & Jaggi, A. S. Advanced glycation end products and diabetic complications. *Korean J Physiol Pharmacol* **18**, 1-14 (2014). https://doi.org:10.4196/kjpp.2014.18.1.1

474 Recabarren-Leiva, D. *et al.* Effects of the age/rage axis in the platelet activation. *Int J Biol Macromol* **166**, 1149-1161 (2021). https://doi.org:10.1016/j.ijbiomac.2020.10.270

475 Ferreira, I. A., Eybrechts, K. L., Mocking, A. I., Kroner, C. & Akkerman, J. W. IRS-1 mediates inhibition of Ca2+ mobilization by insulin via the inhibitory G-protein Gi. *J Biol Chem* **279**, 3254-3264 (2004). https://doi.org:10.1074/jbc.M305474200

476 Cattaneo, M. Platelet P2 receptors: old and new targets for antithrombotic drugs. *Expert Rev Cardiovasc Ther* **5**, 45-55 (2007). https://doi.org:10.1586/14779072.5.1.45

477 Watson, B. R. *et al.* Zinc is a transmembrane agonist that induces platelet activation in a tyrosine phosphorylation-dependent manner. *Metallomics* **8**, 91-100 (2016). https://doi.org:10.1039/c5mt00064e

478 Kahn, S. E. *et al.* Evidence of cosecretion of islet amyloid polypeptide and insulin by beta-cells. *Diabetes* **39**, 634-638 (1990). https://doi.org:10.2337/diab.39.5.634

479 Hartter, E. *et al.* Basal and stimulated plasma levels of pancreatic amylin indicate its co-secretion with insulin in humans. *Diabetologia* **34**, 52-54 (1991). https://doi.org:10.1007/BF00404025

480 Abedini, A. *et al.* RAGE binds preamyloid IAPP intermediates and mediates pancreatic beta cell proteotoxicity. *J Clin Invest* **128**, 682-698 (2018). https://doi.org:10.1172/JCI85210

481 Sturchler, E., Galichet, A., Weibel, M., Leclerc, E. & Heizmann, C. W. Site-specific blockade of RAGE-Vd prevents amyloid-beta oligomer neurotoxicity. *J Neurosci* **28**, 5149-5158 (2008). https://doi.org:10.1523/JNEUROSCI.4878-07.2008

482 Konarkowska, B., Aitken, J. F., Kistler, J., Zhang, S. & Cooper, G. J. The aggregation potential of human amylin determines its cytotoxicity towards islet beta-cells. *FEBS J* **273**, 3614-3624 (2006). https://doi.org:10.1111/j.1742-4658.2006.05367.x

483 Herczenik, E. *et al.* Activation of human platelets by misfolded proteins. *Arterioscler Thromb Vasc Biol* **27**, 1657-1665 (2007). https://doi.org:10.1161/ATVBAHA.107.143479

484 Barale, C. *et al.* Glucagon-like peptide 1-related peptides increase nitric oxide effects to reduce platelet activation. *Thromb Haemost* **117**, 1115-1128 (2017). https://doi.org:10.1160/TH16-07-0586

485 Thornalley, P. J. *et al.* Quantitative screening of advanced glycation endproducts in cellular and extracellular proteins by tandem mass spectrometry. *Biochem J* **375**, 581-592 (2003). https://doi.org:10.1042/BJ20030763

486 Liu, K., Liu, H., Zhang, Z., Ye, W. & Xu, X. The role of N-glycosylation in high glucose-induced upregulation of intercellular adhesion molecule-1 on bovine retinal endothelial cells. *Acta Ophthalmol* **94**, 353-357 (2016). https://doi.org:10.1111/aos.13028

487 Zhang, W. *et al.* A humanized single-chain antibody against beta 3 integrin inhibits pulmonary metastasis by preferentially fragmenting activated platelets in the tumor microenvironment. *Blood* **120**, 2889-2898 (2012). https://doi.org:10.1182/blood-2012-04-425207

488 Bastida, E., Almirall, L. & Ordinas, A. Tumor-cell-induced platelet aggregation is a glycoprotein-dependent and lipoxygenase-associated process. *Int J Cancer* **39**, 760-763 (1987). https://doi.org:10.1002/ijc.2910390617

489 Mannori, G. *et al.* Differential colon cancer cell adhesion to E-, P-, and L-selectin: role of mucin-type glycoproteins. *Cancer Res* **55**, 4425-4431 (1995).

490 Nikolova, G. *et al.* The vascular basement membrane: a niche for insulin gene expression and Beta cell proliferation. *Dev Cell* **10**, 397-405 (2006). https://doi.org:10.1016/j.devcel.2006.01.015

491 Kaido, T. *et al.* Impact of defined matrix interactions on insulin production by cultured human beta-cells: effect on insulin content, secretion, and gene transcription. *Diabetes* **55**, 2723-2729 (2006). https://doi.org:10.2337/db06-0120

492 Gan, W. J. *et al.* Local Integrin Activation in Pancreatic beta Cells Targets Insulin Secretion to the Vasculature. *Cell Rep* **24**, 2819-2826 e2813 (2018). https://doi.org:10.1016/j.celrep.2018.08.035

493 Huang, G. *et al.* alpha3(V) collagen is critical for glucose homeostasis in mice due to effects in pancreatic islets and peripheral tissues. *J Clin Invest* **121**, 769-783 (2011). https://doi.org:10.1172/JCI45096

494 Porro, B., Songia, P., Squellerio, I., Tremoli, E. & Cavalca, V. Analysis, physiological and clinical significance of 12-HETE: a neglected platelet-derived 12-lipoxygenase product. *J Chromatogr B Analyt Technol Biomed Life Sci* **964**, 26-40 (2014). https://doi.org:10.1016/j.jchromb.2014.03.015

495 Koya, D. & King, G. L. Protein kinase C activation and the development of diabetic complications. *Diabetes* **47**, 859-866 (1998). https://doi.org:10.2337/diabetes.47.6.859

496 Latour, M. G. *et al.* GPR40 is necessary but not sufficient for fatty acid stimulation of insulin secretion in vivo. *Diabetes* **56**, 1087-1094 (2007). https://doi.org:10.2337/db06-1532

497 Kebede, M. *et al.* The fatty acid receptor GPR40 plays a role in insulin secretion in vivo after high-fat feeding. *Diabetes* **57**, 2432-2437 (2008). https://doi.org:10.2337/db08-0553

498 Pascale, J. V. *et al.* Uncovering the signalling, structure and function of the 20-HETE-GPR75 pairing: Identifying the chemokine CCL5 as a negative regulator of GPR75. *Br J Pharmacol* **178**, 3813-3828 (2021). https://doi.org:10.1111/bph.15525

499 Jansson, L. *et al.* Pancreatic islet blood flow and its measurement. *Ups J Med Sci* **121**, 81-95 (2016). https://doi.org:10.3109/03009734.2016.1164769

500 Muratore, M., Santos, C. & Rorsman, P. The vascular architecture of the pancreatic islets: A homage to August Krogh. *Comp Biochem Physiol A Mol Integr Physiol* **252**, 110846 (2021). https://doi.org:10.1016/j.cbpa.2020.110846

501 Epshtein, A. *et al.* Neonatal pancreatic pericytes support beta-cell proliferation. *Mol Metab* **6**, 1330-1338 (2017). https://doi.org:10.1016/j.molmet.2017.07.010

502 Sasson, A. *et al.* Islet Pericytes Are Required for beta-Cell Maturity. *Diabetes* **65**, 3008-3014 (2016). https://doi.org:10.2337/db16-0365

503 Baron, C. L. & Malhotra, V. Role of diacylglycerol in PKD recruitment to the TGN and protein transport to the plasma membrane. *Science* **295**, 325-328 (2002). https://doi.org:10.1126/science.1066759

504 Rozengurt, E. Protein kinase D signaling: multiple biological functions in health and disease. *Physiology (Bethesda)* **26**, 23-33 (2011). https://doi.org:10.1152/physiol.00037.2010

505 Cobbaut, M. & Van Lint, J. Function and Regulation of Protein Kinase D in Oxidative Stress: A Tale of Isoforms. *Oxid Med Cell Longev* **2018**, 2138502 (2018). https://doi.org:10.1155/2018/2138502

506 Bossard, C., Bresson, D., Polishchuk, R. S. & Malhotra, V. Dimeric PKD regulates membrane fission to form transport carriers at the TGN. *J Cell Biol* **179**, 1123-1131 (2007). https://doi.org:10.1083/jcb.200703166

507 Liljedahl, M. *et al.* Protein kinase D regulates the fission of cell surface destined transport carriers from the trans-Golgi network. *Cell* **104**, 409-420 (2001). https://doi.org:10.1016/s0092-8674(01)00228-8

508 Kong, K. C. *et al.* M3-muscarinic receptor promotes insulin release via receptor phosphorylation/arrestin-dependent activation of protein kinase D1. *Proc Natl Acad Sci U S A* **107**, 21181-21186 (2010). https://doi.org:10.1073/pnas.1011651107

509 Khan, S. *et al.* A role for PKD1 in insulin secretion downstream of P2Y1 receptor activation in mouse and human islets. *Physiol Rep* **7**, e14250 (2019). https://doi.org:10.14814/phy2.14250

510 Shi, L. C., Wang, H. Y., Horwitz, J. & Friedman, E. Guanine nucleotide regulatory proteins, Gq and Gi1/2, mediate platelet-activating factor-stimulated phosphoinositide metabolism in immortalized hippocampal cells. *J Neurochem* **67**, 1478-1484 (1996). https://doi.org:10.1046/j.1471-4159.1996.67041478.x

511 Ni, R. *et al.* Effect of Different Doses of Acetylsalicylic Acid on the Antithrombotic Activity of Clopidogrel in a Mouse Arterial Thrombosis Model. *Arterioscler Thromb Vasc Biol* **38**, 2338-2344 (2018). https://doi.org:10.1161/ATVBAHA.118.311404

512 Vogelsang, A. *et al.* Platelet Inhibition by Low-Dose Acetylsalicylic Acid Reduces Neuroinflammation in an Animal Model of Multiple Sclerosis. *Int J Mol Sci* **22** (2021). https://doi.org:10.3390/ijms22189915

513 Reilly, I. A. & FitzGerald, G. A. Inhibition of thromboxane formation in vivo and ex vivo: implications for therapy with platelet inhibitory drugs. *Blood* **69**, 180-186 (1987).

514 Sane, D. C., McKee, S. A., Malinin, A. I. & Serebruany, V. L. Frequency of aspirin resistance in patients with congestive heart failure treated with antecedent aspirin. *Am J Cardiol* **90**, 893-895 (2002). https://doi.org:10.1016/s0002-9149(02)02718-2

515 Frelinger, A. L., 3rd *et al.* Residual arachidonic acid-induced platelet activation via an adenosine diphosphate-dependent but cyclooxygenase-1- and cyclooxygenase-2-independent pathway: a 700-patient study of aspirin

resistance. *Circulation* **113**, 2888-2896 (2006). https://doi.org:10.1161/CIRCULATIONAHA.105.596627

516 Fitzgerald, R. & Pirmohamed, M. Aspirin resistance: effect of clinical, biochemical and genetic factors. *Pharmacol Ther* **130**, 213-225 (2011). https://doi.org:10.1016/j.pharmthera.2011.01.011

517 Crescente, M. *et al.* Profiling the eicosanoid networks that underlie the anti- and pro-thrombotic effects of aspirin. *FASEB J* **34**, 10027-10040 (2020). https://doi.org:10.1096/fj.202000312R

518 Williams, J. M., Murphy, S., Burke, M. & Roman, R. J. 20-hydroxyeicosatetraeonic acid: a new target for the treatment of hypertension. *J Cardiovasc Pharmacol* **56**, 336-344 (2010). https://doi.org:10.1097/FJC.0b013e3181f04b1c

519 Chuang, S. S. *et al.* CYP2U1, a novel human thymus- and brain-specific cytochrome P450, catalyzes omega- and (omega-1)-hydroxylation of fatty acids. *J Biol Chem* **279**, 6305-6314 (2004). https://doi.org:10.1074/jbc.M311830200

520 Xu, S. F. *et al.* Age-associated changes of cytochrome P450 and related phase-2 gene/proteins in livers of rats. *PeerJ* **7**, e7429 (2019). https://doi.org:10.7717/peerj.7429

521 Perl, S. *et al.* Significant human beta-cell turnover is limited to the first three decades of life as determined by in vivo thymidine analog incorporation and radiocarbon dating. *J Clin Endocrinol Metab* **95**, E234-239 (2010). https://doi.org:10.1210/jc.2010-0932

522 Rankin, M. M. & Kushner, J. A. Adaptive beta-cell proliferation is severely restricted with advanced age. *Diabetes* **58**, 1365-1372 (2009). https://doi.org:10.2337/db08-1198

523 Helman, A. *et al.* p16(Ink4a)-induced senescence of pancreatic beta cells enhances insulin secretion. *Nat Med* **22**, 412-420 (2016). https://doi.org:10.1038/nm.4054

524 Avrahami, D. *et al.* Aging-Dependent Demethylation of Regulatory Elements Correlates with Chromatin State and Improved beta Cell Function. *Cell Metab* **22**, 619-632 (2015). https://doi.org:10.1016/j.cmet.2015.07.025

525 Arda, H. E. *et al.* Age-Dependent Pancreatic Gene Regulation Reveals Mechanisms Governing Human beta Cell Function. *Cell Metab* **23**, 909-920 (2016). https://doi.org:10.1016/j.cmet.2016.04.002

526 Smedmyr, B., Wibell, L., Simonsson, B. & Oberg, G. Impaired glucose tolerance after autologous bone marrow transplantation. *Bone Marrow Transplant* **6**, 89-92 (1990).

527 Taskinen, M., Saarinen-Pihkala, U. M., Hovi, L. & Lipsanen-Nyman, M. Impaired glucose tolerance and dyslipidaemia as late effects after bone-marrow transplantation in childhood. *Lancet* **356**, 993-997 (2000). https://doi.org:10.1016/S0140-6736(00)02717-3

528 Griffith, M. L., Jagasia, M. & Jagasia, S. M. Diabetes mellitus after hematopoietic stem cell transplantation. *Endocr Pract* **16**, 699-706 (2010). https://doi.org:10.4158/EP10027.RA

529 Baker, K. S. *et al.* Diabetes, hypertension, and cardiovascular events in survivors of hematopoietic cell transplantation: a report from the bone marrow transplantation survivor study. *Blood* **109**, 1765-1772 (2007). https://doi.org:10.1182/blood-2006-05-022335

530 Zhou, B. *et al.* Rapidly in situ forming platelet-rich plasma gel enhances angiogenic responses and augments early wound healing after open abdomen. *Gastroenterol Res Pract* **2013**, 926764 (2013). https://doi.org:10.1155/2013/926764

531 Roy, S. *et al.* Platelet-rich fibrin matrix improves wound angiogenesis via inducing endothelial cell proliferation. *Wound Repair Regen* **19**, 753-766 (2011). https://doi.org:10.1111/j.1524-475X.2011.00740.x

532 Kisucka, J. *et al.* Platelets and platelet adhesion support angiogenesis while preventing excessive hemorrhage. *Proc Natl Acad Sci U S A* **103**, 855-860 (2006). https://doi.org:10.1073/pnas.0510412103

533 Carramolino, L. *et al.* Platelets play an essential role in separating the blood and lymphatic vasculatures during embryonic angiogenesis. *Circ Res* **106**, 1197-1201 (2010). https://doi.org:10.1161/CIRCRESAHA.110.218073

534 Lo, S. K., Burhop, K. E., Kaplan, J. E. & Malik, A. B. Role of platelets in maintenance of pulmonary vascular permeability to protein. *Am J Physiol* **254**, H763-771 (1988). https://doi.org:10.1152/ajpheart.1988.254.4.H763

535 Deppermann, C. *et al.* Gray platelet syndrome and defective thrombo-inflammation in Nbeal2-deficient mice. *J Clin Invest* (2013). https://doi.org:10.1172/JCI69210

5 APPENDIX

5.1 Figures

5.2 Tables

5.3 Abbreviations

3D	*Three dimensional*
AA	*Arachidonic acid*
AC	*Adenylyl cyclase*
ACD	*Acid citrate dextrose*

AEA	*N-arachidonoylethanolamine*
AGE	*Advanced glycation end products*
Akt	*Protein kinase B*
ALA	*α-Linolenic acid*
ALDH	*Aldehyde dehydrogenas*
AM	*Acetoxymethyl ester*
ANOVA	*Analysis of variance*
APS	*Ammonium peroxidisulphate*
AR	*Aldose reductase*
ASA	*Acetylsalicylic acid*
BM	*Basement membrane*
BW	*Body weight*
BSA	*Bovine serum albumin*
$CaCl_2$	*Calcium chloride*
cGMP	*Cyclic guanosine monophosphate*
CMLE	*Classic maximum likelihood estimation*
CoA	*Coenzyme A*
COX	*Cyclooxygenase*
CO_2	*Carbon dioxide*
CPT	*Carnitine-palmitoyl-transferase*
CRP	*Collagen related peptide*
CTLA	*Cytotoxic T-lymphocyte associated protein*
CY	*Cytochrom*
DAG	*Diacylglycerol*
DAPI	*4’,6-diamidino-2-phenylindole*
DHA	*Docosahexaenoic acid*
DHC	*Dehydrocholesterol*
DMEM	*Dulbecco's Modified Eagle's Medium*
DMSO	*Dimethyl sulfoxide*
DNA	*Deoxyribonucleic acid*
dNTP	*2'-deoxynucleoside 5'-triphosphate*

DTS	*Dense tubular system*
ECL	*Enhanced chemiluminescence*
EDTA	*Ethylenediaminetetraacetic acid*
EET	*Epoxyeicosatrienoic acids*
EGF	*Epidermal growth factor*
ELISA	*Enzyme-linked immunosorbent assay*
eNOS	*Endothelial nitric oxide synthase*
EOS	*Eosinophil*
EPA	*Eicosapentaenoic acid*
EPAC	*Exchange protein directly activated by cAMP*
ER	*Endoplasmic reticulum*
FA	*Fatty acid*
FACL	*Fatty acyl Co-A ligase*
$FADH_2$	*Flavin adenine dinucleotide*
FBS	*Fetal bovine serum*
FCS	*Fetal calf serum*
f/f	*Flox/flox*
FGF	*Fibroblast growth factor*
GABA	*γ-Aminobutyric acid*
GAD	*Glutamic acid decarboxylase*
GC	*Guanylate cyclase*
GCK	*Glucokinase*
GCGR	*Glucagon receptor*
GIP	*Glucose-dependent insulinotropic polypeptide*
GLUT	*Glucose transporter*
GLP	*Glucagon-like peptide*
GPCR	*G-protein coupled receptors*
GRA	*Granulocyte*
GSIS	*Glucose-stimulated insulin secretion*
GTT	*Glucose tolerance test*
G6P	*Glucose-6-phosphate*

H&E	*Hematoxylin and eosin*
Hb	*Hemoglobin*
HCl	*Hydrogen chloride*
HEPES	*(4-(2-hydroxyethyl)-1-piperazineethanesulfonic acid)*
HETE	*Hydroxyeicosatetraenoic acid*
HLA	*Human leukocyte antigen*
hPS	*Supernatant of activated human platelets*
HRP	*Horseradish peroxidase*
IA	*Insulinoma-associated antigen*
ICAM	*Intercellular adhesion molecule*
IL	*Interleukin*
IL2RA	*Interleukin-2 receptor subunit alpha*
IF	*Immunofluorescence*
IFN	*Interferon*
IP_3	*Inositol (3,4,5)-trisphosphate*
i.p.	*Intraperitoneal*
ITAM	*Immunoreceptor tyrosine-based activation motif*
ITT	*Insulin tolerance test*
i.v.	*Intravenous*
K_2HPO_4	*Dipotassium phosphate*
KCl	*Potassium chloride*
LOX	*Lipoxygenase*
LPA	*Lysophosphatidic acid*
LPC	*Lysophosphatidylcholine*
LPE	*Lysophosphatidylethanolamine*
LPI	*L-α-lysophosphatidylinositol*
LPS	*Lysophosphatidylserine*
LYM	*Lymphocyte*
lysoPAF	*Lyso-precursor of platelet-activating factor*
MAC-1	*Macrophage-1 antigen*
MAG	*Monoacylgycerol*

$MgCl_2$	*Magnesium chloride*
$MgSO_4$	*Magnesium sulfate*
MK	*Megakaryocyte*
MON	*Monocyte*
mPS	*Supernatant of activated mouse platelets*
munc	*Mammalian uncoordinated*
N	*Asparagine*
NaCl	*Natrium chloride*
NADH	*Nicotinamide adenine dinucleotide*
$NaHCO_3$	*Sodium hydrogencarbonate*
Na_2HPO_4	*Disodium hydrogen phosphate*
NaH_2PO_4	*Sodium dihydrogen phosphate*
$NaIO_4$	*Sodium periodate*
NaOH	*Sodium hydroxide*
NBEAL	*Neurobeachin-like*
NO	*Nitric oxide*
NOS	*Nitric oxide synthase*
NS	*Not significant*
NSCC	*Nonselective cation channel*
OCS	*Open canalicular system*
OEA	*Oleoylethanolamide*
PACAP	*Pituitary adenylate cyclase-activating polypeptide*
PAF	*Platelet activating factor*
PAR	*Protease activated receptor*
PBS	*Phosphate buffered saline*
PC	*Phosphatidylcholine*
PDGF	*Platelet derived growth factor*
PE	*Phosphatidylethanolamine*
PEA	*Phosphatidylethanolamine*
PF4	*Platelet factor 4*
PG	*Prostaglandin*

PH	*Pleckstrin homology*
PIP_2	*Phosphatidylinositol-4,5-bisphosphate*
PIP_3	*Phosphatidylinositol (3,4,5)-trisphosphate*
PI3K	*Phosphoinositide 3 kinase*
PKC	*Protein kinase C*
PL	*Phospholipid*
PLC	*Phospholipase C*
PP	*Pancreatic polypeptide*
PPAR	*Peroxisome proliferator-activated receptor*
PRP	*Platelet rich plasma*
PS	*Phosphatidylserine*
PSIS	*Platelet-stimulated insulin secretion*
PSGL-1	*P-selectin glycoprotein ligand-1*
PVDF	*Polyvinylidene fluoride*
RAGE	*Receptor for advanced glycation end products*
RBC	*Red blood cell*
RIPA	*Radioimmunoprecipitation assay buffer*
ROS	*Reactive oxygen species*
RPMI	*Roswell Park memorial institute*
S1P	*Sphingosine-1-phosphate*
SD	*Standard deviation*
SDS	*Sodium dodecyl sulfate*
SEM	*Standard error of the mean*
SERCA	*Sarcoendoplasmic reticulum* Ca^{2+}*-ATPase*
SNAP	*Synaptosomal-associated protein*
SNARE	*Soluble N-ethylmaleimide-sensitive-factor attachment receptor*
STIM	*Stromal interaction molecule*
TAE	*TRIS-acetic acid-EDTA*
TBS	*TRIS-buffered saline*
TBST	*TRIS-buffered saline + Tween 20*
TCA	*Tricarboxylic acid*

TEMED	*Tetramethylethylenediamine*
TF	*Tissue Factor*
THC	*Tetrahidrocannabinol*
TNF	*Tumor necrosis factor*
TRAP	*Thrombin receptor agonist peptide*
TRIS	*Tris(hydroxymethyl)aminomethane*
TRP	*Transient receptor potential*
Tspan	*Tetraspanin*
Tx	*Thromboxane*
VDCC	*Voltage-dependent Ca^{2+} channel*
VEGF	*Vascular endothelial growth factor*
vWF	*Von Willebrand factor*
WBC	*White blood cell*
ZnT	*Zinc transporter*
2-AG	*2-arachidonoyglycerol*
5HT	*5-hydroxytryptamine / serotonin*

5.4 Acknowledgment

The work presented here was performed at the Rudolf Virchow Center for Experimental Biomedicine, University of Würzburg, and University Hospital of Würzburg in the working group of Dr. Grzegorz Sumara between November 2017 and December 2022.

During my PhD studies, many people supported and assisted me in different ways. Without them, it would have been impossible to accomplish this work, which is why I would like to express my sincere gratitude to them:

I would especially like to thank Dr. Grzegorz Sumara for giving me the opportunity to do my PhD in his research group and for his continuous support, encouragement, and mentoring over the past years. The scientific passion and knowledge he transmitted were essential for the achievement of this work. His amazing style of supportive, eye-to-eye, and pragmatic supervision allowed me to fully develop and gave me a time that could not have been better.

The members of my thesis committee: Prof. Dr. Bernhard Nieswandt, Prof. Dr. Patrik Rorsman, and Prof. Dr. Antje Gohla. Thank you for the fruitful scientific discussions and the valuable input which significantly contributed to the development of the project. Additional thanks to Prof. Dr. Bernhard Nieswandt for the continuous provision of laboratory materials and resources.

My colleagues and friends from Würzburg, Rabih, Jonathan, Angel, Stefano, Mona, Alex, and Manu for their unlimited support and for making the time inside and outside the lab so enjoyable.

All the members of the Sumara group in Warsaw for their frequent help, assistance, and input. A special thank goes to Kasia for her dedicated collaboration on this project - it was always a pleasure to work with her.

Prof. Dr. Stegner, Dr. Werner Schmitz, Dr. Benoit Hastoy, and Prof. Dr. Katrin Heinze for their excellent collaborations, ideas, and expertise, which were of tremendous value to this work.

All others who have contributed to this work and are not mentioned here by name.

The Graduate School of Life Sciences for their helpful workshops, support, and coordination of the PhD program.

And last but most importantly, I want to dedicate my greatest gratitude to my family, friends, and to Ale, for always promoting me, having my back, and being patient. They made it possible to master this project.

5.5 Publications

T. Karwen, K. Kolczynska, C. Gross, M. C. Löffler, M. Friedrich, A. Loza-Valdes, W. Schmitz, F. Dziaczkowski, J. Trujillo-Viera, R. El-Merahbi, S. Nawaz, B. Hastoy, A. Demczuk, M. Wit, M. Erk, M. R. Wieckowski, P. Rorsman, K. G. Heinze, D. Stegner, B. Nieswandt, G. Sumara, *Platelet-derived lipids promote insulin secretion of pancreatic β-cells*. Currently in revision at EMBO Molecular Medicine.

A. Loza-Valdes, R. El-Merahbi, T. Kassouf, A. Demczuk, S. Reuter, J. T. Viera, T. Karwen, M. Noh, M. C. Loffler, R. Romero-Becerra, J. L. Torres, M. Marcos, G. Sabio, U. Wojda, G. Sumara, (2022). *Targeting ERK3/MK5 complex for treatment of obesity and diabetes*. Biochemical and Biophysical Research Communications.

J. Trujillo-Viera, R. El-Merahbi, V. Schmidt, T. Karwen, A. Loza-Valdes, A. Strohmeyer, S. Reuter, M. Noh, M. Wit, I. Hawro, S. Mocek, C. Fey, A. E. Mayer, M. C. Loffler, I. Wilhelmi, M. Metzger, E. Ishikawa, S. Yamasaki, M. Rau, A. Geier, M. Hankir, F. Seyfried, M. Klingenspor, G. Sumara, (2021). *Protein Kinase D2 drives chylomicron-mediated lipid transport in the intestine and promotes obesity*. EMBO Molecular Medicine.

R. El-Merahbi, J. T. Viera, A. L. Valdes, K. Kolczynska, S. Reuter, M. C. Loffler, M. Erk, C. P. Ade, T. Karwen, A. E. Mayer, M. Eilers, G. Sumara, (2020). *The adrenergic-induced ERK3 pathway drives lipolysis and suppresses energy dissipation*. Genes & Development.

M. C. Löffler, A. E. Mayer, J. Trujillo Viera, A. Loza Valdes, R. El-Merahbi, C. P. Ade, T. Karwen, W. Schmitz, A. Slotta, M. Erk, S. Janaki-Raman, N. Matesanz, J. L. Torres, M. Marcos, G. Sabio, M. Eilers, A. Schulze, G. Sumara, (2018). *Protein kinase D1 deletion in adipocytes enhances energy dissipation and protects against adiposity*. The EMBO Journal.

5.7 Affidavit

I hereby declare that my thesis entitled, "*Platelets promote insulin secretion of pancreatic β-cells*" is the result of my own work. I did not receive any help or support from commercial consultants. All sources and/or materials applied are listed and specified in the thesis.

Furthermore, I confirm that this thesis has not yet been submitted as part of another examination process neither in identical nor in similar form.

Würzburg, November 2022 _____

Till Karwen

5.8 Eidesstattliche Erklärung

Hiermit erkläre ich an Eides statt, die Dissertation „*Thrombozyten fördern die Insulinsekretion von pankreatischen β-Zellen*" eigenständig, d.h. insbesondere selbstständig und ohne Hilfe eines kommerziellen Promotionsberaters, angefertigt und keine anderen als die von mir angegebenen Quellen und Hilfsmittel verwendet zu haben.

Ich erkläre außerdem, dass die Dissertation weder in gleicher noch in ähnlicher Form bereits in einem anderen Prüfungsverfahren vorgelegen hat.

Würzburg, November 2022 _____

Till Karwen